Studies on Anion Chemistry of Silyl-Substituted π-Electron System Based on 4- and 5-Membered Rings

Tsukasa MATSUO

A dissertation submitted to the Doctoral Program
in Chemistry, the University of Tsukuba
in partial fulfillment of the requirements for the
degree of Doctor of Philosophy (Science)

January, 1999

Contents

Preface

The studies described in this dissertation have been carried out under the direction of Professor Akira Sekiguchi at the Department of Chemistry, University of Tsukuba.

This dissertation is concerned with the chemistry of a variety of anion species of silyl-substituted π-electron systems mainly based on four- and five-membered rings. Anion species of π-electron systems have many interesting and important problems. The author is convinced that the present studies have contributed not only to the progress of the field of organosilicon chemistry but also to the advance in organic chemistry and organometallic chemistry.

Particular thanks are due to Professor Akira Sekiguchi, who made many perceptive suggestions and provided the unflagging support throughout the whole course of the studies. The author wishes to express his grateful acknowledgement to Professor Hideki Sakurai (Science University of Tokyo) for his continuing guidance and valuable discussions. It is a great pleasure to thank Professor Mitsuo Kira (Tohoku University) for his helpful discussions and encouragement. The author is also very grateful to Dr. Keisuke Ebata (NTT Basic Research Laboratory) for his generous instruction and practical suggestions. The author would like to express appreciation to Associate Professor Kenkichi Sakamoto, Dr. Masaaki Ichinohe, and Dr. Vladimir Ya. Lee for their helpful advice and suggestions, and also to all of the members of Professor Sekiguchi's group, Professor Sakurai's group, and Professor Kira's group for their valuable discussions and providing the comfortable environment in research. And special thanks go to Dr. Masato Nanjo who made very useful suggestions and greatly contributed to the establishment of the Professor Sekiguchi's new laboratory. The author thanks Dr. Chizuko Kabuto (Tohoku University) and Ms. Akiko Nakao and Mr. Akira Komai (Mac Science) for the X-ray crystallography. The author also thanks Associate Professor

Ryoichi Akaba (Gunma College of technology) for the PM3 calculation and the cyclic voltammetry.

Finally, the author would like to thank his parents Mr. Toji Matsuo and Ms. Wakano Matsuo, and his sister Ms. Aya Matsuo for their kindly continuous encouragements and supports.

Tsukasa MATSUO

Department of Chemistry

University of Tsukuba

January 1999

General Introduction

π-Electron systems with alternating carbon-carbon single and double bonds are fundamental and essential species in organic chemistry. Various π-electron systems are hitherto known and their properties depend primarily on the number and arrangement of double bonds. The basic concepts concerning π-electron systems, such as conjugation, aromaticity, and Hückel's rule, have been established by both experimentaters and theoreticians thus far.[1]

Double bonds which are separated by just one single bond interact with each other and are called conjugated double bonds. Because of the interaction between the double bonds, systems containing conjugated double bonds tend to be more stable than similar systems with isolated double bonds. This extra stability in the conjugated molecule is called the resonance energy of the system. The origin of this additional stability of conjugated systems is best explained by examination of their molecular orbitals.

1,3-Butadiene with 4C / 4π–electron system has two conjugated double bonds. The most stable conformation of 1,3-butadiene is planar, with the *p* orbitals on the two double bonds aligned. The carbon-carbon single bond in 1,3-butadiene is considerably shorter than a carbon-carbon single bond in alkanes: 1.48 vs. 1.54 Å. Although this bond is shortened by the increased *s* character of the sp^2 hybrid orbitals, the most important reason is the π-bonding overlap and partial double bond character of the bond. The planar conformation, with the *p* orbitals of the two double bonds aligned, allows overlap between the π-bonds. In fact, the electrons of the two double bonds are delocalized over the entire molecule, creating some π-overlap and π-bonding in the carbon-carbon single bond. The length of this bond is something intermediate between the normal length of a single bond and that of a double bond. That is 1,3-butadiene can not be considered as two independent ethylene molecules.

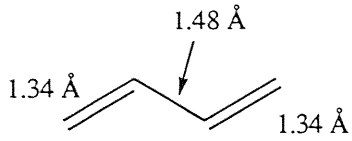

1,3-butadiene

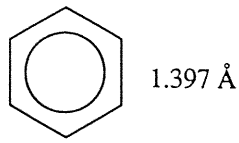

benzene

Benzene with 6C / 6π-electron system has a cyclic structure with three double bonds. Benzene is actually a resonance hybrid of two Kekule structures. This representation suggests that the π-electrons are delocalized, with a bond order of 1.5 between adjacent carbon atoms. The carbon-carbon bond lengths in benzene are shorter than typical single bond lengths, but longer than typical double bond lengths. There are no localized single or double bonds in benzene. Actually benzene represents a ring which consist of sp^2 hybrid carbon atoms, each of them is bonded with one hydrogen atom. The molecular structure of benzene is a planar equilateral hexagon. All the carbon-carbon bonds have the same lengths and all the bond angles are exactly 120°. Each sp^2 carbon atom has an unhybridized *p* orbital perpendicular to the ring plane, and six electrons occupy this circle of *p* orbitals.

The special stability of benzene is called aromaticity. An aromatic compound is a cyclic compound containing definite number of conjugated double bonds with an unusual large resonance energy. Benzene is actually unwilling to undergo typical alkene reactions such as bromination, and is much more stable than the other acyclic polyenes. Aromatic compounds are those that correspond to the following criteria. 1) The structure must be cyclic, containing definite number of conjugated π-bonds. 2) Each atom in the ring must have an unhybridized *p* orbital. The ring atoms are usually sp^2 hybridized, or occasionally *sp* hybridized. 3) The unhybridized *p* orbitals must overlap to form a continuous ring of parallel orbitals. In most cases, the structure must be planar or nearly planar for effective overlap. 4) Delocalization of the π-electrons over the ring must result

in a lowering of the electronic energy.

Cyclobutadiene with 4C / 4π-electron system meets the first three criteria for a continuous ring of overlapping *p* orbitals, but the delocalization of the π-electrons results in an increase in the electronic energy. Cyclobutadiene is less stable than its open-chain analogue, 1,3-butadiene, and it is antiaromatic.

cyclobutadiene

Cyclic hydrocarbons with alternating single and double bonds are called annulenes. Benzene is [6]annulene and cyclobutadiene is [4]annulene, respectively. Hückel developed a shortcut to predict which of annulenes and related compounds are aromatic and which are antiaromatic. In accordance with Hückel's rule, we must be certain that the compound under consideration corresponds to the criteria of aromaticity. Hückel's rule is the following. 1) If the number of π-electrons in the cyclic system is $(4N + 2)$, with N an integer, the system is aromatic. Common aromatic systems have 2, 6, 10 π-electrons, for $N = 0$, 1, and 2. 2) Systems with $4N$ π-electrons, with N an integer, are antiaromatic. Common examples are the systems with 4, 8, 12 π-electrons. There are six π-electrons in benzene, so it is a $(4N + 2)$ system, with $N = 1$. Hückel's rule predicts benzene to be aromatic. On the other hand, cyclobutadiene has four π-electrons and Hückel's rule predicts cyclobutadiene to be antiaromatic.

Anion species of π-electron systems having extra electrons in the molecule, have been studied from the beginning of nineteen hundreds. Cyclopentadienide ion with 5C / 6 π-electron system was formed by the hydrogen abstraction reaction of cyclopentadiene using a base in 1900.[2] A negative charge of cyclopentadienide ion is equally delocalized over the five carbon atoms. The structure of cyclopentadienide ion is a planar, equilateral pentagon. Thus, cyclopentadienide ion is a stable, closed-shell anion species, which is stabilized by aromatic 6π-electron system. It is a $(4N + 2)$ system, with $N = 1$. A sodium salt of cyclopentadienide ion is indeed thermally stable up to 300 °C, but it is highly air

and moisture sensitive.[3] Cyclopentadienide ion has a high reactivity towards electrophilic reagents and cyclopentadiene derivatives are easily formed.

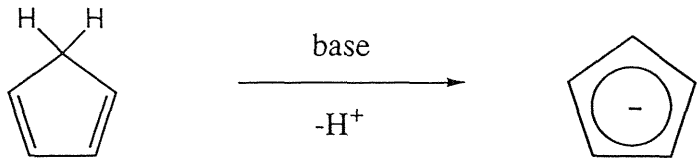

cyclopentadienide ion

Cyclooctatetraene dianion with 8C / 10π-electron system was prepared from the same point of view of aromaticity.[4] Neutral cyclooctatetraene is [8]annulene with 8π-electrons of four double bonds. It is a $4N$ system, with $N = 2$. If Hückel's rule is applied to cyclooctatetraene, it would predict antiaromaticity. However, cyclooctatetraene is a stable hydrocarbon. It does not show the high reactivity associated with antiaromaticity. Its reactions are typical for alkenes. Cyclooctatetraene is more flexible than cyclobutadiene, and it assumes a nonplanar conformation that avoids most of the overlap between adjacent π-bonds. In fact, structural studies have shown that cyclooctatetraene is not planar but has a tub conformation. That is, cyclooctatetraene is a nonaromatic compound.

Cyclooctatetraene dianion was prepared by a reaction of cyclooctatetraene with alkali metal. Two negative charge of cyclooctatetraene dianion is equally delocalized over the eight carbon atoms. Structural studies have shown that the molecular structure of cyclooctatetraene dianion is different from that of neutral cyclooctatetraen with the tub structure. It is planar, equilateral octagon. Thus, cyclooctatetraene dianion is a stable, closed-shell dianion species, which is stabilized by aromatic 10π-electron system. It is a $(4N + 2)$ system, with $N = 2$. The molecular structure of the dipotassium salt of 1,3,5,7-tetramethylcyclooctatetraene dianion was unequivocally confirmed by X-ray crystallography.[5]

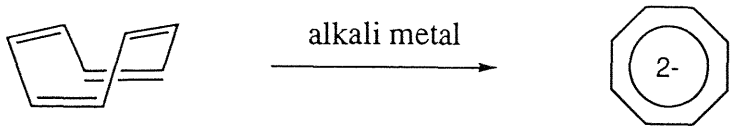

cyclooctatetraene dianion

Anion species of π-electron systems have many interesting and important problems. Delocalization of π-electrons, distribution of negative charge, complexation with metal cation, formation of ion pairs, solvation of counter cation, and so on. Various anion species of π-electron systems have been studied so far, and some of them were isolated as a corresponding alkali metal complex such as the sodium salt of cyclopentadienide ion.[3] However, anion species of π-electron systems are not stable and highly sensitive to the air and moisture. An oxidation reaction of anion species of π-electron systems is readily occurred to form neutral starting molecule. For example, cyclooctatetraene dianion is immediately reverted to cyclooctatetraene by oxygen.[4] Anion species of π-electron systems are also easily reacted with water in the air to form the corresponding hydrogen addition products. Thus, there has been a few reports in regard to an exact structure and properties of anion species.[6] The special techniques, such as Schlenk tube method and a glove box filled with inert gas, are essential for the handling of these unstable compounds.

Dianion species of π-electron systems have become remarkable interest owing to their unique structures and electronic properties resulting from the high density of π-electrons. Dianion species are considerably unstable due to their electrostatic repulsion of two negative charges. Therefore, two electron reduction of π-electron systems does not usually proceed with the formation of dianion species. Only part of special π-electron systems undergoes the two electron reduction, such as cyclooctatetraene dianion with a contribution of aromatic stabilization.

The introduction of a silyl group causes remarkable steric and electronic perturbations to the π-electron systems.[7] First, the silyl groups have a remarkable steric effect. Trimethylsilyl group is a most popular substituent as trialkyl-substituted silyl groups and is widely used for a variety of organic synthesis. Because silicon-carbon single bond (1.89 Å) is longer than carbon-carbon single bond (1.54 Å), trimethylsilyl group is bulkier than *t*-butyl group. Thus, trimethylsilyl group is regarded as one of the bulky substituent.

Hexakis(trimethylsilyl)benzene has a highly distorted structure due to the steric effect of six trimethylsilyl groups.[8] The benzene ring of hexakis(trimethylsilyl)benzene is significantly distorted to a chair form. Photolysis of hexakis(trimethylsilyl)benzene with a light ($\lambda > 300$ nm) afforded the hexakis(trimethylsilyl)Dewar benzene quantitatively. The Dewar benzene is a thermally labile molecule and is readily reverted to the benzene by heating. The Dewar benzene was irradiated with a light ($\lambda = 254$ nm) to produce the hexakis(trimethylsilyl)prismane. The prismane is also readily converted to the benzene by heating.

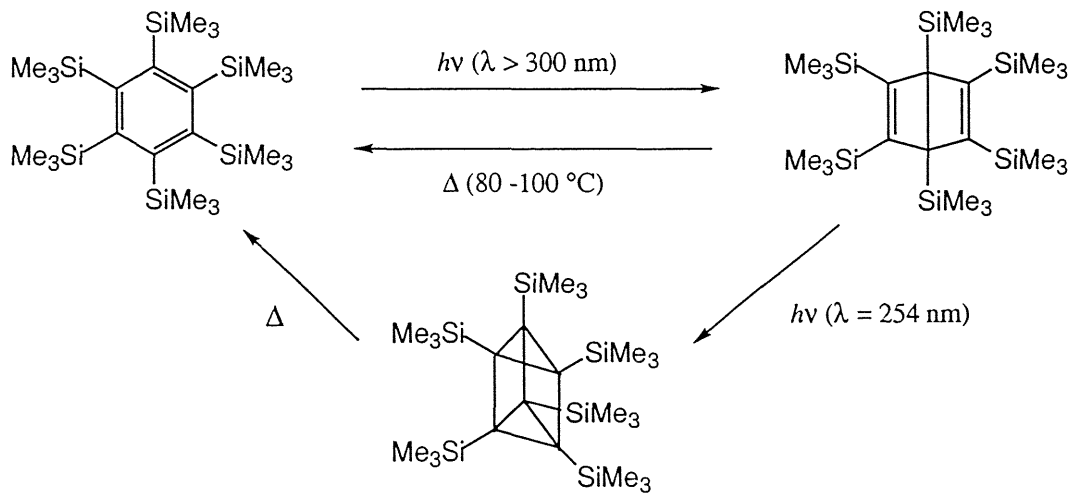

A variety of hexakis(trimethylsilyl)benzene isomers were produced not only by photochemical reaction but also by thermal reaction. Thermolysis of hexakis(trimethyl-

silyl)benzene at 200 °C gave the bisallene derivative quantitatively by the rupture of the benzene ring. In this reaction, several isomers were also isolated as the intermediates. These unusual photochemical and thermal reactivities of hexakis(trimethylsilyl)benzene are considered as a consequence of steric effect of trimethylsilyl groups.

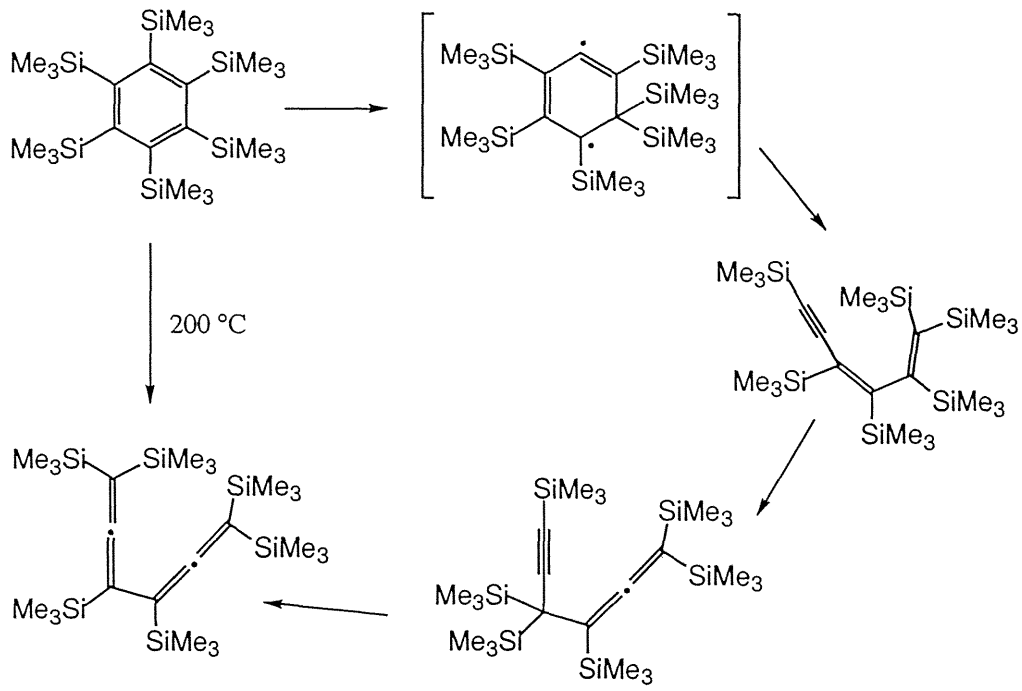

The other very important effect of silyl groups is their electronic effect. The electronic effect of silyl groups is well-known as the α-effect and β-effect. The α-effect is the following: anion on the atom which is located at an α-position of silicon atom, is stabilized by the antibonding σ* orbital of the silicon-carbon bond of alkylsilyl group. When alkylsilyl group is substituted by the π-electron systems, the level of LUMO of π-electron system is stabilized by the interaction between the antibonding σ* orbital of the silicon-carbon bond and π* orbital of π-electron system. It is a σ*-π* conjugation.

The β-effect is the following: cation on the atom which is situated at a β-position of silicon atom, is stabilized by the bonding σ orbital of the silicon-carbon bond at the base of silyl group. When a silyl group attaches to the π-electron systems, the level of HOMO of π-electron system is risen by the interaction between the bonding σ orbital of the

silicon-carbon bond and π orbital of π-electron system. It is a σ-π conjugation. Both the σ*-π* conjugation and the σ-π conjugation are considered as a kind of hyperconjugation.

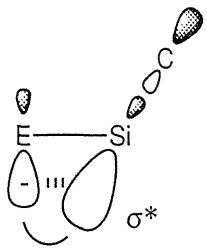

α-effect

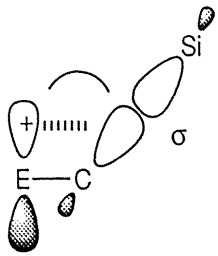

β-effect

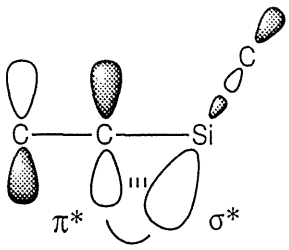

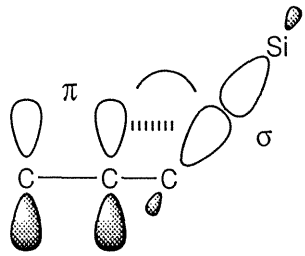

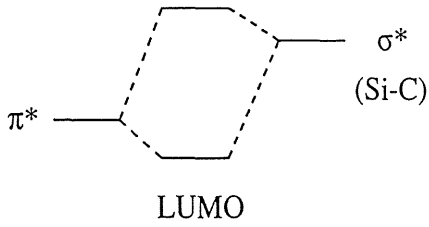

σ*-π* conjugation

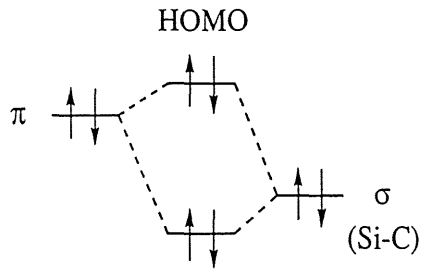

σ-π conjugation

As above mentioned, silyl group has quite different from simple alkyl group electronic properties. One of the most interesting features of silyl-substituted π-electron systems is the ability to form dianion species by two electron reduction with alkali metals due to the stabilization of their level of LUMO. Recently, several dianion species of silyl-substituted π-electron systems have been actually isolated as the dialkali metal complexes, and their structures and properties were revealed.

First, dianion species of silyl-substituted ethylene has been investigated.[9] Reaction of tetrakis(trimethylsilyl)ethylene with excess of lithium metal in dry oxygen-free THF at room temperature under argon gave a dark red solution of the dianion species within a few hours. Crystallization at -10 °C in hexane afforded yellow crystals of the 1,2-dilithio[tetrakis(trimethylsilyl)]ethane containing two molecules of THF. The structure of the dilithium compound was unequivocally determined by X-ray crystallography. Two lithium atoms are three-coordinated, being bonded to the THF in addition to two carbon atoms. It is a doubly-bridged structure. The bond length of the dianionic carbon-carbon bond is significantly increased from 1.368 Å in the precursor, tetrakis(trimethylsilyl)-ethylene to 1.597 Å in the dilithium compound. 1,2-dilithio[tetrakis(trimethylsilyl)]ethane is the first structural characterization of nonconjugated 1,2-dilithioethane. After that, a variety of dianion species of silyl-substituted ethylene have been prepared.[10]

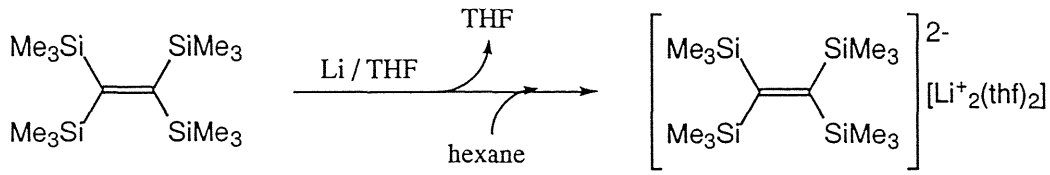

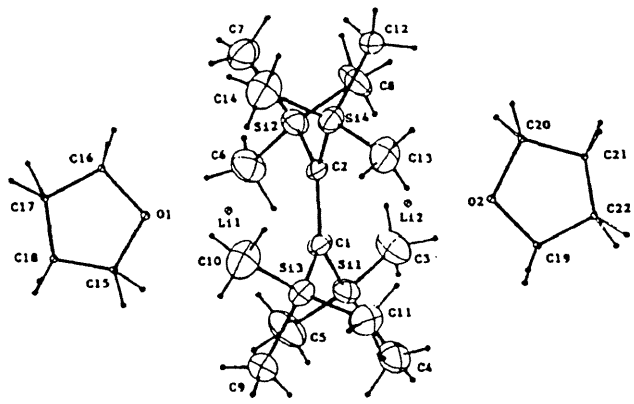

Next, two dianion species of silyl-substituted benzene have been studied.[11] One is the dilithium salt of hexakis(trimethylsilyl)benzene dianion, and the other is the dilithium salt of 1,2,4,5-tetrakis(trimethylsilyl)benzene dianion. The former is a nonaromatic

compound, whereas the latter is an antiaromatic compound with 6C / 8π-electron system. It is a $4N$ system, with $N = 2$.

Reaction of hexakis(trimethylsilyl)benzene with excess of lithium metal in dry-oxygen free THF at room temperature led to the formation of a dark red solution of the benzene dianion within 1 hour. Crystallization from hexane afforded red crystals of bis[(tetrahydrofuran)lithium(I)]hexakis(trimethylsilyl)benzenide containing two molecules of THF. The structure of the dilithium compound has been unequivocally confirmed by X-ray crystallography. Both lithium atoms are located on the same side of the benzene ring. The lithium-lithium distance is only 2.722 Å despite of the expected electrostatic repulsion. The benzene ring is appreciably deformed into a boat form. The steric factors may play an important role to determine the structure of the benzene dianion. The molecular structure of the dilithium compound found in the crystals seems to be maintained in solution. In the ^{7}Li NMR spectra, one signal is appearing at -1.48 ppm. The dilithium salt of hexakis(trimethylsilyl)benzene dianion is the first nonconjugated mononuclear benzene dianion.

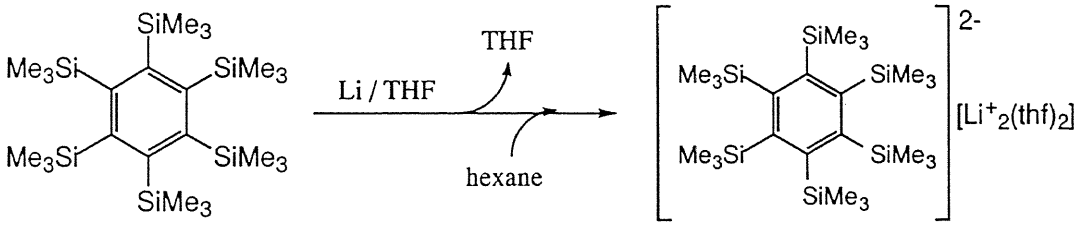

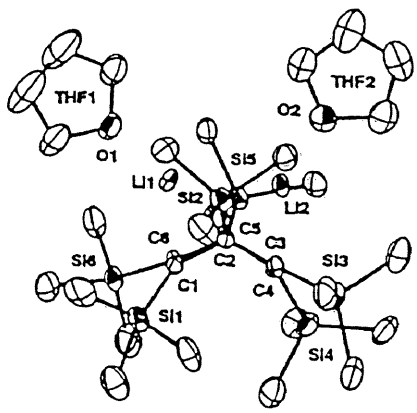

The similar two electron reduction was proceeded in tetrakis(trimethylsilyl)benzene. Reaction of 1,2,4,5-tetrakis(trimethylsilyl)benzene with lithium metal in dry oxygen-free DME at room temperature immediately gave the formation of a dark red solution of the benzene dianion. Crystallization from hexane yielded dark brown crystals of bis[(1,2-dimethoxyethane)lithium(I)]1,2,4,5-tetrakis(trimethylsilyl)benzenide. The structure of the dilithium compound was also determined by X-ray crystallography. The two lithium atoms are exactly located above and below the center of the benzene ring. The benzene ring is nearly planar. The molecular structure of the dilithium compound found in the crystals is retained in solution. Of particular interest is ^{7}Li resonance at 10.7 ppm. The appreciable downfield shift is caused by the strong deshielding effect on the lithium atoms by the paratropic ring current resulting from 8π-electron antiaromatic system. Thus, the dilithium salt of 1,2,4,5-tetrakis(trimethylsilyl)benzene dianion has nearly the planar antiaromatic character with the negative charge stabilized by the four silyl groups. Afterward, as an approach to a triplet benzene dianion, the planar hexasilylbenzene dianion species have been investigated.[12]

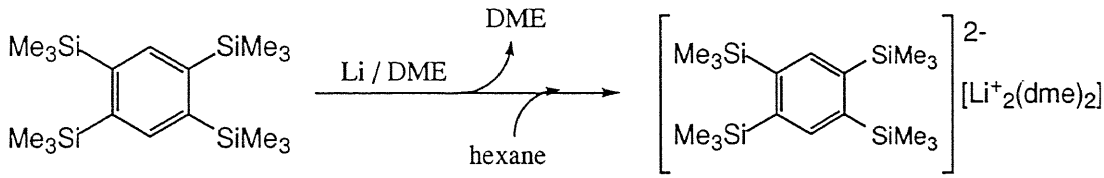

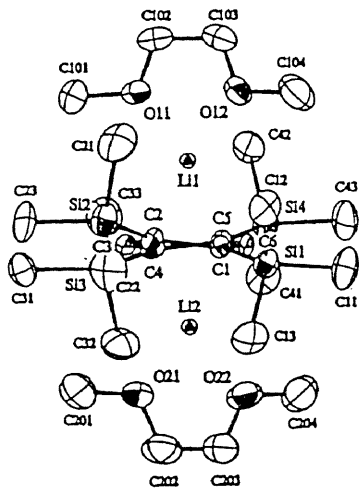

From the foregoing examples, the electronic effect of silyl groups is very useful for the stabilization of dianion species of π-electron systems. The bulky silyl groups also accelerate the formation of a monomer of dialkali metal compounds with an improvement of the solubility.

This dissertation is concerned with the synthesis of a variety of anion species of silyl-substituted π-electron systems mainly based on four- and five-membered rings. The molecular structure of these anion species were determined by X-ray crystallography. The structural parameters of anion species are compared with those of the precursor, neutral silyl-substituted π-electron systems. The structure of anion species in solution are also discussed on the basis of the NMR spectroscopic data. Especially, the Li NMR is very available to gain the information of anion species. Further, the PM3 calculation is efficiently used for the understanding of the properties of anion species.

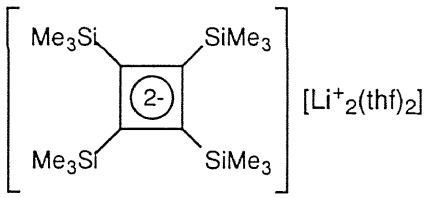

Chapter 1

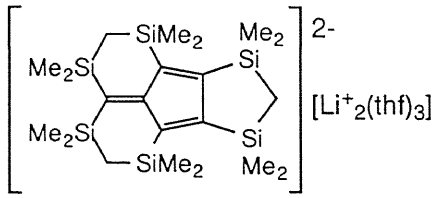

Chapter 4

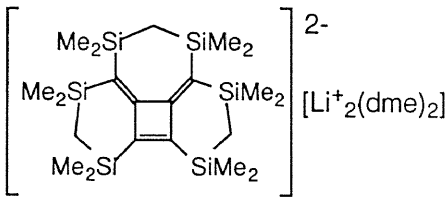

Chapter 2

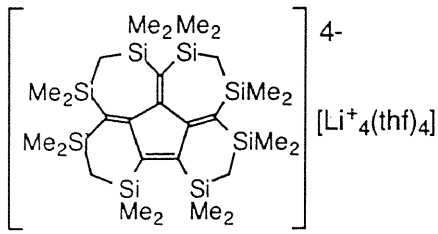

Chapter 5

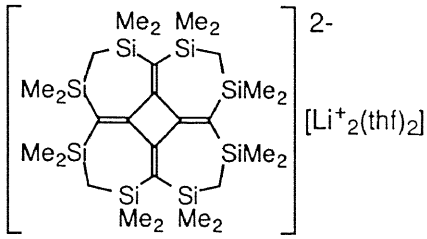

Chapter 3

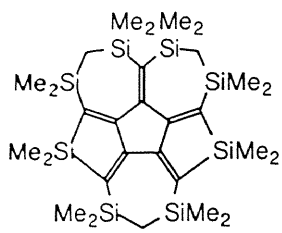

Chapter 6

References

(1) L. G. Wade, Jr., "Organic Chemistry, second edition" Prentice-Hall, Inc., New Jersey (1991).

(2) (a) J. Thiele, *Chem. Ber.*, **33,** 666 (1900). (b) J. Thiele, *Chem. Ber.*, **34,** 68 (1901).

(3) K. Ziegler, H. Froitzheim-Kühlhorn, and K. Hafner, *Chem. Ber.*, **89,** 434 (1956).

(4) (a) A. R. Ubbelohde, *Chem. Ind.*, **1956,** 153. (b) T. J. Katz, *J. Am. Chem. Soc.*, **82,** 3784 (1960). (c) T. J. Katz and H. L. Strauss, *J. Chem. Phys.*, **32,** 1873 (1960).

(5) S. Z. Goldgerg, K. N. Raymond, C. A. Harmon, and D. H. Templeton, *J. Am. Chem. Soc.*, **96,** 1348 (1974).

(6) For the recent reviews on the various anion species, see: (a) K. Müllen, *Chem. Rev.*, **84,** 603 (1984). (b) W. N. Setzer and P. v. R. Schleyer, *Adv. Organomet. Chem.*, **24,** 353 (1985). (c) C. Schade and P. v. R. Schleyer, *Adv. Organomet. Chem.*, **27,** 169 (1987). (d) M. Rabinovitz, *Top. Curr. Chem.*, **14,** 99 (1988). (e) A. B. Sannigrahi, T. Kar, B. G. Niyogi, P. Hobza, and P. v. R. Schleyer, *Chem. Rev.*, **90** 1061 (1990). (f) H. Bock, K. Ruppert, C. Näther, Z. Havlas, H. F. Herrmann, C. Arad, I. Gögel, A. John, J. Meuret, S. Nick, A. Rauschenbach, W. Seitz, T. Vaupel, and B. Solouki, *Angew. Chem., Int. Ed. Engl.*, **31,** 550 (1992).

(7) (a) H. Sakurai, *Nippon Kagaku Kaishi,* **1990,** 439. (b) H. Sakurai, *Pure Appl. Chem.*, **68,** 327 (1996).

(8) (a) H. Sakurai, K. Ebata, C. Kabuto, and A. Sekiguchi, *J. Am. Chem. Soc.*, **112,** 1799 (1990). (b) A. Sekiguchi, K. Ebata, Y. Terui, and H. Sakurai, *Chem.*

Lett., **1991**, 1417.

(9) (a) A. Sekiguchi, T. Nakanishi, C. Kabuto, and H. Sakurai, *J. Am. Chem. Soc.*, **111**, 3748 (1989). (b) A. Sekiguchi, M. Ichinohe, T. Nakanishi, and H. Sakurai, *Chem. Lett.*, **1993**, 267.

(10) (a) A. Sekiguchi, T. Nakanishi, C. Kabuto, and H. Sakurai, *Chem. Lett.*, **1992**, 867. (b) A. Sekiguchi, M. Ichinohe, C. Kabuto, and H. Sakurai, *Organometallics*, **14**, 1092 (1995). (c) A. Sekiguchi, M. Ichinohe, C. Kabuto, and H. Sakurai, *Bull. Chem. Soc. Jpn.*, **68**, 2981 (1995). (d) A. Sekiguchi, M. Ichinohe, T. Nakanishi, C. Kabuto, and H. Sakurai, *Bull. Chem. Soc. Jpn.*, **68**, 3215 (1995). (e) A. Sekiguchi, M. Ichinohe, M. Takahashi, C. Kabuto, and H. Sakurai, *Angew. Chem., Int. Ed. Engl.*, **36**, 1533 (1997).

(11) (a) A. Sekiguchi, K. Ebata, C. Kabuto, and H. Sakurai, *J. Am. Chem. Soc.*, **113**, 1464 (1991). (b) A. Sekiguchi, K. Ebata, C. Kabuto, and H. Sakurai, *J. Am. Chem. Soc.*, **113**, 7081 (1991).

(12) K. Ebata, W. Setaka, T. Inoue, C. Kabuto, M. Kira, and H. Sakurai, *J. Am. Chem. Soc.*, **120**, 1335 (1998).

Chapter 1

Silyl-Substituted Cyclobutadiene Dianion with 4C / 6π-Electron System

Summary

The reaction of tetrakis(trimethylsilyl)cyclobutadienyl cyclopentadienyl cobalt [$C_4(TMS)_4CoCp$] (**6**) with lithium metal in THF at room temperature led to the dilithium salt of tetrakis(trimethylsilyl)cyclobutadiene dianion (**8**) with 4 center / 6π-electron system. Crystallization from hexane afforded air and moisture sensitive pale yellow crystals of **8** containing two molecules of THF. The structure of **8** in solution has been discussed on the basis of NMR spectroscopic data. In the ^7Li NMR spectrum of **8** in benzene-d_6 only one signal appeared at -5.29 ppm. This appreciable upfield shift is evidently caused by the strong shielding effect by the diamagnetic ring current resulting from the 6π aromatic system. The NMR data indicate that the cyclobutadiene dianion **8** is an aromatic compound stabilized by the four silyl groups.

Introduction

"Aromatic or nonaromatic; that is the question!"

Hückel's rule predicts cyclobutadiene dianion (**1**) to be aromatic. There are six π-electrons in cyclobutadiene dianion, so it is a $(4N + 2)$ system, with $N = 1$. However, there has been no clear evidence for the aromaticity of cyclobutadiene dianion, so far.

In 1970's, the parent cyclobutadiene (**2**) was *Mona Lisa* in organic chemistry. Many chemists have tried to synthesize free cyclobutadiene, but no one achieved it successfully due to the antiaromaticity resulting from 4π-electron system. According to the spectroscopic evidence by matrix isolation, free cyclobutadiene is not square but rectangular structure, and is not triplet but singlet species owing to the Jahn-Teller effect.[1] After that, there has been some reports on the cyclobutadiene derivatives which have been confirmed by X-ray crystallography, such as tetrakis(*t*-butyl)cyclobutadiene.[2] These compounds have shown the rectangular structure with the considerably elongated carbon-carbon single bond.

In 1972, McKennis et al. obtained evidence for the formation of cyclobutadiene dianion (**1**); but they characterized it as being highly reactive since it apparently abstracted protons from THF.[3] In 1978, Garratt et al. successfully used ester groups to delocalize the negative charge so extensively that the dianion (**3**) was stable at room temperature (Chart 1-1).[4] According to the authors, only 40% of the negative charge in **3** remains in the four-membered ring. pK_a measurements indicate that the dianion **3** does not experience any aromatic stabilization.

In 1982, the ^1H and ^{13}C NMR data of dilithium salt of 1,2-diphenylbenzocyclobutadienediide (**4**) and dipotassium salt of 1,2,3,4-tetraphenylcyclobutadienediide (**5**) were continuously reported by Boche et al. (Schemes 1-1 and 1-2).[5,6] The negative charge of **5** resides predominantly (64%) on the phenyl groups.

Chart 1-1

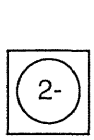

1

2

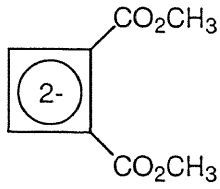

3

Scheme 1-1

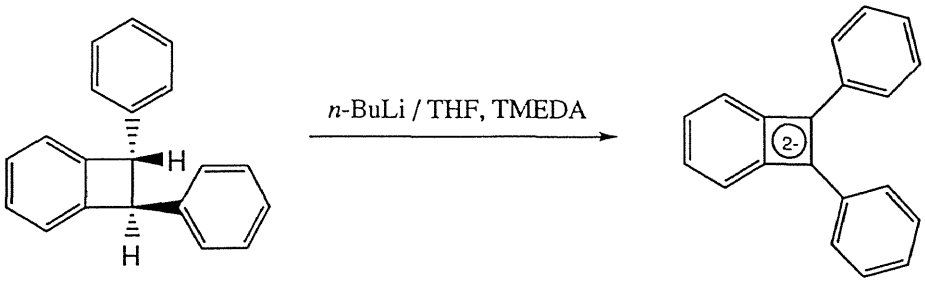

4

Scheme 1-2

5

More recently, Boche et al. have determined the molecular structure of dilithium salt of 1,2-diphenylbenzocyclobutadienediide (4) with 2 molecules of TMEDA (Figure 1-1).[7] Two types of molecular structure (I and II) were found in the crystals of 4. But they have not commented on the aromaticity of 4.

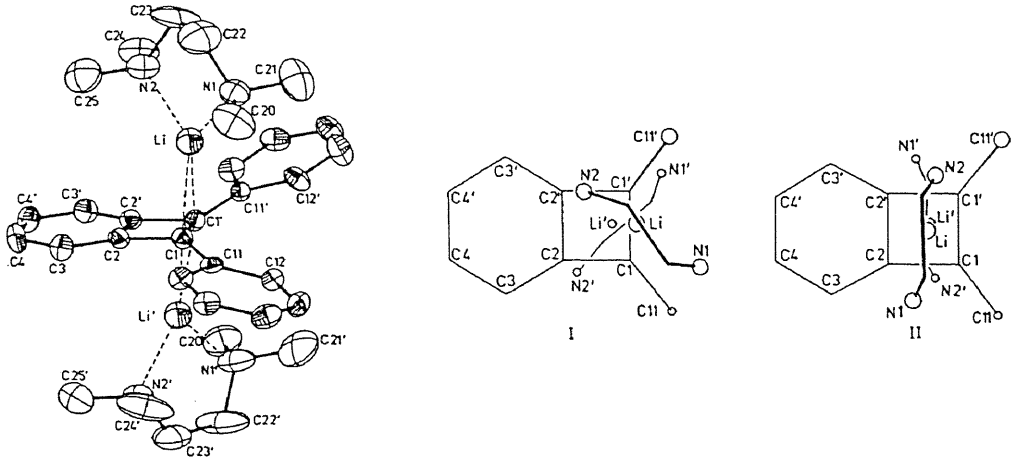

Figure 1-1. Crystal structure of dilithium 1,2-diphenylbenzocyclobutadiene dianion **4**.

Elaborate calculations indicate that cyclobutadiene dianion (**1**) should be regarded as a nonaromatic compound because of destabilizing 1,3-interactions. In other words, the stabilization due to cyclic delocalization is not sufficient in this doubly charged system. Accordingly, the Hückel-type D_{4h} geometry is not to be expected. A vibrational analysis demonstrated that the minimum of cyclobutadiene dianion is occupied by the C_s conformation (**1'**), which is composed of an allyl anion and a localized negative charge (Figure 1-2).[8] For the dianion computed with 6-31G* basis , the dihedral angles made by C1-C2-C3 and C1-C3-C4 planes is 163.1°, and C1-C2-C4 and C2-C3-C4 planes is 167.6°, respectively. The MP2 optimization was also found to give a bent structure with C_s symmetry as **1'**.

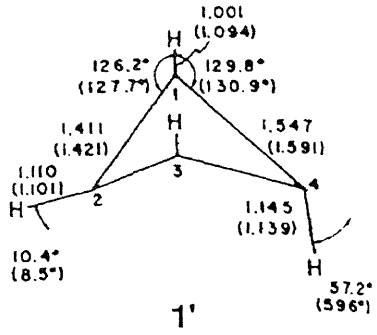

Figure 1-2. Optimal geometry of cyclobutadiene dianion (**1'**) computed with 6-31G* basis and 3-21G (in parentheses).

To evaluate the influence of a counterion, $Li^+C_4H_4^{2-}$ was also examined with 3-21G basis (Figure 1-3).[8] Its geometry was optimized with the C_{4v} symmetry constraint. It is seen that the major effect of the lithium on the structure is the distortion of the hydrogens out of the plane of the carbons and away from the lithium, but C-C bond distances and skeleton angles correspond to the square dianion. The lithium lies 1.078 Å above the plane of the carbons.

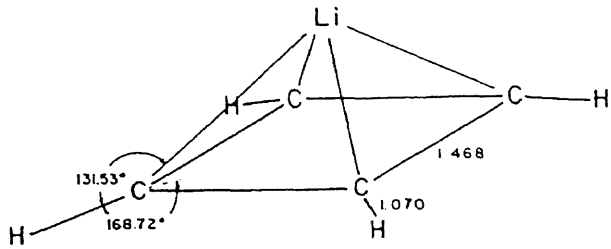

Figure 1-3. Optimized geometry (3-21G) of $Li^+C_4H_4^{2-}$ with a C_{4v} symmetry constraint.

In this chapter, the synthesis, isolation, and characterization of dilithium tetrasilylcyclobutadiene dianion with a novel 4C / 6π-electron system are described.

Results and Discussion

Synthesis of Tetrasilylcyclobutadienyl Cyclopentadienyl Cobalt

The preparation of free cyclobutadiene by photolytic methods in low temperature matrices (8-20 K) is a relatively recent accomplishment.[1] The stabilization of cyclobutadiene by coordination to a transition metal had been predicted on theoretical grounds by Longuet-Higgins and Orgel in 1956, the first synthesis of a cyclobutadiene transition metal complex being carried out by Criegee in 1959.[9] Since then various transition metal complexes of cyclobutadiene (η^4-coordination) have been hitherto prepared such as cyclobutadienyl(tricarbonyl)iron [$C_4H_4Fe(CO)_3$].[10] However, only one example of (π-cyclopentadienyl)[π-tetrakis(trimethylsilyl)cyclobutadiene]cobalt (**6**) has been reported so far as the tetrasilyl-substituted cyclobutadiene transition complex.[11]

First, the cobalt complex **6** was prepared according to the Vollhardt's method.[11b] A mixture of bis(trimethylsilyl)acetylene and cyclopentadienyl(dicarbonyl)cobalt [CpCo $(CO)_2$] was reacted under the refluxing temperature of bis(trimethylsilyl)acetylene to produce yellow crystals of [$C_4(TMS)_4CoCp$] (**6**) in 55% yield with a small amount of tetrakis(trimethylsilyl)butatriene (Scheme 1-3).

Scheme 1-3

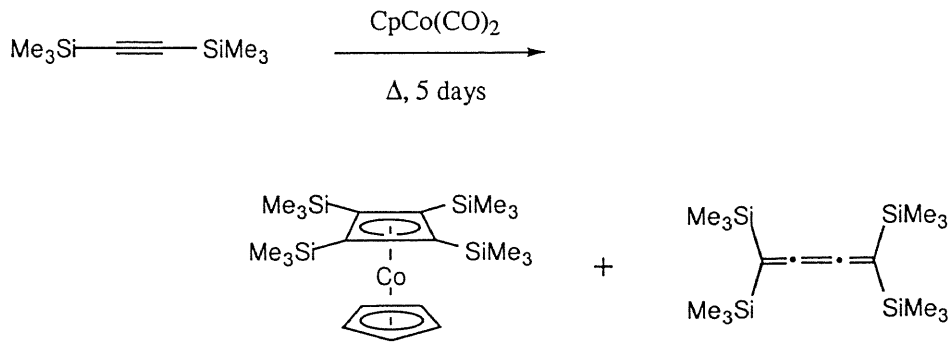

6

Butatriene is a valence isomer (C_4H_4) of cyclobutadiene, tetrahedrane, and methylenecyclopropene. Tetrakis(trimethylsilyl)butatriene was reported as an only example of the valence isomers of $(TMS)_4C_4$.[11b,12] Tetrakis(trimethylsilyl)cyclobutadiene, tetrakis(trimethylsilyl)tetrahedrane, and tetrakis(trimethylsilyl)methylenecyclopropene are hitherto unknown.

Next, tetrasilylcyclobutadiene cobalt complex bridged by $Me_2Si(CH_2)_2SiMe_2$ chains (**7**) was prepared in a similar manner (Scheme 1-4). Cobalt complex **7** was also isolated as yellow crystals in 16% yield. Similar reaction using cyclic diyne compounds and $[CpCo(CO)_2]$ have been reported by Gleiter et al., and a variety of cobalt complexes, such as metal-capped cyclobutadienosuperphanes, were successfully prepared.[13]

Scheme 1-4

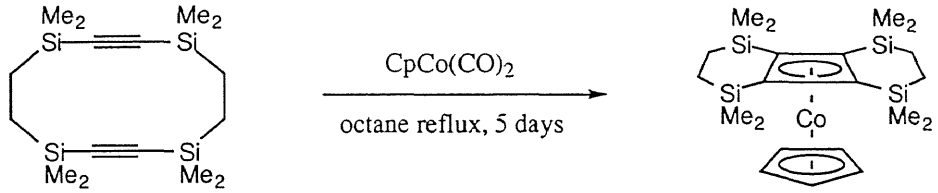

7

Cobalt complexes **6** and **7** are fully characterized by NMR spectroscopies. These compounds are thermally stable but slightly moisture sensitive, and are slowly decomposed in the air.

Reaction of Tetrasilylcyclobutadienyl Cyclopentadienyl Cobalt with Lithium Metal

Reaction of $[C_4(TMS)_4CoCp]$ (**6**) with excess of lithium metal in dry oxygen-free THF at room temperature gave the formation of a dark brown solution containing the tetrakis(trimethylsilyl)cyclobutadiene dianion (**8**) (Scheme 1-5). This transmetalation reaction completed about 20 hours. The solvent was removed in vacuo, and then dry degassed hexane was introduced by vacuum transfer. A hexane soluble brown solution and hexane insoluble dark materials were separated in a glove box filled with argon gas. The dark materials may be a reactive residue of cobalt complex. Crystallization of the hexane solution at 5 °C afforded air and moisture sensitive pale yellow crystals of the dilithium salt of tetrakis(trimethylsilyl)cyclobutadiene dianion (**8**) containing two molecules of THF.

Scheme 1-5

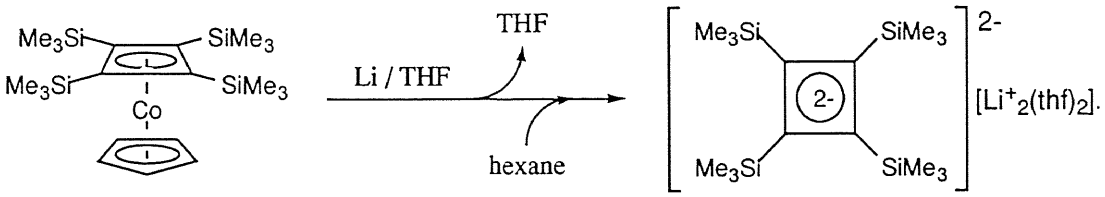

6 **8**

Cobalt complex **7** bridged by disilethylene chains also underwent a transmetalation in THF to yield a dark brown solution including the corresponding dilithium salt of tetrasilylcyclobutadiene dianion (**9**) (Scheme 1-6). The structure of dianions **8** and **9** were deduced on the basis of NMR spectroscopic data.

Scheme 1-6

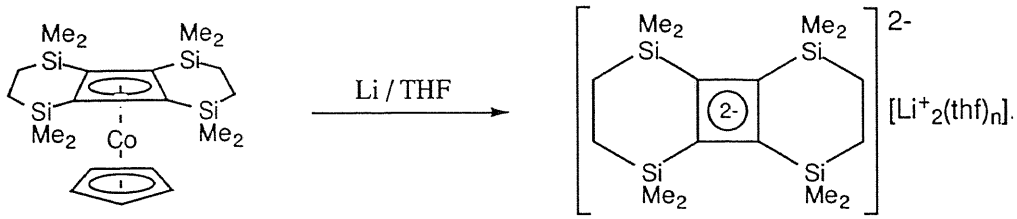
Me2
Si
Me2
Si
Si
Me2
Co
Si
Me2
Li / THF
Me2
Si
Me2
Si
2-
Si
Me2
Si
Me2
[Li+2(thf)n].

7 9

PM3 Calculation of Tetrakis(trimethylsilyl)cyclobutadiene 10

The geometry optimization of tetrakis(trimethylsilyl)cyclobutadiene **10** and its dianion $\mathbf{10}^{2-}$ were carried out by PM3 calculation.[14] The calculated structure of **10** is shown in Figure 1-4. The LUMO of **10** is depicted in Figure 1-5. The selected bond angles and lengths of **10** calculated by PM3 are also shown in Figures 1-6 and 1-7. The charge distribution of **10** is also shown in Figure 1-8.

The four-membered ring of cyclobutadiene **10** is not completely planar but slightly distorted due to the steric hindrance of four trimethylsilyl groups. The dihedral angle of C1-C2-C3-C4 is 4.6°. The C-C single and double bond lengths are 1.548 and 1.354 Å, respectively. This suggests that **10** is not a conjugated diene and there are no resonance energy in the π-system. In other words, the optimal structure of **10** has two isolated double bonds to avoid its antiaromaticity resulting from the delocalization of 4π-electrons.

The energy diagram of **10** calculated by PM3 is shown in Figure 1-9. Originally, non-substituted cyclobutadiene (C_4H_4) is a square structure by simple Hückel method, and has the degenerate two orbitals of HOMO. However, trimethylsilyl-substituted **10** is an almost rectangular structure by PM3 calculation as shown in Figure 1-4. Thus, the level of LUMO (0.20 eV) is quite different from that of HOMO (-7.57 eV). The schematic drawing of the LUMO of **10** is shown in Figure 1-10. In the LUMO, C1-C2 and C3-C4 bonds are antibonding, whereas C2-C3 and C1-C4 bonds are bonding. The π-MO coefficients at four carbon atoms (C1, C2, C3, and C4) are almost same size as shown in Figure 1-10. Thus, two electron reduction of **10** may produce dianion dimetal complex so that the counter cations may equally interact with the four carbon atoms. The resulting dianion may be stabilized by four silicon atoms (Si1, Si2, Si3, and Si4).

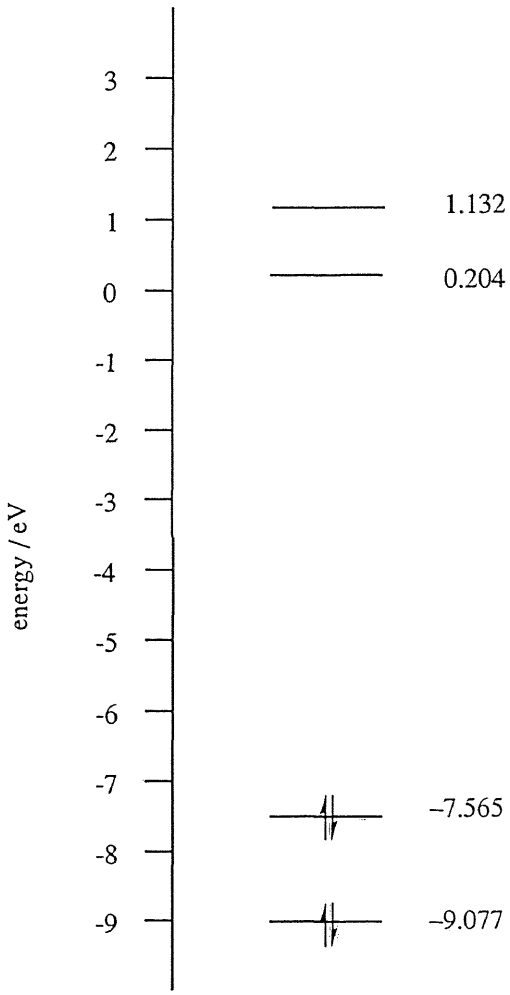

Figure 1-9. Energy diagram of **10** calculated by PM3.

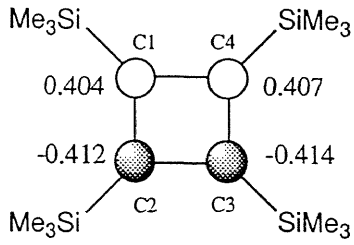

Figure 1-10. Schematic representation of the LUMO of **10** calculated by PM3.

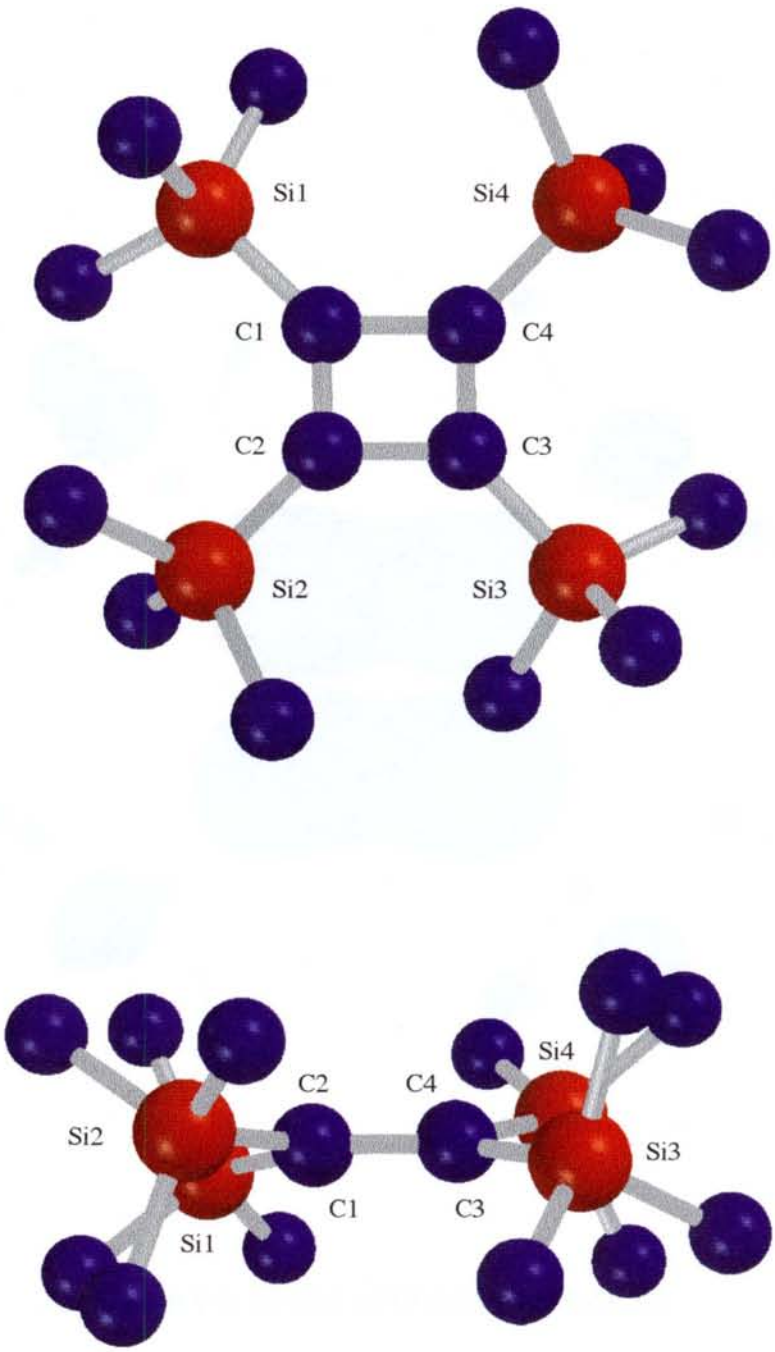

Figure 1-4. Calculated structure of **10** by PM3 (hydrogen atoms are omitted for the clarity): upper, top view; below, side view.

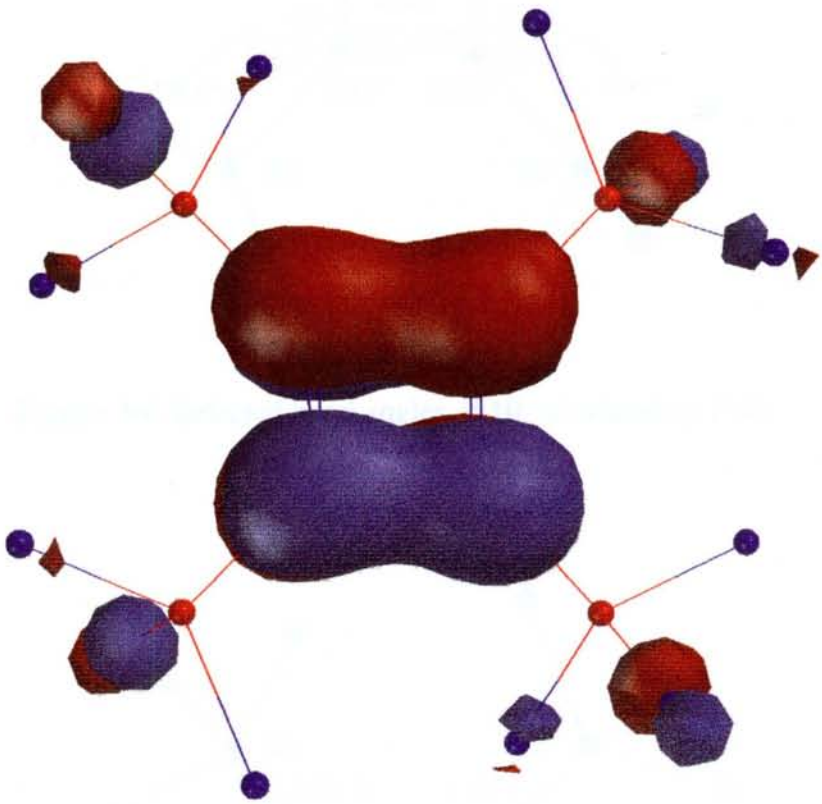

Figure 1-5. LUMO of **10** calculated by PM3.

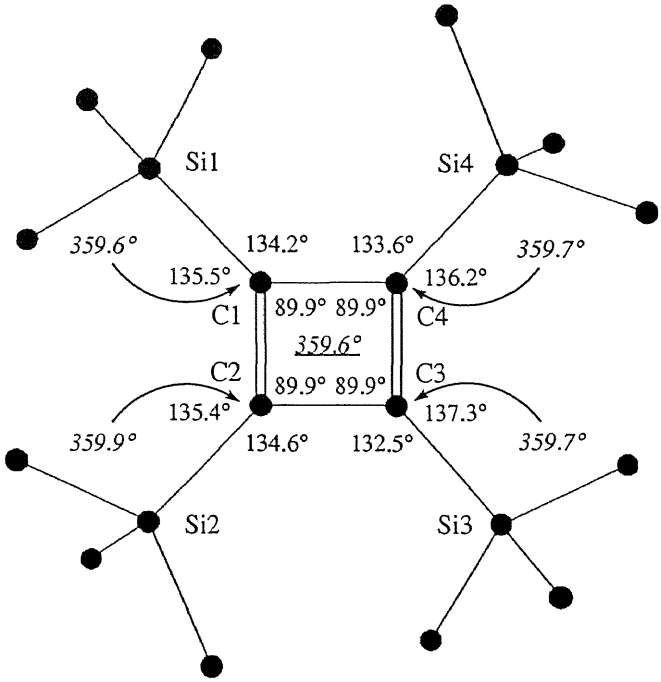

Figure 1-6. Selected bond angles of **10** calculated by PM3.

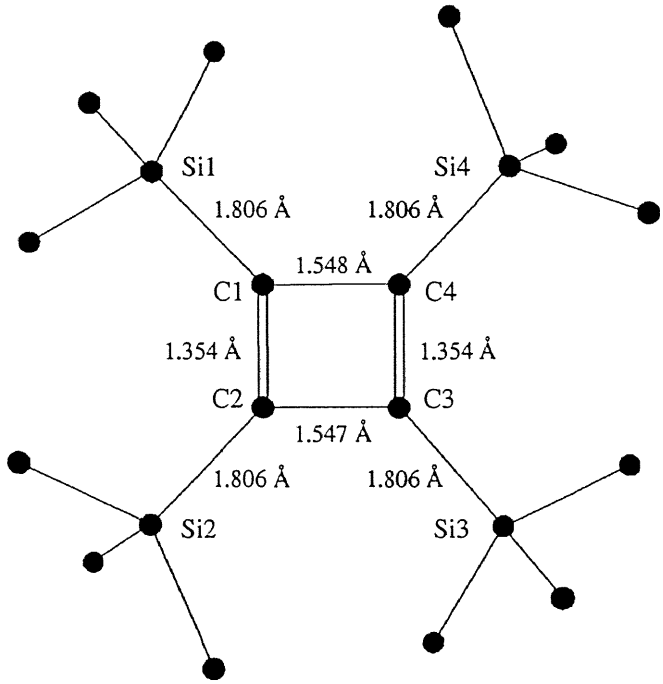

Figure 1-7. Selected bond lengths of **10** calculated by PM3.

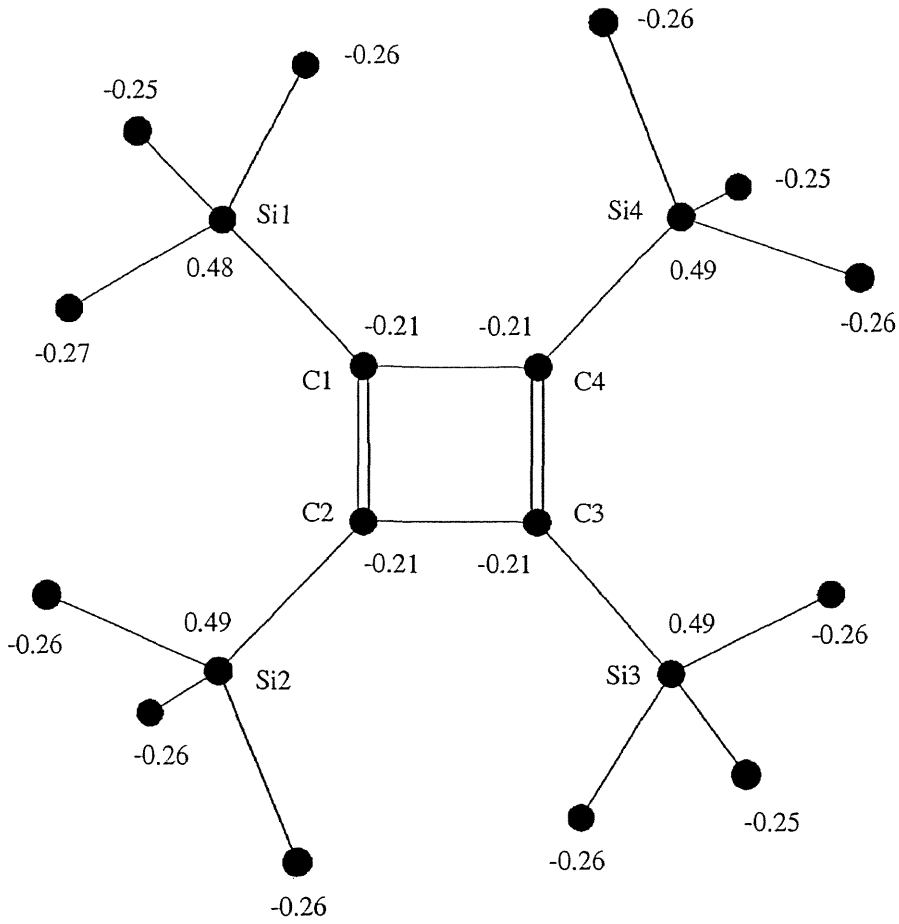

Figure 1-8. Mulliken charge distribution of **10** calculated by PM3.

PM3 Calculation of Tetrakis(trimethylsilyl)cyclobutadiene Dianion 10^{2-}

The geometry optimization of tetrakis(trimethylsilyl)cyclobutadiene dianion (counter ion free) $\mathbf{10}^{2-}$ was also carried out by PM3 calculation.[12] The calculated structure of $\mathbf{10}^{2-}$ is shown in Figure 1-11. The selected bond angles and lengths of $\mathbf{10}^{2-}$ are also shown in Figures 1-12 and 1-13. The charge distribution of $\mathbf{10}^{2-}$ is depicted in Figure 1-14.

The four-membered ring of dianion $\mathbf{10}^{2-}$ becomes more planar structure by two electron reduction due to the delocalization of negative charge. The dihedral angle of C1-C2-C3-C4 is 2.2°. The four C-C bond lengths (C1-C2, C2-C3, C3-C4, and C1-C4) are nearly equal (1.446 to 1.448 Å (av 1.447 Å)). Thus, the resulted four-membered ring is almost square. This indicates that $\mathbf{10}^{2-}$ calculated by PM3 is an aromatic molecule with a 6π-electron system.

Comparison of the calculated parameters of **10** and $\mathbf{10}^{2-}$ is very interesting. The change of bond lengths by two electron reduction are reflected by the LUMO of **10** (Figure 1-10). The distances of C1-C2 and C3-C4 bonds of $\mathbf{10}^{2-}$ are elongated by 0.094 Å relative to those of **10**. By contrast, the distances of C1-C4 and C2-C3 bonds of $\mathbf{10}^{2-}$ are shortened by 0.102 Å. Thus, C1-C4 and C2-C3 bonds are bonding, whereas C1-C2 and C3-C4 bonds are antibonding. The Si-C(sp^2) single bond lengths of $\mathbf{10}^{2-}$ calculated by PM3 are 1.737 Å, which are shorter than those of **10** (1.806 Å) due to the pπ-σ* conjugation.

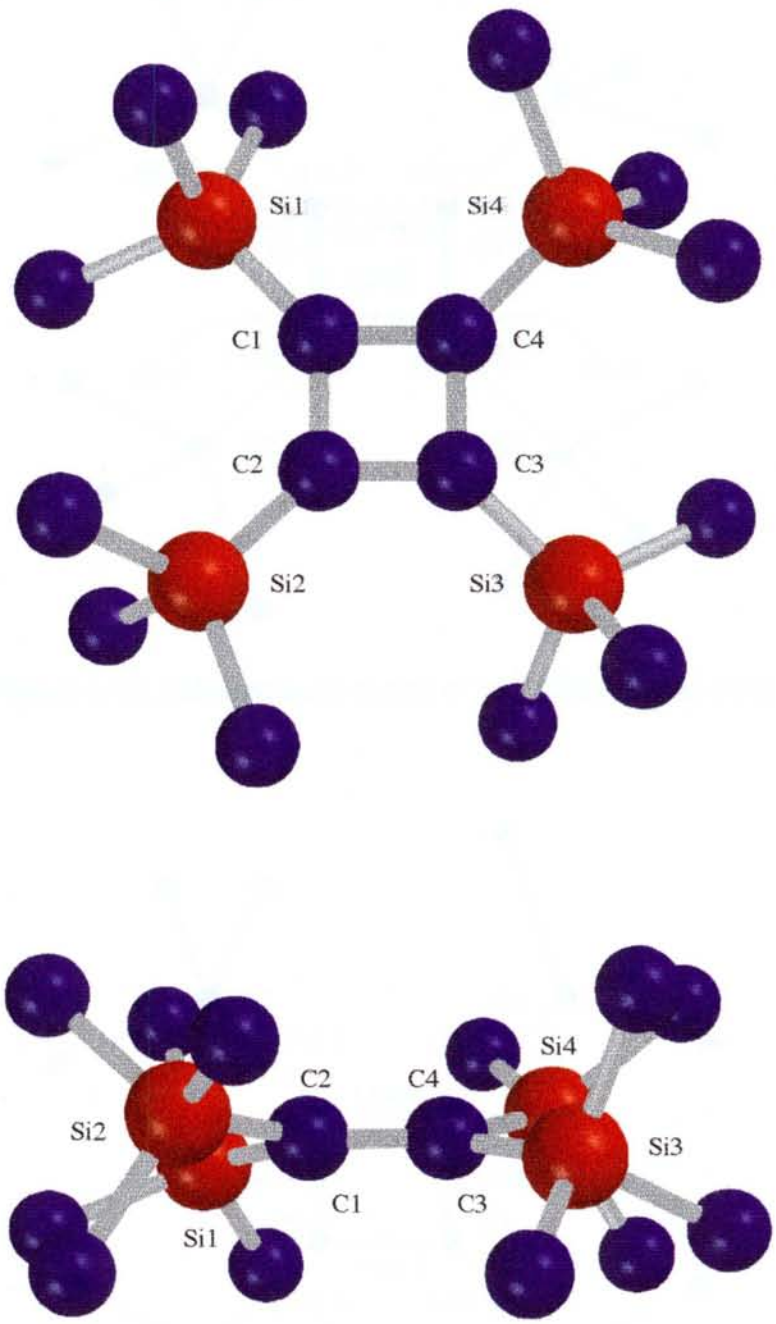

Figure 1-11. Calculated structure of $\mathbf{10}^{2-}$ by PM3 (hydrogen atoms are omitted for the clarity): upper, top view; below, side view.

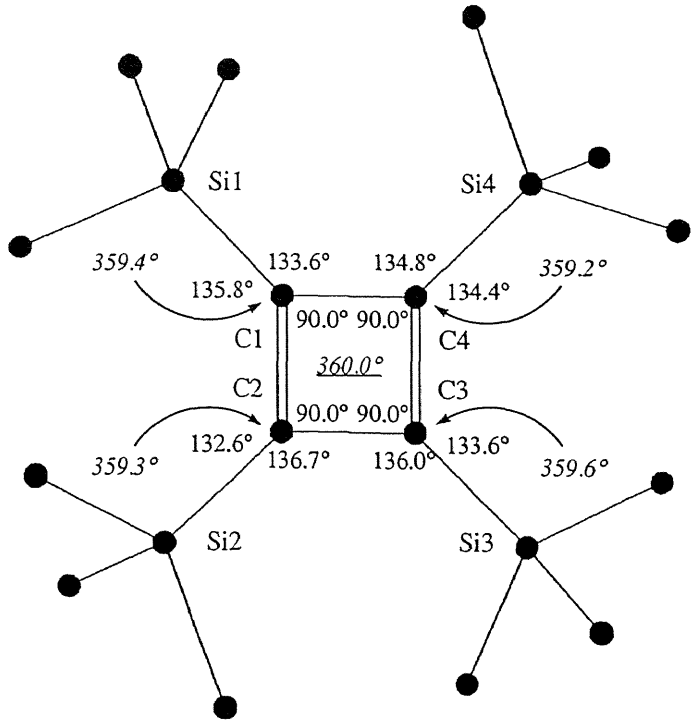

Figure 1-12. Selected bond angles of 10^{2-} calculated by PM3.

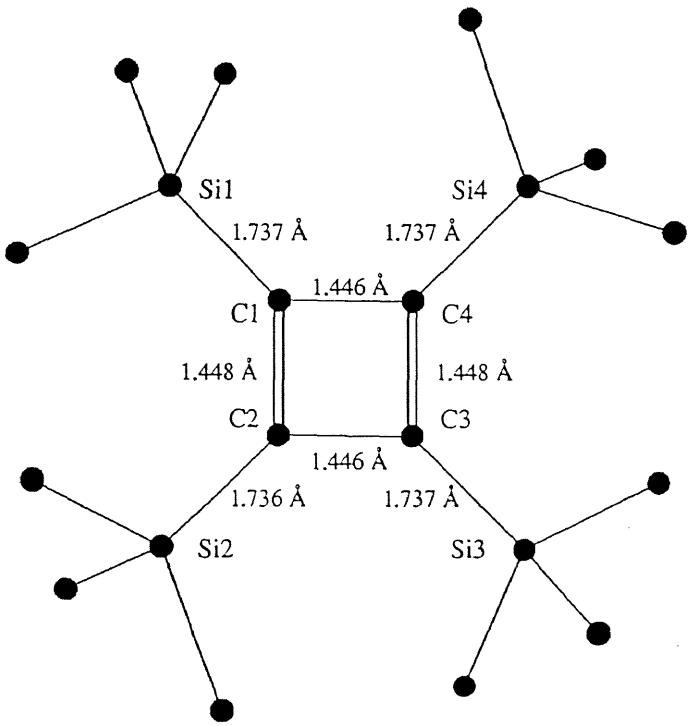

Figure 1-13. Selected bond lengths of 10^{2-} calculated by PM3.

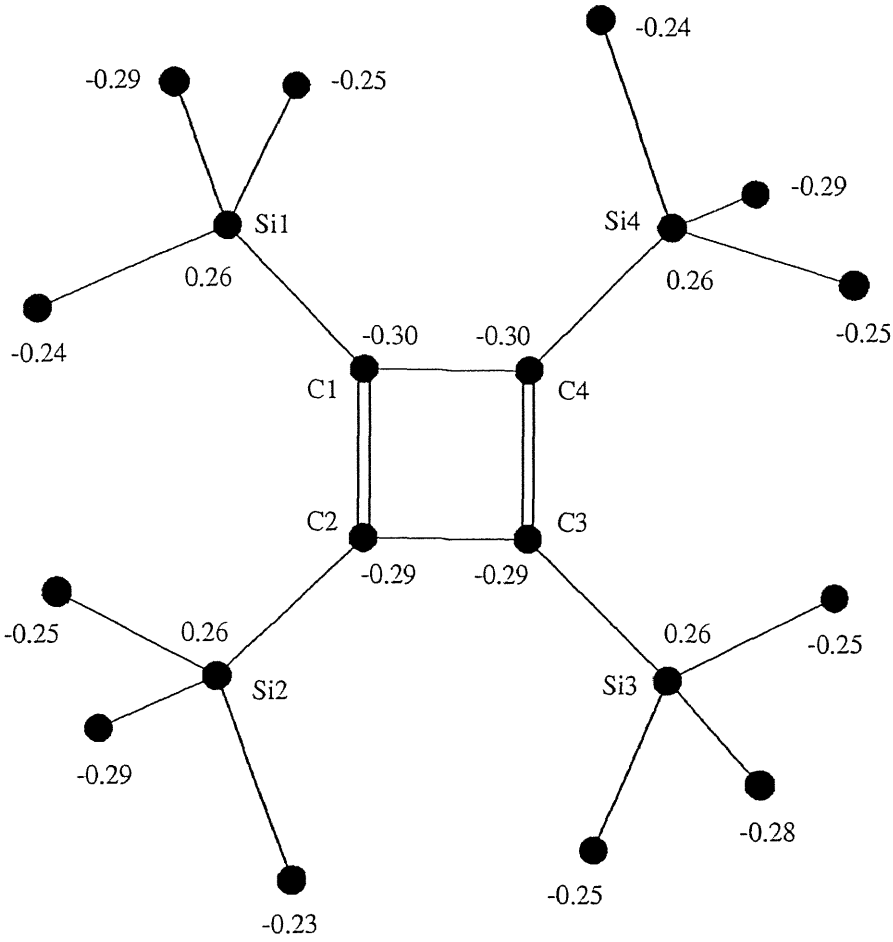

Figure 1-14. Mulliken charge distribution of $\mathbf{10}^{2-}$ calculated by PM3.

Structure of Dilithium Tetrasilylcyclobutadiene Dianion in Benzene-d_6

The structure of dilithium tetrakis(trimethylsilyl)cyclobutadiene dianion **8** in benzene-d_6 was deduced by ^1H, ^{13}C, ^{29}Si, and ^7Li NMR spectroscopies. These NMR data on the structure of **8** indicate a highly symmetric bis-CIP formation in solution.

In the ^1H NMR spectrum of **8**, only one signal is observed at 0.51 ppm for the methyl protons together with the signals due to THF. As well, only one ^{13}C NMR signal is observed at 5.4 ppm for the methyl carbon atoms. ^{13}C NMR signal of quaternary carbon atoms is observed at 104.0 ppm, which is similar to that of dipotassium 1,2,3,4-tetraphenylcyclobutadiene dianion **5** (108.8 ppm). It is thought that the negative charge is largely delocalized on the four quaternary carbon atoms of the π-skeleton of **8**. The ^{29}Si NMR signal is observed at -23.7 ppm relative to upper field than the precursor cobalt complex **6** (-7.8 ppm, $\Delta\delta = 15.9$). The negative charge on the quaternary carbon atoms is considerably stabilized by the four silyl groups in **8** (pπ-σ* conjugation).

Interestingly, the ^7Li NMR spectrum of **8** yielded only one signal appearing at –5.29 ppm as shown in Figure 1-15. The appreciable upfield shift at -5.29 ppm is evidently caused by the strong shielding effect by the diamagnetic ring current resulting from the 6π-electron system. These NMR data suggest that the cyclobutadiene dianion **8** is aromatic compound with 4C / 6π-electron system.

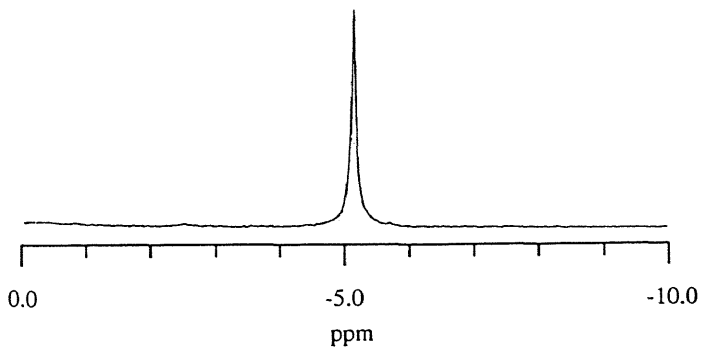

Figure 1-15. ^7Li NMR spectrum of **8** in C_6D_6 at 298 K.

The structure of dilithium tetrasilylcyclobutadiene dianion **9** bridged by disilethylene chains in benzene-d_6 was also deduced on the basis of the NMR spectroscopic data. In the ^1H NMR spectrum of **9**, only one signal is observed at 0.35 and 1.19 ppm for the methyl and methylene protons, respectively, together with the signals due to THF. As well, only one ^{13}C NMR signal is observed at 2.5 and 12.4 ppm for the methyl and methylene carbon atoms, respectively. ^{13}C NMR signal of quaternary carbon atoms is found at 101.9 ppm, which is similar to that of **8** (104.0 ppm). Only one ^{29}Si signal is observed at -24.2 ppm. The ^7Li NMR spectrum of **9** shows only one signal at -5.37 ppm.

It was expected that the four-membered ring of **9** has more planar structure relative to that of **8** due to the bridge-building of $Me_2Si(CH_2)_2SiMe_2$. However, the significant difference of ^7Li chemical shift between **8** (-5.29 ppm) and **9** (-5.37 ppm) could not be found at all. This indicates that the shielding effect by the aromatic ring current of the two cyclobutadiene dianions (**8** and **9**) is almost the same state. That is, the aromaticity of **8** and **9** resulting from 4C / 6π-electron system are nearly equal and must be a characteristic of cyclobutadiene dianion.

In the case of lithium cyclopentadienide ($Li^+ \cdot C_5H_5^-$), the strongly high field shift of the ^7Li signal is observed at -8.37 ppm in THF.[9a] This points to a structure in which the Li^+ cation resides above the plane of the cyclopentadienide ring, that is in the shielding region of the aromatic ring current. The ^6Li NMR chemical shift of lithium pentakis(dimethylsilyl)cyclopentadienide [$(Ph_2C{=}O)Li \cdot \{C_5(SiMe_2H)_5\}$] is also observed in upper field (-7.51 ppm).[15] The ^7Li NMR chemical shifts of cyclobutadiene dianions (**8** and **9**) are somewhat lower field than those of cyclopentadienide. This indicates that the degree of the aromaticity of cyclobutadiene dianion with 4C / 6π-electron system may be slightly weaker than that of cyclopentadienide ion with 5C / 6π-electron system.

The NMR data show that the structure of the dilithium tetrasilyl-substituted cyclobutadiene dianions (**8** and **9**) is a stable, closed-shell dianion, which is stabilized not only by the four silyl groups but also by the aromatic 6π-electron system. The predicted structure of **8** is shown in Figure 1-16. The dilithium salt **8** has a monomeric structure and forms contact ion pair (bis-CIP). Two lithium atoms are located almost completely above and below the center of the four-membered ring (η^4-coordination). One THF molecule is coordinated to each lithium atom. Two lithium atoms are located at the shielding region of the diamagnetic ring current resulting from 4C / 6π-electron system.

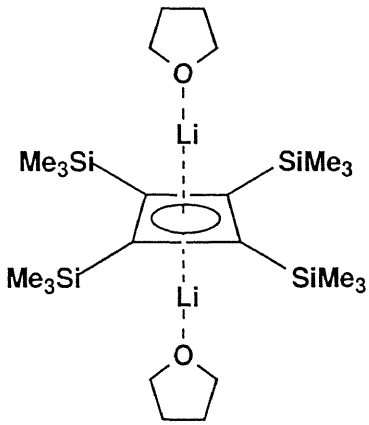

Figure 1-16. Possible structure of **8**.

Experimental Section

General Methods

^{1}H NMR spectra were recorded on a Bruker AC-300 FT spectrometer. ^{13}C, ^{29}Si, and ^{7}Li NMR spectra were collected on a Bruker AC-300 at 75.5, 59.6, and 116.6 MHz, respectively. ^{7}Li NMR spectra are referenced to 1 M LiCl (1 M = 1 mol dm^{-3}) in methanol / benzene-d_6. Mass spectra were obtained on a Shimadzu QP-5000. Electronic spectra were recorded on a Shimadzu UV-2100 spectrometer. The sampling of **8** was carried out by using a MBRAUN MB-150 B-G gas-replacement type glove box.

Materials

Tetrahydrofuran and hexane were dried and distilled from sodium benzophenone ketyl. These solvents were further dried and degassed over a potassium mirror in vacuo prior to use. Benzene-d_6 was dried over molecular sieves, and then transferred into a tube covered with potassium mirror prior to use. Octane was dried and distilled from calcium hydride.

Preparation of Tetrakis(trimethylsilyl)cyclobutadienyl Cyclopentadienyl Cobalt (6)

A mixture of the bis(trimethylsilyl)acetylene (40 ml) and [$CpCo(CO)_2$] (2.80 g, 15.6 mmol) was added dropwise slowly to refluxing bis(trimethylsilyl)acetylene (50 ml). After then, the reaction mixture was heated under the refluxing temperature of bis-(trimethylsilyl)acetylene over a period of 5 days. Excess bis(trimethylsilyl)acetylene was removed by vacuum transfer and the products were chromatographed on silica gel to produce yellow crystals of tetrakis(trimethylsilyl)cyclobutadienyl cyclopentadienyl cobalt (**6**) in 55% yield with a small amount of orange crystals of tetrakis(trimethylsilyl)-

butatriene. This compound had already been isolated by Sakurai et al. for the first time[11a] and this procedure follows the secondly reported Vollhardt's method.[11b] mp 213-214 °C; ^{1}H NMR ($CDCl_3$) δ = 0.17 (s, 36 H, CH_3), 4.91 (s, 5 H, CH); ^{13}C NMR ($CDCl_3$) δ = 2.4 (CH_2), 79.5 (CH), 82.0 (C); ^{29}Si NMR ($CDCl_3$) δ = -7.8; UV (hexane) λ_{max}/nm (ε) 217 (30600), 237 (sh. 15700), 290 (9700), 404 (300).

Preparation of Tetrasilylcyclobutadienyl Cyclopentadienyl Cobalt Bridged by Disilethylene Chains (7)

A mixture of the 3,3,6,6,9,9,12,12-octamethyl-3,6,9,12-tetrasilacyclododeca-1,7-diyne (501 mg, 1.49 mmol) and [$CpCo(CO)_2$] (320 mg, 1.78 mmol) in octane (10 ml) was heated under the refluxing temperature of octane over a period of 5 days. The reaction mixture was chromatographed on silica gel to produce yellow crystals of tetrasilylcyclobutadienyl cyclopentadienyl cobalt bridged by disilethylene chains (7) in 16% yield. mp 252-254 °C; ^{1}H NMR ($CDCl_3$) δ = 0.02 (s, 12 H, CH_3), 0.13 (s, 12 H, CH_3), 0.59–0.69 (m, 4 H, CH_2), 0.73–0.83 (m, 4 H, CH_2), 4.92 (s, 5 H, CH); ^{13}C NMR ($CDCl_3$) δ = -1.0 (CH_3), -0.3 (CH_3), 8.6 (CH_2), 79.1 (CH), 80.6 (C); ^{29}Si NMR ($CDCl_3$) δ = -9.0; UV (hexane) λ_{max}/nm (ε) 218 (30500), 236 (sh. 15700), 262 (5500), 292 (8900), 410 (400). Found: C, 54.44; H 8.14%. Calcd for $C_{21}H_{37}CoSi_4$: C, 54.74; H 8.09%.

Preparation of Dilithium Tetrakis(trimethylsilyl)cyclobutadiene Dianion (8).

The crystals of 7 (49 mg, 0.105 mmol) and lithium metal (30 mg, 4.3 mmol) were placed in a reaction tube with a magnetic stirrer. After degassing, dry oxygen-free THF (1.0 mL) was introduced by vacuum transfer and the mixture was stirred at room temperature to give a dark brown solution containing the tetrakis(trimethylsilyl)-

cyclobutadiene dianion **8**. This transmetalation completed for about 20 hours. After the solvent was removed in vacuo, degassed hexane was introduced by vacuum transfer. A hexane soluble brown solution and hexane insoluble dark materials were separated in a glove box. The hexane solution was cooled to afford pale yellow crystals of **8**. ^{1}H NMR (C_6D_6) δ = 0.51 (s, 36 H, CH_3), 1.14 (s, 8 H, THF), 3.39 (s, 8 H, THF); ^{13}C NMR (C_6D_6) δ = 5.4 (CH_3), 25.3 (THF), 69.5 (THF), 104.0 (C); ^{29}Si NMR (C_6D_6) δ = –23.7; ^{7}Li NMR (C_6D_6) δ = -5.29.

NMR Spectral Data of 8 in THF-d_8 at 298 K.

^{1}H NMR (THF-d_8) δ = 0.09 (s, 36 H, CH_3); ^{13}C NMR (THF-d_8) δ = 5.1 (CH_3), 104.0 (C); ^{29}Si NMR (THF-d_8) δ = –24.3; ^{7}Li NMR (THF-d_8) δ = -4.92.

Preparation of Dilithium Tetrasilylcyclobutadiene Dianion Bridged by Disilethylene Chains (9).

The crystals of **7** (49 mg, 0.106 mmol) and lithium metal (30 mg, 4.3 mmol) were placed in a reaction tube with a magnetic stirrer. After degassing, dry oxygen-free THF (1.0 mL) was introduced by vacuum transfer and the mixture was stirred at room temperature to give a dark brown solution containing the tetrasilylcyclobutadiene dianion **9**. This transmetalation completed for about 20 hours. After the solvent was removed in vacuo, degassed benzene-d_6 was introduced by vacuum transfer. ^{1}H NMR (C_6D_6) δ = 0.35 (s, 24 H, CH_3), 1.19 (s, 8 H, CH_2), 1.34 (br.s, THF), 3.49 (br.s, THF); ^{13}C NMR (C_6D_6) δ = 2.5 (CH_3), 12.4 (CH_2), 25.5 (THF), 68.7 (THF), 101.9 (C); ^{29}Si NMR (C_6D_6) δ = –24.2; ^{7}Li NMR (C_6D_6) δ = -5.37.

Molecular Orbital Calculations.

PM3 calculations were performed by Power Macintosh 7600/200 with MACSPARTAN plus program (Ver. 1.1.7).[14] All the calculations were performed with the geometry optimization.

References

(1) G. Maier, *Angew. Chem., Int. Ed. Engl.*, **27,** 309 (1988).

(2) (a) H. Kimling and A. Krebs, *Angew. Chem., Int. Ed. Engl.*, **11,** 932 (1972). (b) L. T. J. Delbaere, M. N. G. James, N. Nakamura, and S. Masamune, *J. Am. Chem. Soc.*, **97,** 1973 (1975). (c) H. Irngartinger, N. Riegler, K.-D. Malsch, K. -A. Schneider, and G. Maier, *Angew. Chem., Int. Ed. Engl.*, **19,** 211 (1980). (d) H. Irngartinger and M. Nixdorf, *Angew. Chem., Int. Ed. Engl.*, **22,** 403 (1983).

(3) J. S. McKennis, L. Brener, J. R. Schweiger, and R. Pettit, *J. Chem. Soc., Chem. Commun.*, **1972,** 365.

(4) P. J. Garratt and R. Zahler, *J. Am. Chem. Soc.*, **100,** 7753 (1978).

(5) G. Boche, H. Etzrodt, M. Marsch, and W. Thiel, *Angew. Chem., Int. Ed. Engl.*, **21,** 132 (1982).

(6) G. Boche, H. Etzrodt, M. Marsch, and W. Thiel, *Angew. Chem., Int. Ed. Engl.*, **21,** 133 (1982).

(7) G. Boche, H. Etzrodt, W. Massa, and G. Baum, *Angew. Chem., Int. Ed. Engl.*, **24,** 864 (1985).

(8) B. A. Hess, Jr. C. S. Ewig, and L. J. Schaad, *J. Org. Chem.*, **50,** 5869 (1985).

(9) (a) Ch. Elschenbroich and A. Salzer, "Organometallics: A Concise Introduction", VCH, Weinheim, 1992. (b) H. C. Longuett-Higgins and L. E. Orgel, *J. Chem. Soc.*, **1956,** 1969. (c) R. Criegee, *Angew. Chem.*, **71,** 70 (1959).

(10) (a) R. Pettit, *J. Am. Chem. Soc.*, **87,** 131 (1965). (b) R. Pettit, *J. Am. Chem. Soc.*, **87,** 3254 (1965). (c) R. Pettit, *J. Am. Chem. Soc.*, **88,** 1328 (1966).

(11) (a) H. Sakurai and J. Hayashi, *J. Organomet. Chem.*, **70,** 85 (1974). (b) J. R. Fritch, K. P. C.Vollhardt, M. R. Thompson, and V. W. Day, *J. Am. Chem. Soc.*, **101,** 2768 (1979).

(12) (a) G. Maier, H. W. Lange, and H. P. Reisenauer, *Angew. Chem., Int. Ed. Engl.*, **20,** 976 (1981). (b) W. Kaim and H. Bock, *J. Organomet. Chem.*, **164,** 218 (1979). (c) T. Kusumoto and T. Hiyama, *Tetrahedron Lett.*, **28,** 1807 (1987). (d) T. Kusumoto and T. Hiyama, *Tetrahedron Lett.*, **28,** 1811 (1987).

(13) R. Gleiter and M. Merger, *Angew. Chem., Int. Ed. Engl.*, **36,** 2426 (1997).

(14) J. J. P. Stewart, *J. Comput. Chem.*, **10,** 209 (1989).

(15) A. Sekiguchi, Y. Sugai, K. Ebata, C. Kabuto, and H. Sakurai, *J. Am. Chem. Soc.*, **115,** 1144 (1993).

Chapter 2

Silyl-Substituted Dimethylenecyclobutene Dianion with 6C / 8π-Electron System

Summary

The intramolecular reaction of 3,3,5,5,8,8,10,10,13,13,15,15-dodecamethyl-3,5,8,10,13,15-hexasilacyclopentadeca-1,6,11-triyne (**11**) with $[Mn(CO)_3(Me\text{-}Cp)]$ in THF under photochemical and refluxing conditions produced hexasilyldimethylenecyclobutene derivative (**12**). The reaction of **12** with lithium metal in 1,2-dimethoxyethane (DME) immediately gave the dilithium salt of dimethylenecyclobutene dianion (**13**) with 6 center / 8π-electron system. The molecular structure of dilithium salt of dianion **13** was clearly determined by X-ray diffraction. The dilithium salt **13** has a monomeric structure and forms contact ion pair (bis-CIP) in the crystals. Two lithium atoms are located above and below the π-skeleton and one DME molecule is coordinated to each lithium atom. The structural parameters of **13** are discussed in comparison to those of the neutral starting molecule **12**. The structure of **13** in solution has also been discussed on the basis of NMR spectroscopic data. The X-ray crystallography and the NMR data indicate that the structure of the dimethylenecyclobutene dianion **13** is evidently 6C / 8π allyl anion system stabilized by the silyl groups.

Introduction

Allyl anion with 3C / 4π-electron system is one of the most simple and important conjugated system. Allyl anion is an interesting anionic species with regard to its structure, bonding, and delocalization of the negative charge. Especially, allyllithium is a useful reagent for organic synthesis, however, the structural proof is still controversial.[1] Most NMR studies and X-ray crystallographic investigation favors the delocalized π-bonding.[2] In the case of 1,3-(diphenyl)allyllithium·diethyl ether complex, a columnar structure with bridging η^3-allyl units is realized (Figure 2-1).[3] More recently, the monomer structure of 1,3-bis(trimethylsilyl)allyllithium·TMEDA complex both in solution and crystals have been reported (Figure 2-2).[4]

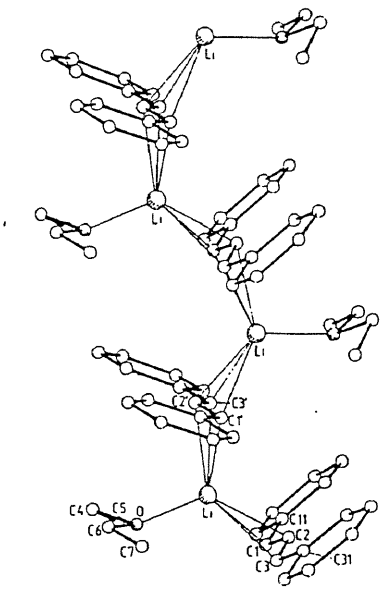

Figure 2-1. Crystal structure of 1,3-diphenylallyllithium.

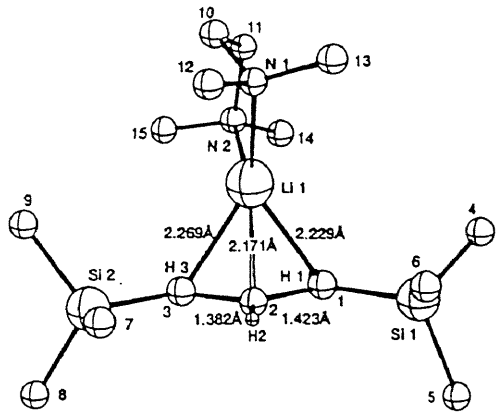

Figure 2-2. Crystal structure of 1,3-bis(trimethylsilyl)allyllithium.

The structure is represented by the π-bonding of lithium with allyl anions (Figure 2-3). This figure shows the interaction between the π-electrons of allyl anion and the vacant 2*p*-orbital of lithium cation creating some π-overlap and π-bonding.

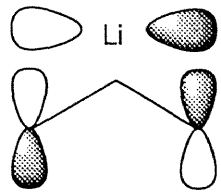

Figure 2-3. π-bonding of allyllithium.

3,4-Dimethylenecyclobutene with 6C / 6π-electron system is one of the most important cross-conjugated π-electron system based on four-membered ring. One double bond is located in the four-membered ring and two double bonds are situated in the exo position. Dimethylenecyclobutene is a benzene isomer, however, the properties of dimethylenecyclobutene is quite different from that of benzene. Non-substituted dimethylenecyclobutene is thermally labile and an intermolecular Diels-Alder reaction is readily occurred. Because dimethylenecyclobutene possesses an unique 6π-electron system, there has been no studies concerning the anion species of dimethylenecyclobutene derivatives thus far.

Silyl-substituted π-electron systems can be readily reduced by alkali metals to dianions, which were described in the general introduction. In this chapter, isolation, characterization, and molecular structure of dilithium hexasilyldimethylenecyclobutene dianion as a new silyl-substituted 6C / 8π-electron system with allyl anion character are described.

Results and Discussion

Synthesis of Hexasilyldimethylenecyclobutene 12

Hexasilyldimethylenecyclobutene derivative (**12**) bridged by $Me_2SiCH_2SiMe_2$ chains was prepared by the intramolecular cyclotrimerization of the macrocyclic silyltriyne (**11**). Preparation of the silmethylene-bridged cyclic triacetylene (**11**) is rather straightforward by the coupling reaction of the respective bis(chlorosilane) with bis(ethynyl) Grignard reagent in 36% yield (Scheme 2-1).

Scheme 2-1

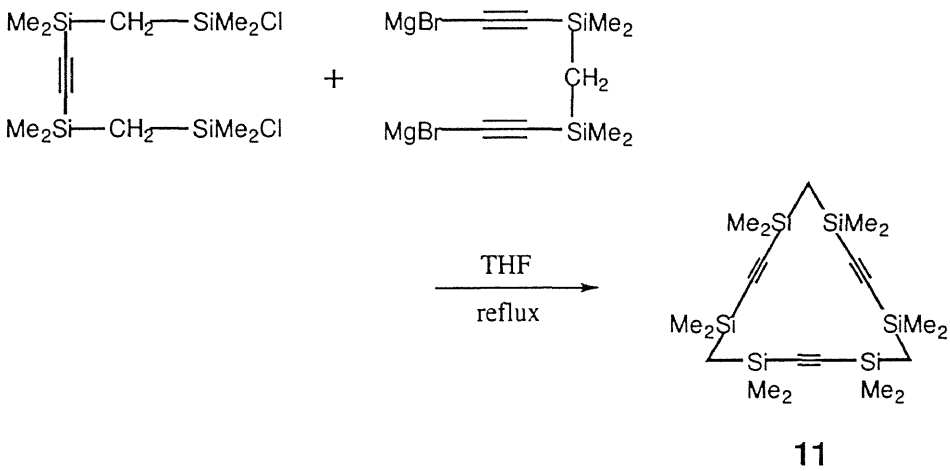

11

A mixture of the 3,3,5,5,8,8,10,10,13,13,15,15-dodecamethyl-3,5,8,10,13,15-hexasilacyclopentadeca-1,6,11-triyne (**11**) and one molar amount of $[Mn(CO_3)(Me\text{-}Cp)]$ in THF was irradiated with a 500 W high-pressure mercury lamp under the refluxing temperature of THF to produce pale yellow crystals of the persilylated dimethylene-cyclobutene derivative (**12**) in 50% yield (Scheme 2-2).

Scheme 2-2

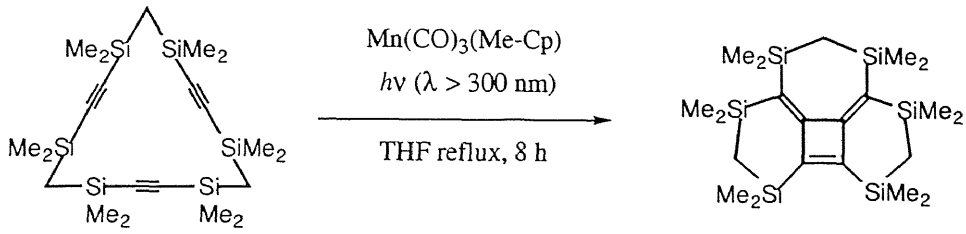

11 **12**

Oligomerization of acetylene, catalyzed by transition-metal complexes, is an interesting class of reactions to lead to benzene as a trimer and cyclooctatetraene as a tetramer.[5] In previous studies, it is demonstrated that macrocyclic polyacetylenes tethered by disiloxane bridges ($SiMe_2OSiMe_2$) undergo intramolecular cyclization to a variety of π-electron system.[6] More recently, it was shown that not only cyclic but also acyclic acetylenes substituted by two silyl groups on each end undergo facile 1,2-silyl shift in the reaction with (cyclopentadienyl)tricarbonylmanganese under photochemical conditions to give 2,2-disilylvinylidene complexes.[7] Compound **12** is the first example of the formation of dimethylenecyclobutene by trimerization of acetylenes. The reaction mechanism to form **12** is not clear at the moment, but a double 1,2-silyl shift can be involved. The possible mechanism is shown in Scheme 2-3.

Compound **12** was fully characterized by NMR spectroscopies and the molecular structure of **12** was determined by X-ray crystallography.

Scheme 2-3

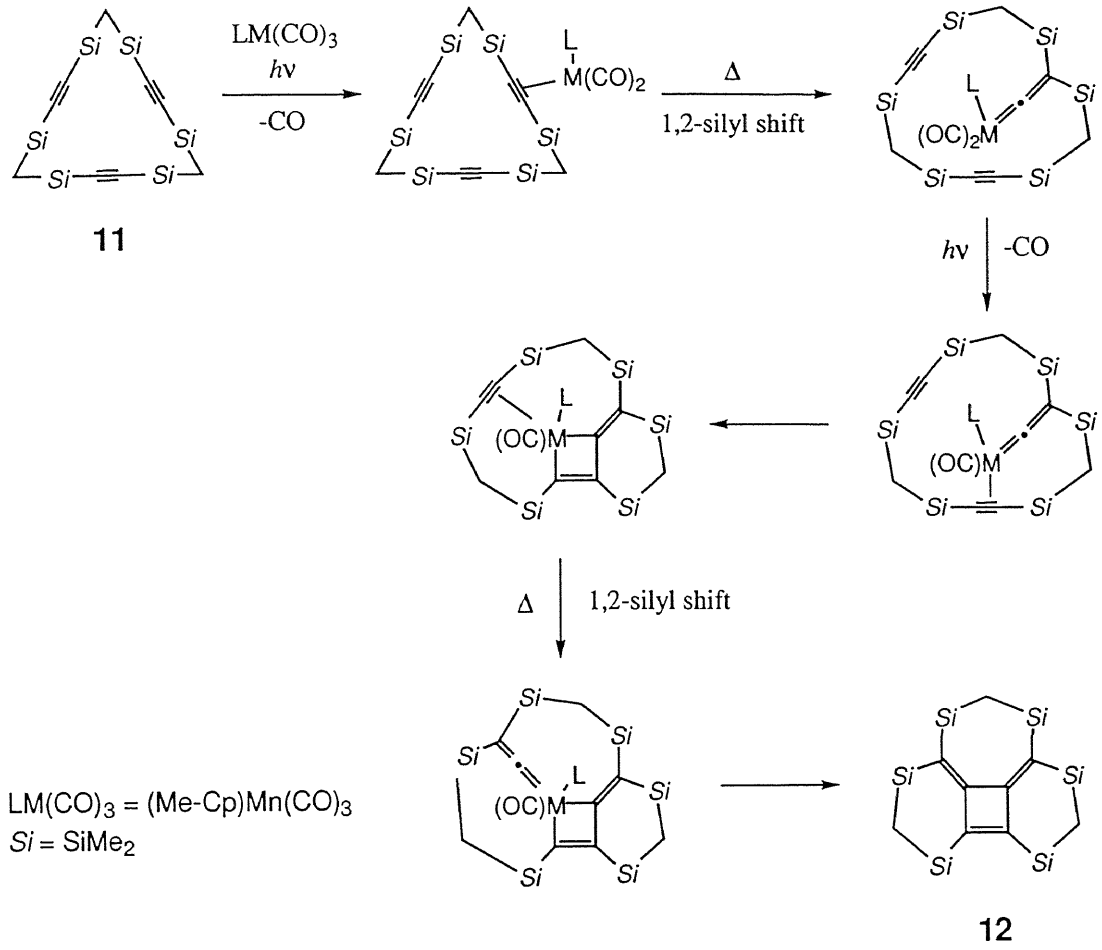
LM(CO)3
hν
-CO
Δ
1,2-silyl shift
hν
-CO
Δ
1,2-silyl shift
11
12
LM(CO)3 = (Me-Cp)Mn(CO)3
Si = SiMe2

Molecular Structure of Hexasilyldimethylenecyclobutene 12

Hexasilyldimethylenecyclobutene **12** bridged by silmethylene chains could be recrystallized from ethanol. The molecular structure of **12** was unequivocally confirmed by X-ray crystallography. Only one example of highly distorted 1,2-di-*t*-butyl-3,4-diisopropylidene-1-cyclobutene has been reported so far as the structure of 3,4-dimethylenecyclobutene.[8] Although the latter is strongly folded due to the steric compression, the π-skeleton of **12** is almost planar due to the silmethylene bridge-building. The ORTEP drawing of **12** are shown in Figure 2-4. The crystal packing of **12** is also shown in Figure 2-5. The final atomic parameters of **12** are listed in Tables 2-1 and 2-2. The bond lengths of **12** are summarized in Tables 2-3 and 2-4. The bond angles of **12** are also summarized in Table 2-5.

The selected bond angles of **12** is shown in Figure 2-6. The central four-membered ring has an almost planar structure. The internal bond angles of the central four-membered ring of **12** are 86.1(3)-94.2(4)° (av 90.0°), and the sum of the bond angles is 359.9°.

The selected bond lengths of **12** is also shown in Figure 2-7. The substantial bond alternation between the single and double bonds of the π-skeleton of **12** shows the structural feature as a typical cross-conjugated diene. C3-C4 single bond length is 1.563(7) Å, which is somewhat longer than a C-C single bond in alkanes (1.54 Å). On the other hand, C1-C4 and C2-C3 single bond lengths are 1.493(7) and 1.501(7) Å, which is shorter than a C-C single bond in alkanes. The C-C double bond lengths of **12** are 1.346(7)-1.371(7) Å (av 1.355 Å). Thus, the conjugation of π-skeleton of **12** is not extended to entire π-system, but is broken at C3-C4 bond. The six- and seven-membered rings containing the $Me_2SiCH_2SiMe_2$ fragments of **12** have almost envelope conformations.

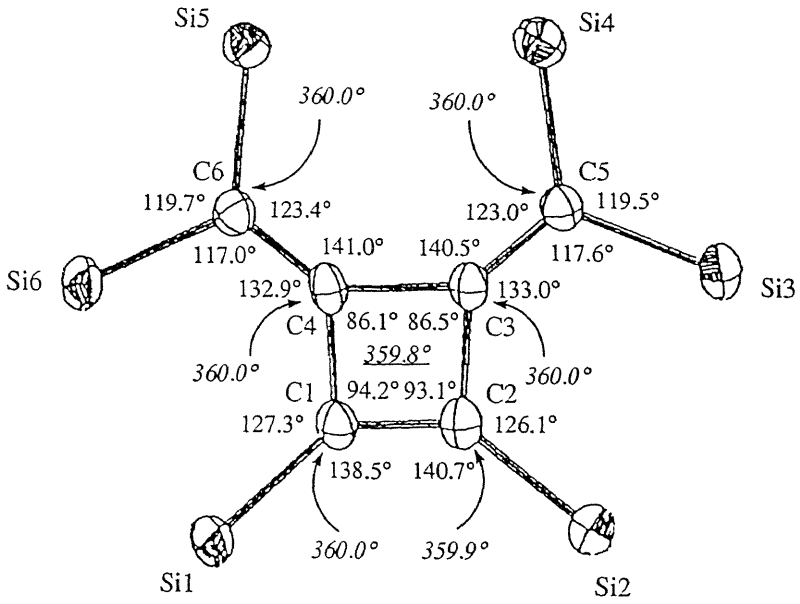

Figure 2-6. Selected bond angles of **12**.

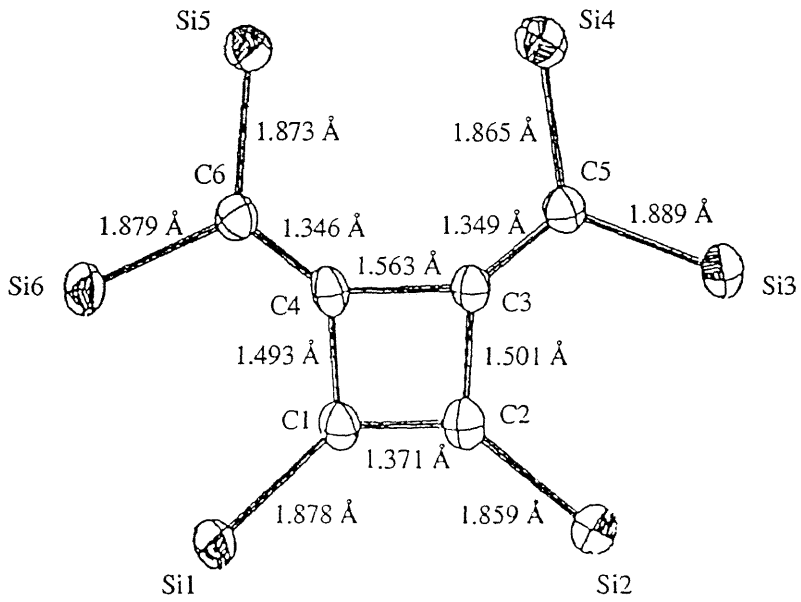

Figure 2-7. Selected bond lengths of **12**.

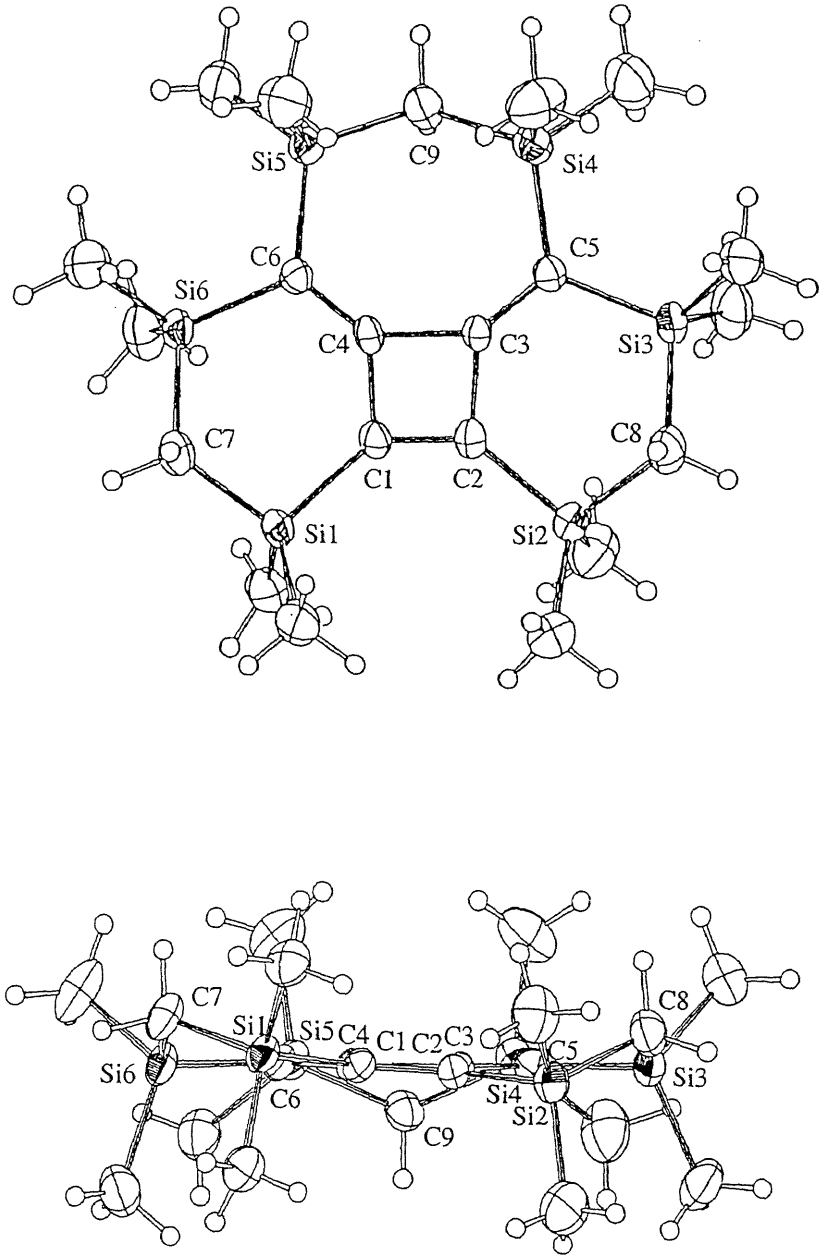

Figure 2-4. ORTEP drawing of **12**: upper, top view; below, side view.

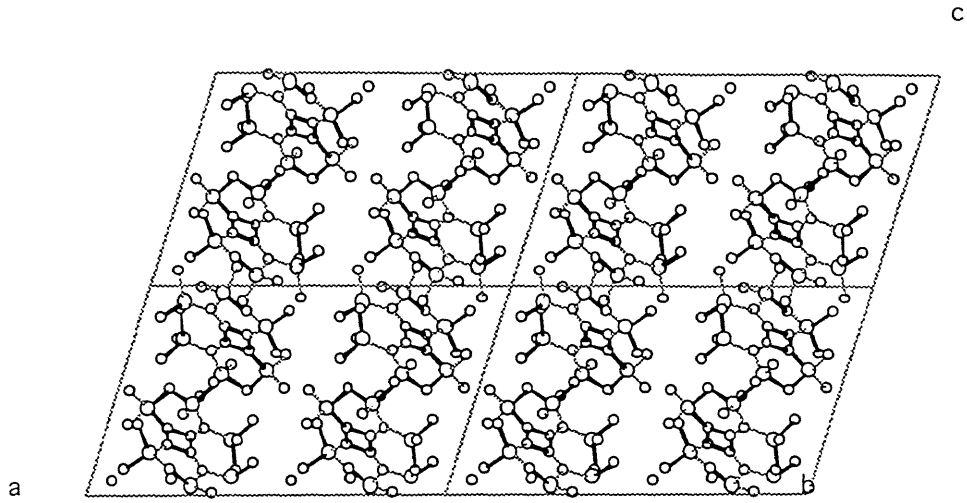

Figure 2-5. Crystal packing of **12**.

Table 2-1. Atomic Parameters[a] for Non-Hydrogen Atoms of **12**

ATOM	X	Y	Z	BEQV
SI1	3586(1)	406(1)	2071(1)	2.1
SI2	3999(1)	3523(2)	4142(1)	2.5
SI3	2796(1)	5115(1)	4321(1)	2.5
SI4	1382(1)	4388(2)	2633(1)	2.6
SI5	1075(1)	2155(1)	849(1)	2.4
SI6	2140(1)	206(1)	468(1)	2.5
C 1	3151(3)	1776(5)	2433(4)	1.9
C 2	3292(3)	2763(5)	3136(4)	2.0
C 3	2590(2)	3183(5)	2824(4)	1.7
C 4	2439(3)	2086(4)	1993(4)	1.8
C 5	2282(3)	4099(5)	3190(4)	1.9
C 6	1939(3)	1569(5)	1217(4)	2.0
C 7	2901(3)	-607(5)	1301(5)	3.0
C 8	3600(3)	4359(6)	5033(5)	3.2
C 9	1046(3)	3832(5)	1213(4)	2.8
C10	4123(3)	931(6)	1258(5)	3.0
C11	4112(3)	-430(6)	3303(5)	3.5
C12	4389(4)	4594(7)	3385(6)	4.4
C13	4625(3)	2396(7)	4934(6)	4.4
C14	2363(3)	5385(7)	5362(5)	3.8
C15	2954(4)	6656(6)	3777(6)	4.3
C16	944(3)	3634(8)	3528(6)	4.8
C17	1195(4)	6115(7)	2580(6)	5.4
C18	594(4)	1166(7)	1527(7)	4.5
C19	664(3)	2066(6)	-660(5)	3.9
C20	2271(4)	810(6)	-819(5)	4.2
C21	1469(4)	-984(6)	113(7)	5.0

[a] Positional parameters are multiplied by 10^4. Thermal parameters are given by the equivalent temperature factors (A^2).

Table 2-2. Atomic Parameters[a] for Hydrogen Atoms of **12**

ATOM	X	Y	Z	B
H(C 7)1	301(3)	-123(6)	79(5)	3.8(1.4)
H(C 7)2	279(3)	-117(6)	179(5)	3.9(1.4)
H(C 8)1	391(3)	499(6)	547(5)	3.3(1.3)
H(C 8)2	350(3)	371(6)	555(5)	4.5(1.5)
H(C 9)1	126(3)	431(5)	75(4)	2.3(1.2)
H(C 9)2	56(3)	405(6)	93(5)	3.9(1.4)
H(C10)1	389(3)	123(6)	49(5)	3.7(1.4)
H(C10)2	441(3)	156(6)	161(5)	5.2(1.6)
H(C10)3	444(3)	30(6)	122(5)	3.3(1.3)
H(C11)1	432(3)	-114(6)	311(5)	4.4(1.5)
H(C11)2	450(3)	14(6)	373(5)	5.4(1.6)
H(C11)3	379(4)	-67(7)	374(6)	7.5(1.9)
H(C12)1	402(3)	511(6)	286(5)	4.7(1.5)
H(C12)2	473(3)	501(7)	390(5)	5.9(1.7)
H(C12)3	462(3)	412(7)	299(5)	5.7(1.7)
H(C13)1	499(3)	277(6)	556(5)	5.1(1.6)
H(C13)2	442(3)	179(7)	523(6)	6.6(1.8)
H(C13)3	489(3)	199(6)	455(5)	5.4(1.7)
H(C14)1	264(3)	593(6)	599(5)	4.8(1.5)
H(C14)2	195(3)	582(6)	503(5)	3.6(1.4)
H(C14)3	224(3)	463(7)	565(6)	6.2(1.8)
H(C15)1	319(3)	722(7)	430(5)	5.5(1.7)
H(C15)2	324(3)	658(7)	332(5)	6.0(1.7)
H(C15)3	250(3)	704(7)	339(6)	6.0(1.7)
H(C16)1	111(3)	383(6)	429(5)	5.5(1.7)
H(C16)2	43(3)	387(7)	321(6)	6.1(1.7)
H(C16)3	104(4)	276(7)	352(6)	7.1(1.9)
H(C17)1	74(3)	630(7)	222(5)	5.6(1.7)
H(C17)2	135(3)	654(6)	333(5)	4.2(1.4)
H(C17)3	149(4)	657(7)	218(6)	7.2(1.9)
H(C18)1	83(3)	113(6)	235(5)	3.5(1.4)
H(C18)2	15(3)	157(6)	137(5)	5.0(1.6)
H(C18)3	52(3)	39(7)	120(6)	5.9(1.7)
H(C19)1	87(3)	251(6)	-105(5)	4.0(1.4)
H(C19)2	58(3)	130(7)	-94(6)	6.4(1.8)
H(C19)3	21(3)	239(6)	-81(5)	5.0(1.6)
H(C20)1	256(3)	20(6)	-103(5)	5.4(1.6)
H(C20)2	185(4)	102(7)	-134(6)	7.1(1.9)
H(C20)3	257(3)	160(7)	-68(6)	6.4(1.8)
H(C21)1	159(3)	-170(7)	-32(5)	5.7(1.7)
H(C21)2	147(3)	-130(6)	86(5)	4.8(1.6)
H(C21)3	102(3)	-63(6)	-42(5)	4.4(1.5)

[a] Positional parameters are multiplied by 10^4. Thermal parameters are given by the equivalent temperature factors (A^2).

Table 2-3. List of Bond Lengths (Å) for Non-Hydrogen Atoms of **12**

ATOM	-	ATOM		LENGTH(SIG)
SI1	-	C 1	=	1.878(6)
SI1	-	C 7	=	1.856(7)
SI1	-	C10	=	1.867(7)
SI1	-	C11	=	1.878(7)
SI2	-	C 2	=	1.859(6)
SI2	-	C 8	=	1.862(7)
SI2	-	C12	=	1.867(7)
SI2	-	C13	=	1.866(7)
SI3	-	C 5	=	1.889(6)
SI3	-	C 8	=	1.872(7)
SI3	-	C14	=	1.877(7)
SI3	-	C15	=	1.872(9)
SI4	-	C 5	=	1.865(6)
SI4	-	C 9	=	1.858(7)
SI4	-	C16	=	1.881(9)
SI4	-	C17	=	1.898(9)
SI5	-	C 6	=	1.873(6)
SI5	-	C 9	=	1.872(7)
SI5	-	C18	=	1.874(9)
SI5	-	C19	=	1.886(7)
SI6	-	C 6	=	1.879(6)
SI6	-	C 7	=	1.874(7)
SI6	-	C20	=	1.888(7)
SI6	-	C21	=	1.873(9)
C 1	-	C 2	=	1.371(7)
C 1	-	C 4	=	1.493(7)
C 2	-	C 3	=	1.501(7)
C 3	-	C 4	=	1.563(7)
C 3	-	C 5	=	1.349(7)
C 4	-	C 6	=	1.346(7)

Table 2-4. List of Bond Lengths (Å) for Hydrogen Atoms of **12**

ATOM	-	ATOM		LENGTH(SIG)
C 7	-	H(C 7)1	=	1.01(6)
C 7	-	H(C 7)2	=	0.96(6)
C 8	-	H(C 8)1	=	1.00(6)
C 8	-	H(C 8)2	=	1.04(6)
C 9	-	H(C 9)1	=	1.00(5)
C 9	-	H(C 9)2	=	1.01(6)
C10	-	H(C10)1	=	1.02(6)
C10	-	H(C10)2	=	0.93(7)
C10	-	H(C10)3	=	0.97(6)
C11	-	H(C11)1	=	0.95(6)
C11	-	H(C11)2	=	1.04(6)
C11	-	H(C11)3	=	1.05(7)
C12	-	H(C12)1	=	1.03(6)
C12	-	H(C12)2	=	0.94(7)
C12	-	H(C12)3	=	0.96(7)
C13	-	H(C13)1	=	1.02(6)
C13	-	H(C13)2	=	0.93(7)
C13	-	H(C13)3	=	0.97(7)
C14	-	H(C14)1	=	1.03(6)
C14	-	H(C14)2	=	0.97(6)
C14	-	H(C14)3	=	0.96(7)
C15	-	H(C15)1	=	0.93(7)
C15	-	H(C15)2	=	0.97(7)
C15	-	H(C15)3	=	1.03(7)
C16	-	H(C16)1	=	0.96(7)
C16	-	H(C16)2	=	1.08(7)
C16	-	H(C16)3	=	0.97(7)
C17	-	H(C17)1	=	0.97(7)
C17	-	H(C17)2	=	1.03(6)
C17	-	H(C17)3	=	1.05(7)
C18	-	H(C18)1	=	1.03(6)
C18	-	H(C18)2	=	1.01(6)
C18	-	H(C18)3	=	0.93(7)
C19	-	H(C19)1	=	0.90(6)
C19	-	H(C19)2	=	0.90(7)
C19	-	H(C19)3	=	0.98(6)
C20	-	H(C20)1	=	1.00(7)
C20	-	H(C20)2	=	0.98(7)
C20	-	H(C20)3	=	1.05(7)
C21	-	H(C21)1	=	1.02(7)
C21	-	H(C21)2	=	1.02(6)
C21	-	H(C21)3	=	1.06(6)

Table 2-5. List of Bond Angles (Å) for Non-Hydrogen Atoms of **12**

ATOM -	ATOM	ATOM	ANGLE(SIG)
C 1 -	SI1 -	C 7 =	103.0(2)
C 1 -	SI1 -	C10 =	109.9(2)
C 1 -	SI1 -	C11 =	112.2(2)
C 7 -	SI1 -	C10 =	113.4(2)
C 7 -	SI1 -	C11 =	110.3(2)
C10 -	SI1 -	C11 =	108.1(2)
C 2 -	SI2 -	C 8 =	102.6(2)
C 2 -	SI2 -	C12 =	107.6(2)
C 2 -	SI2 -	C13 =	113.2(2)
C 8 -	SI2 -	C12 =	112.9(3)
C 8 -	SI2 -	C13 =	111.2(3)
C12 -	SI2 -	C13 =	109.2(3)
C 5 -	SI3 -	C 8 =	111.2(2)
C 5 -	SI3 -	C14 =	110.4(2)
C 5 -	SI3 -	C15 =	110.5(3)
C 8 -	SI3 -	C14 =	107.1(3)
C 8 -	SI3 -	C15 =	109.0(3)
C14 -	SI3 -	C15 =	108.5(3)
C 5 -	SI4 -	C 9 =	111.8(2)
C 5 -	SI4 -	C16 =	109.8(3)
C 5 -	SI4 -	C17 =	111.1(3)
C 9 -	SI4 -	C16 =	110.8(3)
C 9 -	SI4 -	C17 =	105.4(3)
C16 -	SI4 -	C17 =	107.8(3)
C 6 -	SI5 -	C 9 =	111.5(2)
C 6 -	SI5 -	C18 =	109.3(3)
C 6 -	SI5 -	C19 =	111.1(2)
C 9 -	SI5 -	C18 =	111.4(3)
C 9 -	SI5 -	C19 =	105.6(3)
C18 -	SI5 -	C19 =	107.9(3)
C 6 -	SI6 -	C 7 =	111.3(2)
C 6 -	SI6 -	C20 =	107.8(3)
C 6 -	SI6 -	C21 =	112.4(3)
C 7 -	SI6 -	C20 =	109.4(3)
C 7 -	SI6 -	C21 =	106.8(3)
C20 -	SI6 -	C21 =	109.1(3)
SI1 -	C 1 -	C 2 =	138.5(4)
SI1 -	C 1 -	C 4 =	127.3(3)
C 2 -	C 1 -	C 4 =	94.2(4)
SI2 -	C 2 -	C 1 =	140.7(4)
SI2 -	C 2 -	C 3 =	126.1(3)
C 1 -	C 2 -	C 3 =	93.1(4)
C 2 -	C 3 -	C 4 =	86.5(3)
C 2 -	C 3 -	C 5 =	133.0(5)
C 4 -	C 3 -	C 5 =	140.5(5)
C 1 -	C 4 -	C 3 =	86.1(3)
C 1 -	C 4 -	C 6 =	132.9(5)
C 3 -	C 4 -	C 6 =	141.0(5)
SI3 -	C 5 -	SI4 =	119.5(2)
SI3 -	C 5 -	C 3 =	117.6(4)
SI4 -	C 5 -	C 3 =	123.0(4)
SI5 -	C 6 -	SI6 =	119.7(2)
SI5 -	C 6 -	C 4 =	123.4(4)
SI6 -	C 6 -	C 4 =	117.0(4)
SI1 -	C 7 -	SI6 =	116.2(3)
SI2 -	C 8 -	SI3 =	115.5(3)
SI4 -	C 9 -	SI5 =	121.8(3)

PM3 Calculation of Hexasilyldimethylenecyclobutene 12

The geometry optimization of hexasilyldimethylenecyclobutene **12** was carried out by PM3 calculation.[9] The calculated structure of **12** is shown in Figure 2-8. The LUMO of **12** is also shown in Figure 2-9. The geometry of **12** by the X-ray diffraction is wellreproduced by PM3 calculation. The selected bond angles and lengths of **12** calculated by PM3 are shown in Figures 2-10 and 2-11. The charge distribution of **12** is also shown in Figure 2-12.

Consideration of π-MO of **12** is very important to understand the nature of π-electron system. The energy diagram of **12** calculated by PM3 is shown in Figure 2-13. The schematic drawing of the LUMO of **12** is shown in Figure 2-14. In the LUMO, C1-C4 and C2-C3 bonds are bonding, while C1-C2, C3-C4, C3-C5, and C4-C6 bonds are antibonding. The π-MO coefficients at the C1 and C2 carbon atoms are larger than that of other carbon atoms as shown in Figure 2-14. Thus, two electron reduction of **12** may produce dianion dimetal complex so that the counter cations may strongly interact with the C1 and C2 carbon atoms. The resulting dianion may be stabilized by Si1 and Si2 silicon atoms. In addition, the C1-C4-C6 and C2-C3-C5 units have similar π-MO to allyl anion with 3 center / 4π-electron system. Thus, it is reasonable to accept that reduction of **12** may yield the corresponding dianion species; one negative charge is delocalized on the C1-C4-C6 unit stabilized by Si1, Si5, and Si6 atoms, and the other one is delocalized on the C2-C3-C5 unit stabilized by Si2, Si3, and Si4 atoms, respectively.

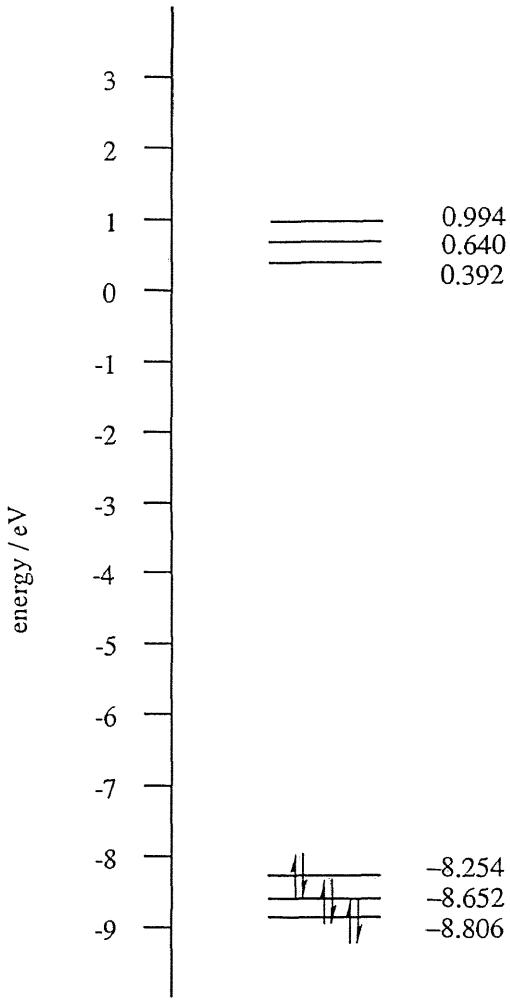

Figure 2-13. Energy diagram of **12** calculated by PM3.

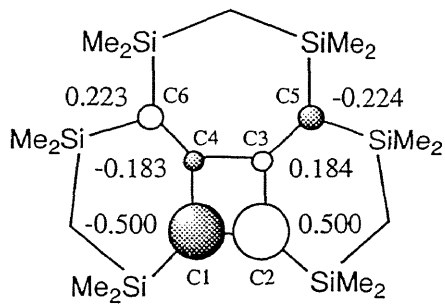

Figure 2-14. Schematic representation of the LUMO of **12** calculated by PM3.

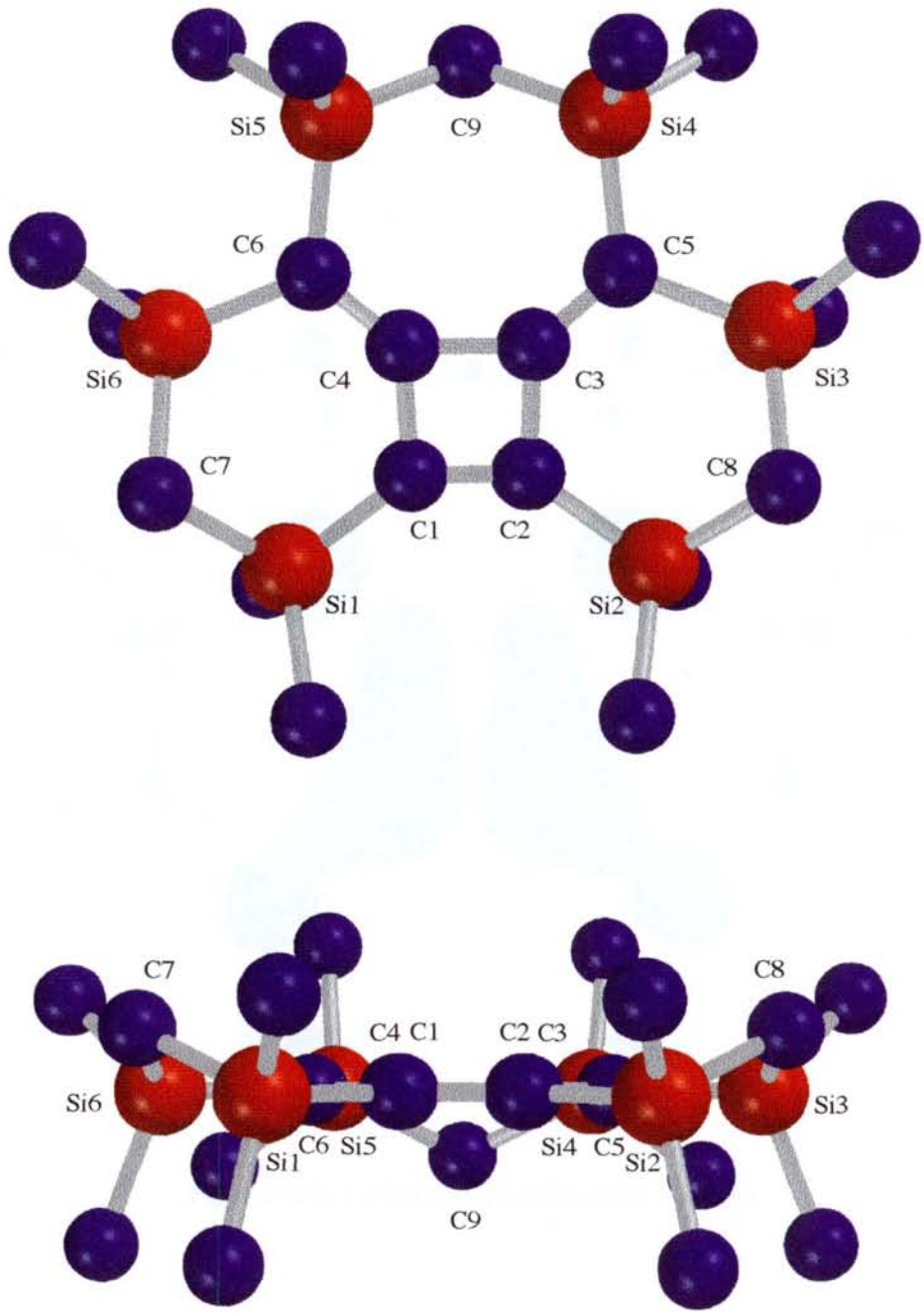

Figure 2-8. Calculated structure of **12** by PM3 (hydrogen atoms are omitted for the clarity): upper, top view; below, side view.

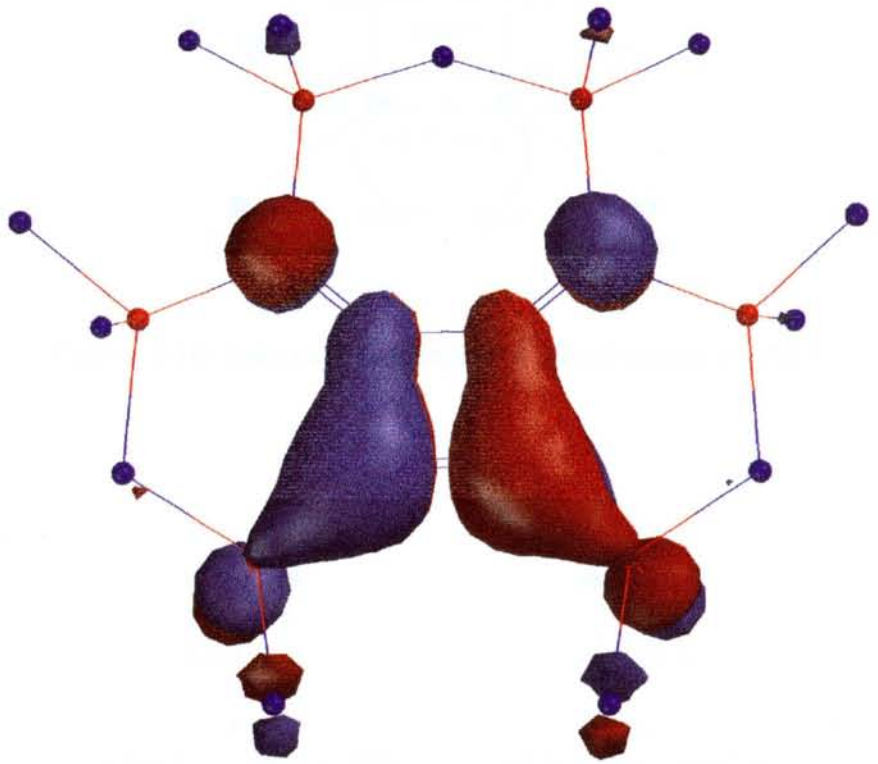

Figure 2-9. LUMO of **12** calculated by PM3.

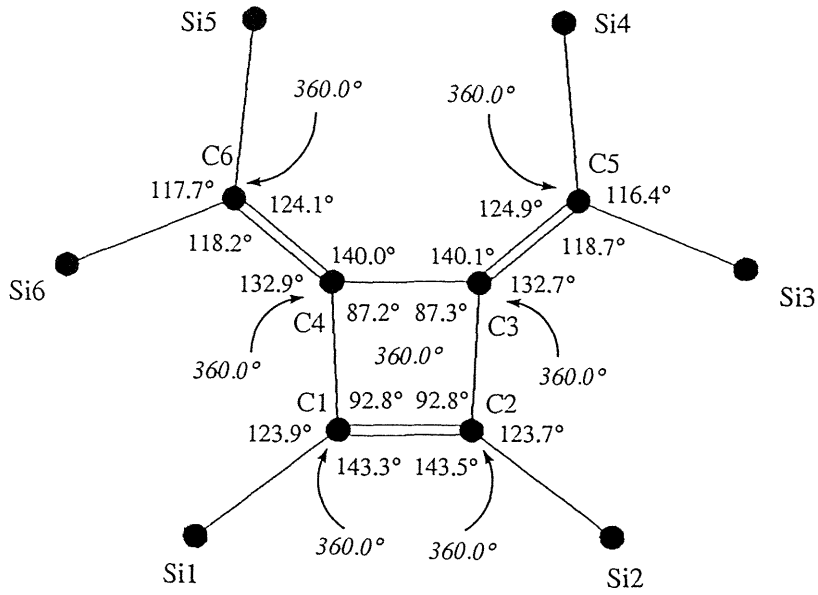

Figure 2-10. Selected bond angles of **12** calculated by PM3.

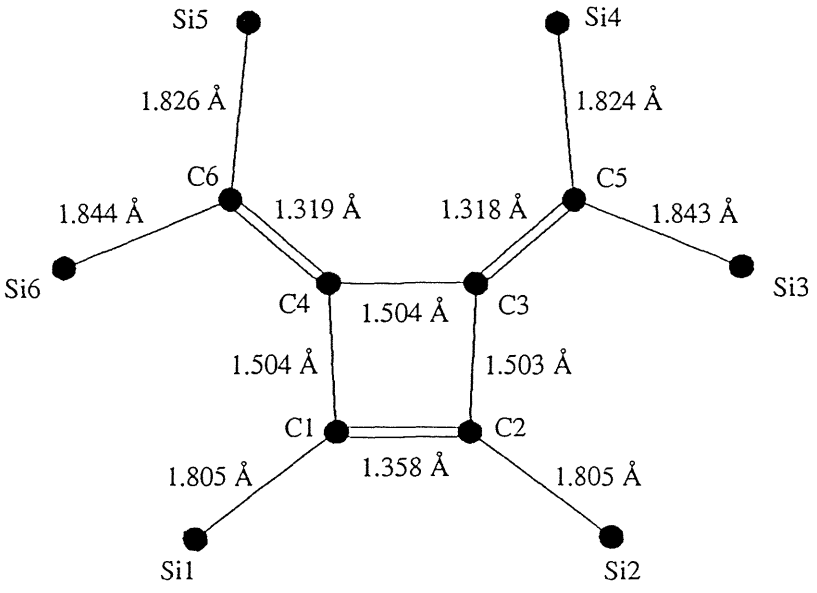

Figure 2-11. Selected bond lengths of **12** calculated by PM3.

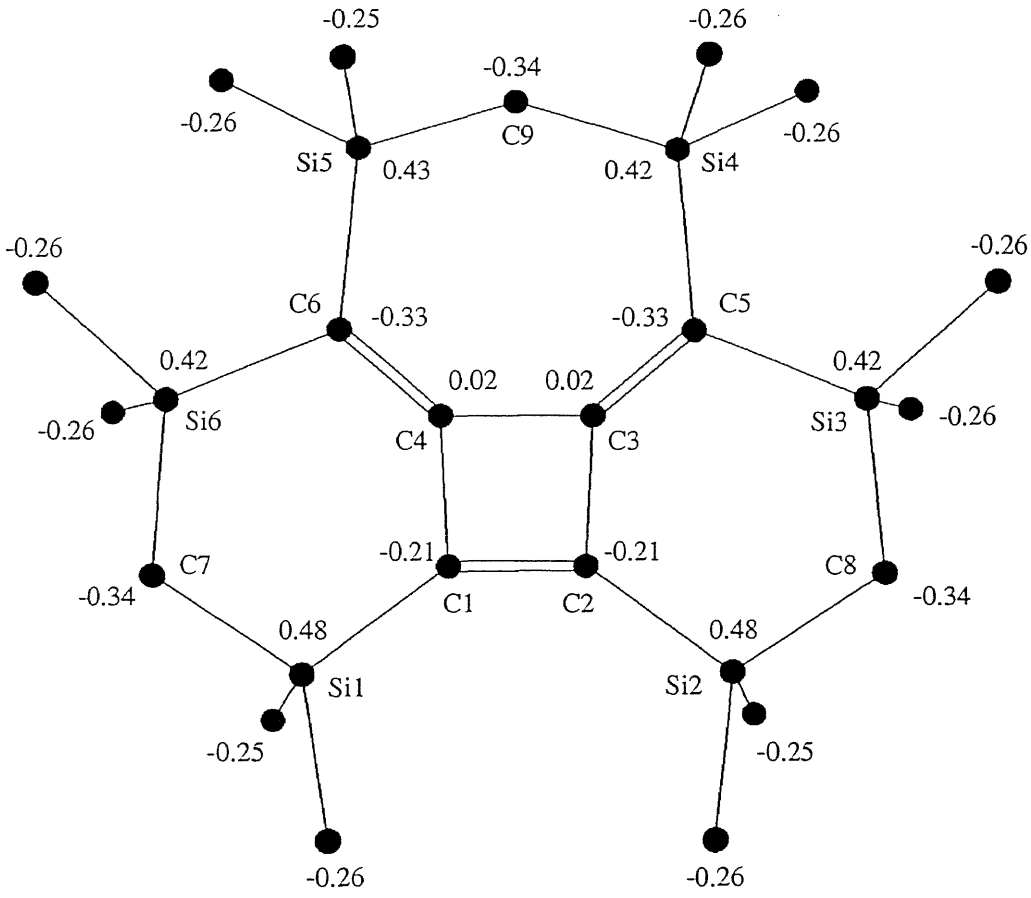

Figure 2-12. Mulliken charge distribution of **12** calculated by PM3.

Two Electron Reduction of Hexasilyldimethylenecyclobutene 12 with Lithium Metal

Reduction of **12** with excess lithium metal in dry oxygen-free 1,2-dimethoxyethane (DME) at room temperature led to the formation of a green solution of the dianion of **12** (Scheme 2-4). The reaction completed within 5 min. The solvent was removed in vacuo, and then dry degassed hexane was introduced by vacuum transfer. Crystallization from hexane at -20 °C afforded air and moisture sensitive green crystals of the dilithium salt of hexasilyldimethylenecyclobutene dianion (**13**) containing two molecules of DME. The structure of **13** was unequivocally confirmed by NMR spectroscopy and X-ray crystallography.

Scheme 2-4

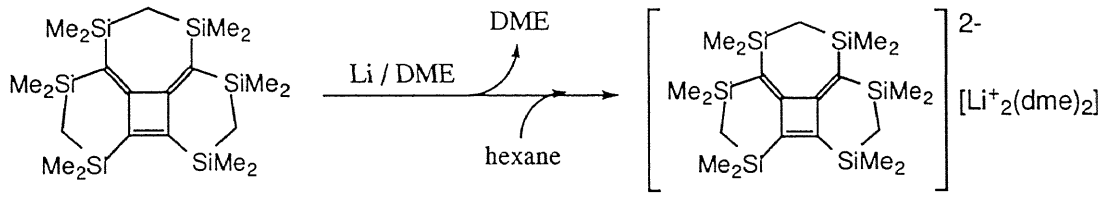

12 **13**

Molecular Structure of Dilithium Hexasilyldimethylenecyclobutene Dianion 13

The dilithium salt **13** has a monomeric structure and forms contact ion pairs (bis-CIP) in the crystals. The ORTEP drawing of 13 is shown in Figure 2-15. The crystal packing of **13** is shown in Figure 2-16. The final atomic parameters of **13** are listed in Tables 2-6 and 2-7. The atomic distances of 13 are summarized in Tables 2-8 and 2-9. The bond angles of **13** are also summarized in Table 2-10.

Several interesting features of the structure of **13** can be pointed out. Two lithium atoms are located up and below the π-skeleton. One DME molecule is coordinated to each lithium atom. The selected bond lengths of **13** are shown in Figure 2-17. Li1 is located above the C1-C2 bond (C1-Li1, 2.323(7); C2-Li1, 2.084(7) Å) and Li2 is below the C4-C6 bond (C4-Li2, 2.209(9); C6-Li2, 2.211(9) Å). Six carbon atoms (C1, C2, C3, C4, C5, and C6) of π-skeleton are maintained nearly coplanar.

Comparison of the structural parameters of **12** and **13** is quite interesting. The distance of C1-C2 bond of **13** is considerably elongated by 0.180 Å relative to that of **12**. As well, the distances of C3-C5 and C4-C6 bonds are stretched by 0.027 and 0.090 Å, respectively. The distances of C3-C4 bond is slightly lengthened by 0.010 Å. By contrast, the distances of C1-C4 and C2-C3 bonds of **13** are shortened by 0.079 and 0.037 Å, respectively. These structural features are reflected by the LUMO of **12** (Figure 2-14). Thus, C1-C4 and C2-C3 bonds are bonding, whereas C1-C2, C3-C5, C4-C6, and C3-C4 bonds are antibonding.

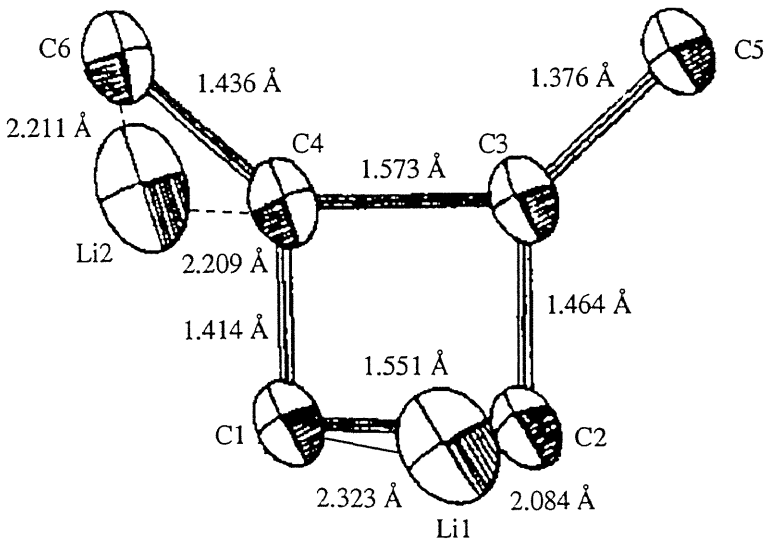

Figure 2-17. Selected bond lengths of **13**.

The selected bond angles and lengths of **13** are shown in Figures 2-18 and 2-19. The four-membered ring is almost planar, as determined by the internal bond angles of 88.3(2)-92.6(3)° (av 90.0°) and the sum of the bond angles (359.9°). The bond lengths of the Si-C bonds (C1-Si1, 1.828(2); C2-Si2, 1.805(2); C5-Si3, 1.870(2); C5-Si4, 1.835(2), C6-Si5, 1.824(4), C6-Si6, 1.851(4) Å) for **13** are remarkably shortened compared to those of **12** (1.878(6), 1.859(6), 1.889(6), 1.865(6), 1.873(6), and 1.879(6), respectively), due to the delocalization of the negative charge onto the silicon centers by $p\pi$-σ^* conjugation. The bond lengths of the Si-C (Si-Me and Si-CH_2) bonds of **13** are slightly elongated (about 0.01 Å) relative to those of **12**.

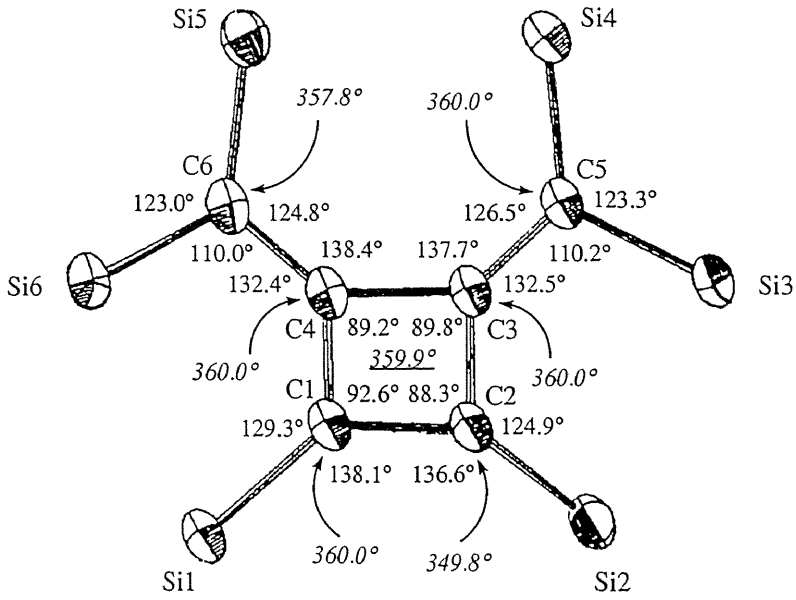

Figure 2-18. Selected bond angles of **13**.

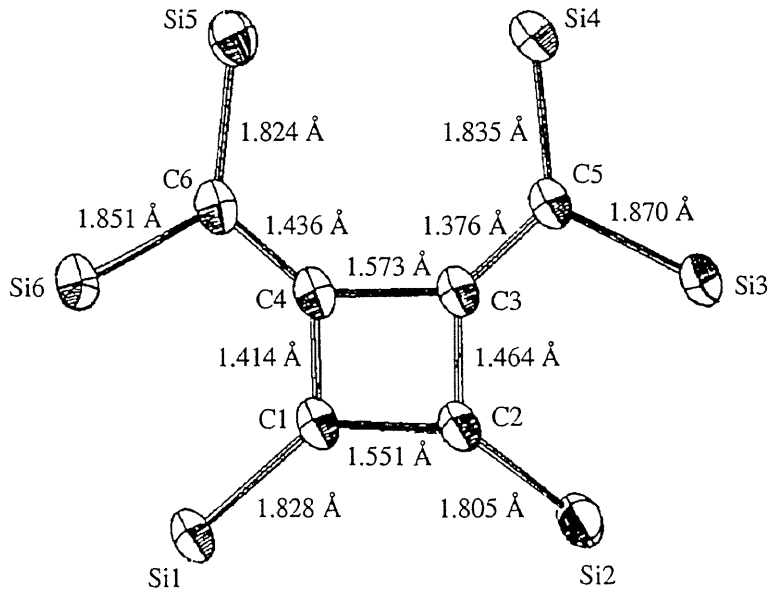

Figure 2-19. Selected bond lengths of **13**.

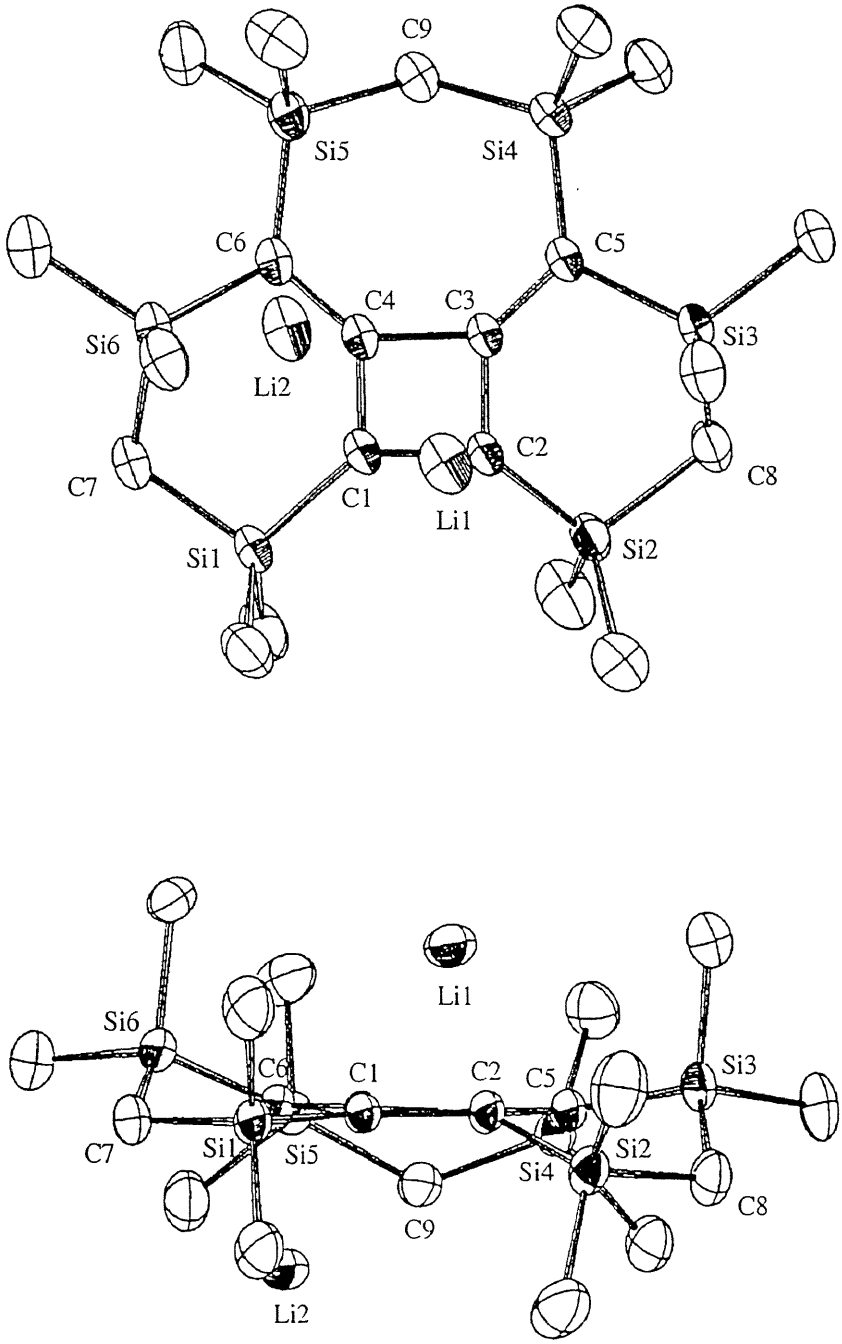

Figure 2-15. ORTEP drawing of **13** (DME molecules and hydrogen atoms are omitted for the clarity): upper, top view; below, side view.

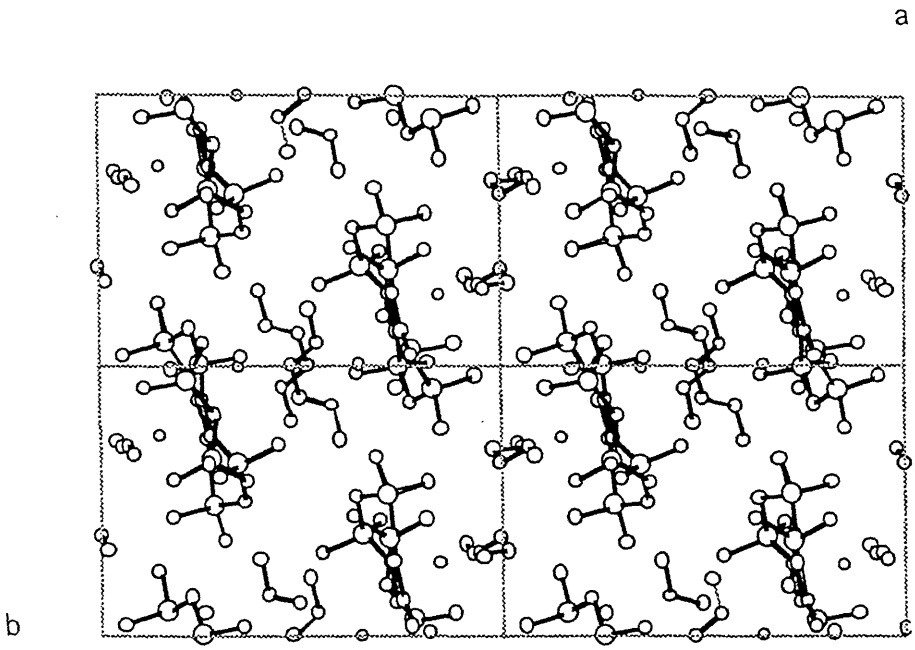

Figure 2-16. Crystal packing of **13**.

Table 2-6. Atomic Parameters[a] for Non-Hydrogen Atoms of **13**

ATOM	X	Y	Z	BEQV
SI1	-46(1)	2534(1)	5237(1)	4.0
SI2	3684(1)	3437(1)	7181(1)	4.4
SI3	5211(1)	2826(1)	9978(1)	4.1
SI4	3526(1)	2764(1)	11532(1)	3.8
SI5	584(1)	2185(1)	10114(1)	4.0
SI6	-900(1)	1667(1)	7051(1)	4.1
O 1	3055(3)	542(1)	8156(3)	5.8
O 2	3037(3)	703(2)	5906(3)	6.1
O 3	846(3)	4562(1)	8535(3)	7.0
O 4	-1506(3)	4179(2)	7268(3)	7.6
C 1	1276(3)	2579(2)	6863(3)	3.4
C 2	2687(3)	2770(2)	7491(3)	3.5
C 3	2731(3)	2673(2)	8768(3)	3.1
C 4	1308(3)	2450(2)	8083(3)	3.2
C 5	3684(3)	2732(2)	10017(3)	3.5
C 6	370(3)	2213(2)	8443(3)	3.5
C 7	-1400(3)	2244(2)	5515(3)	4.7
C 8	5086(3)	3614(2)	8806(3)	5.2
C 9	1873(3)	2878(2)	11246(3)	4.2
C10	144(4)	1780(3)	4056(4)	6.7
C11	-317(4)	3553(3)	4468(4)	6.8
C12	2998(5)	4460(3)	6494(5)	8.5
C13	4188(4)	2990(3)	5955(4)	8.2
C14	6558(3)	3103(3)	11603(4)	6.5
C15	5668(3)	1815(3)	9451(4)	6.0
C16	4279(4)	1850(3)	12545(4)	6.1
C17	4351(4)	3682(3)	12622(4)	5.8
C18	-840(4)	2590(3)	10257(4)	6.5
C19	845(4)	1136(2)	10805(4)	6.5
C20	-380(4)	625(2)	6700(4)	5.6
C21	-2326(4)	1469(3)	7280(4)	6.3
C22	2860(5)	427(3)	9259(4)	7.5
C23	3109(4)	-191(2)	7476(4)	6.8
C24	3628(4)	-5(3)	6576(4)	6.9
C25	3350(5)	855(3)	4876(5)	8.0
C26	2108(4)	4768(3)	9273(6)	8.5
C27	19(5)	5201(3)	8133(6)	8.7
C28	-1222(5)	4986(3)	7367(6)	9.1
C29	-2785(5)	3987(3)	6728(6)	9.3
LI1	2669(6)	1512(4)	7102(7)	5.5
LI2	38(6)	3497(4)	7854(7)	5.8

[a] Positional parameters are multiplied by 10^4. Thermal parameters are given by the equivalent temperature factors (A^2).

Table 2-7. Atomic Parameters[a] for Hydrogen Atoms of **13**

ATOM	X	Y	Z	B
H(C 7)1	-200(3)	187(2)	473(3)	5.8(0.8)
H(C 7)2	-187(3)	280(2)	559(3)	6.4(0.8)
H(C 8)1	501(3)	422(2)	922(3)	6.9(0.9)
H(C 8)2	588(3)	362(2)	871(3)	6.1(0.8)
H(C 9)1	187(3)	286(2)	1212(3)	5.8(0.8)
H(C 9)2	158(3)	345(2)	1091(3)	5.1(0.7)
H(C10)1	-63(3)	178(2)	317(3)	7.5(0.9)
H(C10)2	87(3)	193(2)	391(3)	7.1(0.9)
H(C10)3	25(3)	120(2)	439(3)	7.2(0.9)
H(C11)1	-101(3)	352(2)	357(3)	7.4(0.9)
H(C11)2	-48(3)	401(2)	505(3)	8.0(0.9)
H(C11)3	46(3)	372(2)	439(3)	7.7(0.9)
H(C12)1	365(3)	481(2)	638(3)	8.2(0.9)
H(C12)2	225(3)	438(2)	560(4)	8.8(1.0)
H(C12)3	274(3)	479(2)	714(4)	8.9(1.0)
H(C13)1	472(3)	340(2)	580(3)	7.6(0.9)
H(C13)2	467(3)	242(2)	629(4)	8.3(1.0)
H(C13)3	341(3)	286(2)	509(3)	7.0(0.9)
H(C14)1	735(3)	313(2)	1149(3)	6.8(0.9)
H(C14)2	642(3)	370(2)	1195(3)	6.7(0.8)
H(C14)3	667(3)	266(2)	1225(3)	6.2(0.8)
H(C15)1	648(3)	185(2)	945(4)	8.6(1.0)
H(C15)2	572(3)	139(2)	1007(4)	8.9(1.0)
H(C15)3	505(3)	161(2)	855(4)	8.4(1.0)
H(C16)1	422(3)	190(2)	1339(3)	7.6(0.9)
H(C16)2	385(3)	130(2)	1207(3)	6.7(0.9)
H(C16)3	518(3)	180(2)	1274(3)	7.6(0.9)
H(C17)1	418(3)	371(2)	1342(3)	7.5(0.9)
H(C17)2	526(3)	367(2)	1292(3)	7.5(0.9)
H(C17)3	403(3)	423(2)	1212(3)	7.1(0.9)
H(C18)1	-70(3)	261(2)	1122(3)	7.2(0.9)
H(C18)2	-105(3)	320(2)	992(3)	7.6(0.9)
H(C18)3	-157(3)	223(2)	974(3)	7.9(0.9)
H(C19)1	94(3)	116(2)	1171(3)	6.9(0.9)
H(C19)2	10(3)	75(2)	1024(3)	7.0(0.9)
H(C19)3	164(3)	86(2)	1084(3)	7.9(0.9)
H(C20)1	-108(3)	34(2)	588(3)	6.4(0.8)
H(C20)2	37(3)	67(2)	654(3)	6.6(0.8)
H(C20)3	-16(3)	24(2)	750(3)	6.6(0.8)
H(C21)1	-297(3)	115(2)	647(3)	7.0(0.9)
H(C21)2	-208(3)	108(2)	809(3)	6.8(0.8)
H(C21)3	-271(3)	201(2)	744(3)	6.9(0.9)
H(C22)1	284(3)	97(2)	969(3)	7.4(0.9)
H(C22)2	353(3)	10(2)	988(3)	7.5(0.9)
H(C22)3	205(3)	12(2)	900(3)	7.3(0.9)
H(C23)1	216(3)	-42(2)	692(3)	7.5(0.9)
H(C23)2	363(3)	-64(2)	812(3)	7.3(0.9)
H(C24)1	460(3)	13(2)	715(3)	8.0(0.9)
H(C24)2	351(3)	-52(2)	587(3)	6.4(0.8)
H(C25)1	291(3)	139(2)	440(3)	8.0(0.9)
H(C25)2	430(3)	96(2)	528(3)	8.3(0.9)
H(C25)3	309(3)	35(2)	416(3)	8.2(0.9)
H(C26)1	264(3)	428(2)	949(4)	9.1(1.0)
H(C26)2	221(4)	510(2)	1009(4)	9.7(1.1)
H(C26)3	237(3)	516(2)	879(4)	9.4(1.0)
H(C27)1	10(3)	553(2)	895(4)	10.0(1.0)
H(C27)2	31(3)	564(2)	773(4)	9.5(1.0)
H(C28)1	-149(3)	518(2)	649(4)	10.0(1.0)
H(C28)2	-177(4)	533(2)	772(4)	10.2(1.0)
H(C29)1	-289(3)	335(2)	672(3)	8.4(1.0)
H(C29)2	-320(3)	428(2)	727(3)	8.5(1.0)
H(C29)3	-320(4)	418(2)	574(4)	9.6(1.1)

[a] Positional parameters are multiplied by 10^4. Thermal parameters are given by the equivalent temperature factors (A^2).

Table 2-8. List of Atomic Distances (Å) for Non-Hydrogen Atoms of **13**

ATOM	-	ATOM		LENGTH(SIG)
SI1	-	C 1	=	1.828(2)
SI1	-	C 7	=	1.875(4)
SI1	-	C10	=	1.875(4)
SI1	-	C11	=	1.878(4)
SI2	-	C 2	=	1.805(2)
SI2	-	C 8	=	1.885(4)
SI2	-	C12	=	1.890(6)
SI2	-	C13	=	1.880(6)
SI3	-	C 5	=	1.870(2)
SI3	-	C 8	=	1.868(4)
SI3	-	C14	=	1.885(4)
SI3	-	C15	=	1.885(4)
SI4	-	C 5	=	1.835(2)
SI4	-	C 9	=	1.870(4)
SI4	-	C16	=	1.888(4)
SI4	-	C17	=	1.893(4)
SI5	-	C 6	=	1.824(4)
SI5	-	C 9	=	1.875(4)
SI5	-	C18	=	1.893(4)
SI5	-	C19	=	1.888(4)
SI6	-	C 6	=	1.851(4)
SI6	-	C 7	=	1.885(4)
SI6	-	C20	=	1.887(4)
SI6	-	C21	=	1.889(4)
O 1	-	C22	=	1.413(7)
O 1	-	C23	=	1.414(6)
O 1	-	LI1	=	1.963(7)
O 2	-	C24	=	1.411(6)
O 2	-	C25	=	1.431(7)
O 2	-	LI1	=	2.044(7)
O 3	-	C26	=	1.406(7)
O 3	-	C27	=	1.368(7)
O 3	-	LI2	=	1.967(9)
O 4	-	C28	=	1.360(7)
O 4	-	C29	=	1.414(7)
O 4	-	LI2	=	1.995(9)
C 1	-	C 2	=	1.551(4)
C 1	-	C 3	=	2.100(4)
C 1	-	C 4	=	1.414(4)
C 1	-	LI1	=	2.323(7)
C 2	-	C 3	=	1.464(4)
C 2	-	C 4	=	2.146(4)
C 2	-	LI1	=	2.084(7)
C 3	-	C 4	=	1.573(4)
C 3	-	C 5	=	1.376(4)
C 4	-	C 6	=	1.436(4)
C 4	-	LI2	=	2.209(9)
C 6	-	LI2	=	2.211(9)
C23	-	C24	=	1.478(7)
C27	-	C28	=	1.393(9)

Table 2-9. List of Bond Lengths (Å) for Hydrogen Atoms of **13**

ATOM	-	ATOM		LENGTH(SIG)
C 7	-	H(C 7)1	=	1.04(3)
C 7	-	H(C 7)2	=	1.08(3)
C 8	-	H(C 8)1	=	1.09(3)
C 8	-	H(C 8)2	=	1.02(3)
C 9	-	H(C 9)1	=	1.01(3)
C 9	-	H(C 9)2	=	1.02(3)
C10	-	H(C10)1	=	1.03(3)
C10	-	H(C10)2	=	1.00(3)
C10	-	H(C10)3	=	1.03(3)
C11	-	H(C11)1	=	0.99(3)
C11	-	H(C11)2	=	1.05(4)
C11	-	H(C11)3	=	1.02(3)
C12	-	H(C12)1	=	1.04(4)
C12	-	H(C12)2	=	1.02(4)
C12	-	H(C12)3	=	1.05(4)
C13	-	H(C13)1	=	1.02(3)
C13	-	H(C13)2	=	1.07(4)
C13	-	H(C13)3	=	1.03(3)
C14	-	H(C14)1	=	1.03(3)
C14	-	H(C14)2	=	1.07(3)
C14	-	H(C14)3	=	1.02(3)
C15	-	H(C15)1	=	0.98(4)
C15	-	H(C15)2	=	1.00(4)
C15	-	H(C15)3	=	1.02(4)
C16	-	H(C16)1	=	1.00(3)
C16	-	H(C16)2	=	1.05(3)
C16	-	H(C16)3	=	1.00(3)
C17	-	H(C17)1	=	1.03(3)
C17	-	H(C17)2	=	0.99(3)
C17	-	H(C17)3	=	1.07(3)
C18	-	H(C18)1	=	1.04(3)
C18	-	H(C18)2	=	1.07(3)
C18	-	H(C18)3	=	0.99(4)
C19	-	H(C19)1	=	0.99(3)
C19	-	H(C19)2	=	1.04(3)
C19	-	H(C19)3	=	1.03(4)
C20	-	H(C20)1	=	1.04(3)
C20	-	H(C20)2	=	1.00(3)
C20	-	H(C20)3	=	1.07(3)
C21	-	H(C21)1	=	1.03(3)
C21	-	H(C21)2	=	1.08(3)
C21	-	H(C21)3	=	1.03(3)
C22	-	H(C22)1	=	1.00(3)
C22	-	H(C22)2	=	0.97(3)
C22	-	H(C22)3	=	1.02(3)
C23	-	H(C23)1	=	1.10(3)
C23	-	H(C23)2	=	1.04(3)
C24	-	H(C24)1	=	1.08(4)
C24	-	H(C24)2	=	1.11(3)
C25	-	H(C25)1	=	1.05(4)
C25	-	H(C25)2	=	1.04(4)
C25	-	H(C25)3	=	1.09(4)
C26	-	H(C26)1	=	0.98(4)
C26	-	H(C26)2	=	1.02(4)
C26	-	H(C26)3	=	1.01(4)
C27	-	H(C27)1	=	1.03(4)
C27	-	H(C27)2	=	1.02(4)
C28	-	H(C28)1	=	0.98(4)
C28	-	H(C28)2	=	1.05(4)
C29	-	H(C29)1	=	1.06(4)
C29	-	H(C29)2	=	1.05(4)
C29	-	H(C29)3	=	1.08(4)

Table 2-10. List of Bond Angles (Å) for Non-Hydrogen Atoms of **13**

ATOM -	ATOM	ATOM	ANGLE(SIG)
C 1 -	SI1 -	C 7 =	104.6(1)
C 1 -	SI1 -	C10 =	114.4(1)
C 1 -	SI1 -	C11 =	110.8(1)
C 7 -	SI1 -	C10 =	110.2(1)
C 7 -	SI1 -	C11 =	111.1(1)
C10 -	SI1 -	C11 =	105.8(2)
C 2 -	SI2 -	C 8 =	105.3(1)
C 2 -	SI2 -	C12 =	116.4(2)
C 2 -	SI2 -	C13 =	113.5(2)
C 8 -	SI2 -	C12 =	109.0(2)
C 8 -	SI2 -	C13 =	109.9(2)
C12 -	SI2 -	C13 =	102.7(2)
C 5 -	SI3 -	C 8 =	109.7(1)
C 5 -	SI3 -	C14 =	114.5(1)
C 5 -	SI3 -	C15 =	110.2(1)
C 8 -	SI3 -	C14 =	108.2(2)
C 8 -	SI3 -	C15 =	109.1(2)
C14 -	SI3 -	C15 =	104.9(2)
C 5 -	SI4 -	C 9 =	112.9(1)
C 5 -	SI4 -	C16 =	112.2(1)
C 5 -	SI4 -	C17 =	111.3(1)
C 9 -	SI4 -	C16 =	110.4(1)
C 9 -	SI4 -	C17 =	104.8(1)
C16 -	SI4 -	C17 =	104.9(2)
C 6 -	SI5 -	C 9 =	111.5(1)
C 6 -	SI5 -	C18 =	111.4(1)
C 6 -	SI5 -	C19 =	115.4(2)
C 9 -	SI5 -	C18 =	104.4(1)
C 9 -	SI5 -	C19 =	109.2(2)
C18 -	SI5 -	C19 =	104.2(2)
C 6 -	SI6 -	C 7 =	110.5(1)
C 6 -	SI6 -	C20 =	111.7(1)
C 6 -	SI6 -	C21 =	115.0(1)
C 7 -	SI6 -	C20 =	105.9(1)
C 7 -	SI6 -	C21 =	108.3(2)
C20 -	SI6 -	C21 =	105.0(2)
C22 -	O 1 -	C23 =	114.4(3)
C22 -	O 1 -	LI1 =	128.1(3)
C23 -	O 1 -	LI1 =	113.4(3)
C24 -	O 2 -	C25 =	112.5(3)
C24 -	O 2 -	LI1 =	110.4(3)
C25 -	O 2 -	LI1 =	129.7(3)
C26 -	O 3 -	C27 =	116.4(4)
C26 -	O 3 -	LI2 =	131.0(4)
C27 -	O 3 -	LI2 =	112.4(4)
C28 -	O 4 -	C29 =	116.4(4)
C28 -	O 4 -	LI2 =	110.3(4)
C29 -	O 4 -	LI2 =	133.3(4)
SI1 -	C 1 -	C 2 =	138.1(2)
SI1 -	C 1 -	C 4 =	129.3(2)
SI1 -	C 1 -	LI1 =	111.1(2)
C 2 -	C 1 -	C 4 =	92.6(2)
C 2 -	C 1 -	LI1 =	61.3(2)
C 4 -	C 1 -	LI1 =	92.3(2)
SI2 -	C 2 -	C 1 =	136.6(2)
SI2 -	C 2 -	C 3 =	124.9(2)
SI2 -	C 2 -	LI1 =	121.4(2)
C 1 -	C 2 -	C 3 =	88.3(2)
C 1 -	C 2 -	LI1 =	77.9(2)
C 3 -	C 2 -	LI1 =	93.0(2)

Table 2-10 (continued). List of Bond Angles (Å) for Non-Hydrogen Atoms of **13**

C	2	-	C	3	-	C 4 =	89.8(2)
C	2	-	C	3	-	C 5 =	132.5(2)
C	4	-	C	3	-	C 5 =	137.6(2)
C	1	-	C	4	-	C 3 =	89.2(2)
C	1	-	C	4	-	C 6 =	132.4(2)
C	1	-	C	4	-	LI2 =	91.3(2)
C	3	-	C	4	-	C 6 =	138.4(2)
C	3	-	C	4	-	LI2 =	114.6(2)
C	6	-	C	4	-	LI2 =	71.1(2)
SI	3	-	C	5	-	SI4 =	123.3(1)
SI	3	-	C	5	-	C 3 =	110.2(2)
SI	4	-	C	5	-	C 3 =	126.5(2)
SI	5	-	C	6	-	SI6 =	123.0(1)
SI	5	-	C	6	-	C 4 =	124.8(2)
SI	5	-	C	6	-	LI2 =	108.3(2)
SI	6	-	C	6	-	C 4 =	110.0(2)
SI	6	-	C	6	-	LI2 =	102.4(2)
C	4	-	C	6	-	LI2 =	71.0(2)
SI	1	-	C	7	-	SI6 =	112.3(2)
SI	2	-	C	8	-	SI3 =	111.5(2)
SI	4	-	C	9	-	SI5 =	123.9(2)
O	1	-	C23		-	C24 =	108.6(4)
O	2	-	C24		-	C23 =	109.0(4)
O	4	-	C28		-	C27 =	117.1(5)
O	3	-	C27		-	C28 =	115.6(5)
O	1	-	LI	1	-	O 2 =	81.1(3)
O	1	-	LI	1	-	C 1 =	130.1(3)
O	1	-	LI	1	-	C 2 =	134.9(4)
O	2	-	LI	1	-	C 1 =	137.0(3)
O	2	-	LI	1	-	C 2 =	138.9(4)
C	1	-	LI	1	-	C 2 =	40.8(1)
O	3	-	LI	2	-	O 4 =	82.4(3)
O	3	-	LI	2	-	C 4 =	115.6(4)
O	3	-	LI	2	-	C 6 =	137.3(4)
O	4	-	LI	2	-	C 4 =	161.5(4)
O	4	-	LI	2	-	C 6 =	130.1(4)
C	4	-	LI	2	-	C 6 =	37.9(1)

PM3 Calculation of Hexasilyldimethylenecyclobutene Dianion 12^{2-}

The geometry optimization of hexasilyldimethylenecyclobutene dianion 12^{2-} (counter ion free) was also carried out by PM3 calculation.[9] The calculated structure of 12^{2-} is shown in Figure 2-20. The geometry of 12^{2-} calculated by PM3 is close to that of dilithium hexasilyldimethylenecyclobutene dianion **13** by the X-ray diffraction. Some differences between crystal structure and calculated structure may be due to the existence of counter lithium cation and DME bidentate ligands. The selected bond angles and lengths of 12^{2-} calculated by PM3 are shown in Figures 2-21 and 2-22. The charge distribution of 12^{2-} is also shown in Figure 2-23.

Comparison of the calculated parameters of **12** and 12^{2-} is also interesting. The change of bond lengths by two electron reduction is wellreproduced by PM3 calculation. The C-C single and double bond lengths of **12** calculated by PM3 are 1.503-1.504 Å (av 1.504 Å) and 1.318-1.358 Å (av 1.331 Å), respectively. Those of 12^{2-} are 1.404-1.546 Å (av 1.451 Å) and 1.367-1.498 Å (av 1.411 Å), respectively. The Si-C(sp^2) single bond lengths of 12^{2-} calculated by PM3 are 1.737-1.793 Å (av 1.765 Å), which are shorter than those of **12** (1.805-1.844 Å (av 1.823 Å)) due to the $p\pi$-σ^* conjugation.

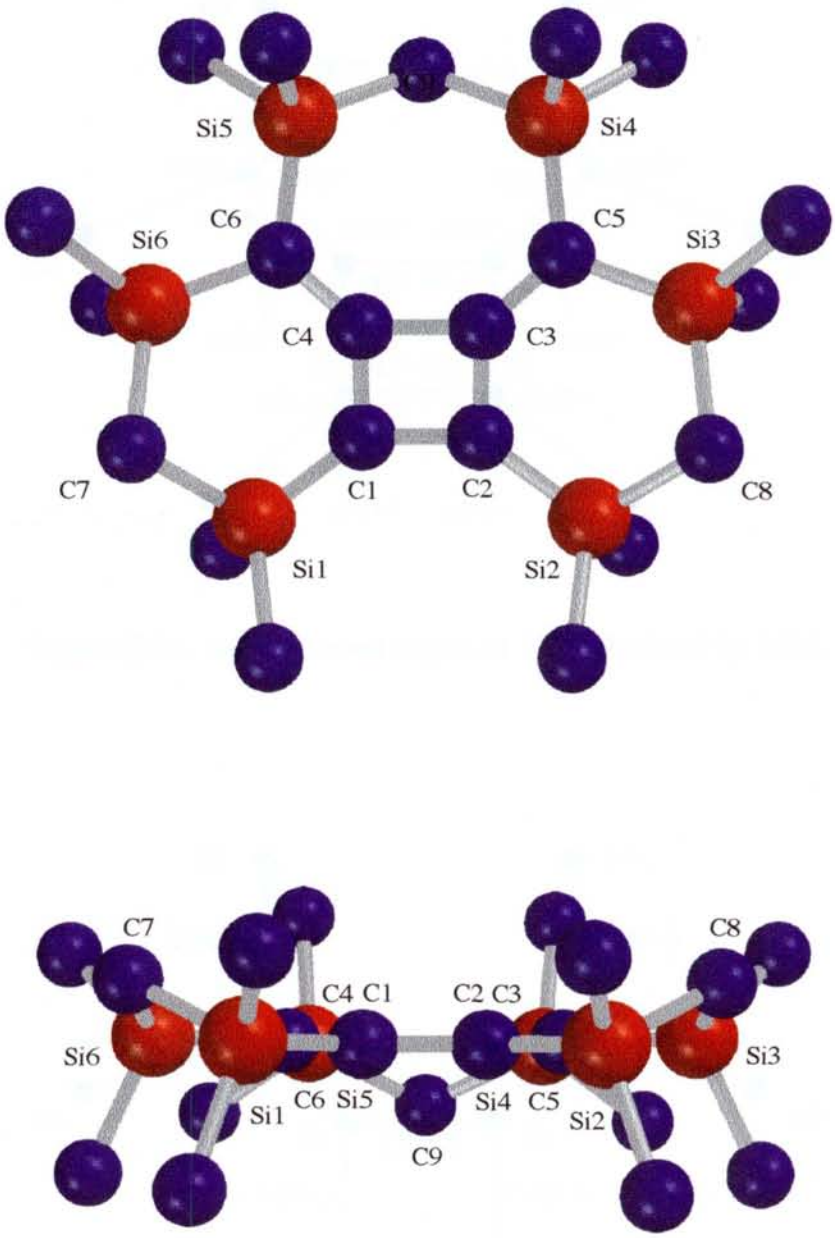

Figure 2-20. Calculated structure of $\mathbf{12}^{2-}$ by PM3 (hydrogen atoms are omitted for the clarity): upper, top view; below, side view.

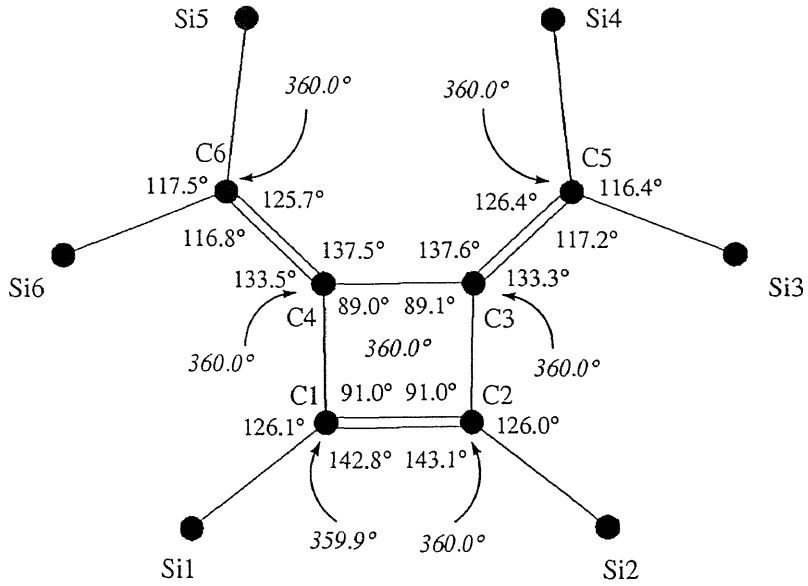

Figure 2-21. Selected bond angles of $\mathbf{12}^{2-}$ calculated by PM3.

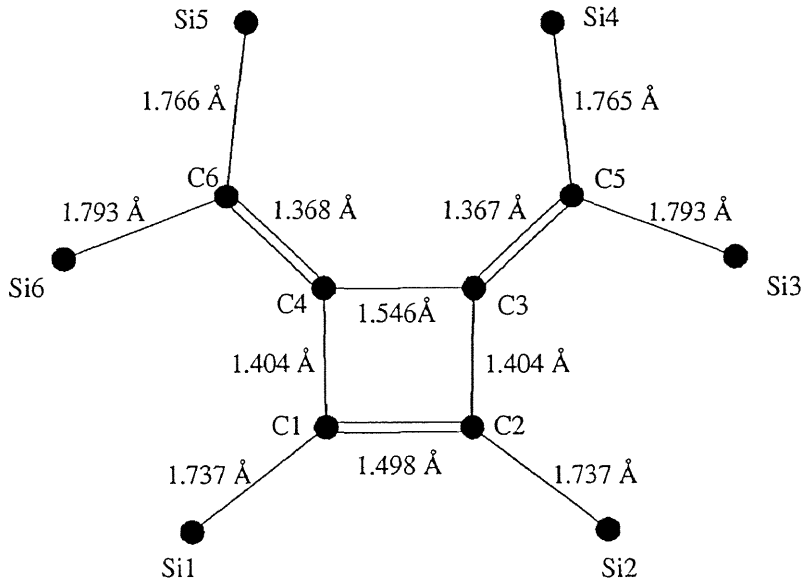

Figure 2-22. Selected bond lengths of $\mathbf{12}^{2-}$ calculated by PM3.

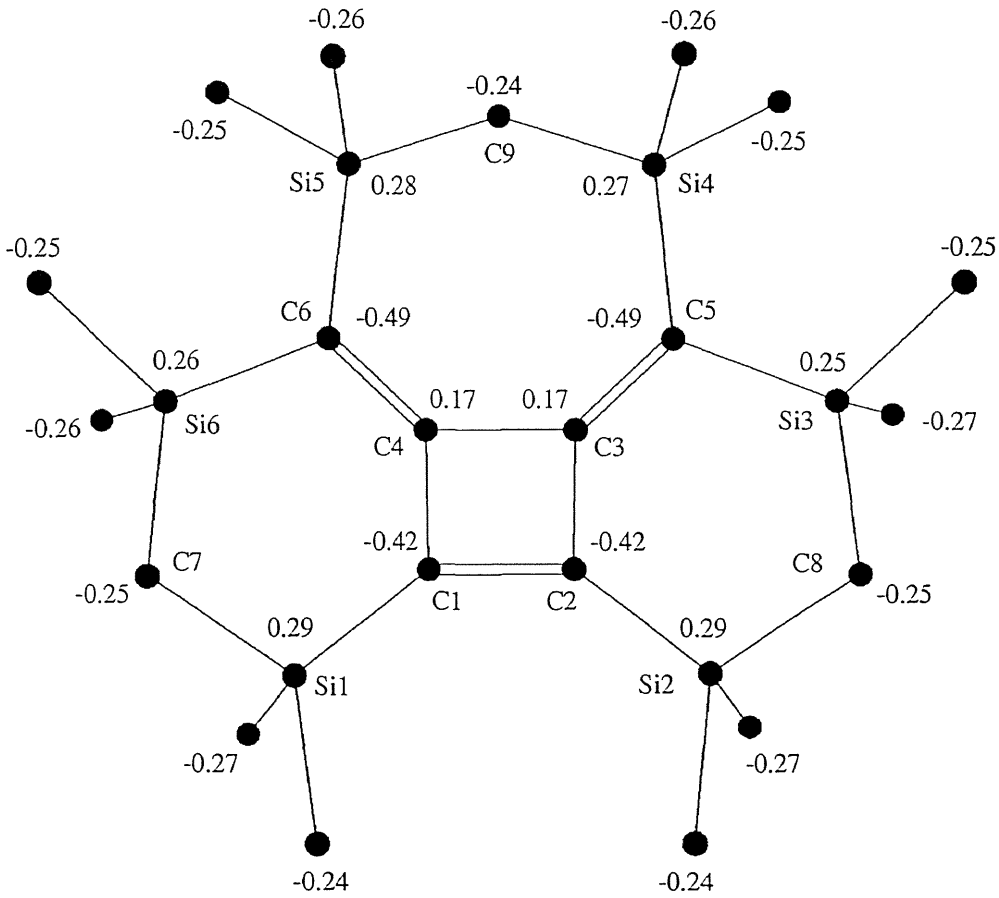

Figure 2-23. Mulliken charge distribution of $\mathbf{12}^{2-}$ calculated by PM3.

Structure of Dilithium Hexasilyldimethylenecyclobutene Dianion 13 in Toluene-d_8

The structure of **13** in toluene-d_8 was deduced on the basis of the NMR spectroscopic data. In the ^1H NMR spectrum of **13** in toluene-d_8, three sets of methyl groups were observed at 0.14, 0.29, and 0.38 ppm, and two sets of methylene groups at -0.13 and 0.05 ppm, together with the signals due to DME. Three sets of ^{29}Si signals were found at -30.1, -13.3, and -11.7 ppm, shifting to upper field relative to those of **12** (–17.5, -7.3, and -7.1 ppm). This suggests that the negative charge is stabilized by the six silyl groups in **13** ($p\pi$-σ^* conjugation). The carbon atoms assigned to the methyl groups were observed at 3.6, 4.5, and 5.3 ppm, and methylene groups at 2.8 and 11.5 ppm. ^7Li NMR spectrum of **13** yielded only one signal appearing at 0.20 ppm in toluene-d_8 at temperature range 298-193 K (Figure 2-24).

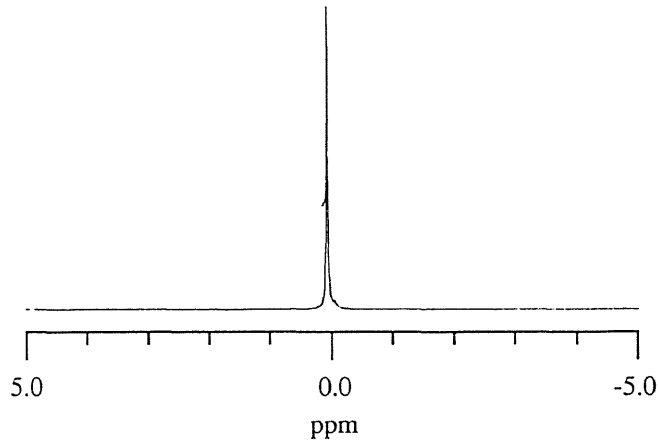

Figure 2-24. ^7Li NMR spectrum of **13** in C_7D_8 at 298 K.

The negative charge is largely delocalized on the four carbon atoms (C1, C2, C5, and C6) in the π-skeleton of **13** as evidenced by ^{13}C NMR spectral data. Thus, these carbons were observed at 74.4 and 87.4 ppm, and significantly shifted to upper field about 100 ppm relative to those of **12** (173.5 and 177.1 ppm). On the other hand, the central carbon atoms assigned C3 and C4 remarkably moved to lower field appearing at 180.6 ppm (126.3 ppm for **12**). No scalar coupling between ^{7}Li and the anionic carbons (C1, C6, and C2, C5) was observed.

The X-ray crystallography and the NMR data indicate that the structure of the dilithium hexasilyldimethylenecyclobutene dianion (**13**) is evidently 6C / 8π-electron, bis(allyl anion) system. Two negative charge is delocalized on C1, C2, C5, and C6 carbon atoms. Thus, the dimethylenecyclobutene dianion has allyl anion character stabilized by the silyl groups.

Experimental Section

General Methods

^{1}H NMR spectra were recorded on a Bruker AC-300 FT spectrometer. ^{13}C, ^{29}Si, and ^{7}Li NMR spectra were collected on a Bruker AC-300 at 75.5, 59.6, and 116.6 MHz, respectively. ^{7}Li NMR spectra are referenced to 1 M LiCl (1 M = 1 mol dm^{-3}) in methanol / toluene-d_8. Mass spectra were obtained on a Shimadzu QP-1000. Electronic spectra were recorded on a Shimadzu UV-2100 spectrometer. The sampling of **13** for X-ray crystallography was carried out by using a Giken Engineering Service GBX-1200 gas-replacement type glove box.

Materials

Tetrahydrofuran, 1,2-dimethoxyethane (DME), and hexane were dried and distilled from sodium benzophenone ketyl. These solvents were further dried and degassed over a potassium mirror in vacuo prior to use. Toluene-d_8 was dried over molecular sieves, and then transferred into a tube covered with potassium mirror prior to use.

Preparation of 3,3,5,5,8,8,10,10,13,13,15,15-dodecamethyl-3,5,8,10,13,15-hexasilacyclopentadeca-1,6,11-triyne (11)

3,3,5,5-tetramethyl-3,5-disilahepta-1,6-diyne (10.97 g, 0.061 mol) in THF (20 ml) was added to a THF solution of ethylmagnesium bromide (100 ml, 0.124 mol) to produce the Grignard reagent of the 1,6-diyne. The THF solution of the resulting Grignard reagent and 2,9-dichloro-2,4,4,7,7,9-hexamethyl-2,4,7,9-tetrasiladeca-5-yne (20.01 g, 0.056 mol) in THF (20 ml) were added dropwise to refluxing THF (500 ml), and the mixture was heated overnight. The reaction mixture was poured into hexane and hydrolyzed with dilute hydrochloric acid, followed by extraction with hexane. The

organic layer was washed with water and dried over anhydrous sodium sulfate. After evaporation of the solvent, the residue was distilled under reduced pressure to give the triyne (**11**) (100-150 °C / 0.15 mmHg, Kugelrohr distillation). Recrystallization from ethanol gave pure colorless crystals of **11** in 38% yield. This compound had already been isolated from the reaction mixture of $BrMgC{\equiv}CMgBr$ and $ClMe_2SiCH_2SiMe_2Cl$ in very low yield.[10] mp 112–113 °C. ^1H NMR ($CDCl_3$) δ = -0.08 (s, 6 H, CH_2), 0.23 (s, 36 H, CH_3); ^{13}C NMR ($CDCl_3$) δ = 1.2 (CH_3), 2.9 (CH_2), 115.0 (C); ^{29}Si NMR ($CDCl_3$) δ = -19.9; UV (hexane) λ_{max} /nm (ε) 209 (2100), 216 (1400); HRMS Found: m/z 462.1902. Calcd for $C_{21}H_{42}Si_6$: M, 462.1902.

Preparation of Hexasilyldimethylenecyclobutene (12)

A mixture of the 3,3,5,5,8,8,10,10,13,13,15,15-dodecamethyl-3,5,8,10,13,15-hexasilacyclopentadeca-1,6,11-triyne (**11**) (1000 mg, 2.16 mmol) and $[Mn(CO)_3(Me\text{-}Cp)]$ (477 mg, 2.19 mmol) in THF (30 ml) was irradiated with a 500 W high-pressure mercury lamp for 10 h through the cutoff filter (λ > 300 nm) under the refluxing temperature of THF. After removal of the manganese complex, the reaction mixture was chromatographed on silica gel to produce pale yellow crystals of **12** in 50% yield. mp 199-200 °C; ^1H NMR ($CDCl_3$) δ = -0.13 (s, 4 H, CH_2), 0.01 (s, 2 H, CH_2), 0.15 (s, 12 H, CH_3), 0.18 (s, 12 H, CH_3), 0.20 (s, 12 H, CH_3); ^{13}C NMR ($CDCl_3$) δ = 0.4 (CH_2), 0.4 (CH_3), 2.7 (CH_3), 3.0 (CH_2), 7.4 (CH_2), 126.3 (C), 173.5 (C), 177.1 (C); ^{29}Si NMR ($CDCl_3$) δ = -17.5, -7.3, -7.1; UV (hexane) λ_{max}/nm (ε) 240 (sh. 26900), 248 (32400), 256 (sh. 26900), 290 (8300); HRMS Found: m/z 462.1914. Calcd for $C_{21}H_{42}Si_6$: M, 462.1902.

X-ray Crystallography of Hexasilyldimethylenecyclobutene (12)

Single crystal of **12** for X-ray diffractions was grown from an ethanol solution. The X-ray crystallographic experiment of **12** was performed on a Rigaku-Denki AFC 5R diffractometer equipped with graphite-monochromatized Cu-$K\alpha$ radiation (λ = 1.54178 Å). Crystal data for **12** at 200 K: MF = $C_{21}H_{42}Si_6$, MW = 463.08, monoclinic, a = 21.400(1) Å, b = 10.761(1) Å, c = 12.948(1) Å, β = 107.721(6)°, V = 2840.4(5) Å^3, space group = $P2_1/a$, Z = 4, D_{calcd} = 1.083 g/cm^3. The final R factor was 0.0733 (R_w = 0.0848) for 4094 reflections with $F_o > 3\sigma(F_o)$. The details of the X-ray experiment are given in Table 2-11.

Table 2-11. Detail of the X-ray Experiment for **12**

molecular formula	$C_{21}H_{42}Si_6$
molecular weight	463.08
crystal system	monoclinic
space group	$P2_1/a$
cell constants	a = 21.400(1) Å, b = 10.761(1) Å,
	c = 12.948(1) Å, β = 107.721(6)°,
	V = 2840.4(5) Å^3
Z value	4
D_{calcd}	1.083 g cm^{-3}
μ (Cu $K\alpha$)	0.28265 mm^{-1}
crystal size	0.30 x 0.30 x 0.30 mm
crystal shape	prism
crystal color	pale yellow
diffractometer	Rigaku AFC-5R
radiation	Cu$K\alpha$ (λ = 1.541780 Å)
	graphite monochromatized rotating anode
temperature	200 K
2θ range	3 - 125°
number of unique reflections	4523
number of used reflections	4094 ($F > 3\sigma(F)$)
number of parameters	413
data correction	Lorenz and polarization effects
	no absorption, no extinction
structure analysis	direct method
refinement	block diagonal least squares methods
temperature factors	anisotropic (C and Si)
	isotropic (H, generated by calculation)
$R = \sum \|\|F_o\| - \|F_c\|\| / \sum \|F_o\|$	0.0733
$R_w = [\sum w(\|F_o\| - \|F_c\|)^2 / \sum \|F_o\|^2]^{1/2}$	0.0848

Preparation of Dilithium Hexasilyldimethylenecyclobutene Dianion (13).

The crystals of **12** (72 mg, 0.155 mmol) and lithium metal (30 mg, 4.3 mmol) were placed in a reaction tube with a magnetic stirrer. After degassing, dry oxygen-free DME (1.0 mL) was introduced by vacuum transfer and the mixture was stirred at room temperature to give a green solution of the dianion of **12** within 5 min. After the solvent was removed in vacuo, degassed hexane was introduced by vacuum transfer. Then, after the lithium metal was removed, the solution was cooled to afford green crystals of **13** quantitatively. ^{1}H NMR (C_7D_8) δ = -0.13 (s, 4 H, CH_2), 0.05 (s, 2 H, CH_2), 0.14 (s, 12 H, CH_3), 0.29 (s, 12 H, CH_3), 0.38 (s, 12 H, CH_3), 2.95 (s, 8 H, DME), 3.13 (s, 12 H, DME); ^{13}C NMR (C_7D_8) δ = 2.8 (CH_2), 3.6 (CH_3), 4.5 (CH_3), 5.3 (CH_3), 11.5 (CH_2), 59.7 (DME), 70.7 (DME), 74.4 (C), 84.4 (C), 180.6 (C); ^{29}Si NMR (C_7D_8) δ = -30.1, -13.3, -11.7; ^{7}Li NMR (C_7D_8) δ = 0.20.

X-ray Crystallography of Dilithium Hexasilyldimethylenecyclobutene Dianion (13)

Single crystal of **13** for X-ray diffractions was grown from a hexane solution. The X-ray crystallographic experiment of **13** was performed on a Rigaku-Denki AFC 5R diffractometer equipped with graphite-monochromatized Cu-*K*α radiation (λ = 1.54718 Å). Crystal data for **13** at 286 K: MF = $C_{29}H_{62}Li_2O_4Si_6$, MW = 657.20, triclinic, a = 12.040(2) Å, b = 16.367(2) Å, c = 11.509(1) Å, α = 92.91(1)°, β = 116.86(0)°, γ = 88.37(1)°,V = 2020.6(5) Å^3, space group = p_1-, Z = 2, D_{calcd} = 1.081 g/cm^3. The final R factor was 0.0434 (R_w = 0.0431) for 5449 reflections with $F_o > 3\sigma(F_o)$. The details of the X-ray experiment are given in Table 2-12.

Table 2-12. Detail of the X-ray Experiment for **13**

molecular formula	$C_{29}H_{62}Li_2O_4Si_6$
molecular weight	657.20
crystal system	triclinic
space group	P_1-
cell constants	a = 12.040(2) Å, b = 16.367(2) Å,
	c = 11.509(1) Å, α = 92.91(1)°,
	β = 97.94(2)°, γ = 88.37(1)°,
	V = 2020.6(5) Å^3
Z value	2
D_{calcd}	1.081 g cm^{-3}
μ (Cu $K\alpha$)	0.21716 mm^{-1}
crystal size	0.30 x 0.30 x 0.25 mm
crystal shape	prism
crystal color	green
diffractometer	Rigaku AFC-5R
radiation	Cu$K\alpha$ (λ = 1.541780 Å)
	graphite monochromatized rotating anode
temperature	286 K
2θ range	3 - 125°
number of unique reflections	6406
number of used reflections	5449 ($F > 3\sigma(F)$)
number of parameters	619
data correction	Lorenz and polarization effects
	no absorption, no extinction
structure analysis	direct method
refinement	block diagonal least squares methods
temperature factors	anisotropic (C, Li, O, and Si)
	isotropic (H, generated by calculation)
$R = \sum \|\|F_o\| - \|F_c\|\| / \sum \|F_o\|$	0.0434
$R_w = [\sum w(\|F_o\| - \|F_c\|)^2 / \sum \|F_o\|^2]^{1/2}$	0.0431

Molecular Orbital Calculations.

PM3 calculations were performed by Power Macintosh 7600/200 with MACSPARTAN plus program (Ver. 1.1.7).[9] All the calculations were performed with the geometry optimization.

References

(1) G. Fraenkel and F. Qiu, *J. Am. Chem. Soc.*, **118,** 5828 (1996).

(2) (a) P. West, J. I. Purmort, and S. V. McKinley, *J. Am. Chem. Soc.*, **90,** 797 (1968). (b) T. B. Thompson and W. T. Ford, *J. Am. Chem. Soc.*, **101,** 5459 (1979). (c) S. Brownstein, S. Bywater, and D. J. Worsfold, *J. Organomet. Chem.*, **199,** 1 (1980). (d) M. Schlosser and M. Stähle, *Angew. Chem. Int., Ed, Engl.*, **19,** 487 (1980). (e) M. Stähle and M. Schlosser, *J. Organomet. Chem.*, **220,** 277 (1981). (f) R. Benn and A. Rufinska, *J. Organomet. Chem.*, **239,** C19 (1982). (g) H. Köster and E. Weiss, *Chem. Ber.*, **115,** 3422 (1982). (h) U. Schümann, E. Weiss, H. Dietrich, and W. Mahdi, *J. Organomet. Chem.*, **322,** 299 (1987).

(3) G. Boche, H. Etzrodt, M. Marsh, W. Massa, G. Baum, H. Dietrich, and W. Mahdi, *Angew. Chem. Int., Ed. Engl.*, **98,** 104 (1986).

(4) G. Boche, G. Fraenkl, J. Cabral, K. Harms, N. J. P. van Eikema-Hommes, J. Lohrenz, M. Marsch, and P. v. R. Schleyer, *J. Am. Chem. Soc.*, **114,** 1562 (1992).

(5) (a) W. Reppe, O. Schlichting, K. Klager, and T. Toepel, *Ann. Chem.*, **560,** 1 (1948). (b) W. Reppe and W. J. Schweckendiek, *Ann. Chem.*, **560,** 104 (1948).

(6) (a) H. Sakurai, Y. Nakadaira, A. Hosomi, Y. Eriyama, K. Hirama, and C. Kabuto, *J. Am. Chem. Soc.*, **106,** 8316 (1984). (b) H. Sakurai, K. Hirama, Y. Nakadaira, and C. Kabuto, *Chem. Lett.*, **1988,** 485. (c) H. Sakurai, K. Hirama, Y. Nakadaira, and C. Kabuto, *J. Am. Chem. Soc.*, **109,** 6880 (1987). (d) H. Sakurai, *Nippon Kagaku Kaishi,* **1990,** 439. (e) H. Sakurai, *Pure Appl. Chem.*, **68,** 327 (1996).

(7) H. Sakurai, T. Fujii, and K. Sakamoto, *Chem. Lett.*, **1992,** 339.

(8) H. J. Bruins Slot, J. Kroon, J. M. Oostween, H. J. T. Bos, and P. Vermeer, *Cryst. Struc. Comm.*, **11,** 741 (1982).

(9) J. J. P. Stewart, *J. Comput. Chem.*, **10,** 209 (1989).

(10) E. Kloster-Jensen and G. A. Eliassen, *Angew. Chem., Int. Ed. Engl.*, **24,** 565 (1985).

Chapter 3

Silyl-Substituted [4]Radialene Dianion with 8C / 10π-Electron System

Summary

The intramolecular reaction of 3,3,5,5,8,8,10,10,13,13,15,15,18,18,20,20-hexadecamethyl-3,5,8,10,13,15,18,20-octasilacycloicosa-1,6,11,16-tetrayne (**14**) with three molar amount of $[Mn(CO)_3(Me\text{-}Cp)]$ in THF under photochemical and refluxing conditions produced octasilyl[4]radialene derivative (**15**). The reaction of **15** with alkali metals (Li, Na, and K) in THF gave dialkali metal salts of the corresponding dianion (**16**) with 8 center / 10π-electron system. The molecular structure of dilithium salt of octasilyl[4]radialene dianion (**16a**) has been established by X-ray crystallography. The two lithium atoms are located above and below the π-skeleton and are bonded to the carbon atoms of the radialene framework to give a bis-CIP structure. The structural parameters of **16a** are discussed in comparison to those of **15**. The structure of **16a** in solution has also been discussed on the basis of NMR spectroscopic data. The two Li^+ ions of **16a** are not fixed to the π-skeleton in toluene-d_8, but are fluxional, giving a symmetric structure (bis-CIP) on the NMR time scale. In a solvating medium such as THF-d_8, one of the Li^+ ions dissociates to yield an ion pair (CIP and SSIP). Some evidence for the Li^+ ion walk on the π-skeleton is demonstrated.

Introduction

Over the last few years, structural studies of various anions, which can be either a solvent-separated ion pair (SSIP) or solvent-shared contact ion pair (CIP), have been reported in both crystals and solution states.[1] The ligand which coordinates or solvates to counter cation, is an important factor for the determination of crystal structure of anion species.

For example, tetraphenylbutadiene disodium dimethoxyethane complex, solvent-shared and solvent-separated ion triples within single crystal has been reported by Bock et al. (Figure 3-1).[2] The crystal contains a stoichiometric 1:1 ratio both as a solvent-shared contact ion triple, $[C_{28}H_{22}^{2-}\{Na^{+}(H_3COCH_2CH_2OCH_3)_2\}_2]$, and as a solvent-separated ion triple, $[C_{28}H_{22}^{2-}][\{Na^{+}(H_3COCH_2CH_2OCH_3)_3\}_2]$.

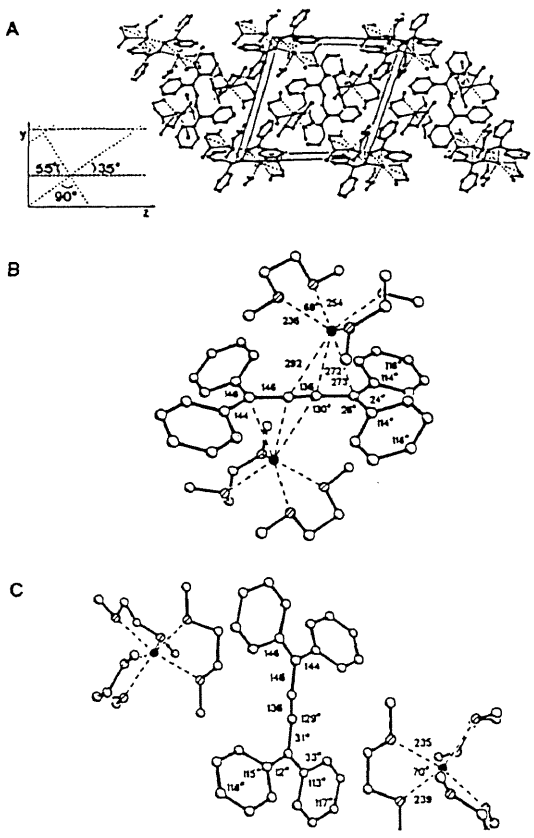

Figure 3-1. Crystal structure of disodium tetraphenylbutadiene dianion.

More recently, the competing Na^+ solvation, ether-shared and ether-separated triple ions of perylene dianion ($C_{20}H_{10}^{2-}$) has also been reported by Bock et al. (Figure 3-2).[3] Disodium salt of perylene dianion tetrakis(dimethoxyethane) [$C_{20}H_{10}^{2-}\{Na^+(H_3COCH_2CH_2OCH_3)_2\}_2$] (A) shows a solvent-shared triple ion with an η^6-half-sandwich sodium π-coordination to the perylene dianion. Disodium perylene dianion bis(tetraglyme) [$C_{20}H_{10}^{2-}\{Na^+(H_3CO(CH_2CH_2O)_4CH_3)\}_2$] (B) exhibits an another solvent-shared triple ion but with an η^2 sodium (π/σ)-coordination to the perylene dianion rim. Disodium perylene dianion tetrakis(triglyme) complex [$C_{20}H_{10}^{2-}$] [$\{Na^+(H_3CO(CH_2CH_2O)_2CH_3)\}_2$] (C) shows a solvent-separated triple ion of perylene dianion and two sodium bis(triglyme) countercations.

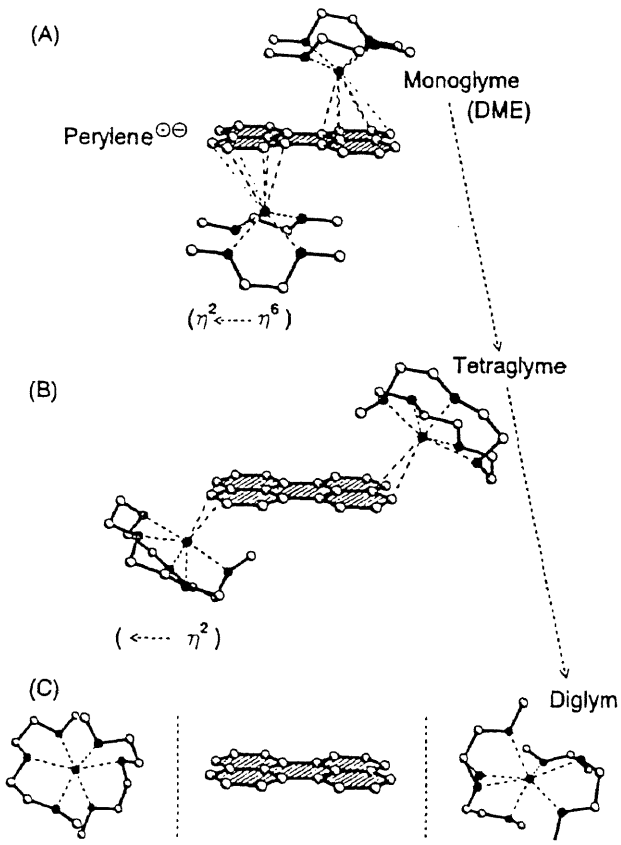

Figure 3-2. Crystal structure of disodium perylene dianion.

The polarity of the solvent has also been recognized as important factor for the SSIP and CIP formations in solution. However, in most of these systems, the dynamic behavior of the counter cation in solution has not been made clear.[4]

In this chapter, synthesis, characterization, and evidence for a lithium walk on the π-skeleton of the dilithium octasilyl[4]radialene dianion as a new silyl-substituted 8C / 10 π-electron system are described.

Synthesis of Octasilyl[4]radialene 15

Radialene (permethylenecycloalkane) has received considerable attention due to its special arrangement of π-electrons. Various radialene derivatives have been reported thus far, but the synthetic methods are still very limited.[5] The silyl-substituted radialene derivative is hitherto unknown. In chapter 2, the intramolecular cyclotrimerization of the silacyclotriyne with manganese complex was described. The persilylated [4]radialene derivative (**15**) has been synthesized in a similar manner via the intramolecular cyclization of 3,3,5,5,8,8,10,10,13,13,15,15,18,18,20,20-hexadecamethyl-3,5,8,10,13,15,18,20-octasilacycloicosa-1,6,11,16-tetrayne (**14**) with $[Mn(CO)_3(Me\text{-}Cp)]$.

The macrocyclic tetrayne (**14**) bridged by $Me_2SiCH_2SiMe_2$ was prepared by the coupling reaction of the respective bis(chlorosilane) with bis(ethynyl) Grignard reagent in 25% yield (Scheme 3-1).

Scheme 3-1

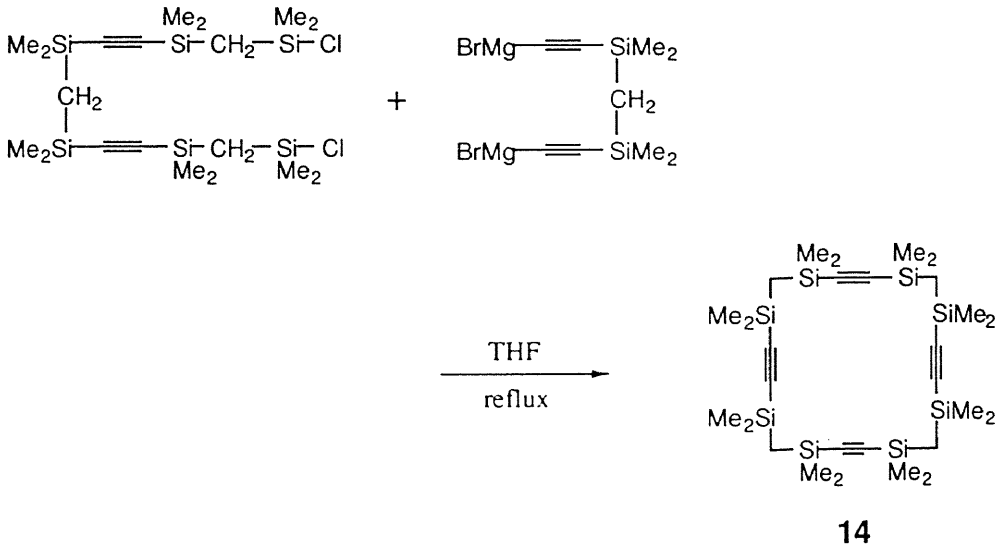

14

A mixture of the macrocyclic tetrayne (**14**) and three molar amounts of [$Mn(CO)_3$ (Me-Cp)] in THF was irradiated with a 500 W high-pressure mercury lamp under the refluxing temperature of THF to produce yellow crystals of the persilylated [4]radialene (**15**) in 11% yield (Scheme 3-2). The reaction may involve disilylvinylidene complex as a reactive intermediate.[6] The reaction mechanism to produce **15** remains unclear; nevertheless, a quadruple 1,2-silyl shift must be involved for the formation of **15**. The possible mechanism of intramolecular cyclotetramerization is shown in Scheme 3-3. Compound **15** is a first example of the formation of [4]radialene via the tetramerization of acetylene units.

Scheme 3-2

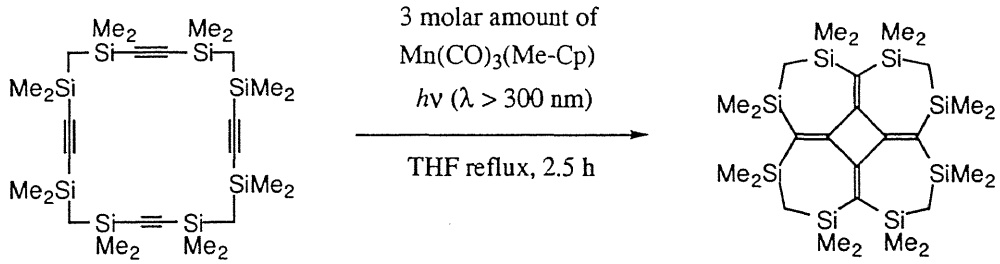

14 **15**

Scheme 3-3

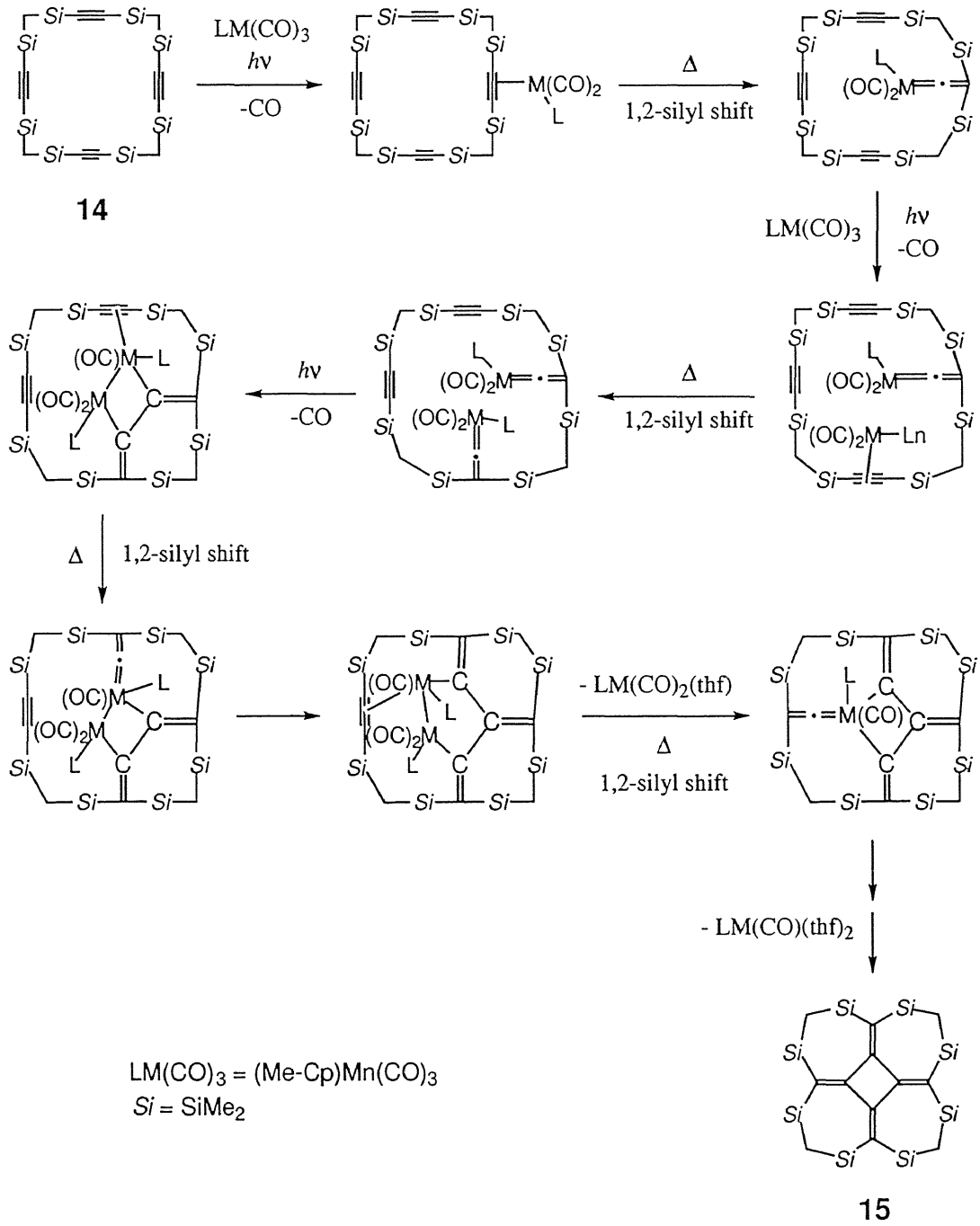
LM(CO)3
hν
-CO
Δ
1,2-silyl shift
14
LM(CO)3
hν
-CO
Δ
1,2-silyl shift
hν
-CO
Δ
1,2-silyl shift
- LM(CO)2(thf)
Δ
1,2-silyl shift
- LM(CO)(thf)2
15
LM(CO)3 = (Me-Cp)Mn(CO)3
Si = SiMe2

Molecular Structure of Octasilyl[4]radialene 15

Octasilyl[4]radialene **15** bridged by silmethylene chains could be recrystallized from ethanol. [4]Radialene has a particular arrangement of 8π-electrons with a symmetric framework. The molecular structure of **15** was unequivocally confirmed by X-ray crystallography. The ORTEP drawing of **15** is shown in Figure 3-3. The crystal packing of **15** is also shown in Figure 3-4. The final atomic parameters of **15** are listed in Tables 3-1 and 3-2. The bond lengths of **15** are summarized in Tables 3-3 and 3-4. The bond angles of **15** are also summarized in Table 3-5.

The central four-membered ring of **15** is not planar, but has a considerably distorted conformation with a puckered angle of 32.5°. The puckered angle of **15** is similar to those of reported: 26.5° for perchloro- and 34.7° for perphenyl-substituted [4]radialenes.[5f, 7] The selected bond angles of **15** are shown in Figure 3-5. The internal bond angles of the four-membered ring of **15** range form 87.6(4) to 87.9(4)° (av 87.7°), and the sum of the bond angles is 357.8°.

The selected bond lengths of **15** are also shown in Figure 3-6. The appreciable bond alternation between the single and double bonds of the π-skeleton of **15** shows the structural feature as a cross-conjugated diene. The C-C single and double bond lengths are 1.517(9)-1.523(9) Å (av 1.520 Å) and 1.333(9)-1.361(9) Å (av 1.350 Å), respectively. The four seven-membered rings containing the $Me_2SiCH_2SiMe_2$ fragments have twist and boat conformations.

NMR data of **15** show a highly symmetric structure in solution on the NMR time scale. Thus, in the ^1H NMR spectrum of **15**, only one signal is found at 0.14 and 0.04 ppm for the methyl and methylene protons, respectively. In the ^{13}C NMR spectrum, the signal is observed at 2.1 and 10.8 ppm for the methyl and methylene carbon atoms, respectively. The endocyclic and exocyclic quaternary ^{13}C NMR signals appear at 134.7 and 167.5 ppm. Only one ^{29}Si signal is observed at -7.8 ppm.

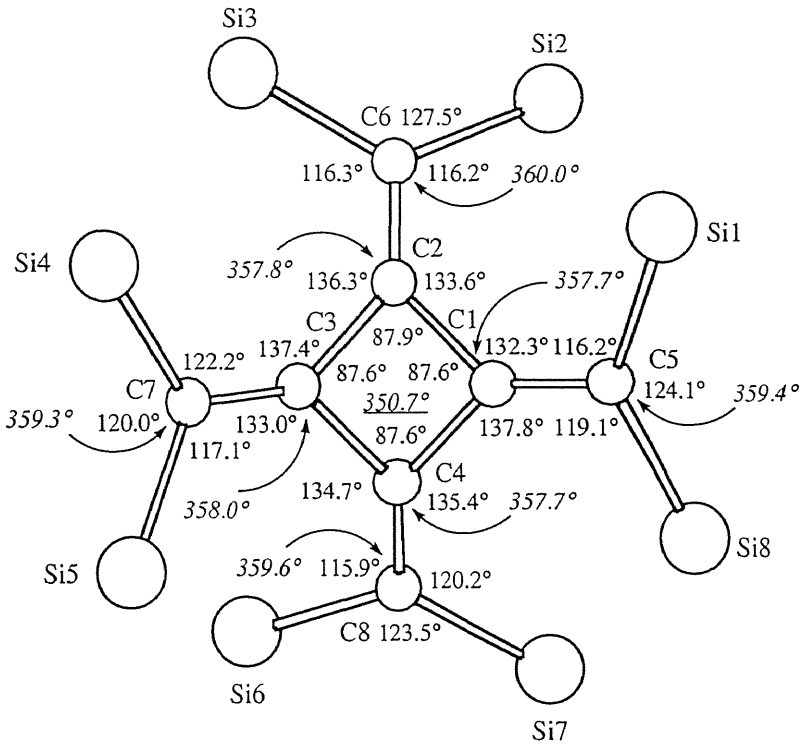

Figure 3-5. Selected bond angles of **15**.

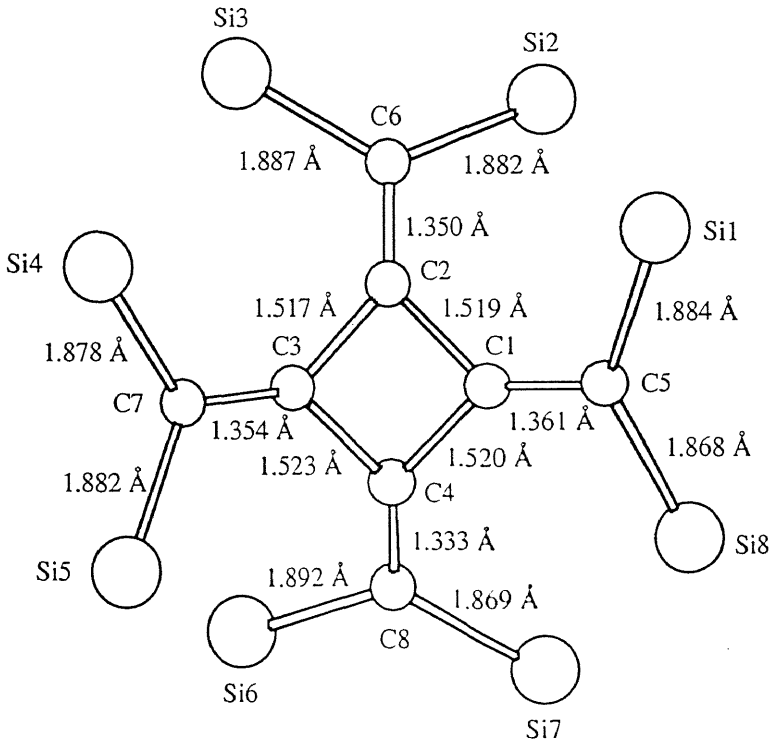

Figure 3-6. Selected bond lengths of **15**.

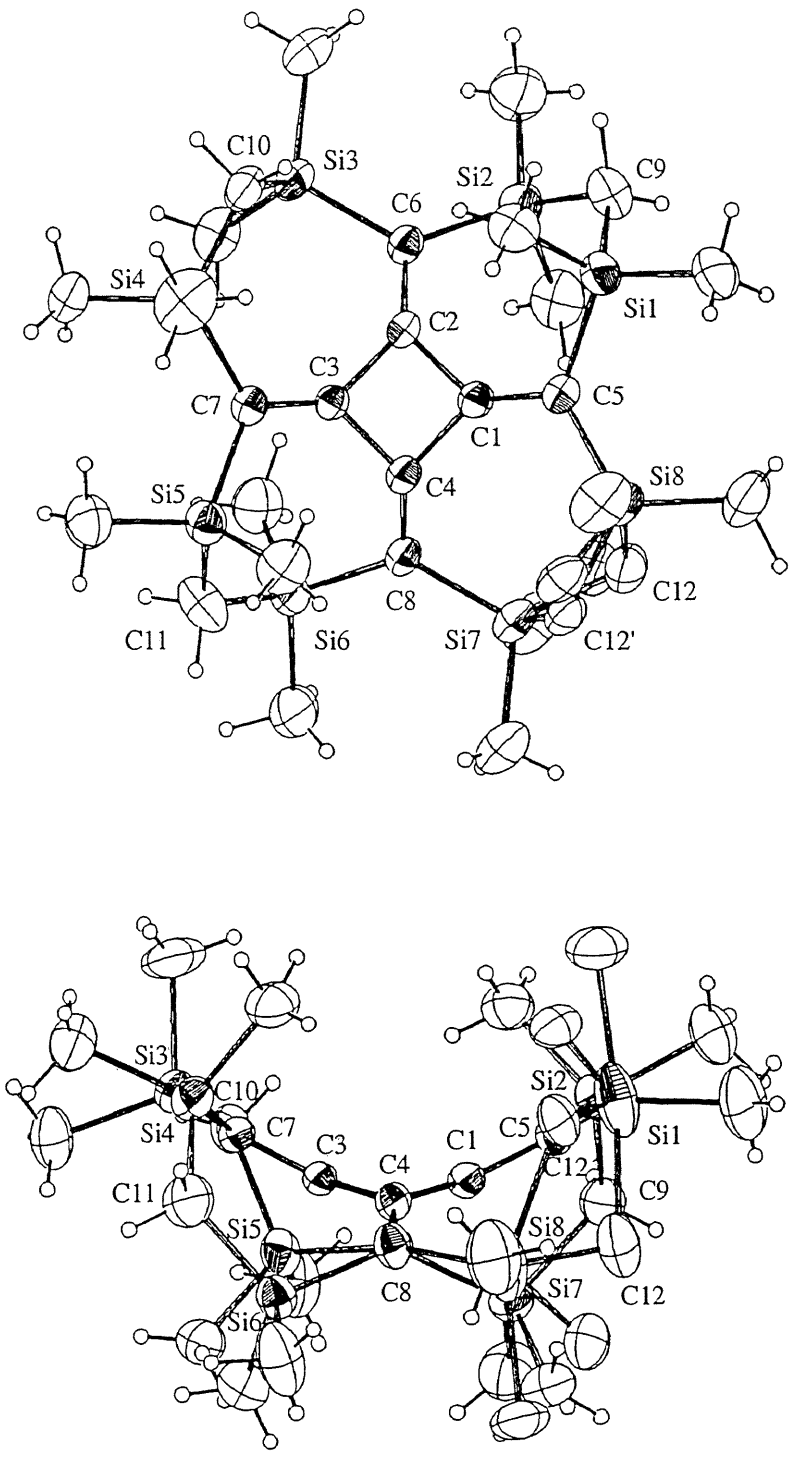

Figure 3-3. ORTEP drawing of molecule **15**: upper, top view; below, side view.

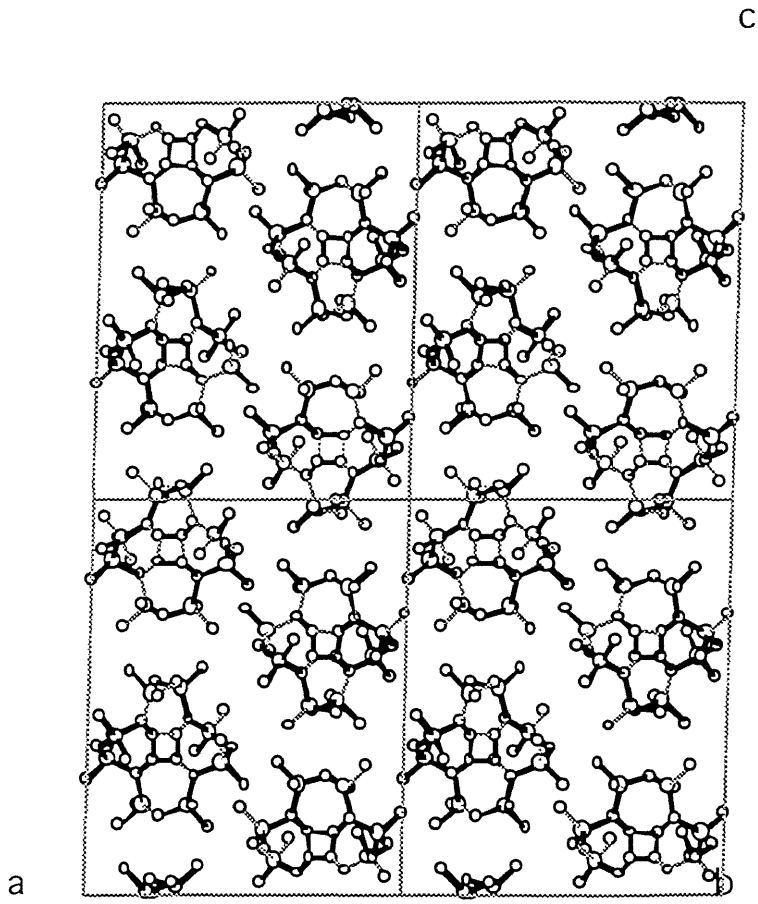

Figure 3-4. Crystal packing of **15**.

Table 3-1. Atomic Parameters[a] for Non-Hydrogen Atoms of **15**

ATOM	X	Y	Z	BEQV
SI1	4338(1)	658(3)	1660(1)	5.1
SI2	3940(1)	-2178(3)	895(1)	5.6
SI3	2959(1)	-741(3)	-223(1)	5.2
SI4	2050(1)	2182(2)	-86(1)	5.3
SI5	957(1)	2350(2)	989(1)	5.4
SI6	711(1)	-786(3)	1574(1)	5.2
SI7	1819(1)	-1046(4)	2717(1)	8.2
SI8	3250(1)	876(4)	2770(1)	8.7
C 1	2908(3)	27(7)	1621(3)	3.8
C 2	2864(3)	-149(7)	959(2)	3.7
C 3	2135(3)	543(7)	972(2)	3.5
C 4	2105(3)	65(7)	1610(3)	4.0
C 5	3449(3)	400(8)	1996(3)	4.4
C 6	3234(3)	-940(7)	573(3)	4.2
C 7	1747(3)	1493(7)	641(3)	4.1
C 8	1601(3)	-463(8)	1948(3)	4.7
C 9	4625(4)	-1045(9)	1286(4)	6.5
C10	2855(4)	1271(9)	-347(3)	5.8
C11	350(4)	959(11)	1278(5)	8.0
C21	5054(4)	1185(12)	2207(4)	8.3
C22	4273(4)	2221(10)	1135(4)	6.9
C23	3505(5)	-3447(10)	1421(4)	7.9
C24	4375(6)	-3397(12)	354(4)	9.2
C25	2117(5)	-1735(10)	-392(4)	7.1
C26	3630(5)	-1426(13)	-729(4)	9.1
C27	2245(6)	4175(10)	-15(5)	9.6
C28	1338(5)	1911(12)	-665(4)	8.0
C29	430(5)	3583(11)	482(4)	8.3
C30	1301(5)	3538(10)	1591(4)	7.9
C31	850(5)	-2143(11)	980(4)	8.1
C32	32(5)	-1565(15)	2068(4)	10.1
C33	1126(6)	-689(15)	3228(4)	10.4
C34	3933(6)	392(15)	3309(4)	10.4
C35	2379(10)	-2521(22)	2801(7)	7.8
C36	1631(11)	-3409(19)	2709(8)	8.2
C37	2668(12)	2280(22)	2881(8)	6.4
C38	3407(10)	3215(16)	2757(7)	8.8
C12	2699(9)	-1188(24)	2987(7)	7.7
C12'	2355(8)	928(19)	2997(6)	5.7

[a] Positional parameters are multiplied by 10^4. Thermal parameters are given by the equivalent temperature factors (A^2).

Table 3-2. Atomic Parameters[a] for Hydrogen Atoms of **15**

ATOM	X	Y	Z	B
H(C 9)1	499(4)	-74(9)	94(3)	9.9(2.3)
H(C 9)2	480(4)	-162(8)	154(3)	7.8(2.0)
H(C10)1	326(3)	178(7)	-22(3)	5.8(1.7)
H(C10)2	287(3)	158(8)	-77(3)	7.2(1.9)
H(C11)1	2(4)	153(10)	155(4)	10.9(2.6)
H(C11)2	4(3)	73(8)	96(3)	7.0(1.8)
H(C21)1	550(4)	131(8)	201(3)	8.5(2.0)
H(C21)2	491(4)	204(9)	239(4)	9.4(2.3)
H(C21)3	514(4)	33(10)	250(4)	10.3(2.4)
H(C22)1	404(4)	194(9)	80(3)	9.4(2.3)
H(C22)2	401(4)	287(9)	124(3)	9.2(2.2)
H(C22)3	473(4)	256(9)	98(3)	9.4(2.3)
H(C23)1	315(4)	-402(9)	122(3)	9.1(2.2)
H(C23)2	385(4)	-414(10)	152(4)	11.0(2.6)
H(C23)3	328(4)	-284(10)	176(4)	11.7(2.7)
H(C24)1	475(4)	-255(9)	11(3)	8.4(2.1)
H(C24)2	463(4)	-414(9)	58(3)	10.1(2.4)
H(C24)3	407(5)	-386(11)	10(4)	13.2(3.0)
H(C25)1	177(4)	-181(9)	-11(3)	10.2(2.4)
H(C25)2	192(4)	-148(10)	-75(4)	10.7(2.5)
H(C25)3	229(5)	-274(12)	-45(4)	14.5(3.3)
H(C26)1	374(4)	-246(8)	-73(3)	8.2(2.0)
H(C26)2	351(4)	-112(9)	-112(3)	9.8(2.4)
H(C26)3	414(4)	-94(9)	-63(3)	8.6(2.1)
H(C27)1	241(4)	470(9)	-36(3)	9.0(2.2)
H(C27)2	185(5)	474(12)	17(4)	15.8(3.6)
H(C27)3	262(5)	427(12)	25(4)	15.0(3.3)
H(C28)1	158(4)	191(9)	-101(3)	10.0(2.4)
H(C28)2	104(4)	122(9)	-55(3)	9.2(2.3)
H(C28)3	104(5)	285(13)	-66(5)	16.0(3.6)
H(C29)1	79(4)	419(8)	24(3)	8.1(2.0)
H(C29)2	15(4)	297(8)	22(3)	7.7(2.0)
H(C29)3	11(5)	414(11)	74(4)	12.7(3.0)
H(C30)1	103(4)	437(10)	163(3)	9.9(2.4)
H(C30)2	127(5)	317(12)	190(4)	14.2(3.3)
H(C30)3	177(4)	409(10)	150(4)	11.5(2.7)
H(C31)1	85(5)	-307(11)	112(4)	12.3(2.9)
H(C31)2	52(4)	-206(10)	70(4)	11.2(2.6)
H(C31)3	135(4)	-199(10)	80(4)	11.8(2.7)
H(C32)1	-43(5)	-136(10)	183(4)	11.9(2.8)
H(C32)2	12(5)	-246(11)	203(4)	13.2(3.0)
H(C32)3	5(5)	-119(10)	241(4)	12.2(2.8)
H(C33)1	128(4)	-68(9)	357(3)	9.5(2.3)
H(C33)2	94(5)	7(11)	314(4)	11.9(2.8)
H(C33)3	81(6)	-149(14)	319(5)	19.3(4.5)
H(C34)1	376(5)	36(11)	376(4)	13.0(2.9)
H(C34)2	399(6)	-46(15)	327(5)	19.2(4.4)
H(C34)3	434(5)	82(12)	331(4)	15.2(3.5)

[a] Positional parameters are multiplied by 10^4. Thermal parameters are given by the equivalent temperature factors (A^2).

Table 3-3. List of Bond Lengths (Å) for Non-Hydrogen Atoms of **15**

ATOM		ATOM		LENGTH(SIG)
SI1	-	C 5	=	1.884(7)
SI1	-	C 9	=	1.859(9)
SI1	-	C21	=	1.880(12)
SI1	-	C22	=	1.864(9)
SI2	-	C 6	=	1.882(7)
SI2	-	C 9	=	1.865(9)
SI2	-	C23	=	1.874(9)
SI2	-	C24	=	1.867(10)
SI3	-	C 6	=	1.887(7)
SI3	-	C10	=	1.864(9)
SI3	-	C25	=	1.864(9)
SI3	-	C26	=	1.849(12)
SI4	-	C 7	=	1.878(7)
SI4	-	C10	=	1.848(9)
SI4	-	C27	=	1.858(12)
SI4	-	C28	=	1.878(10)
SI5	-	C 7	=	1.882(7)
SI5	-	C11	=	1.845(10)
SI5	-	C29	=	1.880(10)
SI5	-	C30	=	1.853(9)
SI6	-	C 8	=	1.892(7)
SI6	-	C11	=	1.850(10)
SI6	-	C31	=	1.860(9)
SI6	-	C32	=	1.872(13)
SI7	-	C 8	=	1.869(9)
SI7	-	C33	=	1.809(15)
SI7	-	C35	=	1.719(21)
SI7	-	C36	=	2.181(21)
SI7	-	C12	=	1.765(21)
SI7	-	C12'	=	2.152(18)
SI8	-	C 5	=	1.868(7)
SI8	-	C34	=	1.814(13)
SI8	-	C37	=	1.711(23)
SI8	-	C38	=	2.151(20)
SI8	-	C12	=	2.212(21)
SI8	-	C12'	=	1.788(18)
C 1	-	C 2	=	1.519(9)
C 1	-	C 3	=	2.107(9)
C 1	-	C 4	=	1.520(9)
C 1	-	C 5	=	1.361(9)
C 2	-	C 3	=	1.517(9)
C 2	-	C 4	=	2.103(9)
C 2	-	C 6	=	1.350(9)
C 3	-	C 4	=	1.523(9)
C 3	-	C 7	=	1.354(9)
C 4	-	C 8	=	1.333(9)

Table 3-4. List of Bond Lengths (Å) for Hydrogen Atoms of **15**

ATOM	-	ATOM		LENGTH(SIG)
C 9	-	H(C 9)1	=	1.10(8)
C 9	-	H(C 9)2	=	0.85(7)
C10	-	H(C10)1	=	0.92(6)
C10	-	H(C10)2	=	1.00(7)
C11	-	H(C11)1	=	1.02(8)
C11	-	H(C11)2	=	0.94(7)
C21	-	H(C21)1	=	0.98(7)
C21	-	H(C21)2	=	0.92(8)
C21	-	H(C21)3	=	1.03(8)
C22	-	H(C22)1	=	0.90(8)
C22	-	H(C22)2	=	0.80(8)
C22	-	H(C22)3	=	0.99(8)
C23	-	H(C23)1	=	0.96(8)
C23	-	H(C23)2	=	0.93(9)
C23	-	H(C23)3	=	1.04(9)
C24	-	H(C24)1	=	1.20(7)
C24	-	H(C24)2	=	0.97(8)
C24	-	H(C24)3	=	0.91(10)
C25	-	H(C25)1	=	0.95(8)
C25	-	H(C25)2	=	0.92(8)
C25	-	H(C25)3	=	0.98(10)
C26	-	H(C26)1	=	0.96(7)
C26	-	H(C26)2	=	0.96(8)
C26	-	H(C26)3	=	1.08(7)
C27	-	H(C27)1	=	0.98(7)
C27	-	H(C27)2	=	1.01(11)
C27	-	H(C27)3	=	0.92(11)
C28	-	H(C28)1	=	0.93(8)
C28	-	H(C28)2	=	0.90(8)
C28	-	H(C28)3	=	1.03(11)
C29	-	H(C29)1	=	1.05(7)
C29	-	H(C29)2	=	0.97(7)
C29	-	H(C29)3	=	0.99(10)
C30	-	H(C30)1	=	0.92(8)
C30	-	H(C30)2	=	0.79(10)
C30	-	H(C30)3	=	1.05(9)
C31	-	H(C31)1	=	0.90(9)
C31	-	H(C31)2	=	0.88(9)
C31	-	H(C31)3	=	1.05(9)
C32	-	H(C32)1	=	1.04(9)
C32	-	H(C32)2	=	0.84(10)
C32	-	H(C32)3	=	0.84(9)
C33	-	H(C33)1	=	0.84(8)
C33	-	H(C33)2	=	0.80(9)
C33	-	H(C33)3	=	0.94(13)
C34	-	H(C34)1	=	1.09(10)
C34	-	H(C34)2	=	0.79(13)
C34	-	H(C34)3	=	0.86(11)

Table 3-5. List of Bond Angles (Å) for Non-Hydrogen Atoms of **15**

ATOM -	ATOM	ATOM	ANGLE(SIG)
C 5 -	SI1 -	C 9 =	111.0(3)
C 5 -	SI1 -	C21 =	113.4(4)
C 5 -	SI1 -	C22 =	108.2(3)
C 9 -	SI1 -	C21 =	107.7(4)
C 9 -	SI1 -	C22 =	110.9(4)
C21 -	SI1 -	C22 =	105.5(4)
C 6 -	SI2 -	C 9 =	109.4(3)
C 6 -	SI2 -	C23 =	107.4(3)
C 6 -	SI2 -	C24 =	114.8(4)
C 9 -	SI2 -	C23 =	110.2(4)
C 9 -	SI2 -	C24 =	109.4(4)
C23 -	SI2 -	C24 =	105.4(4)
C 6 -	SI3 -	C10 =	105.4(3)
C 6 -	SI3 -	C25 =	111.5(3)
C 6 -	SI3 -	C26 =	113.1(4)
C10 -	SI3 -	C25 =	111.1(4)
C10 -	SI3 -	C26 =	107.9(4)
C25 -	SI3 -	C26 =	107.8(4)
C 7 -	SI4 -	C10 =	114.1(3)
C 7 -	SI4 -	C27 =	108.3(4)
C 7 -	SI4 -	C28 =	110.3(4)
C10 -	SI4 -	C27 =	107.6(4)
C10 -	SI4 -	C28 =	107.3(4)
C27 -	SI4 -	C28 =	109.1(5)
C 7 -	SI5 -	C11 =	112.1(3)
C 7 -	SI5 -	C29 =	113.7(3)
C 7 -	SI5 -	C30 =	106.8(3)
C11 -	SI5 -	C29 =	107.7(4)
C11 -	SI5 -	C30 =	110.2(4)
C29 -	SI5 -	C30 =	106.2(4)
C 8 -	SI6 -	C11 =	110.4(4)
C 8 -	SI6 -	C31 =	106.9(3)
C 8 -	SI6 -	C32 =	113.9(4)
C11 -	SI6 -	C31 =	111.2(4)
C11 -	SI6 -	C32 =	107.0(5)
C31 -	SI6 -	C32 =	107.5(5)
C 8 -	SI7 -	C33 =	114.1(5)
C 8 -	SI7 -	C35 =	116.6(7)
C 8 -	SI7 -	C36 =	103.9(6)
C 8 -	SI7 -	C12 =	122.1(7)
C 8 -	SI7 -	C12'=	97.6(5)
C33 -	SI7 -	C35 =	121.6(8)
C33 -	SI7 -	C36 =	93.5(7)
C33 -	SI7 -	C12 =	118.9(8)
C33 -	SI7 -	C12'=	90.1(6)
C35 -	SI7 -	C36 =	48.0(8)
C35 -	SI7 -	C12 =	48.0(9)
C35 -	SI7 -	C12'=	109.6(8)
C36 -	SI7 -	C12 =	94.8(9)
C36 -	SI7 -	C12'=	154.4(7)
C12 -	SI7 -	C12'=	61.6(8)
C 5 -	SI8 -	C34 =	115.3(5)
C 5 -	SI8 -	C37 =	117.4(8)
C 5 -	SI8 -	C38 =	100.7(5)
C 5 -	SI8 -	C12 =	97.0(6)
C 5 -	SI8 -	C12'=	119.8(6)
C34 -	SI8 -	C37 =	122.1(8)
C34 -	SI8 -	C38 =	98.9(6)
C34 -	SI8 -	C12 =	88.5(7)

Table 3-5 (continued). List of Bond Angles (Å) for Non-Hydrogen Atoms of **15**

C34 -	SI8 -	C12'=	118.3(7)
C37 -	SI8 -	C38 =	49.6(9)
C37 -	SI8 -	C12 =	107.0(9)
C37 -	SI8 -	C12'=	47.0(9)
C38 -	SI8 -	C12 =	155.6(7)
C38 -	SI8 -	C12'=	96.3(7)
C12 -	SI8 -	C12'=	60.0(7)
C 2 -	C 1 -	C 3 =	46.0(3)
C 2 -	C 1 -	C 4 =	87.6(4)
C 2 -	C 1 -	C 5 =	132.3(6)
C 3 -	C 1 -	C 4 =	46.3(3)
C 3 -	C 1 -	C 5 =	152.1(5)
C 4 -	C 1 -	C 5 =	137.8(6)
C 1 -	C 2 -	C 3 =	87.9(4)
C 1 -	C 2 -	C 4 =	46.2(3)
C 1 -	C 2 -	C 6 =	133.6(6)
C 3 -	C 2 -	C 4 =	46.3(3)
C 3 -	C 2 -	C 6 =	136.3(6)
C 4 -	C 2 -	C 6 =	152.6(5)
C 1 -	C 3 -	C 2 =	46.1(3)
C 1 -	C 3 -	C 4 =	46.1(3)
C 1 -	C 3 -	C 7 =	153.1(5)
C 2 -	C 3 -	C 4 =	87.6(4)
C 2 -	C 3 -	C 7 =	137.4(5)
C 4 -	C 3 -	C 7 =	133.0(5)
C 1 -	C 4 -	C 2 =	46.2(3)
C 1 -	C 4 -	C 3 =	87.6(4)
C 1 -	C 4 -	C 8 =	135.4(6)
C 2 -	C 4 -	C 3 =	46.1(3)
C 2 -	C 4 -	C 8 =	152.7(5)
C 3 -	C 4 -	C 8 =	134.7(6)
SI1 -	C 5 -	SI8 =	124.1(3)
SI1 -	C 5 -	C 1'=	116.2(5)
SI8 -	C 5 -	C 1 =	119.1(5)
SI2 -	C 6 -	SI3 =	127.5(3)
SI2 -	C 6 -	C 2 =	116.2(5)
SI3 -	C 6 -	C 2 =	116.3(5)
SI4 -	C 7 -	SI5 =	120.0(3)
SI4 -	C 7 -	C 3 =	122.2(5)
SI5 -	C 7 -	C 3 =	117.1(4)
SI6 -	C 8 -	SI7 =	123.5(4)
SI6 -	C 8 -	C 4 =	115.9(5)
SI7 -	C 8 -	C 4 =	120.2(5)
SI1 -	C 9 -	SI2 =	118.3(4)
SI3 -	C10 -	SI4 =	118.5(4)
SI5 -	C11 -	SI6 =	119.5(5)
SI7 -	C12 -	SI8 =	107.9(10)
SI7 -	C12'-	SI8 =	109.6(8)

PM3 Calculation of Octasilyl[4]radialene 15

The geometry optimization of octasilyl[4]radialene **15** was carried out by PM3 calculation.[8] The calculated structure of **15** is shown in Figure 3-7. The LUMO of **15** is also shown in Figure 3-8. The geometry of **15** by the X-ray diffraction is well-reproduced by PM3 calculation. The selected bond angles and lengths of **15** calculated by PM3 are shown in Figures 3-9 and 3-10. The charge distribution of **15** is also shown in Figure 3-11.

The energy diagram of **15** calculated by PM3 is shown in Figure 3-12. The level of LUMO (-0.22 eV) is considerably stabilized by silyl groups. The schematic drawing of the LUMO of **15** is shown in Figure 3-13. In the LUMO, the exocyclic C-C double bonds (C1-C5, C2-C6, C3-C7, and C4-C8) are antibonding, while the endocyclic C-C single bonds (C1-C2, C2-C3, C3-C4, and C1-C4) are bonding. The π-MO coefficients at the exocyclic carbon atoms (C5, C6, C7, and C8) are larger than that of endocyclic carbon atoms (C1, C2, C3, and C4) as shown in Figure 3-13. Thus, two electron reduction of **15** may produce dianion species so that the negative charge may be largely delocalized on the exocyclic carbon atoms. The resulting dianion may be stabilized by eight silicon atoms (Si1, Si2, Si3, Si4, Si5, Si6, Si7, and Si8).

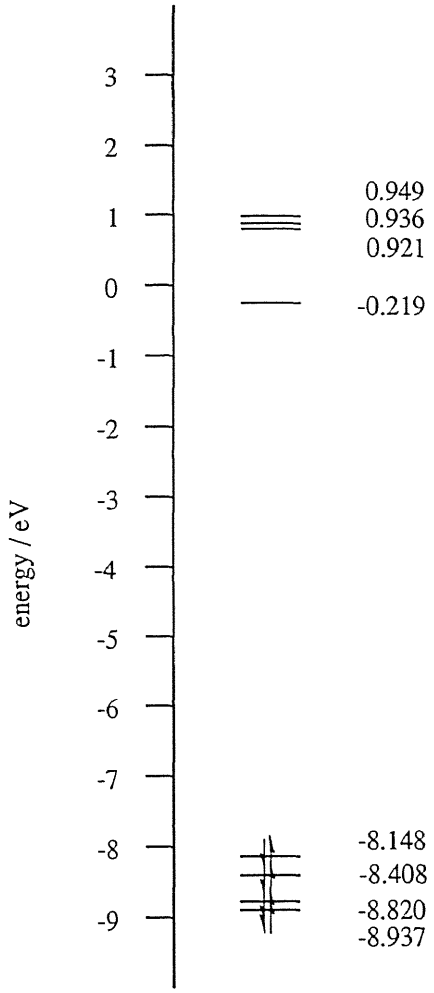

Figure 3-12. Energy diagram of **15** calculated by PM3.

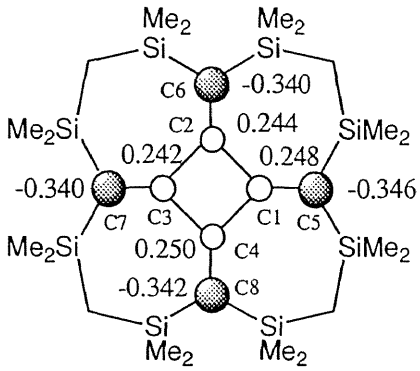

Figure 3-13. Schematic representation of the LUMO of **15** calculated by PM3.

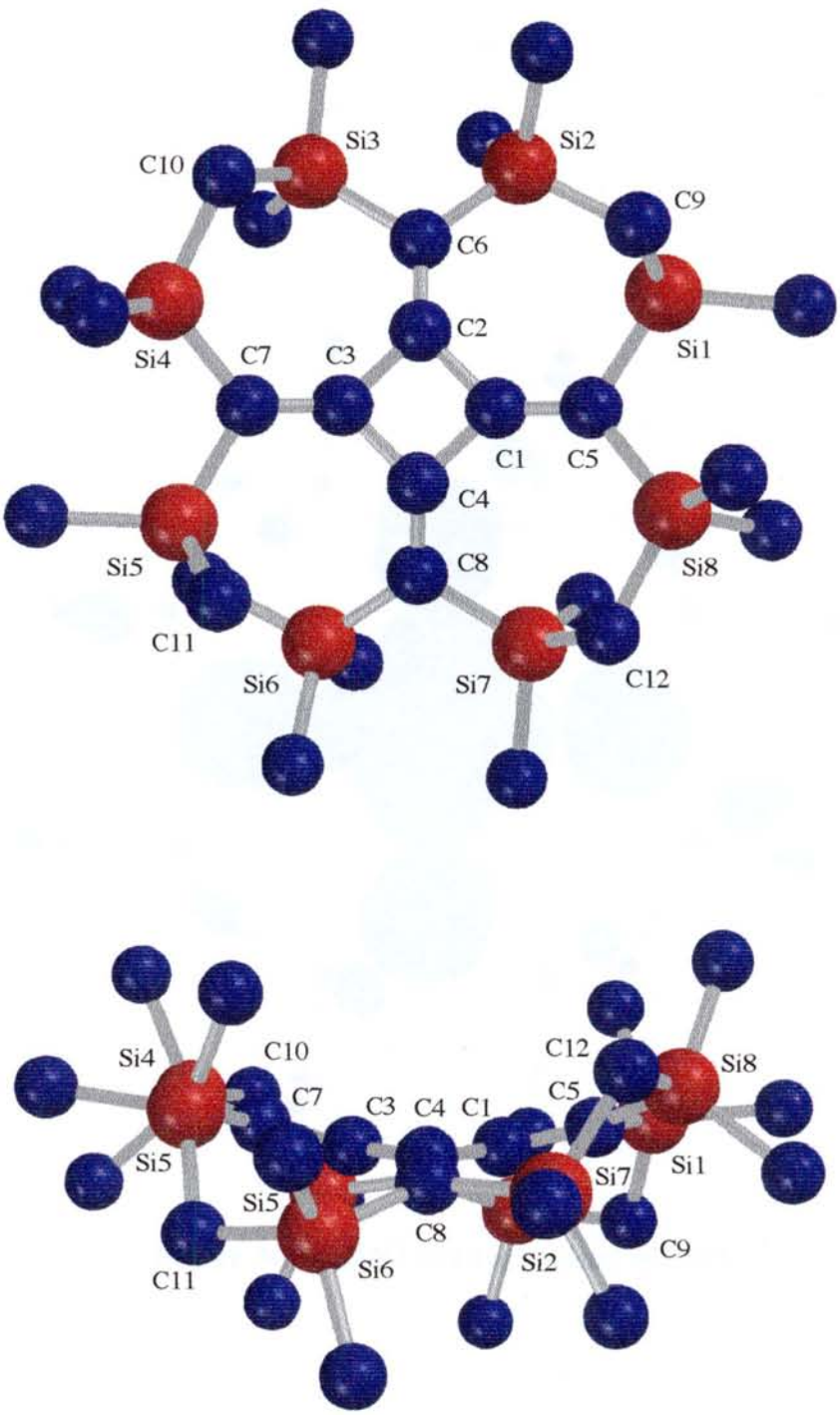

Figure 3-7. Calculated structure of **15** by PM3 (hydrogen atoms are omitted for the clarity): upper, top view; below, side view.

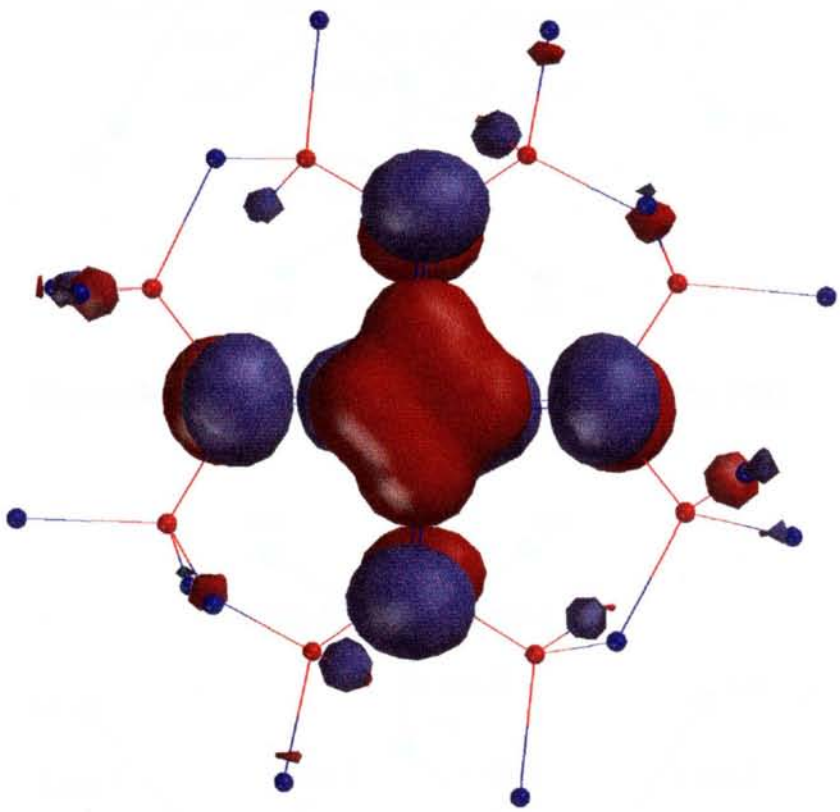

Figure 3-8. LUMO of **15** calculated by PM3.

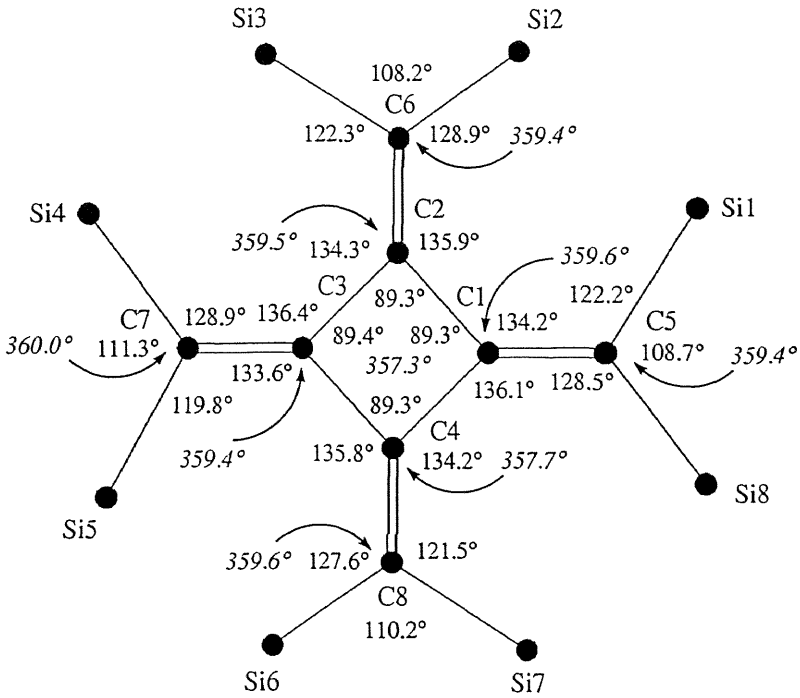

Figure 3-9. Selected bond angles of **15** calculated by PM3.

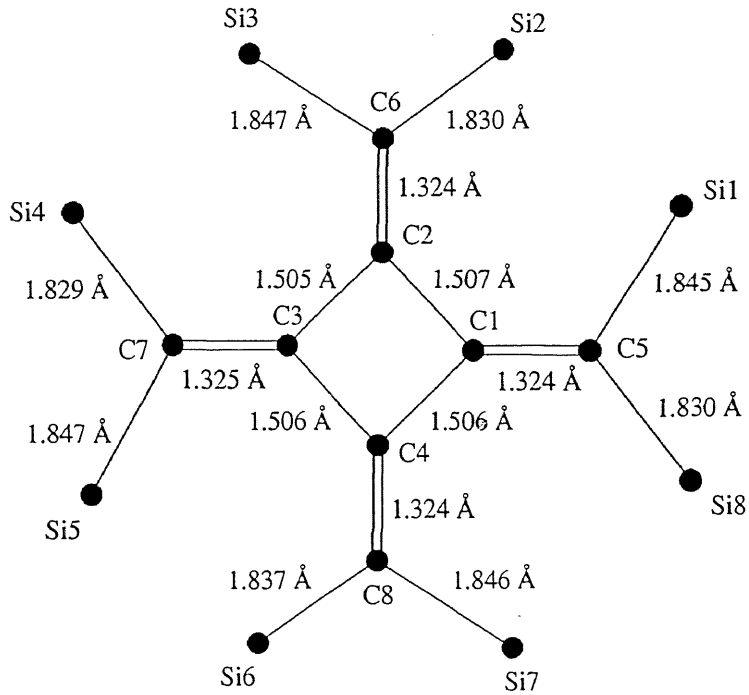

Figure 3-10. Selected bond lengths of **15** calculated by PM3.

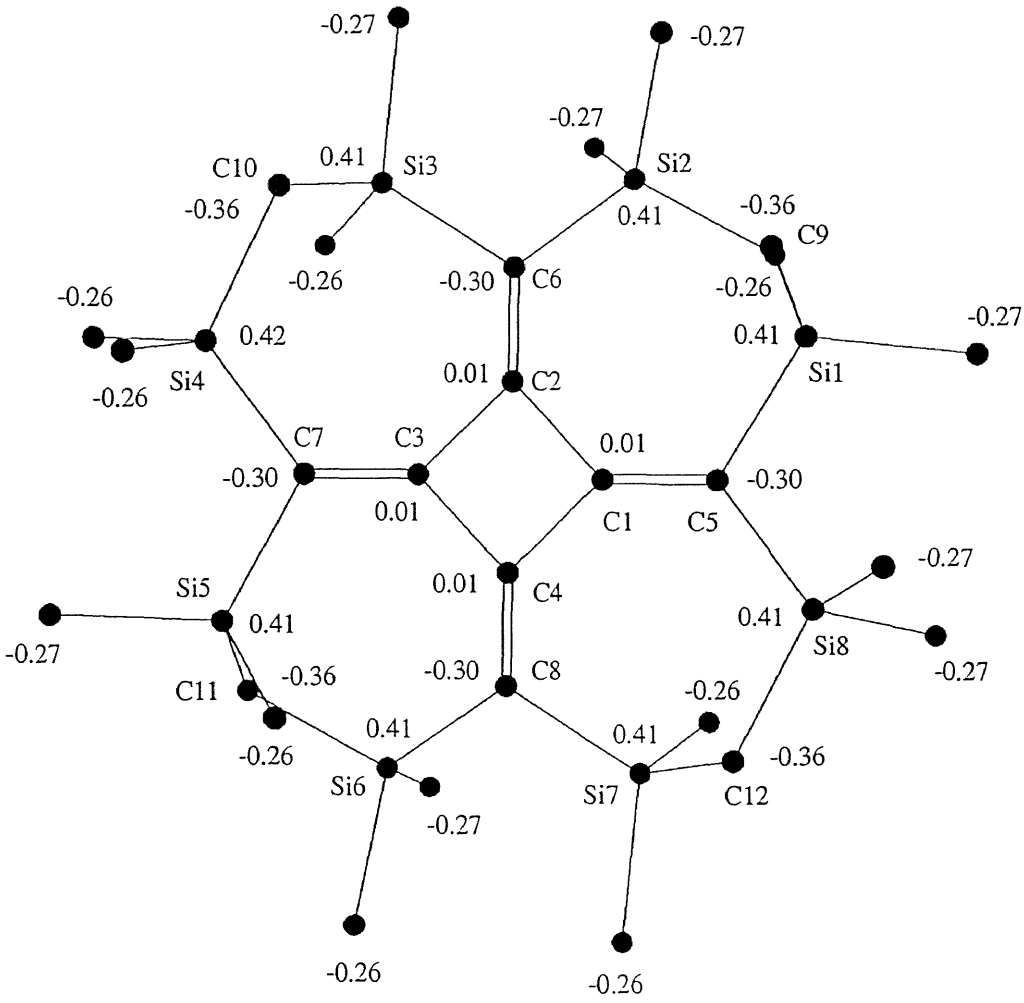

Figure 3-11. Mulliken charge distribution of 15 calculated by PM3.

Two Electron Reduction of Octasilyl[4]radialene 15 with Lithium Metal

[4]Radialene dianion resulting from the metalation of 1,2-dimethyl-3,4-bis-methylenecyclobutene with *n*-BuLi / KO^{t}Bu or *n*-BuLi / TMEDA has been reported, but it was characterized only by the quenching experiments (Scheme 3-4).[9]

Scheme 3-4

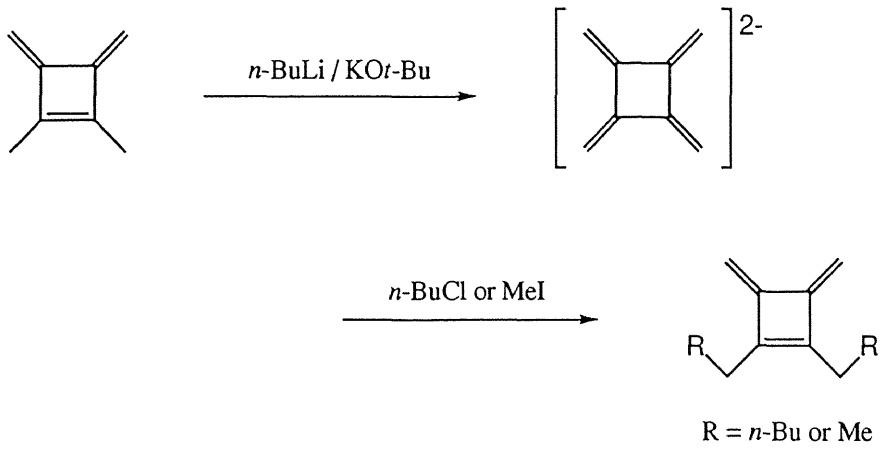

The reaction of **15** with excess of lithium metal in dry oxygen-free THF at room temperature led to the formation of a red solution of the dianion of **15** (Scheme 3-5). The two electron reduction occurred quantitatively and completed within 1 hour. After the solvent was removed in vacuo, dry degassed toluene was introduced by vacuum transfer. Crystallization from a toluene solution afforded air and moisture sensitive dark red crystals of the dilithium salt of the dianion (**16a**) containing two molecules of THF.

The [4]radialene derivative (**15**) underwent a two electron reduction not only by lithium, but also by sodium and potassium in THF to give red solutions of the dianions of **16b** (Na) and **16c** (K) within 1 hour (Scheme 3-5). The structures of **16a** (Li), **16b** (Na), and **16c** (K) were deduced by NMR spectroscopy as well as by X-ray diffraction for **16a** (Li, THF ligand).

Scheme 3-5

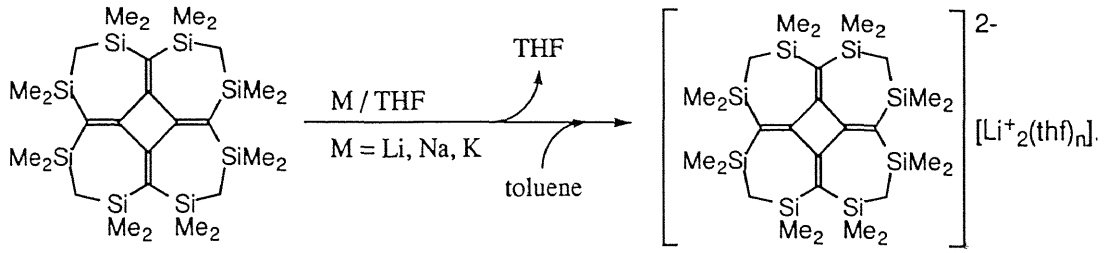

15

16a (Li)
16b (Na)
16c (K)

The reaction of **15** with excess lithium metal in dry oxygen-free DME at room temperature also gave the red solution of the dianion of **15** within 0.5 hour (Scheme 3-6). Crystallization from toluene afforded air and moisture sensitive dark red crystals of the dilithium salt of the dianion (**16a'**) containing four molecules of DME. The molecular structure of **16a'** (Li, DME ligand) was also unequivocally confirmed by X-ray crystallography.

Scheme 3-6

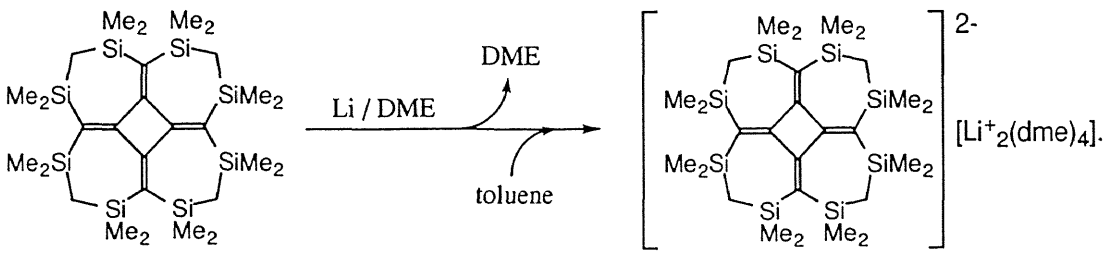

15

16a' (Li)

Molecular Structure of Dilithium Octasilyl[4]radialene Dianion 16a (THF Ligand)

Figure 3-14 shows the molecular structure of **16a** (THF ligand), which has confirmed by X-ray crystallography. The structure shows that the molecule has an inversion center at the center of the four-membered ring of C1-C2-C1*-C2*. The dilithium salt **16a** has a monomeric structure and forms contact ion pairs (bis-CIP) in the crystals. One THF molecule is coordinated to each lithium atom. The ORTEP drawing of **16a** is shown in Figure 3-15. The crystal packing of **16a** is also shown in Figure 3-16. The final atomic parameters of **16a** are listed in Tables 3-6 and 3-7. The atomic distances of **16a** are summarized in Tables 3-8 and 3-9. The bond angles of **16a** are also summarized in Table 3-10.

Several interesting features of the structures of **16a** can be pointed out. Two lithium atoms (Li1 and Li1*) are located up and below the ring, and are bonded to the four carbon atoms of the radialene skeleton as well as to the oxygen atoms of THF. The selected bond lengths of **16a** are shown in Figure 3-17. The distance between Li1 and the four carbon atoms (C1, C2, C3, and C4) ranges from 2.245(2) to 2.315(2) Å (av 2.279 Å). Two of the seven-membered rings, which lie opposite to each other in the projection shown in Figure 3-15 and and contain the $Me_2SiCH_2SiMe_2$ fragments, exhibit a twist conformation, and the other two exhibit a boat conformation.

Comparison of the structural features of **15** and **16a** is quite interesting. Eight carbon atoms of the π-skeleton of **16a** are almost coplanar, following a two-electron reduction due to the delocalization of the negative charge. The selected bond angles and lengths of **16a** are shown in Figures 3-18 and 3-19. The four-membered ring is planar and almost square, as determined by the internal bond angles of 89.8(1)-90.2(1)° (av 90.0°) and the sum of the bond angles (360.0°). The average length of the exocyclic bonds (C1–C3 and C2-C4) is elongated by about 0.06 Å relative to those of **15**

(1.350(9) Å (av) for **15** and 1.409(1) Å (av) for **16a**). In contrast, the average length of endocyclic bonds (C1-C2 and C1-C2*) is shortened by about 0.04 Å (1.520(9) Å (av) for **15** and 1.479(1) Å (av) for **16a**). Thus, the endocyclic bonds in **16a** are bonding, whereas the exocyclic bonds are antibonding. Therefore, the geometry of **16a** reflects the nature of the LUMO of **15**, as shown in Figure 3-13. The bond lengths of the Si-C bonds (Si1-C3, Si2-C4, Si3-C4, and Si4-C3) for **16a** are slightly shortened compared to those of **15** due to the delocalization of the negative charge onto the silicon centers by pπ-σ* conjugation (1.880(7) Å (av) for **15** and 1.860(1) Å (av) for **16a**).

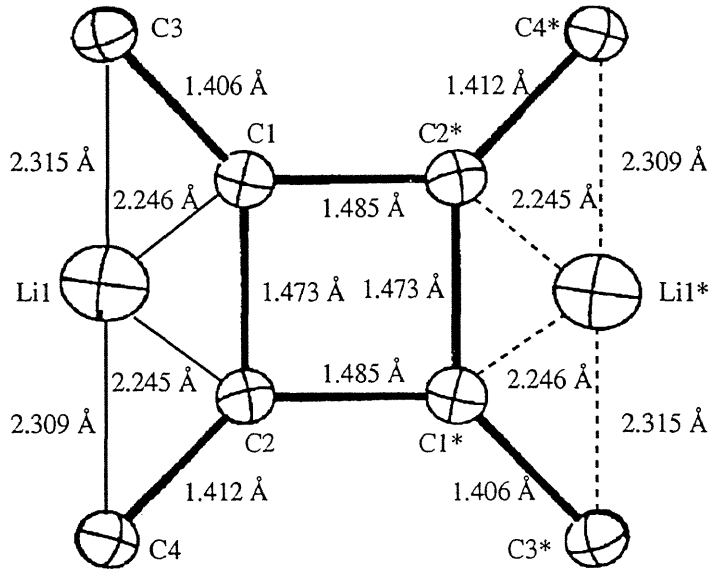

Figure 3-17. Selected bond lengths of **16a**.

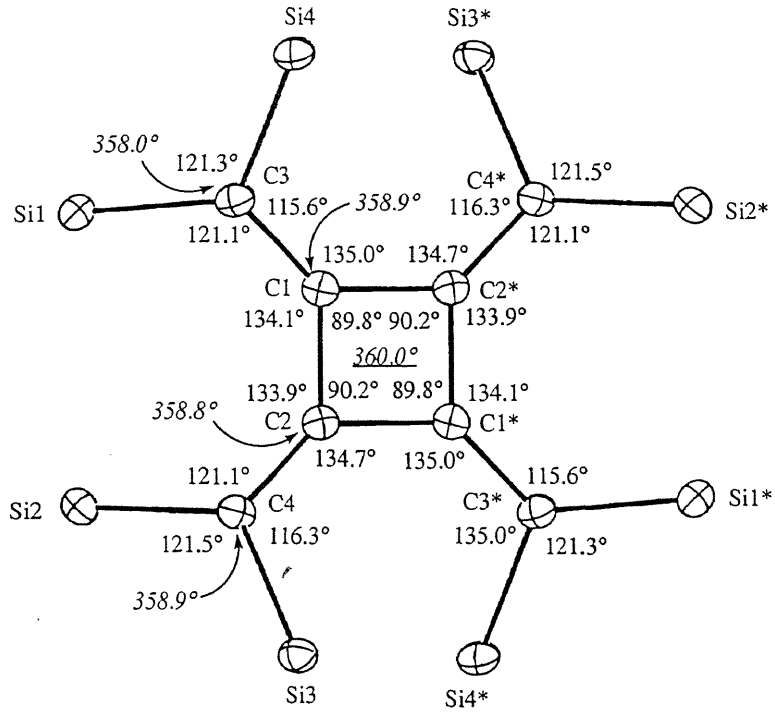

Figure 3-18. Selected bond angles of **16a**.

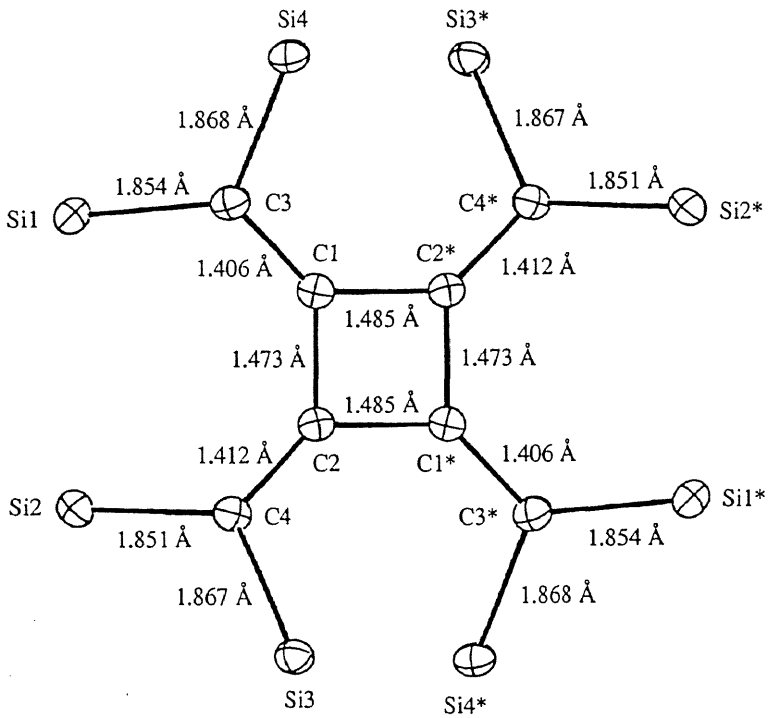

Figure 3-19. Selected bond lengths of **16a**.

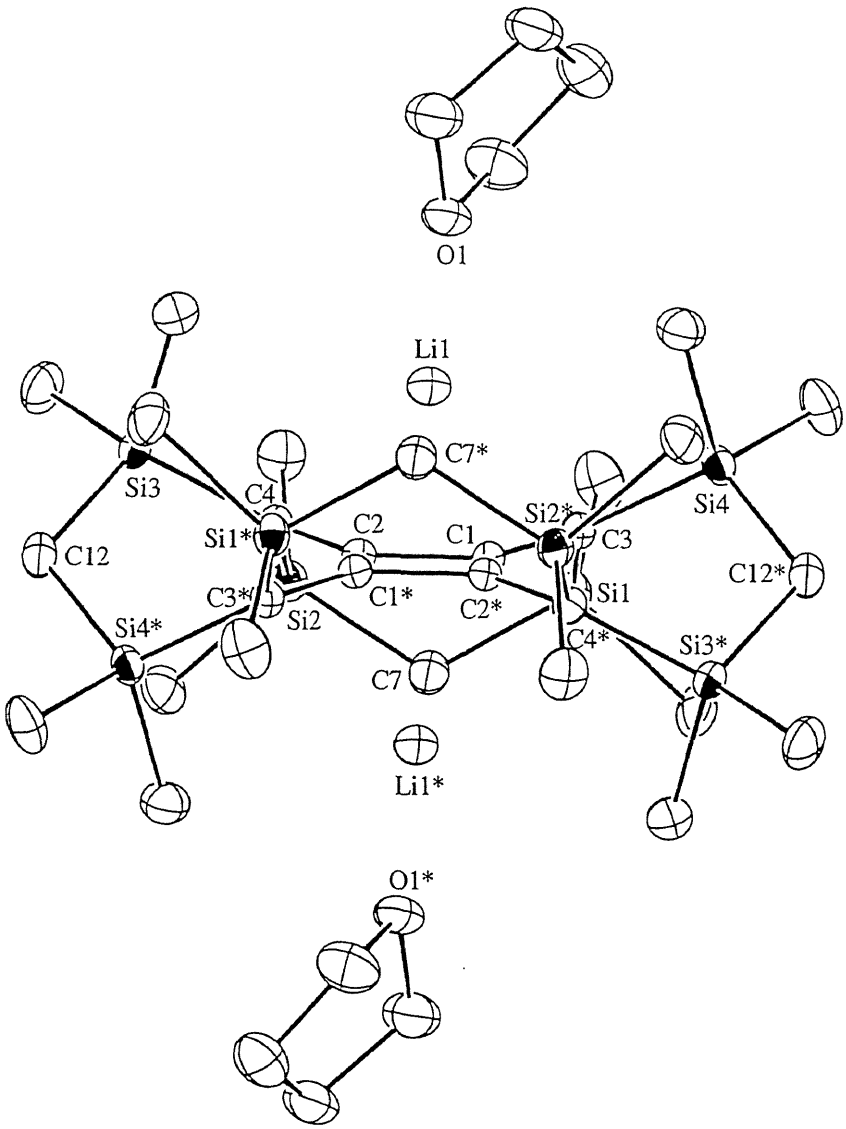

Figure 3-14. ORTEP drawing of **16a** (hydrogen atoms are omitted for the clarity).

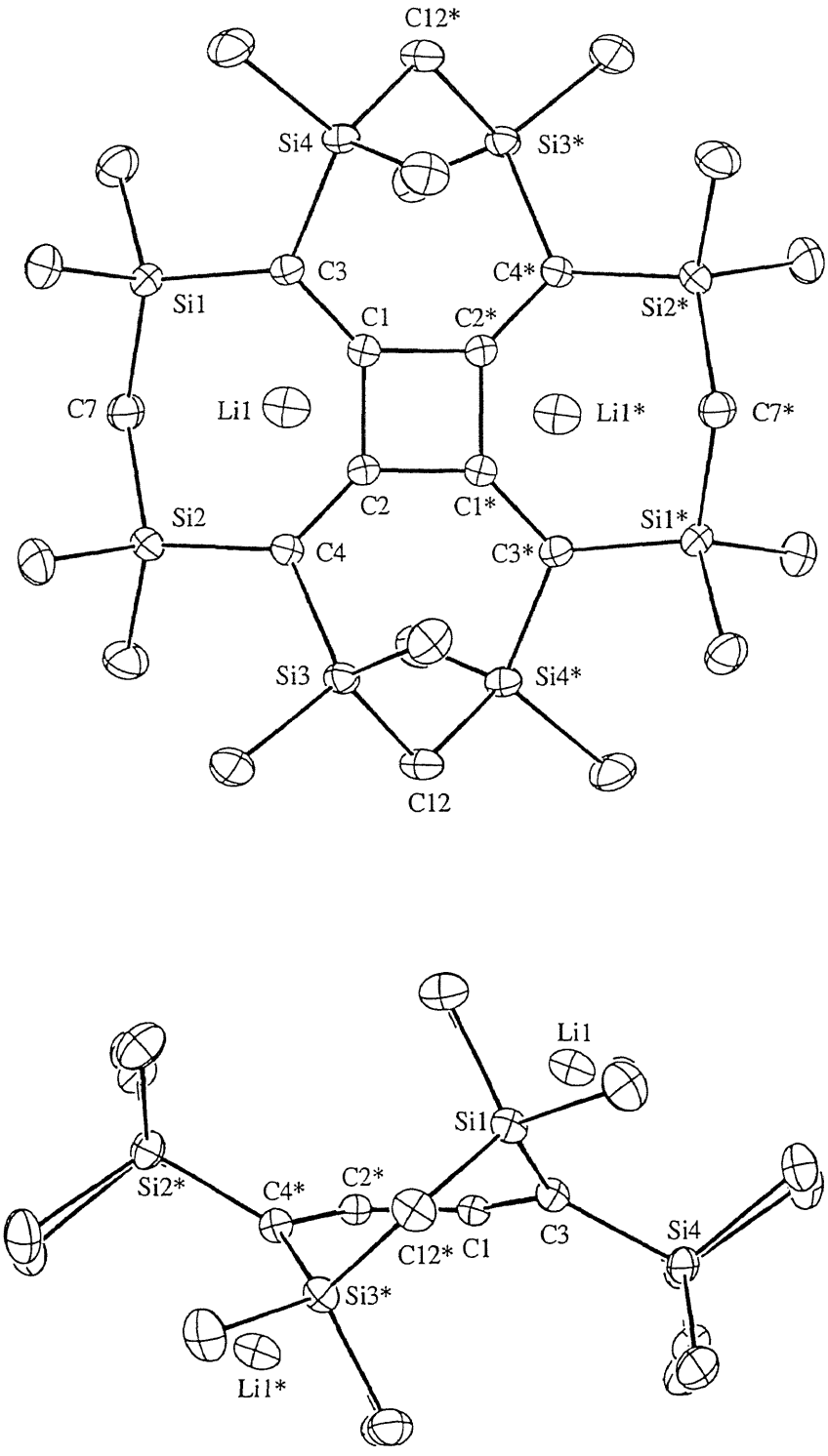

Figure 3-15. ORTEP drawing of **16a** (THF molecules and hydrogen atoms are omitted for the clarity): upper, top view; below, side view.

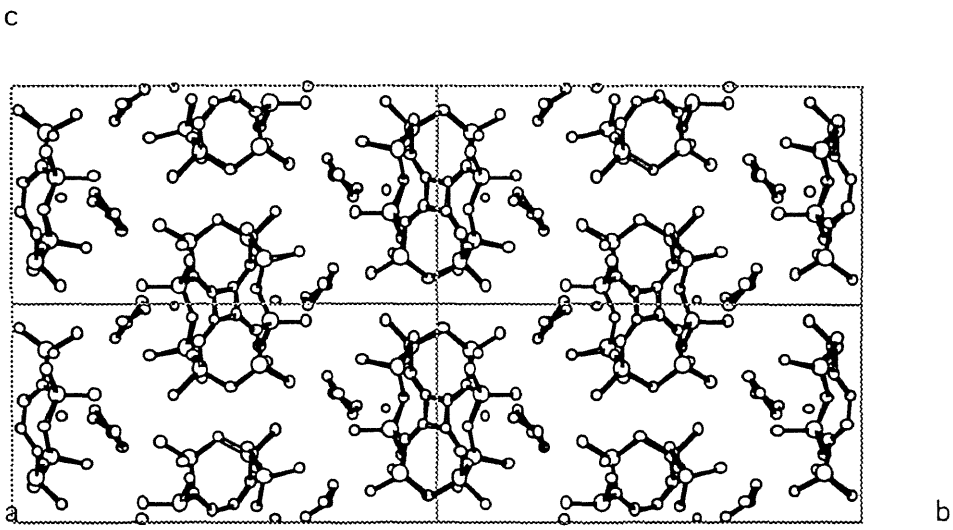

Figure 3-16. Crystal packing of **16a**.

Table 3-6. Atomic Parameters for Non-Hydrogen Atoms of **16a**

Atom	X/a	Y/b	Z/c	U(iso)
Si1	0.85378(2)	0.90888(1)	0.70431(2)	0.02084(8)
Si2	0.66182(2)	0.89416(1)	0.41636(2)	0.01907(8)
Si3	0.81370(2)	0.91681(1)	0.21687(2)	0.01918(8)
Si4	1.21245(2)	0.94224(1)	0.80398(2)	0.01908(8)
O1	1.13904(6)	0.81207(2)	0.52514(5)	0.0323(2)
C1	1.00241(7)	0.97670(3)	0.57761(6)	0.0163(2)
C2	0.91320(7)	0.97148(3)	0.44605(6)	0.0166(3)
C3	1.02056(7)	0.93994(3)	0.67888(6)	0.0179(3)
C4	0.81253(7)	0.92746(3)	0.37255(6)	0.0181(3)
C5	0.83600(10)	0.94677(4)	0.84027(8)	0.0334(4)
C6	0.86156(10)	0.82561(4)	0.74119(9)	0.0348(4)
C7	0.67654(7)	0.92386(3)	0.56809(7)	0.0243(3)
C8	0.46938(8)	0.91772(3)	0.30372(8)	0.0289(3)
C9	0.66192(9)	0.80870(3)	0.41661(8)	0.0314(3)
C10	0.70287(10)	0.84804(3)	0.13880(8)	0.0326(4)
C11	1.01430(9)	0.90119(4)	0.23109(8)	0.0317(4)
C12	0.73940(9)	0.98355(3)	0.11478(7)	0.0254(3)
C13	1.23403(10)	0.88129(4)	0.92010(8)	0.0331(4)
C14	1.36129(8)	0.92565(4)	0.73961(8)	0.0304(3)
C15	1.26781(11)	0.80526(4)	0.49091(10)	0.0445(5)
C16	1.38312(10)	0.76780(4)	0.58998(9)	0.0393(4)
C17	1.29530(11)	0.74213(4)	0.66366(10)	0.0444(5)
C18	1.13239(10)	0.75754(4)	0.58923(10)	0.0444(4)
Li1	1.02185(14)	0.88187(5)	0.51687(12)	0.0287(6)

Table 3-7. Atomic Parameters for Hydrogen Atoms of **16a**

Atom	X/a	Y/b	Z/c	U(iso)
H5A	0.8181(11)	0.9887(5)	0.8234(10)	0.051(3)
H5B	0.9258(12)	0.9433(4)	0.9123(10)	0.048(3)
H5C	0.7510(15)	0.9302(6)	0.8562(12)	0.079(4)
H6A	0.8587(12)	0.7994(5)	0.6735(11)	0.064(3)
H6B	0.9541(14)	0.8190(5)	0.8098(12)	0.068(3)
H6C	0.7710(12)	0.8150(5)	0.7537(10)	0.056(3)
H7A	0.6632(9)	0.9675(4)	0.5552(8)	0.033(2)
H7B	0.5941(11)	0.9066(4)	0.5929(9)	0.046(3)
H8A	0.4552(12)	0.9604(5)	0.3085(10)	0.057(3)
H8B	0.3923(11)	0.8977(5)	0.3246(10)	0.053(3)
H8C	0.4536(11)	0.9061(5)	0.2212(11)	0.052(3)
H9A	0.6295(11)	0.7922(5)	0.3379(11)	0.051(3)
H9B	0.7607(12)	0.7929(5)	0.4581(11)	0.063(3)
H9C	0.5909(10)	0.7937(4)	0.4478(9)	0.045(3)
H10A	0.7119(13)	0.8458(5)	0.0668(12)	0.063(3)
H10B	0.7486(10)	0.8091(5)	0.1838(9)	0.046(3)
H10C	0.5966(13)	0.8506(5)	0.1247(11)	0.062(3)
H12A	0.7802(11)	0.9811(5)	0.0555(10)	0.049(3)
H12B	0.6347(11)	0.9831(4)	0.0779(10)	0.045(3)
H11A	1.0405(10)	0.8623(5)	0.2651(9)	0.042(2)
H11B	1.0937(12)	0.9310(5)	0.2891(11)	0.055(3)
H11C	1.0242(12)	0.9005(5)	0.1505(11)	0.060(3)
H13A	1.3381(12)	0.8823(5)	0.9748(10)	0.052(3)
H13B	1.2225(11)	0.8422(5)	0.8816(10)	0.051(3)
H13C	1.1659(12)	0.8860(5)	0.9582(10)	0.057(3)
H14A	1.3575(11)	0.9534(5)	0.6714(11)	0.060(3)
H14B	1.3598(10)	0.8839(5)	0.7168(9)	0.043(3)
H14C	1.4635(12)	0.9318(4)	0.7985(10)	0.046(3)
H15A	1.2979(11)	0.8479(5)	0.4830(10)	0.049(3)
H15B	1.2370(11)	0.7839(5)	0.4132(10)	0.054(3)
H16A	1.4226(11)	0.7373(5)	0.5553(10)	0.046(3)
H16B	1.4604(10)	0.7897(4)	0.6358(9)	0.036(2)
H17A	1.3021(11)	0.6996(5)	0.6689(10)	0.056(3)
H17B	1.3245(11)	0.7606(5)	0.7404(11)	0.050(3)
H18A	1.0744(11)	0.7660(4)	0.6426(10)	0.043(3)
H18B	1.0714(12)	0.7257(5)	0.5243(10)	0.057(3)

Table 3-8. List of Atomic Disrances (Å) for Non-Hydrogen Atoms of **16a**

Atom	Atom	Length(sig)
Si1	C3	1.854(1)
Si1	C5	1.882(1)
Si1	C6	1.887(1)
Si1	C7	1.872(1)
Si2	C4	1.851(1)
Si2	C7	1.872(1)
Si2	C8	1.886(1)
Si2	C9	1.889(1)
Si3	C4	1.867(1)
Si3	C10	1.882(1)
Si3	C11	1.882(1)
Si3	C12	1.870(1)
Si4	C3	1.868(1)
Si4	C12	1.870(1)
Si4	C13	1.882(1)
Si4	C14	1.881(1)
O1	C15	1.436(2)
O1	C18	1.439(2)
C1	C2	1.473(1)
C1	C2	1.485(1)
C1	C3	1.406(1)
C2	C4	1.412(1)
C15	C16	1.515(2)
C16	C17	1.528(2)
C17	C18	1.504(2)

Table 3-9. List of Bond Lengths (Å) for Hydrogen Atoms of **16a**

Atom	Atom	Length(sig)
C5	H5A	0.950(12)
C5	H5B	0.956(11)
C5	H5C	0.968(13)
C6	H6A	0.982(13)
C6	H6B	0.957(13)
C6	H6C	0.957(11)
C7	H7A	0.977(10)
C7	H7B	1.010(10)
C8	H8A	0.958(12)
C8	H8B	0.966(11)
C8	H8C	0.968(13)
C9	H9A	0.940(12)
C9	H9B	0.947(12)
C9	H9C	0.945(10)
C10	H10A	0.892(13)
C10	H10B	1.020(11)
C10	H10C	0.961(12)
C11	H11A	0.943(10)
C11	H11B	1.042(11)
C11	H11C	0.996(13)
C12	H12A	0.924(11)
C12	H12B	0.923(10)
C13	H13A	0.957(11)
C13	H13B	0.963(11)
C13	H13C	0.925(11)
C14	H14A	1.005(12)
C14	H14B	0.960(11)
C14	H14C	0.969(11)
C15	H15A	0.999(11)
C15	H15B	0.978(12)
C16	H16A	0.939(11)
C16	H16B	0.876(10)
C17	H17A	0.942(12)
C17	H17B	0.939(13)
C18	H18A	1.002(11)
C18	H18B	1.043(12)

Table 3-10. List of Bond Angles (Å) for Non-Hydrogen Atoms of **16a**

Atom	Atom	Atom	Angle(sig)
C3	Si1	C5	109.5(1)
C3	Si1	C6	116.0(1)
C3	Si1	C7	109.9(1)
C5	Si1	C6	104.1(1)
C5	Si1	C7	108.6(1)
C6	Si1	C7	108.5(1)
C4	Si2	C7	110.3(1)
C4	Si2	C8	109.7(1)
C4	Si2	C9	113.5(1)
C7	Si2	C8	106.6(1)
C7	Si2	C9	110.5(1)
C8	Si2	C9	106.1(1)
C4	Si3	C10	112.2(1)
C4	Si3	C11	108.6(1)
C4	Si3	C12	113.6(1)
C10	Si3	C11	104.8(1)
C10	Si3	C12	108.3(1)
C11	Si3	C12	109.0(1)
C3	Si4	C12	114.1(1)
C3	Si4	C13	111.5(1)
C3	Si4	C14	109.3(1)
C12	Si4	C13	108.2(1)
C12	Si4	C14	107.8(1)
C13	Si4	C14	105.5(1)
C15	O1	C18	105.9(1)
C2	C1	C2	89.8(1)
C2	C1	C3	134.1(1)
C2	C1	C3	135.0(1)
C1	C2	C1	90.2(1)
C1	C2	C4	133.9(1)
C1	C2	C4	134.7(1)
Si1	C3	Si4	121.3(1)
Si1	C3	C1	121.1(1)
Si4	C3	C1	115.6(1)
Si2	C4	Si3	121.5(1)
Si2	C4	C2	121.1(1)
Si3	C4	C2	116.3(1)
Si1	C7	Si2	119.0(1)
Si3	C12	Si4	113.5(1)
O1	C15	C16	106.4(1)
C15	C16	C17	104.8(1)
C16	C17	C18	104.1(1)
O1	C18	C17	105.0(1)

Molecular Structure of Dilithium Octasilyl[4]radialene Dianion 16a' (DME Ligand)

The molecular structure of **16a'** (DME ligand) has also been confirmed by X-ray crystallography (Figure 3-20). The structure of **16a'** is quite different from that of **16a** (THF ligand). In the crystals of **16a'**, one of the lithium cation dissociates to yield an ion pair (CIP and SSIP). The structure of **16a'** is shown in Figure 3-21. The crystal packing of **16a'** is also shown in Figures 3-22 and 3-23.

The crystal structure of **16a'** is very interesting. Several unique features can be pointed out. Li1 is bonded to the four carbon atoms of the radialene π-skeleton and forms a contact ion pair (CIP). Two oxygen atoms of one DME is coordinated to Li1. On the other hand, Li2 is solvated by six oxygen atoms of three DME molecules. It's a DME solvated species $[Li^{+}(DME)_3]$ and forms a solvent separated ion pair (SSIP) (Figure 3-24). **16a'** is the first crystal structure of dianion species containing both CIP and SSIP in the molecule. The formation of CIP-SSIP structure of **16a'** is regarded as a result of not only the stabilization of negative charge by the extended 8C / 10π-electron system but also the chelate effect of bidentate DME.

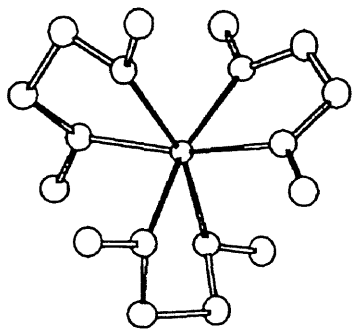

Figure 3-24. Solvation of lithium cation by DME.

The crystal structure can be described as anion [$\mathbf{1}5^{2-}${Li^{+}(DME)}] and cation [$Li^{+}(DME)_3$] salts. The alternating anion and cation layers can be seen from the view of *a*-axis (Figure 3-22). Figure 3-23 shows the column of anion and cation layers from the view of *c*-axis. The distances between anion and cation centers are about 9 Å.

The molecular structure of octasilyl[4]radialene unit of **16a'** is similar to that of **16a**. The π-skeleton of **16a'** has an almost planar structure. However, the final R value (0.197) was too high to discuss its details of the structural parameters.

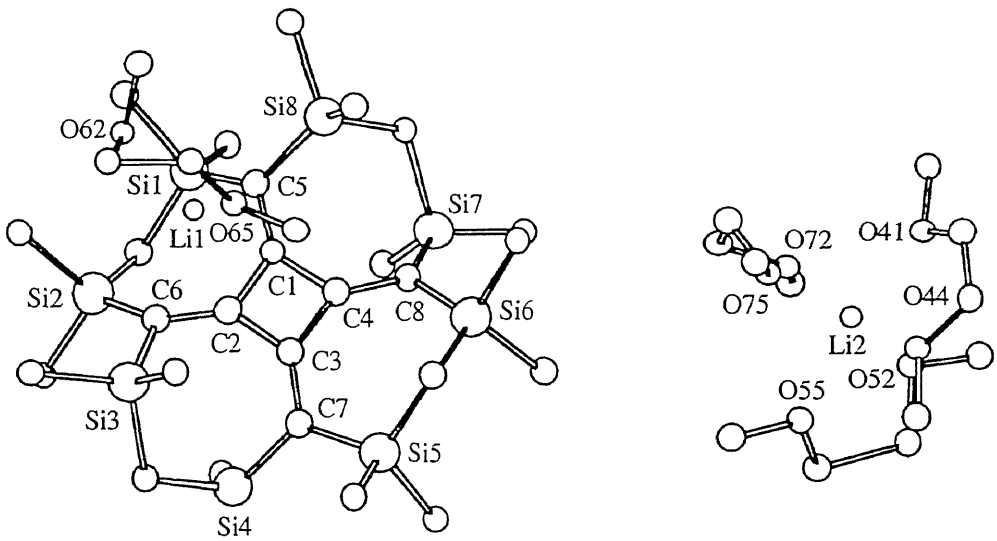

Figure 3-20. Crystal structure of **16a'** (hydrogen atoms are omitted for the clarity).

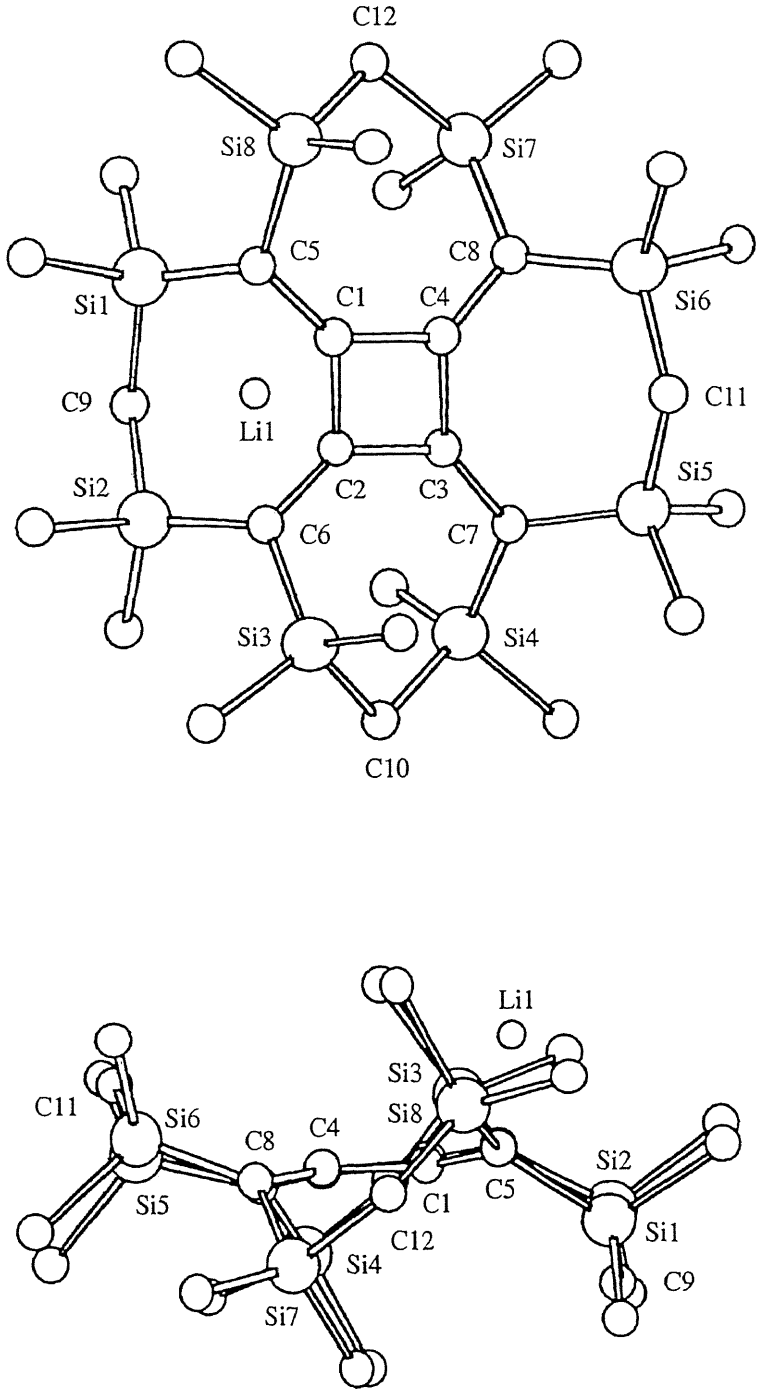

Figure 3-21. Crystal structure of **16a'** (DME molecules and hydrogen atoms are omitted for the clarity): upper, top view; below, side view.

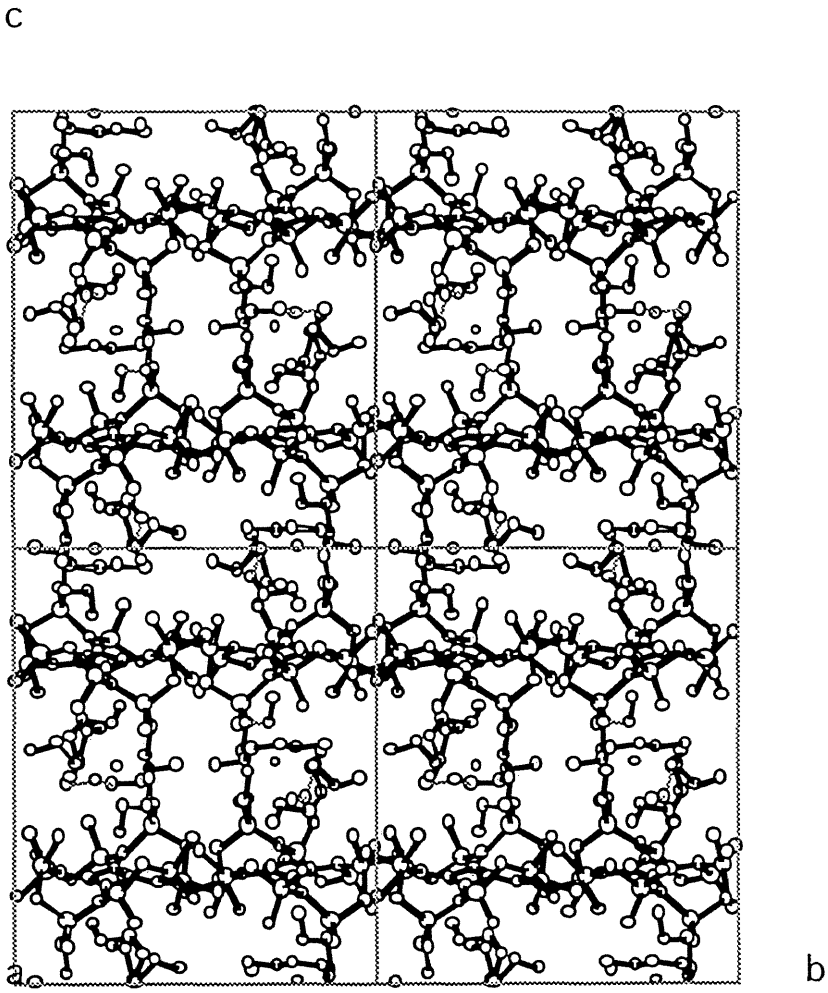

Figure 3-22. Crystal packing of **16a'**.

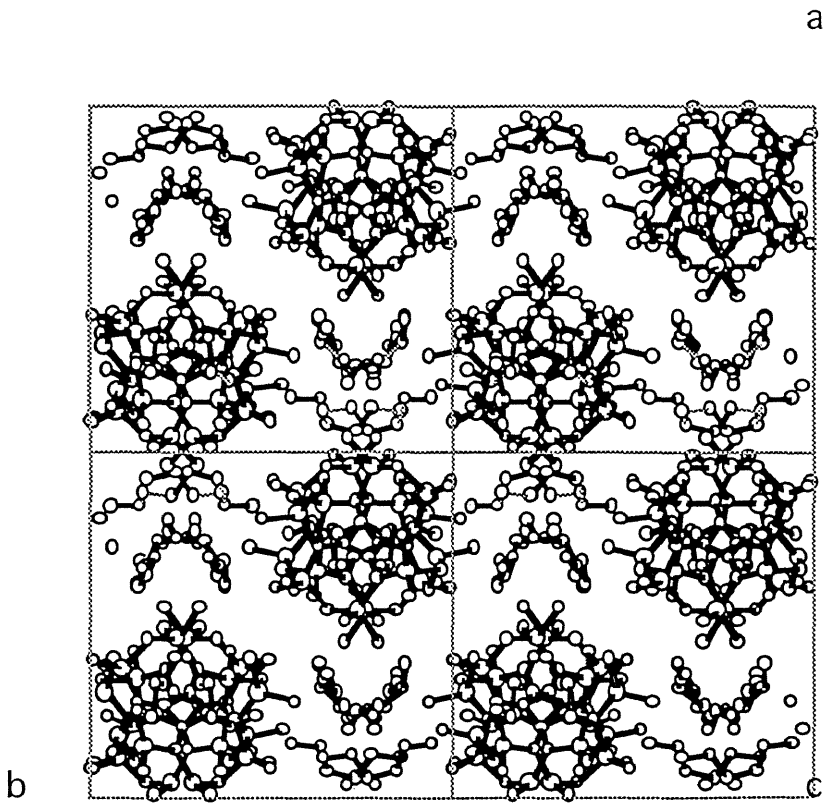

Figure 3-23. Crystal packing of **16a'**.

PM3 Calculation of Octasilyl[4]radialene Dianion 15^{2-}

Both the bis-CIP structure (**16a**, $[15^{2-}\{Li^{+}(THF)\}_2]$) and CIP-SSIP structure (**16a'**, $[15^{2-}\{Li^{+}(DME)\}][Li^{+}(DME)_3]$) have been determined by X-ray crystallography. Therefore, the geometry optimization of octasilyl[4]radialene dianion $\mathbf{15^{2-}}$ (counter ion free) was carried out by PM3 calculation.[8] The calculated structure ($\mathbf{15^{2-}}$) is corresponding to the bis-SSIP structure. A comparison of these structures (**16a**, **16'a**, and $\mathbf{15^{2-}}$) is quite important for the understanding of the properties of dianion species.

The calculated structure of $\mathbf{15^{2-}}$ is shown in Figure 3-25. The geometry of $\mathbf{15^{2-}}$ calculated by PM3 is somewhat different from those of bis-CIP (**16a**) and CIP-SSIP (**16a'**) by the X-ray diffraction. It is thought that the negative charge in SSIP is more efficiently delocalized on the π-skeleton relative to that in CIP. In other words, the density of negative charge on the π-skeleton in CIP is smaller than that in SSIP, due to the π/σ bonds between counter cation and π-skeleton. Some differences between crystal structure and calculated structure may be due to the existence of counter lithium cation and DME ligands. Of course, the packing force is also significant factor for the crystal structures. The selected bond angles and lengths of $\mathbf{15^{2-}}$ calculated by PM3 are shown in Figures 3-26 and 3-27. The charge distribution of $\mathbf{15^{2-}}$ is also shown in Figure 3-28.

Comparison of the calculated parameters of **15** and $\mathbf{15^{2-}}$ is also interesting. The change of bond lengths by two electron reduction is wellreproduced by PM3 calculation. The C-C single and double bond lengths of **15** calculated by PM3 are 1.505-1.507 Å (av 1.506 Å) and 1.324-1.325 Å (av 1.324 Å), respectively. Those of $\mathbf{15^{2-}}$ are 1.466-1.478 Å (av 1.472 Å) and 1.358-1.367 Å (av 1.362 Å), respectively. The Si-C(sp^2) single bond lengths of $\mathbf{15^{2-}}$ calculated by PM3 are 1.774-1.806 Å (av 1.792 Å), which are shorter than those of **15** (1.829-1.847 Å (av 1.839 Å)) due to the pπ-σ* conjugation.

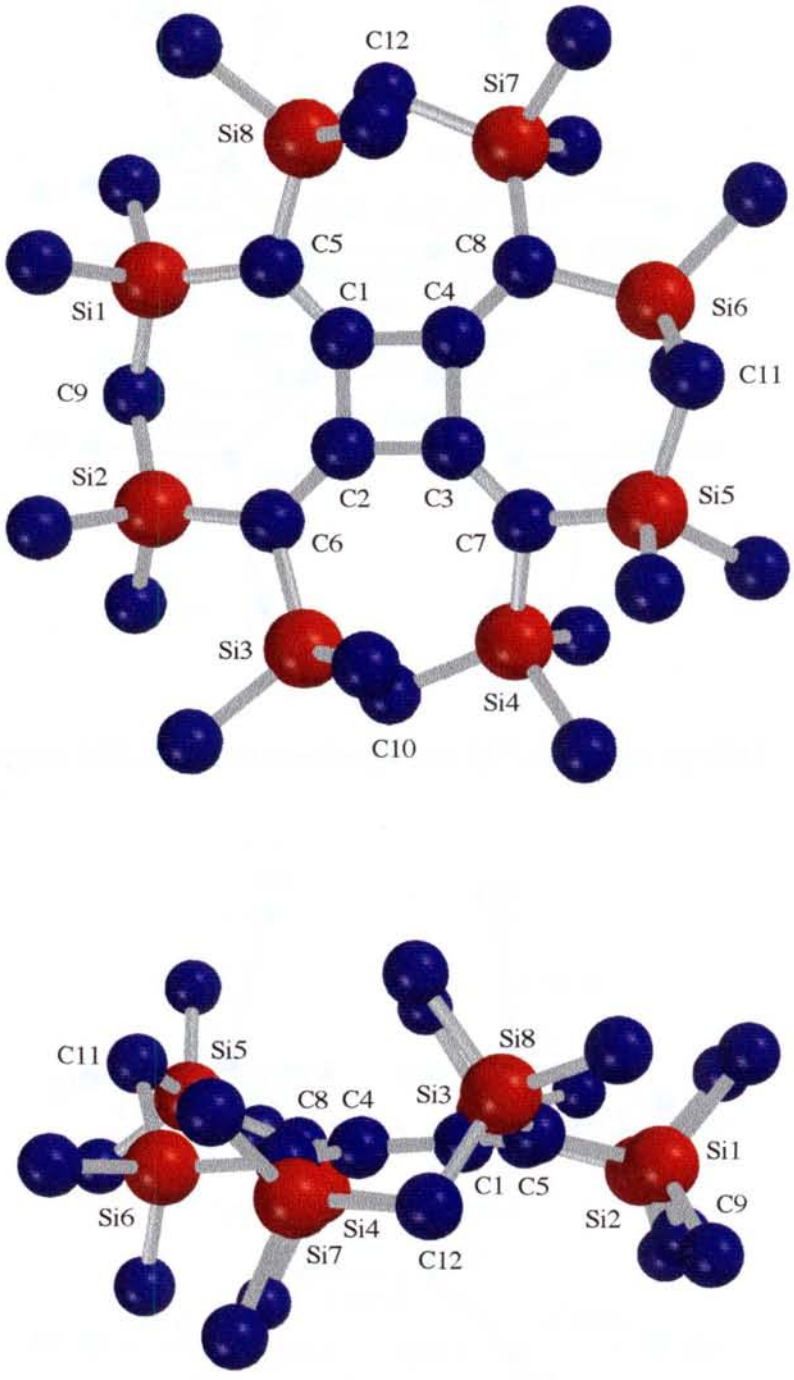

Figure 3-25. Calculated structure of $\mathbf{15}^{2-}$ by PM3 (hydrogen atoms are omitted for the clarity): upper, top view; below, side view.

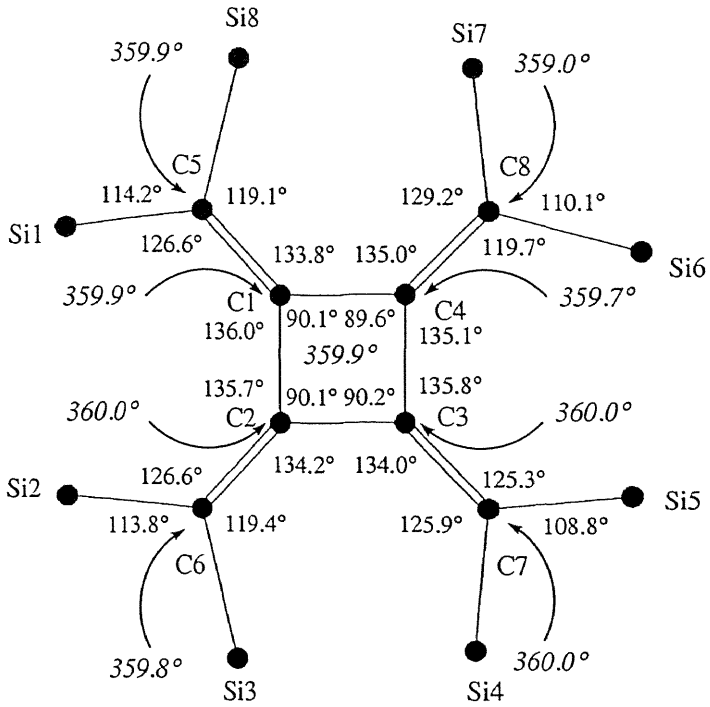

Figure 3-26. Selected bond angles of $\mathbf{15}^{2-}$ calculated by PM3.

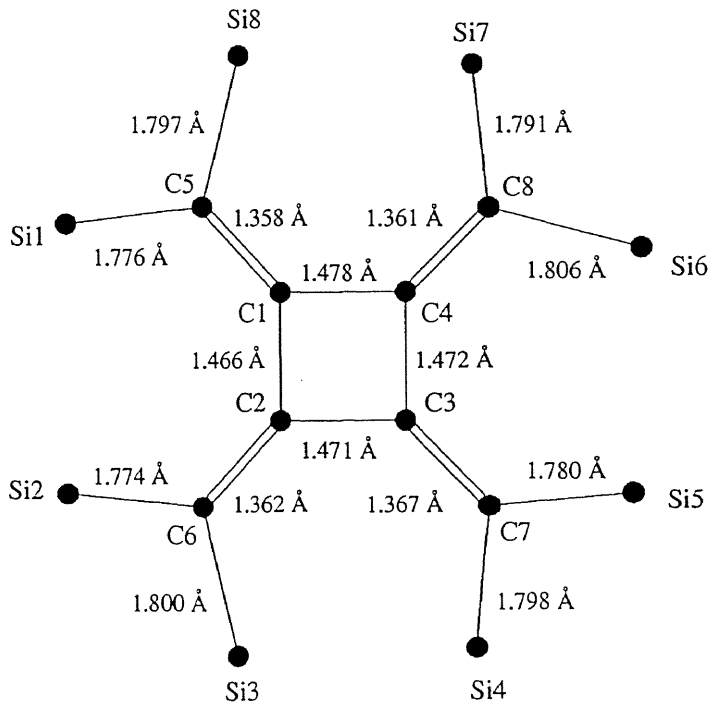

Figure 3-27. Selected bond lengths of $\mathbf{15}^{2-}$ calculated by PM3.

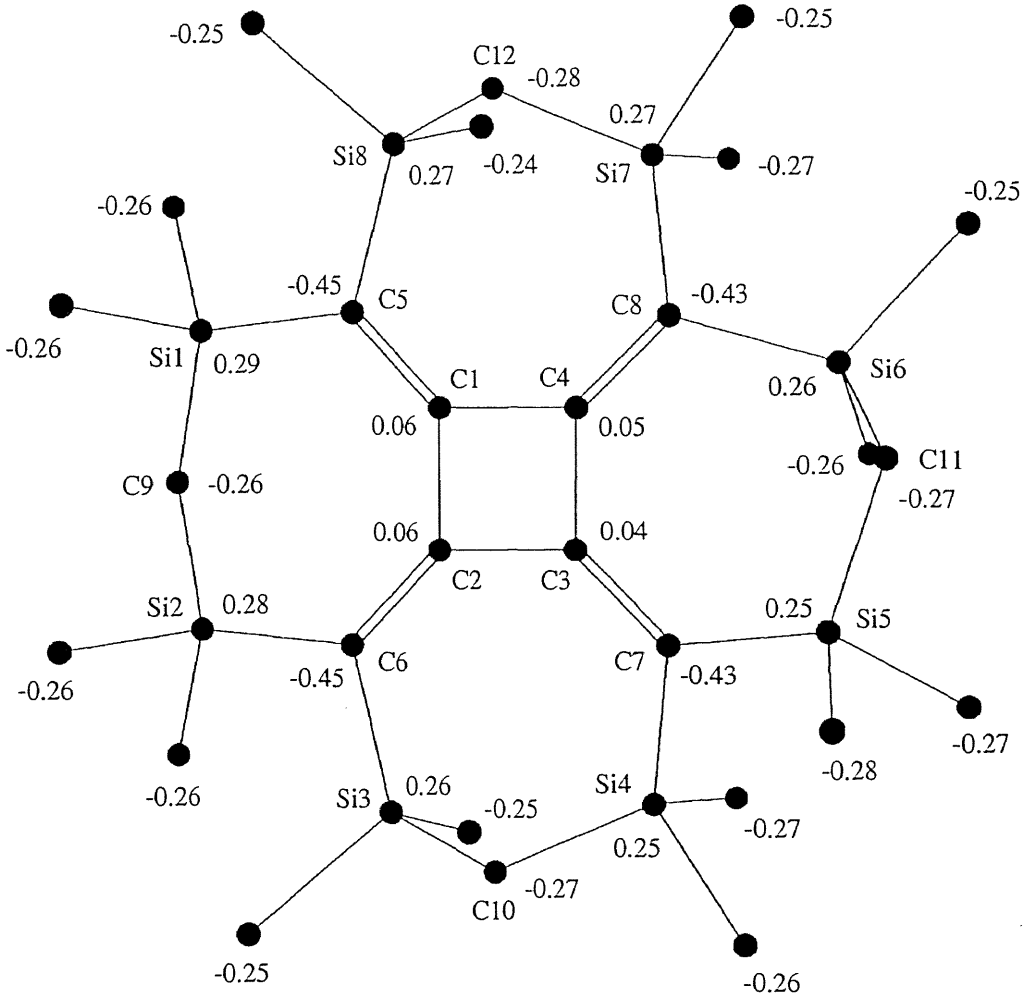

Figure 3-28. Mulliken charge distribution of $\mathbf{15}^{2-}$ calculated by PM3.

Structure of Dilithium Octasilyl[4]radialene Dianion 16a in Toluene-d_8

The structure of **16a** in toluene-d_8 has been deduced on the basis of ^{1}H, ^{13}C, ^{29}Si, and ^{6}Li NMR spectra. These NMR data on the structure of **16a** indicate a symmetric bis-CIP formation in solution. In the ^{1}H NMR spectrum of **16a**, only one signal is observed at 0.32 and 0.13 ppm for the methyl and methylene protons, respectively, together with the signals due to THF. As well, only one ^{13}C NMR signal is observed at 6.0 and 9.5 ppm for the methyl and methylene carbon atoms, respectively. Of particular interest are the chemical shifts of the ^{13}C NMR signals of the exocyclic (C3, C4, C3*, and C4*) and endocyclic (C1, C2, C1*, and C2*) endocyclic carbon atoms. The former ^{13}C NMR signal is observed at 73.2 ppm. This signal has shifted significantly upfield relative to that of **15** ($\Delta\delta = 94.3$). On the other hand, the latter has shifted downfield and appears at 182.8 ppm ($\Delta\delta = 48.1$). The ^{13}C NMR spectral data suggest that the negative charge is largely delocalized on the four exocyclic carbon atoms in the π-skeleton of **16a**. The ^{29}Si signal is observed at -11.8 ppm, which has shifted upfield relative to that of **15** ($\Delta\delta$ = 4.0). This suggests that the negative charge is stabilized by the eight silyl groups in **16a**. The ^{6}Li NMR spectrum of **16a** yields only one signal at -0.66 ppm (Figure 3-29).

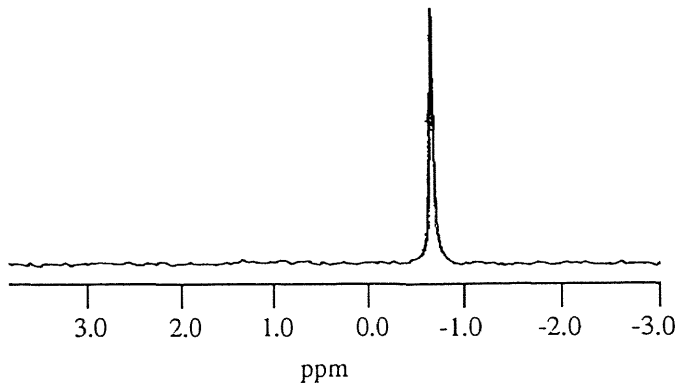

Figure 3-29. ^{6}Li NMR spectrum of **16a** in C_7D_8 at 298 K.

On the basis of these spectral data, it is quite reasonable to assume that the two Li^+ ions of **16a** are not fixed to the π-skeleton, but are fluxional; the two Li^+ ions are walking on the π-skeleton of the radialene on the NMR time scale (Figure 3-30). However, the variable-temperature NMR experiment can not be conducted in toluene-d_8. Due to lowering the temperature, the crystals of bis-CIP have precipitated to hamper the dynamic NMR study. The symmetric structure in toluene-d_8 was also deduced on the bases of the ^1H, ^{13}C, and ^{29}Si NMR spectra of the disodium **16b** and the dipotassium **16c**. It seems that the similar sodium walk and potassium walk on the π-skeleton may also occur to **16b** and **16c** in toluene-d_8, respectively. The solubilities of **16b** and **16c** in toluene-d_8 are also low.

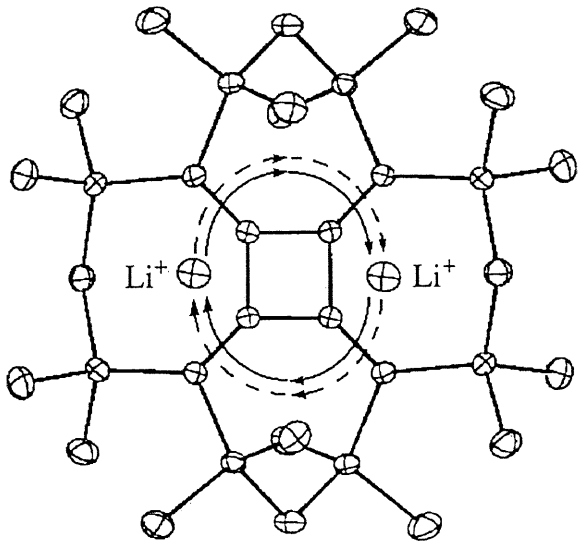

Figure 3-30. Schematic representation of the lithium walk on the π-skeleton of **16a** (bis-CIP) in C_7D_8 at 298 K.

Structure of Dilithium Octasilyl[4]radialene Dianion 16a in THF-d_8

The interesting Li^+ walk on the π-skeleton is evidenced in THF-d_8. In a solvating medium such as THF-d_8, one of the Li^+ ions above the [4]radialene ring dissociates to yield an ion pair (CIP and SSIP) (Scheme 3-7).

Scheme 3-7

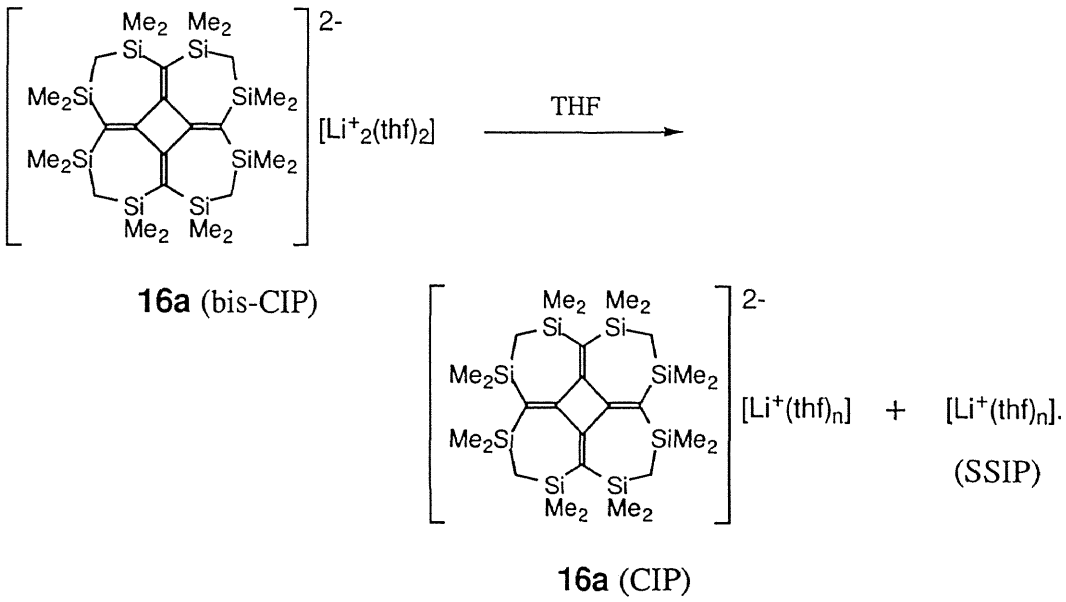

The ^6Li NMR spectrum of **16a** shows two signals with the same intensity at -0.38 and -0.66 ppm; the ratio of the peaks is independent of the concentration (0.03 to 0.13 M, 1 M = 1 mol dm^{-3}) (Figure 3-31). The former signal is assigned to the THF solvated species $[Li^+(thf)_n]$, whereas the latter is assigned to the Li^+ ion that is bonded to the π-skeleton.[10] The signal at -0.38 ppm assigned to the solvated Li^+ ion grows thanks to the ^6LiBr added due to the rapid exchange. However, the intensity of the signal at -0.66 ppm (CIP) bound to the π-framework remains unchanged. No exchange of the two Li^+ ions was observed in the temperature range of 173 to 298 K. Thus, one Li^+ ion of **16a** forms a SSIP and the other one forms a CIP in THF-d_8.

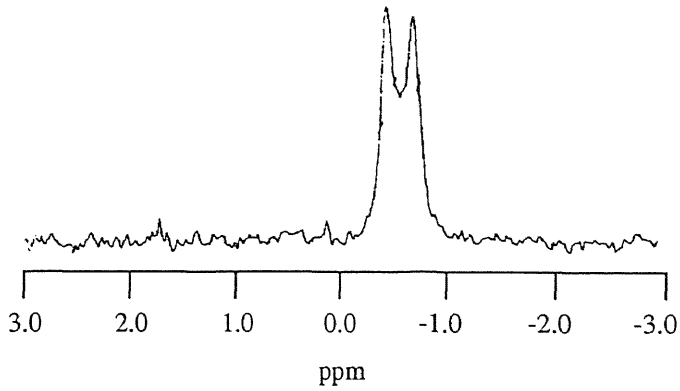

Figure 3-31. ^{6}Li NMR spectrum of **16a** in THF-d_8 at 298 K..

Consequently, the π-skeleton of **16a** has a different environment above and below the plane; methylene group ^{1}H doublet signals, with the geminal coupling of 12.6 Hz, and two ^{13}C signals of $SiMe_2$ can be seen at room temperature. The ^{13}C signal of methylene carbon atoms is found at 11.4 ppm. The endocyclic and exocyclic quaternary carbon atoms are found at 180.7 and 66.8 ppm, respectively. Only one ^{29}Si signal is observed at -13.5 ppm. These spectroscopic data clearly reveal that the Li^+ ion of CIP coordinates with one side of the radialene framework and that it can walk freely on the π-skeleton (Figure 3-32).

Upon lowering the temperature, the ^{13}C signals of the endocyclic and exocyclic carbon atoms broadened and split into two singlets (185.9, 177.8 ppm and 83.5, 50.2 ppm, respectively). The temperature dependent change of the ^{13}C endocyclic carbons in THF-d_8 must be resulted from the dynamics of Li^+ walk on the [4]radialene framework. Experimental and simulated spectra for the ^{13}C NMR signals of the endocyclic carbon atoms are shown in Figure 3-33.

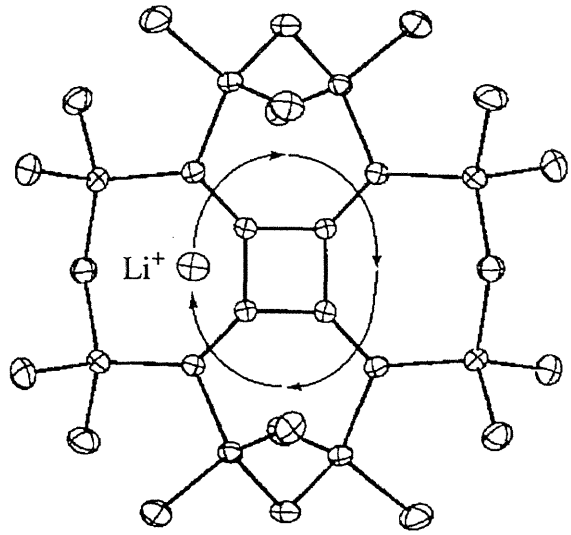

Figure 3-32. Schematic representation of the lithium walk on the π-skeleton of **16a** (CIP) in THF-d_8 at 298 K.

From the Arrhenius and Eyring plots, the values of E_a = 54.9 kJ mol^{-1}, $\Delta H^{\ddagger}$ = 52.7 kJ mol^{-1}, and $\Delta S^{\ddagger}$ = 19.0 J mol^{-1}K^{-1} for the Li^+ walk can be estimated. The Arrhenius and Eyring plots are shown in Figures 3-34 and 3-35, respectively. The data for the dynamic behavior of lithium ion is summarized in Table 3-11.

The present lithium walk is accompanied by the twist-boat interconversion of the seven-membered rings that contain the $Me_2SiCH_2SiMe_2$ fragments, which leads to a high barrier of internal migrations of the Li^+ ion. At 173 K, the Li^+ ion walk of the CIP is suppressed so that Li^+ is fixed at one site of the framework (Figure 3-36), giving eight carbon signals of $SiMe_2$ and three methylene carbons (9.7, 10.4, and 11.4 ppm), two endocyclic carbons (185.9 and 177.8 ppm), and two exocyclic carbons (83.5 and 50.2 ppm). In the ^{29}Si NMR spectrum, four signals were observed at -15.7, -14.3, -12.6, and -11.6 ppm. The Li^+ walk again starts on raising the temperature.

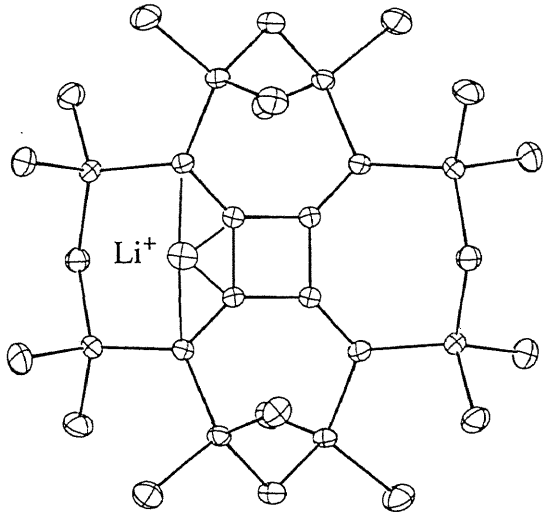

Figure 3-36. Structure of **16a** (CIP) in THF-d_8 at 173 K.

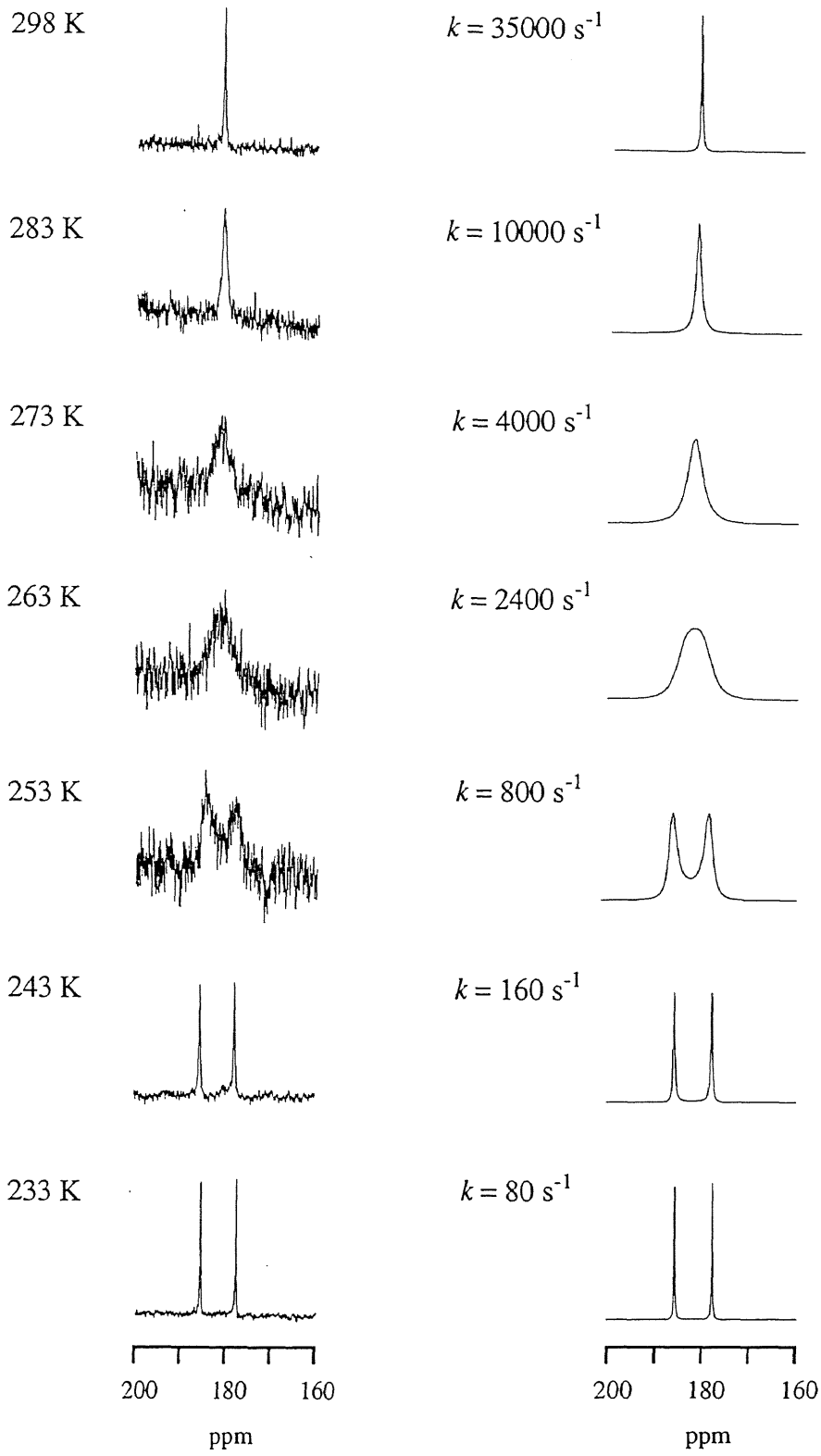

Figure 3-33. Observed (left) and simulated (right) ^{13}C (125 MHz) line shapes of the endocyclic carbons of **16a** in THF-d_8.

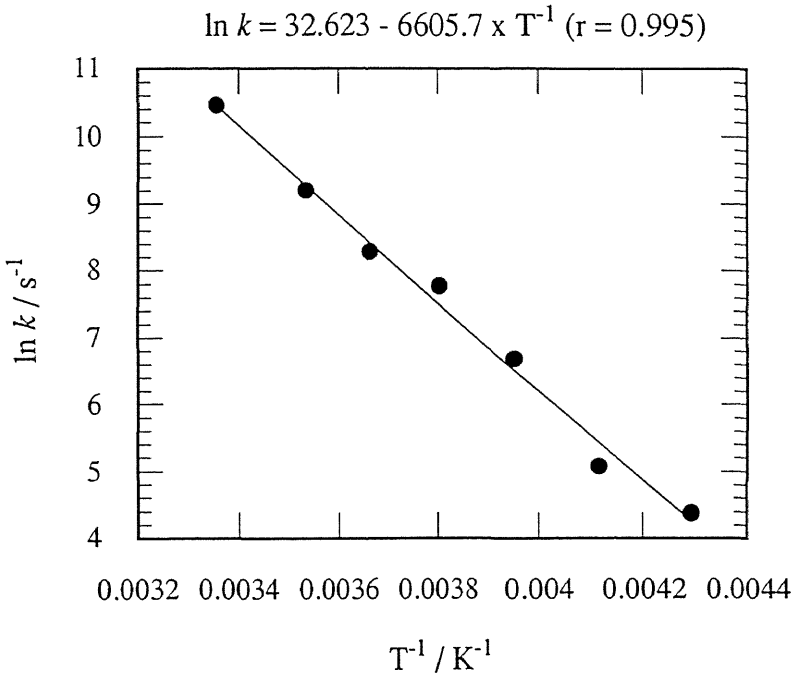

$$k = Ae^{-E_a / RT}$$

$$\ln k = -E_a / RT + \ln A$$

$$E_a = 54.9 \text{ kJmol}^{-1}$$

Figure 3-34. Arrhenius plot (ln k vs. T^{-1}) for the dynamic behavior of lithium ion of **16a** in THF-d_8.

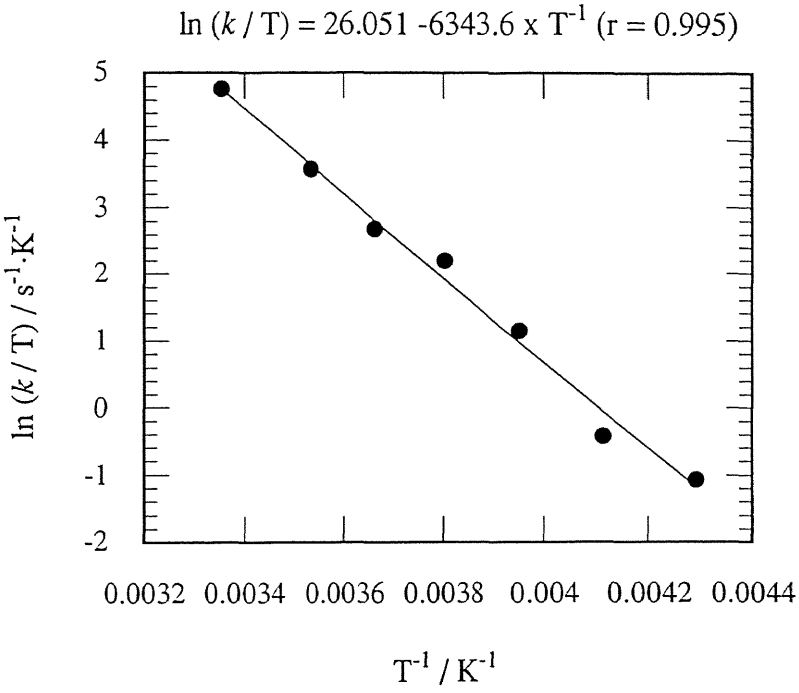

$$k = (k_B / h)Te^{-\Delta G^{\ddagger} / RT}$$

$$k / T = (k_B / h)e^{-\Delta G^{\ddagger} / RT}$$

$$\ln (k / T) = \ln (k_B / h) - \Delta G^{\ddagger} / RT$$

$$\Delta G^{\ddagger} = \Delta H^{\ddagger} - T\Delta S^{\ddagger}$$

$$\ln (k / T) = [\ln (k_B / h) + \Delta S^{\ddagger} / R] - \Delta H^{\ddagger} / RT$$

$$\Delta H^{\ddagger} = 52.7 \text{ kJmol}^{-1}, \Delta S^{\ddagger} = 19.0 \text{ Jmol}^{-1}\text{K}^{-1}$$

Figure 3-35. Eyring plot (ln (*k* / T) vs. T^{-1}) for the dynamic behavior of lithium ion of **16a** in THF-d_8.

Table 3-11. Data for the dynamic behavior of lithium ion of **16a** in THF-d_8 based on ^{13}C NMR (135 MHz)

T / K	T^{-1} / K^{-1}	k / s^{-1}	ln k / s^{-1}	ln (k / T) / $s^{-1}\cdot K^{-1}$
298	3.356×10^{-3}	35000	10.46	4.766
283	3.534×10^{-3}	10000	9.210	3.565
273	3.663×10^{-3}	4000	8.294	2.685
263	3.802×10^{-3}	2400	7.783	2.211
253	3.953×10^{-3}	800	6.685	1.151
243	4.115×10^{-3}	160	5.075	-0.418
233	4.292×10^{-3}	80	4.382	-1.069

Experimental Section

General Methods

^{1}H NMR spectra were recorded on a Bruker AC-300 FT spectrometer. ^{13}C, ^{29}Si, ^{6}Li, and ^{7}Li NMR spectra were collected on a Bruker AC-300 at 75.5, 59.6, 44.2, and 116.6 MHz, respectively. ^{13}C NMR spectra for line shapes of the endocyclic carbons were recorded on a Bruker AC-500 at 125 MHz. Li NMR spectra are referenced to 1 M LiCl (1 M = 1 mol dm^{-3}) in methanol / toluene-d_8 or 1 M LiCl in THF-d_8. Mass spectra were obtained on a Shimadzu QP-1000. Electronic spectra were recorded on a Shimadzu UV-2100 spectrometer. The sampling of **16a** and **16a'** for X-ray crystallography was carried out by using a Giken Engineering Service GBX-1200 gas-replacement type glove box.

Materials

Tetrahydrofuran, 1,2-dimethoxyethane (DME), and toluene were dried and distilled from sodium benzophenone ketyl. These solvents were further dried and degassed over a potassium mirror in vacuo prior to use. Toluene-d_8 and THF-d_8 were dried over molecular sieves, and then transferred into a tube covered with potassium mirror prior to use. Lithium-6 (95 atom%) metal was commercially available (Aldrich Chemical Company).

Preparation of 3,3,5,5,8,8,10,10,13,13,15,15,18,18,20,20-hexadeca-methyl-3,5,8,10,13,15,18,20-octasilacycloicosa-1,6,11,16-tetrayne (14)

3,3,5,5-tetramethyl-3,5-disilahepta-1,6-diyne (7.45 g, 0.041 mol) in THF (20 ml) was added to a THF solution of ethylmagnesium bromide (80 ml, 0.086 mol) to produce the Grignard reagent of the 1,6-diyne. The THF solution of the resulting Grignard

reagent and 2,14-dichloro-2,4,4,7,7,9,9,12,12,14-decamethyl-2,4,7,9,12,14-hexasila-pentadeca-5,10-diyne (21.57 g, 0.042 mol) in THF (20 ml) were added dropwise slowly to refluxing THF (500 ml). After the addition, the reaction mixture was heated overnight. The mixture was poured in hexane and hydrolyzed with dilute hydrochloric acid, followed by extraction with hexane. The organic layer was washed with water and dried over anhydrous sodium sulfate. After evaporation of the solvent, the residue was distilled under reduced pressure to give the crude tetrayne (**14**) (100-160 °C / 0.20 mmHg, Kugelrohr distillation). Recrystallization from ethanol gave pure colorless crystals of **14** in 25% yield. This compound has already been isolated from the reaction mixture of $BrMgC{\equiv}CMgBr$ and $ClMe_2SiCH_2SiMe_2Cl$ in very low yield.[11] mp 120–121 °C. ^1H NMR ($CDCl_3$) δ = -0.01 (s, 8 H, CH_2), 0.22 (s, 48 H, CH_3); ^{13}C NMR ($CDCl_3$) δ = 1.1 (CH_3), 3.3 (CH_2), 114.8 (C); ^{29}Si NMR ($CDCl_3$) δ = -19.7; UV (hexane) λ_{max} /nm (ε) 209 (3700), 217 (2400).

Preparation of Octasilyl[4]radialene (15)

A mixture of the 3,3,5,5,8,8,10,10,13,13,15,15,18,18,20,20-hexadecamethyl-3,5,8,10,13,15,18,20-octasilacycloicosa-1,6,11,16-tetrayne (**14**) (301 mg, 0.49 mmol) and $[Mn(CO)_3(Me\text{-}Cp)]$ (320 mg, 1.47 mmol) in THF (30 ml) was irradiated with a 500 W high-pressure mercury lamp for 2.5 h through the cutoff filter ($\lambda > 300$ nm) under the refluxing temperature of THF. After removal of the manganese complex, the reaction mixture was chromatographed on silica gel to produce yellow crystals of **15** in 11% yield. mp 219-220 °C; ^1H NMR ($CDCl_3$) δ = -0.05 (s, 8 H, CH_2), 0.14 (s, 48 H, CH_3); ^{13}C NMR ($CDCl_3$) δ = 2.1 (CH_3), 10.8 (CH_2), 134.7 (C), 167.5 (C); ^{29}Si NMR ($CDCl_3$) δ = -7.8; UV (hexane) λ_{max}/nm (ε) 229 (19500), 338 (14100), 444 (600). Found: C, 54.35; H 8.99%. Calcd for $C_{28}H_{56}Si_8$: C, 54.47; H 9.14%.

X-ray Crystallography of Octasilyl[4]radialene (15)

Single crystal of **15** for X-ray diffractions was grown from an ethanol solution. The X-ray crystallographic experiment of **15** was performed on a Rigaku-Denki AFC 5R diffractometer equipped with graphite-monochromatized Mo-$K\alpha$ radiation (λ = 0.710690 Å). Crystal data for **15** at 286 K: MF = $C_{28}H_{56}Si_8$, MW = 617.43, monoclinic, a = 18.935(7) Å, b = 9.106(2) Å, c = 22.829(2) Å, β = 91.53(2)°, V = 3935(2) Å^3, space group = $P2_1/c$, Z = 4, D_{calcd} = 1.042 g/cm^3. The final R factor was 0.0787 (R_w = 0.0767) for 4070 reflections with $F_o > 3\sigma(F_o)$. The details of the X-ray experiment are given in Table 3-12.

Table 3-12. Detail of the X-ray Experiment for **15**

molecular formula	$C_{28}H_{56}Si_8$
molecular weight	617.43
crystal system	monoclinic
space group	$P2_1/c$
cell constants	a = 18.935(7) Å, b = 9.106(2) Å,
	c = 22.829(2) Å, β = 91.53(2)°,
	V = 3935(2) Å^3
Z value	4
D_{calcd}	1.042 g cm^{-3}
μ (Mo $K\alpha$)	0.2817 mm^{-1}
crystal size	0.20 x 0.30 x 0.30 mm
crystal shape	prism
crystal color	yellow
diffractometer	Rigaku AFC-5R
radiation	Mo$K\alpha$ (λ = 0.710690 Å)
	graphite monochromatized rotating anode
temperature	286 K
2θ range	3 - 62.5°
number of unique reflections	7902
number of used reflections	4070 ($F > 3\sigma(F)$)
number of parameters	545
data correction	Lorenz and polarization effects
	no absorption, no extinction
structure analysis	direct method
refinement	block diagonal least squares methods
temperature factors	anisotropic (C and Si)
	isotropic (H, generated by calculation)
$R = \sum \|\|F_o\| - \|F_c\|\| / \sum \|F_o\|$	0.0787
$R_w = [\sum w(\|F_o\| - \|F_c\|)^2 / \sum \|F_o\|^2]^{1/2}$	0.0767

Preparation of Dilithium Octasilyl[4]radialene Dianion (16a) (THF Ligand).

The crystals of **15** (20 mg, 0.032 mmol) and lithium metal (30 mg, 4.3 mmol) were placed in a reaction tube with a magnetic stirrer. After degassing, dry oxygen-free THF (1.0 mL) was introduced by vacuum transfer and the mixture was stirred at room temperature to give a red solution of the dianion of **15** within 1 h. After the solvent was removed in vacuo, degassed toluene was introduced by vacuum transfer. Then, after the lithium metal was removed, the solution was cooled to afford dark red crystals of **16a** (THF ligand) quantitatively. ^{1}H NMR (C_7D_8) δ = 0.13 (s, 8 H, CH_2), 0.32 (s, 48 H, CH_3), 1.26 (br.s, 8 H, THF), 3.46 (br.s, 8 H, THF); ^{13}C NMR (C_7D_8) δ = 6.0 (CH_3), 9.5 (CH_2), 25.3 (THF), 69.7 (THF), 73.2 (C), 182.8 (C); ^{29}Si NMR (C_7D_8) δ = -11.8; ^{6}Li NMR (C_7D_8) δ = -0.66.

Preparation of Dilithium Octasilyl[4]radialene Dianion (16a') (DME Ligand).

The crystals of **15** (53 mg, 0.086 mmol) and lithium metal (30 mg, 4.3 mmol) were placed in a reaction tube with a magnetic stirrer. After degassing, dry oxygen-free DME (1.0 mL) was introduced by vacuum transfer and the mixture was stirred at room temperature to give a red solution of the dianion of **15** within 0.5 h. After the solvent was removed in vacuo, degassed toluene was introduced by vacuum transfer. Then, after the lithium metal was removed, the solution was cooled to afford dark red crystals of **16a'** (DME ligand) quantitatively. ^{1}H NMR (C_7D_8) δ = 0.18 (s, 8 H, CH_2), 0.37 (s, 48 H, CH_3), 3.01 (s, 24 H, DME), 3.06 (s, 16 H, DME); ^{13}C NMR (C_7D_8) δ = 6.9 (CH_3), 11.2 (CH_2), 59.1 (DME), 69.2 (C), 71.2 (DME), 180.6 (C); ^{29}Si NMR (C_7D_8) δ = –11.9; ^{7}Li NMR (C_7D_8) δ = -1.51.

X-ray Crystallography of Dilithium Octasilyl[4]radialene Dianion (16a) (THF Ligand)

Single crystal of **16a** (THF ligand) for X-ray diffractions was grown from a toluene solution. The X-ray crystallographic experiment of **16a** was performed on a DIP2020 image plate diffractometer equipped with graphite-monochromatized Mo-$K\alpha$ radiation (λ = 0.71073 Å). Crystal data for **16a** at 150 K: MF = $C_{36}H_{72}Li_2O_2Si_8$, MW = 767.47, monoclinic, a = 9.506(1) Å, b = 22.105(1) Å, c = 11.869(1) Å, β = 112.197 (1)°,V = 2309.20(1) Å^3, space group = $p2_1/c$, Z = 2, D_{calcd} = 1.164 g/cm^3. The final R factor was 0.031 (R_w = 0.038) for 4209 reflections with $I_o > 2\sigma(I_o)$. The details of the X-ray experiment are given in Table 3-13.

X-ray Crystallography of Dilithium Octasilyl[4]radialene Dianion (16a') (DME Ligand)

Single crystal of **16a'** (DME ligand) for X-ray diffractions was grown from a toluene solution. The X-ray crystallographic experiment of **16a'** was performed on a Rigaku-Denki AFC 5R diffractometer equipped with graphite-monochromatized Mo-$K\alpha$ radiation (λ = 0.710690 Å). Crystal data for **16a'** at 286 K: MF = $C_{44}H_{96}Li_2O_8Si_8$, MW = 991.81, monoclinic, a = 16.859(7) Å, b = 17.902(9) Å, c = 21.215(2) Å, β = 100.98(2)°, V = 6285(9) Å^3, space group = $p2_1/c$, Z = 4, D_{calcd} = 1.018 g/cm^3. The final R factor was 0.197 for 6114 reflections with $F_o > 3\sigma(F_o)$. The details of the X-ray experiment are given in Table 3-14.

Table 3-13. Detail of the X-ray Experiment for **16a**

molecular formula	$C_{36}H_{72}Li_2O_2Si_8$
molecular weight	767.47
crystal system	monoclinic
space group	$P2_1/c$
cell constants	a = 9.506(1) Å, b = 22.105(1) Å,
	c = 11.869(1) Å, β = 112.197(2)°,
	V = 2309.20(1) Å^3
Z value	2
D_{calcd}	D_x = 1.104 g cm^{-3}, D_m = 1.164 g cm^{-3}
μ (Mo Kα)	0.254 mm^{-1}
crystal size	0.35 x 0.30 x 0.35 mm
crystal shape	prism
crystal color	red
diffractometer	DIP2020 Image plate
radiation	MoKα (λ = 0.71073 Å)
	graphite monochromatized rotating anode
temperature	150 K
2θ range	4.0 - 40.0°
number of unique reflections	4438
number of used reflections	4208 ($I > 2\sigma(I)$)
number of parameters	361
data correction	DIP2000
structure analysis	*CRYSTAN*
refinement	*CRYSTAN*
temperature factors	anisotropic (C, Li, O and Si)
	isotropic (H)
$R = \sum \|\|F_o\| - \|F_c\|\| / \sum \|F_o\|$	0.031
$R_w = [\sum w(\|F_o\| - \|F_c\|)^2 / \sum \|F_o\|^2]^{1/2}$	0.038
goodness of fit	S = 1.500

Table 3-14. Detail of the X-ray Experiment for **16a'**

molecular formula	$C_{44}H_{96}Li_2O_8Si_8$
molecular weight	991.81
crystal system	monoclinic
space group	$P2_1/c$
cell constants	a = 16.859(7) Å, b = 17.902(9) Å,
	c = 21.215(2) Å, β = 100.98(2)°,
	V = 6285(9) Å^3
Z value	4
D_{calcd}	1.018 g cm^{-3}
μ (Mo $K\alpha$)	0.1906 mm^{-1}
crystal size	0.20 x 0.30 x 0.30 mm
crystal shape	prism
crystal color	red
diffractometer	Rigaku AFC-5R
radiation	Mo$K\alpha$ (λ = 0.710690 Å)
	graphite monochromatized rotating anode
temperature	286 K
2θ range	3 - 45°
number of unique reflections	8474
number of used reflections	6114 ($F > 3\sigma(F)$)
number of parameters	558
data correction	Lorenz and polarization effects
	no absorption, no extinction
structure analysis	direct method
refinement	block diagonal least squares methods
temperature factors	anisotropic (C, Li, O, and Si)
$R = \sum \|\|F_o\| - \|F_c\|\| / \sum \|F_o\|$	0.197

NMR Spectral Data of 16a in THF-d_8 at 298 K.

^{1}H NMR (THF-d_8) δ = -0.23 (d, *J* = 12.6 Hz, 4 H, CH_2), -0.17 (d, *J* = 12.6 Hz, 4 H, CH_2), 0.04 (s, 48 H, CH_3); ^{13}C NMR (THF-d_8) δ = 6.4 (CH_3), 6.9 (CH_3), 11.4 (CH_2), 66.8 (C), 180.7 (C); ^{29}Si NMR (THF-d_8) δ = -13.5; ^{6}Li NMR (THF-d_8) δ = –0.66, -0.38.

NMR spectral data of 16a in THF-d_8 at 173 K.

^{1}H NMR (THF-d_8) δ = -0.82 (d, *J* = 12.8 Hz, 1 H, CH_2), -0.70 (d, *J* = 12.8 Hz, 1 H, CH_2), -0.20 (br.s, 6 H, CH_2) -0.11 (s, 6 H, CH_3), -0.06 (s, 6 H, CH_3), -0.05 (s, 6 H, CH_3), -0.03 (s, 6 H, CH_3), 0.06 (s, 12 H, CH_3 x 2), 0.07 (s, 12 H, CH_3 x 2); ^{13}C NMR (THF-d_8) δ = 6.3 (CH_3 x 2), 6.5 (CH_3 x 2), 7.1 (CH_3), 7.9 (CH_3), 8.5 (CH_3), 9.5 (CH_3), 9.7 (CH_2), 10.4 (CH_2), 11.4 (CH_2), 50.2 (C), 83.5 (C), 177.8 (C), 185.9 (C); ^{29}Si NMR (THF-d_8) δ = -15.7, -14.3, -12.6, -11.6; ^{6}Li NMR (THF-d_8) δ = –1.41, -0.23.

Preparation of Disodium Octasilyl[4]radialene Dianion (16b).

This was obtained by a procedure similar to the preparation of **16a** as dark red crystals. ^{1}H NMR (THF-d_8) δ = -0.22 (s, 8 H, CH_2), 0.04 (s, 48 H, CH_3); ^{13}C NMR (THF-d_8) δ = 7.2 (CH_3), 11.6 (CH_2), 66.5 (C), 182.0 (C); ^{29}Si NMR (THF-d_8) δ = –14.0.

Preparation of Dipotassium Octasilyl[4]radialene Dianion (16c).

This was obtained by a procedure similar to the preparation of **16a** as dark red crystals. ^{1}H NMR (THF-d_8) δ = -0.17 (s, 8 H, CH_2), 0.07 (s, 48 H, CH_3); ^{13}C NMR (THF-d_8) δ = 6.9 (CH_3), 11.1 (CH_2), 70.6 (C), 182.8 (C); ^{29}Si NMR (THF-d_8) δ = –14.0.

Molecular Orbital Calculations.

PM3 calculations were performed by Power Macintosh 7600/200 with MACSPARTAN plus program (Ver. 1.1.7).[8] All the calculations were performed with the geometry optimization.

References

(1) (a) K. Müllen, *Chem. Rev.*, **84,** 603 (1984). (b) W. N. Setzer and P. v. R. Schleyer, *Adv. Organomet. Chem.*, **24,** 353 (1985). (c) C. Schade and P. v. R. Schleyer, *Adv. Organomet. Chem.*, **27,** 169 (1987). (d) M. Rabinovitz, *Top. Curr. Chem.*, **14,** 99 (1988). (e) A. B. Sannigrahi, T. Kar, B. G. Niyogi, P. Hobza, and P. v. R. Schleyer, *Chem. Rev.*, **90** 1061 (1990). (f) H. Bock, K. Ruppert, C. Näther, Z. Havlas, H. F. Herrmann, C. Arad, I. Gögel, A. John, J. Meuret, S. Nick, A. Rauschenbach, W. Seitz, T. Vaupel, and B. Solouki, *Angew. Chem., Int. Ed. Engl.*, **31,** 550 (1992). (g) A. M. Sapse, P. v. R. Schleyer, "Lithium Chemistry: A Theoretical and Experimental Overview", Wiley, New York (1995).

(2) H. Bock, C. Näther, K. Ruppert, and Z. Havlas, *J. Am. Chem. Soc.*, **114,** 6907 (1992).

(3) H. Bock, C. Näther, and Z. Havlas, *J. Am. Chem. Soc.*, **117,** 3869 (1995).

(4) For the recent works on the dynamics of carbanionic inversion, see: (a) H. J. Reich and K. J. Kulicke, *J. Am. Chem. Soc.*, **117,** 6621 (1995). (b) R. W. Hoffmann, R. K. Dress, T. Ruhland, and A. Wenzel, *Chem. Ber.*, **128,** 861 (1995). (c) H. J. Reich and K. J. Kulicke, *J. Am. Chem. Soc.*, **118,** 273 (1996). (d) G. Fraenkel and F. Qui, *J. Am. Chem. Soc.*, **119,** 3571 (1997).

(5) (a) B. Heinrich and A. Roedig, *Angew. Chem., Int. Ed. Engl.*, **7,** 375 (1968). (b) K. Koster and R. West, *J. Org. Chem.*, **40,** 2300 (1975). (c) L. Hagelee, R. West, J. Calabrese, and J. Normant, *J. Am. Chem. Soc.*, **101,** 4888 (1979). (d) F. W. Nader, C.-D. Wacker, H. Inrgartinger, U. Huber-Patz, R. Jahn, and H. Rodewald, *Angew. Chem., Int. Ed. Engl.*, **24,** 852 (1985). (e) B. Hagenbrach, K. Hesse, S. Hünig, and G. Klug, *Ann. Chem.*, **1981,** 256. (f) M. Iyoda, H.

Otani, and M. Oda, *J. Am. Chem. Soc.*, **108,** 5371 (1986). (g) M. Iyoda, M. Tanaka, H. Otani, M. Nose, and M. Oda, *J. Am. Chem. Soc.*, **110,** 8494 (1988).

(6) H. Sakurai, T. Fujii, and K. Sakamoto, *Chem. Lett.*, **1992,** 339.

(7) F. P. Van Remoortere and F. P. Boer, *J. Am. Chem. Soc.*, **92,** 3355 (1970).

(8) J. J. P. Stewart, *J. Comput. Chem.*, **10,** 209 (1989).

(9) W. T. Thorstad, N. S. Mills, D. Q. Buckelew, and L. S. Govea, *J. Org. Chem.*, **54,** 773 (1989).

(10) A. Sekiguchi, M. Ichinohe, T. Nakanishi, and H. Sakurai, *Chem. Lett.*, **1993,** 267.

(11) E. Kloster-Jensen and G. A. Eliassen, *Angew. Chem., Int. Ed. Engl.*, **24,** 565 (1985).

Chapter 4

Silyl-Substituted Fulvene Dianion with 6C / 8π-Electron System

Summary

Reaction of fulvene derivatives bridged by Me_2Si-X-$SiMe_2$ chains (**21a** : X = CH_2, **21b** : X = O) with lithium metal in THF gave the dilithium salts of fulvene dianion (**24a** and **24b**) with 6 center / 8π-electron system. The molecular structure of the dianion dilithium **24a** has been unequivocally established by X-ray crystallography. **24a** has a monomeric structure and forms contact ion pair (bis-CIP) in the crystals. One of lithium atoms is located above the center of the five-membered ring (η^5-coordination), whereas the other one is bonded to the exocyclic carbon atom (η^2-coordination). The structural parameters of **24a** are discussed in comparison to those of the neutral starting molecule **21a**. The structure of **24** in solution has also been discussed on the basis of NMR spectroscopic data. The two lithium ions of **24** are not fixed to the π-skeleton in toluene-d_8, but are fluxional, giving a high symmetrical structure. The spectral data in THF-d_8 at 298 K also suggest the bis-CIP structure of **24**. However, the η^5-coordination lithium ion of **24a** is dissociated to yield an ion pair (CIP-SSIP) at low temperature in THF-d_8, and two dianion species (bis-CIP and CIP-SSIP) were found. The evidence for the unique equilibrium of **24a** in THF-d_8 is demonstrated. The X-ray crystallography and the NMR data indicate that the structure of **24** is a stable, closed-shell dianion, which is stabilized not only by the six silicon atoms but also by the aromatic cyclopentadienyl anion.

Introduction

Fulvene (**17**) (pentafulvene, 5-methylenecyclopentadiene) is one of the most important cross-conjugated π-electron systems based on five-membered ring (Chart 4-1). Fulvene is a benzene isomer with 6π-electron system. Two double bonds are located in the five-membered ring and one double bond is situated in the exo position. Fulvene reacts with nucleophiles selectively at the 6-position (exo carbon) to produce a cyclopentadienide ion.[1] For example, 6,6-dimethylfulvene reacts with methyllithium to produce *t*-butylcyclopentadienide ion (Scheme 4-1).[2] Upon treatment with alkali metals or lithium naphthalenide, fulvene also readily undergoes reduction to afford 6,6'-bifulvenyl through coupling of the intermediate anion radical (**18a**).[3] Fulvene dianion (**18b**), as a result of the two electron reduction, is an interesting anionic species with regard to its structure, bonding, and delocalization of the negative charge.[4] For electronic and steric reasons, the introduction of the phenyl groups at the 6-position allows the formation of a fulvene dianion. Previously, Oku et al. reported that the alkali metal reduction of 6,6-diphenylfulvene produced a dihydro compound via dianion (**19**).[5] Subsequently, Oda et al. reported the NMR observation of **19** in THF (Scheme 4-2).[6] However, the fulvene dianion has not yet been isolated and there is no precedent concerning its molecular structure.

Chart 4-1

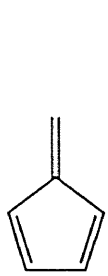

17

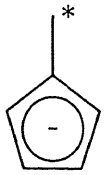

18a (* = •)
18b (* = ⊖)

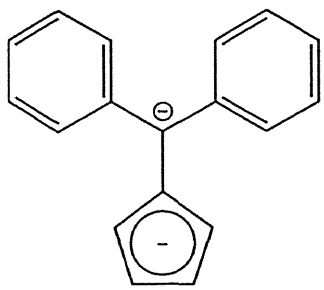

19

Scheme 4-1

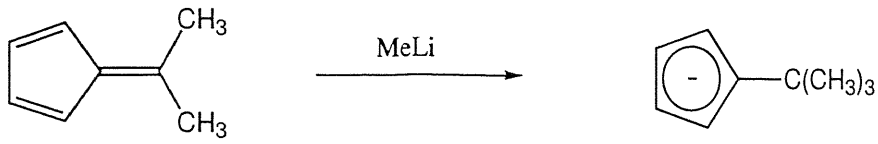

Scheme 4-2

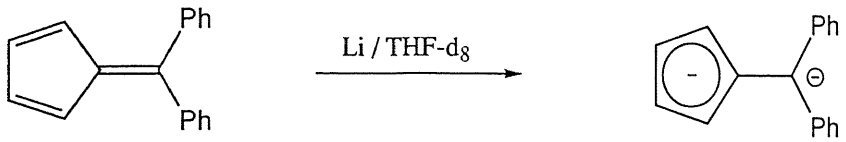

In this chapter, the first successful isolation, full characterization, and molecular structure of dilithium hexasilylfulvene dianion, which has a novel 6C / 8π-electron system, are described.

Results and Discussion

Synthesis of Hexasilylfulvene (21)

Hexasilylfulvene derivatives (**21**) bridged by Me_2Si-X-$SiMe_2$ chains (**21a** : X = CH_2, **21b** : X = O) were prepared by the intramolecular cyclotrimerization of the macrocyclic silyltriynes (**11** and **20**). **21a** linked by silmethylene chains was prepared as red crystals in 26% yield by the intramolecular cyclization of dodecamethyl-3,5,8,10,13, 15-hexasilacyclopentadeca-1,6,11-triyne (**11**) with $Mn(CO)_3$(Me-Cp) by irradiation ($\lambda >$ 300 nm) in the THF at room temperature (Scheme 4-3). **21b** bridged by siloxane chains has also been prepared in a similar manner via the intramolecular cyclization of dodecamethyl-3,5,8,10,13,15-hexasila-4,9,14-trioxacyclopentadeca-1,6,11-triyne (**20**) (Scheme 4-4).[7]

Scheme 4-3

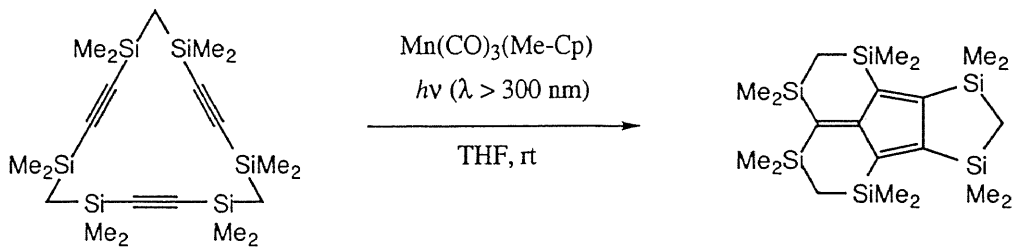

11 **21a**

Scheme 4-4

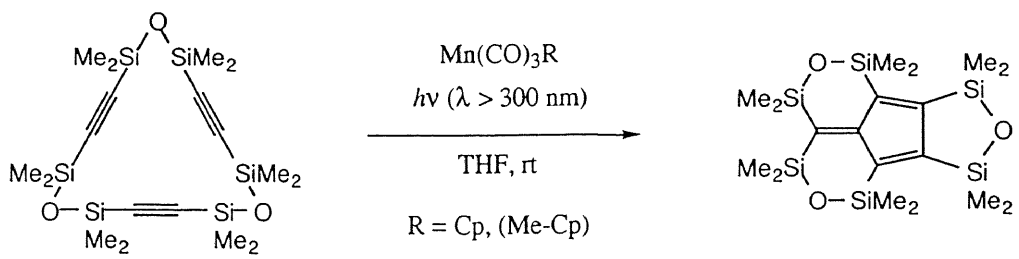

20 **21b**

The reaction involves the 1,2-silyl shift in the 1,2-disilyl-substituted acetylene to give 2,2-disilylvinylidene complexes as a reaction intermediate. In the reaction of fulvene **21b**, the intermediate vinylidene complex (**22**) was successfully isolated. The molecular structure of **22** was confirmed by X-ray crystallography (Figure 4-1).[7] The intriguing 1,2-silyl shift is a general reaction in cyclic and acyclic bissilylacetylene promoted by (cyclopentadienyl or methylcyclopentadienyl)tricarbonylmanganese.[8] The reaction mechanism to form **21** is not clear at this moment, but a single 1,2-silyl shift can be involved (Scheme 4-5).

Scheme 4-5

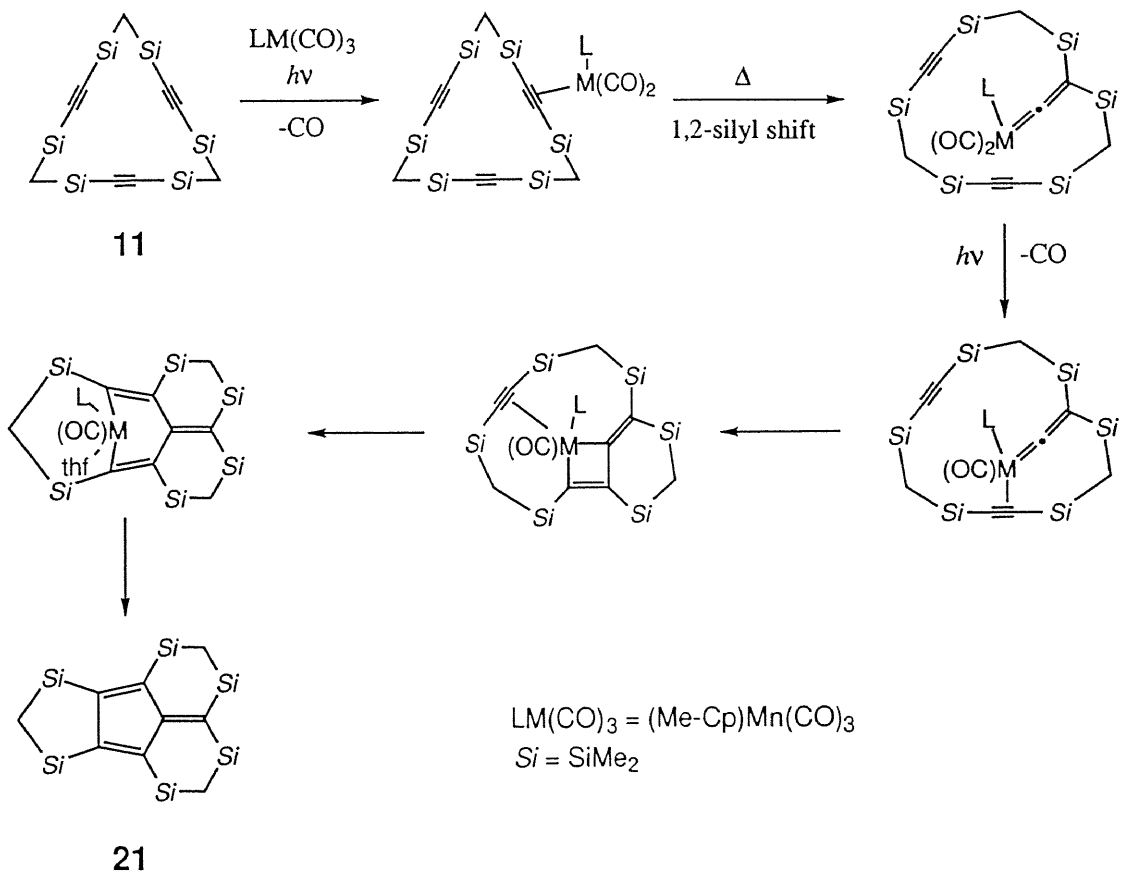

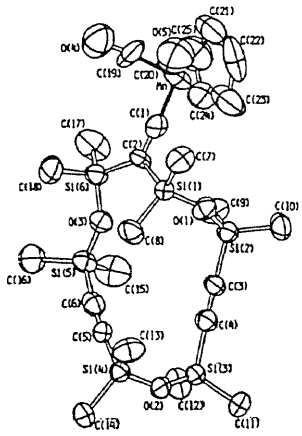

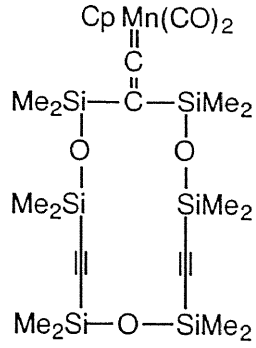

22

Figure 4-1. ORTEP drawing of the vinylidene complex **22**.

Hexakis(trimethylsilyl)fulvene (**23**) was prepared by the photolysis of hexakis-(trimethylsilyl)Dewar benzene with a light (λ = 254 nm) in 23% yield (Scheme 4-6).[9] The molecular structure of **23** is expected to the highly distorted structure due to the steric repulsion of six trimethylsilyl groups. On the other hand, the molecular structures of hexasilylfulvene derivatives **21** are assumed to the almost planar structures due to the bridge-building of Me_2Si-X-$SiMe_2$ chains.

Scheme 4-6

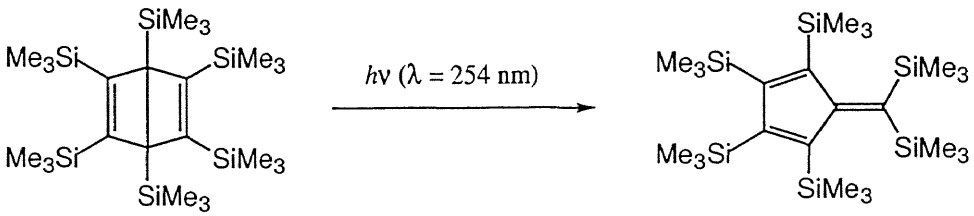

23

Molecular Structure of Hexasilylfulvene 21a

Hexasilylfulvene **21a** bridged by silmethylene chains could be recrystallized from ethanol. The molecular structure of **21a** was unequivocally confirmed by X-ray crystallography. There are two independent molecules in the unit cell. The two molecules have almost same geometry. The ORTEP drawing of molecule 1 and molecule 2 of **21a** are shown in Figure 4-2 and Figure 4-3, respectively. The crystal packing of **21a** is also shown in Figure 4-4. The final atomic parameters of **21a** are listed in Tables 4-1 and 4-2. The bond lengths of **21a** are summarized in Tables 4-3 and 4-4. The bond angles of **21a** are also summarized in Table 4-5.

The selected bond angles of molecule 1 and molecule 2 of **21a** are shown in Figures 4-5 and 4-6, respectively. The π-skeleton of **21a** is almost planar structure as expected. The internal bond angles of the central five-membered ring of molecule 1 are 106.7(2)-109.7(2)° (av 108.0°), and the sum of the bond angles is 539.8°. Those of molecule 2 are 106.7(2)-109.5(2)° (av 108.0°), and 539.9°. The angle formed by C1-C2-C3-C5 and C3-C4-C5 plane is 2.1(3)°. The angle formed by C22-C23-C24-C26 and C24-C25-C26 plane is 2.4(3)°.

The selected bond lengths of molecule 1 and molecule 2 of **21a** are shown in Figures 4-7 and 4-8, respectively. The substantial bond alternation between the single and double bonds of the π-skeleton of **21a** shows the structural feature as a cross-conjugated diene. The C-C single and double bond lengths of molecule 1 are 1.500(4)-1.519(4) Å (av 1.510 Å) and 1.372(4)-1.384(4) Å (av 1.378 Å), respectively. Those of molecule 2 are 1.508(4)-1.511(4) Å (av 1.510 Å) and 1.376(4)-1.378(4) Å (av 1.377 Å), respectively. The five- and six-membered rings containing the $Me_2SiCH_2SiMe_2$ fragments of **21a** have almost envelope conformations.

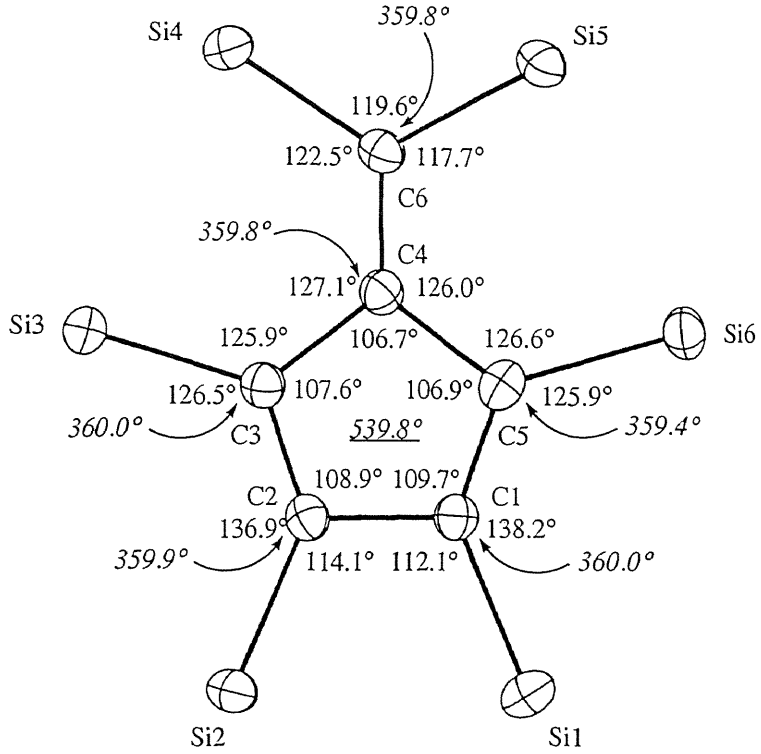

Figure 4-5. Selected bond angles of molecule 1 of **21a**.

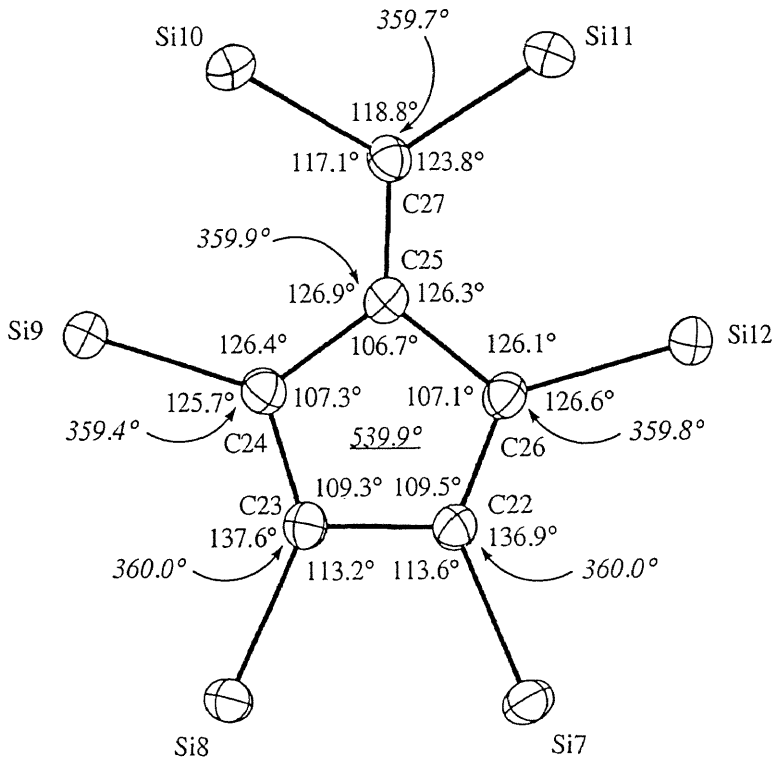

Figure 4-6. Selected bond angles of molecule 2 of **21a**.

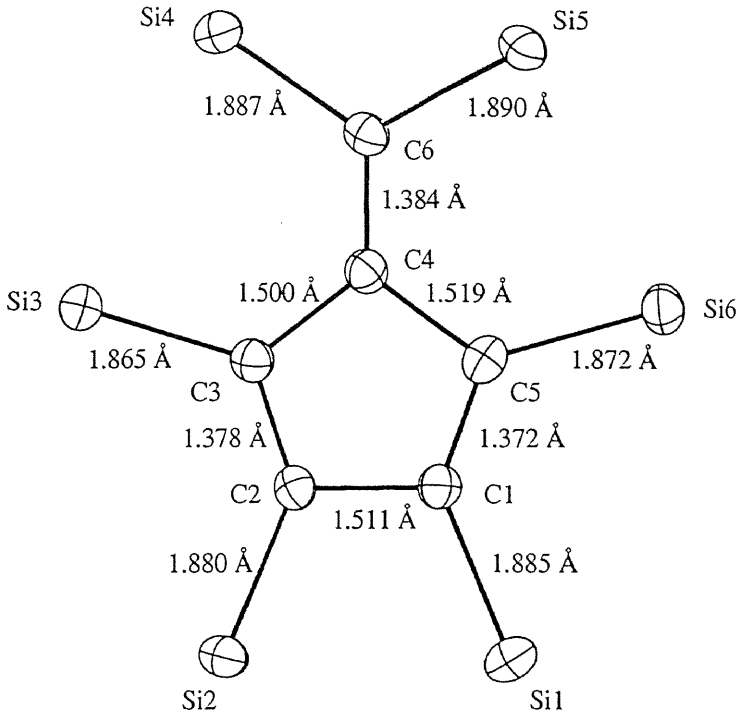

Figure 4-7. Selected bond lengths of molecule 1 of **21a**.

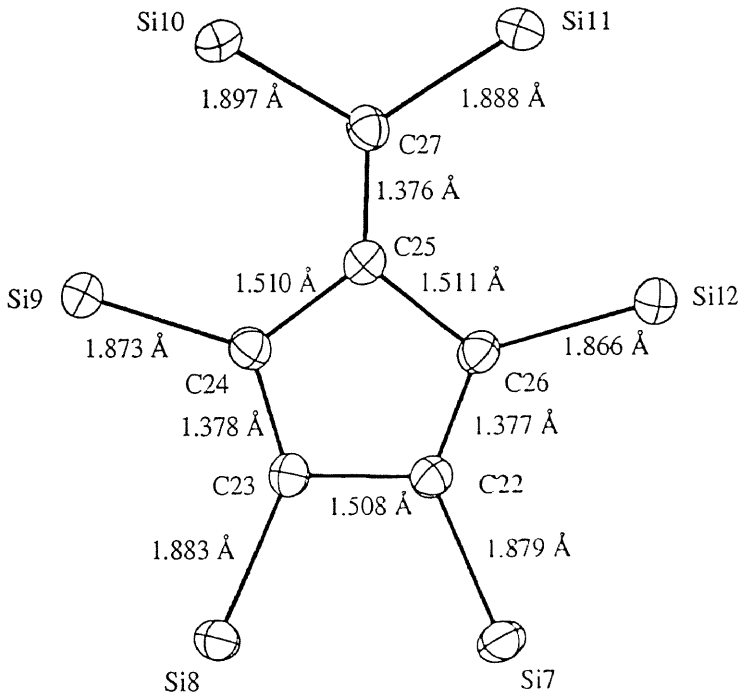

Figure 4-8. Selected bond lengths of molecule 2 of **21a**.

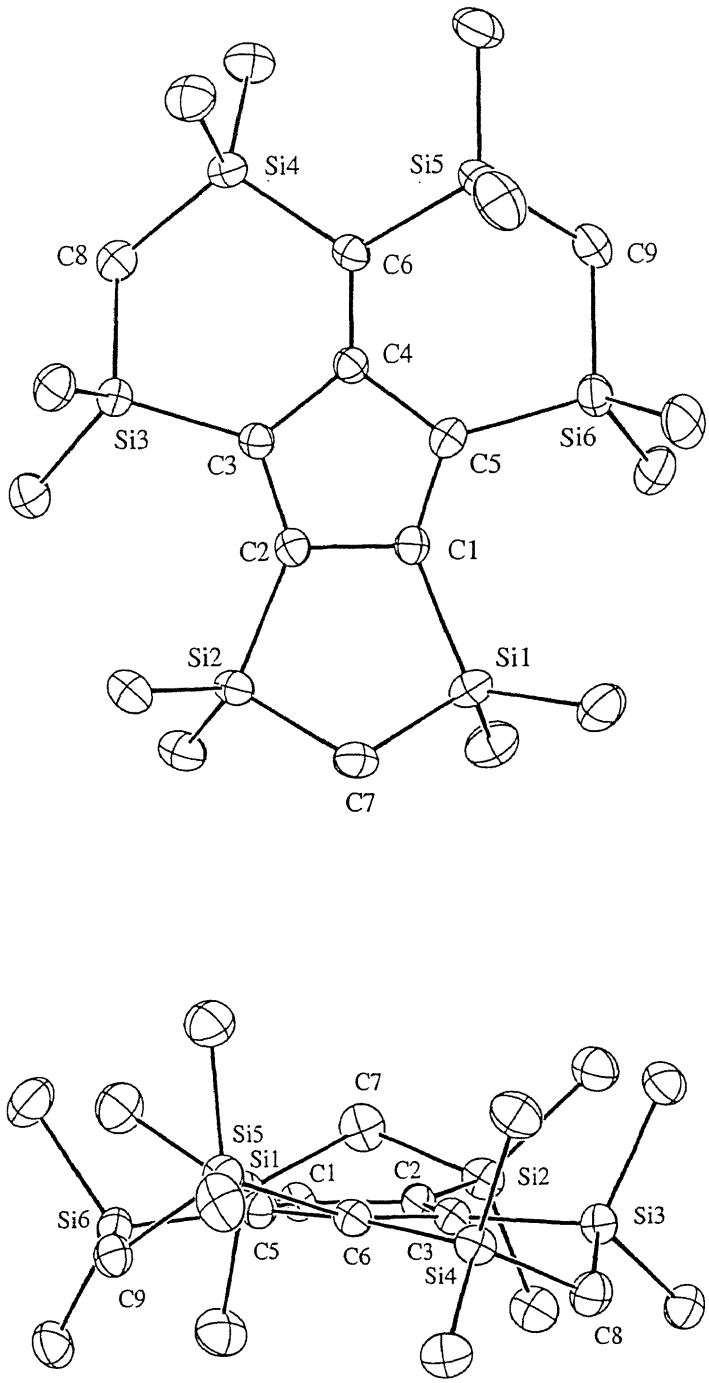

Figure 4-2. ORTEP drawing of molecule 1 of **21a** (hydrogen atoms are omitted for the clarity): upper, top view; below, side view.

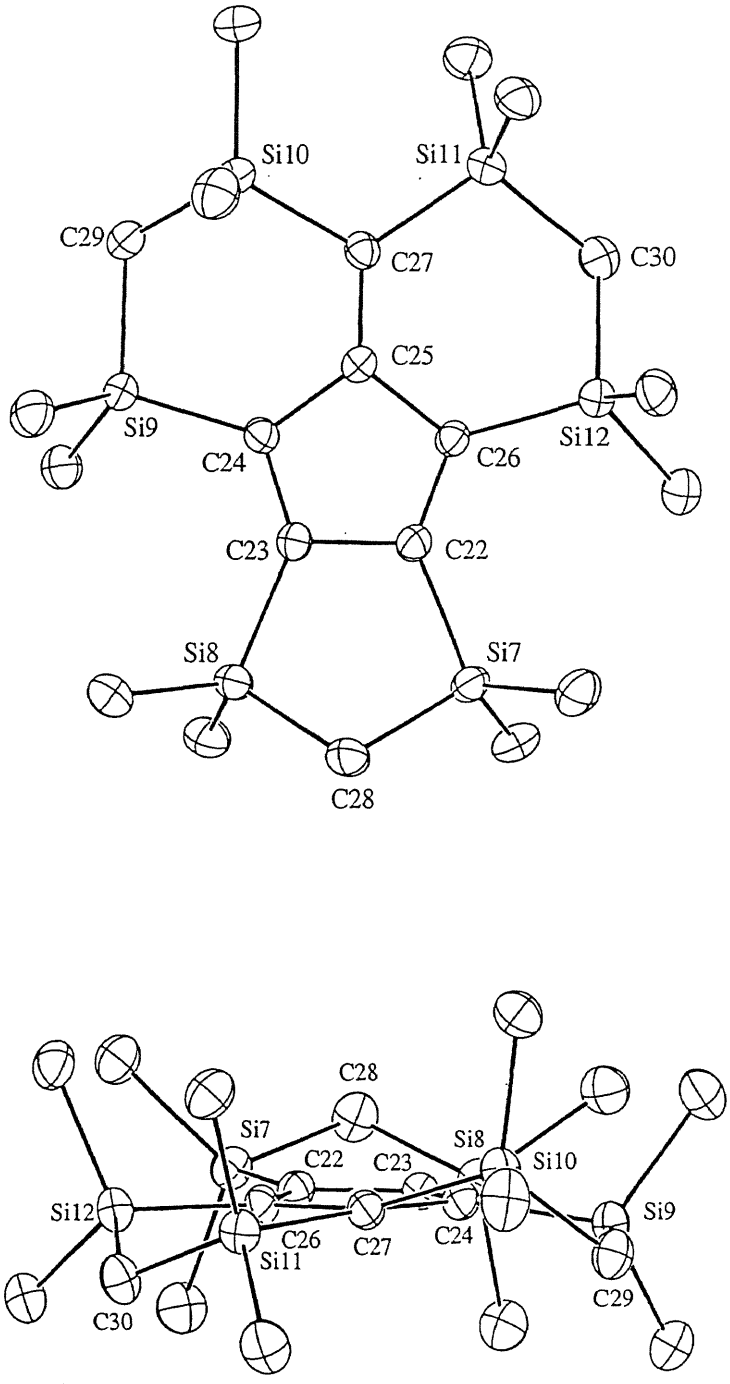

Figure 4-3. ORTEP drawing of molecule 2 of **21a** (hydrogen atoms are omitted for the clarity): upper, top view; below, side view.

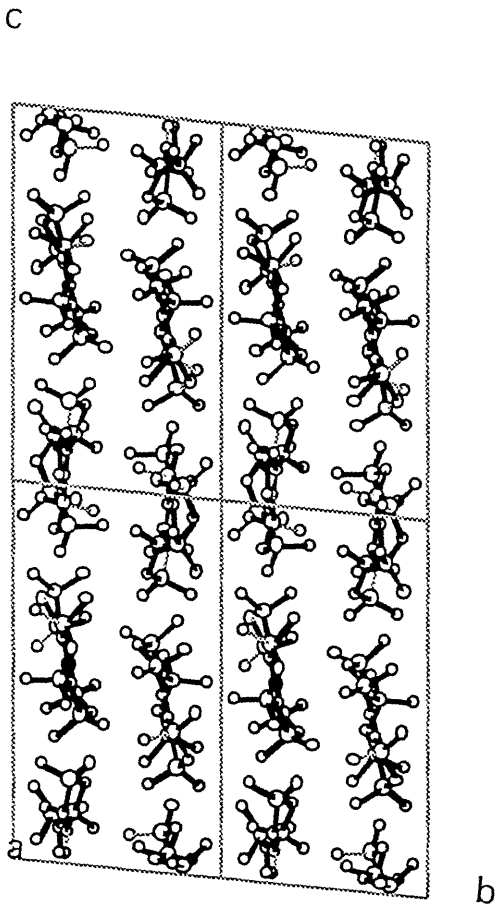

Figure 4-4. Crystal packing of **21a**.

Table 4-1. Atomic Parameters for Non-Hydrogen Atoms of **21a**

Atom	X/a	Y/b	Z/c	U(iso)
Si1	0.61410(7)	0.79490(6)	0.28480(3)	0.0267(3)
Si2	0.83550(7)	0.77990(6)	0.37750(3)	0.0243(3)
Si3	0.76470(6)	0.69530(6)	0.54560(3)	0.0226(3)
Si4	0.52240(7)	0.67100(6)	0.60210(3)	0.0239(3)
Si5	0.30870(7)	0.77150(7)	0.51170(3)	0.0278(3)
Si6	0.32340(7)	0.75020(6)	0.36540(3)	0.0251(3)
Si7	0.90450(7)	0.27860(6)	0.22270(3)	0.0249(3)
Si8	0.67650(7)	0.29600(6)	0.13520(3)	0.0241(3)
Si9	0.71010(6)	0.24710(6)	-0.04820(3)	0.0232(3)
Si10	0.94450(7)	0.27040(6)	-0.10630(3)	0.0261(3)
Si11	1.17240(7)	0.17860(6)	-0.02340(3)	0.0245(3)
Si12	1.16140(7)	0.20170(6)	0.12680(3)	0.0243(3)
C1	0.5812(2)	0.7676(2)	0.3693(1)	0.022(1)
C2	0.6930(2)	0.7527(2)	0.4142(1)	0.021(1)
C3	0.6614(2)	0.7256(2)	0.4735(1)	0.021(1)
C4	0.5290(2)	0.7295(2)	0.4707(1)	0.021(1)
C5	0.4836(2)	0.7556(2)	0.4022(1)	0.023(1)
C6	0.4618(2)	0.7203(2)	0.5217(1)	0.022(1)
C7	0.7758(3)	0.8526(3)	0.3061(1)	0.031(1)
C8	0.6674(3)	0.6135(3)	0.5957(1)	0.029(1)
C9	0.2312(3)	0.7095(3)	0.4300(1)	0.028(1)
C10	0.5262(3)	0.8972(3)	0.2419(1)	0.038(2)
C11	0.6001(3)	0.6585(3)	0.2305(1)	0.038(2)
C12	0.8941(3)	0.6449(3)	0.3489(1)	0.032(1)
C13	0.9555(3)	0.8772(3)	0.4318(1)	0.031(1)
C14	0.8820(3)	0.6069(3)	0.5203(1)	0.030(1)
C15	0.8406(3)	0.8292(3)	0.5939(1)	0.031(1)
C16	0.5395(3)	0.7925(3)	0.6679(1)	0.036(1)
C17	0.4166(3)	0.5531(3)	0.6242(2)	0.035(1)
C18	0.3337(3)	0.9304(3)	0.5185(2)	0.043(2)
C19	0.2149(3)	0.7335(3)	0.5763(1)	0.039(2)
C20	0.2909(3)	0.6436(3)	0.2917(1)	0.033(1)
C21	0.2839(3)	0.8904(3)	0.3402(2)	0.041(2)
C22	0.9184(2)	0.2548(2)	0.1334(1)	0.021(1)
C23	0.8055(2)	0.2683(2)	0.0893(1)	0.021(1)
C24	0.8262(2)	0.2549(2)	0.0252(1)	0.021(1)
C25	0.9544(2)	0.2305(2)	0.0255(1)	0.022(1)
C26	1.0057(2)	0.2278(2)	0.0961(1)	0.021(1)
C27	1.0159(2)	0.2213(2)	-0.0275(1)	0.022(1)
C28	0.7637(3)	0.3503(3)	0.2166(1)	0.031(1)
C29	0.7853(3)	0.2060(3)	-0.1205(1)	0.028(1)
C30	1.2165(3)	0.1244(3)	0.0567(1)	0.031(1)
C31	1.0321(3)	0.3730(3)	0.2721(1)	0.034(1)
C32	0.8784(3)	0.1400(3)	0.2583(1)	0.034(1)
C33	0.5820(3)	0.1605(3)	0.1431(1)	0.033(1)

Table 4-1 (continued). Atomic Parameters for Non-Hydrogen Atoms of **21a**

Atom	X/a	Y/b	Z/c	U(iso)
C34	0.5785(3)	0.4012(3)	0.1030(1)	0.032(1)
C35	0.5807(3)	0.1394(3)	-0.0402(1)	0.031(1)
C36	0.6517(3)	0.3864(3)	-0.0611(2)	0.036(1)
C37	0.9610(3)	0.4288(3)	-0.0953(2)	0.037(2)
C38	1.0176(3)	0.2307(3)	-0.1799(1)	0.039(2)
C39	1.1803(3)	0.0616(3)	-0.0889(1)	0.037(2)
C40	1.2757(3)	0.3055(3)	-0.0363(2)	0.034(1)
C41	1.2599(3)	0.3370(3)	0.1542(1)	0.033(1)
C42	1.1656(3)	0.1116(3)	0.1965(1)	0.033(1)

Table 4-2. Atomic Parameters for Hydrogen Atoms of **21a**

Atom	X/a	Y/b	Z/c	U(iso)
H7A	0.771(3)	0.937(3)	0.320(2)	0.03(1)
H7B	0.814(3)	0.843(3)	0.268(2)	0.03(1)
H8A	0.712(3)	0.608(3)	0.637(2)	0.020(9)
H8B	0.648(3)	0.533(3)	0.575(2)	0.03(1)
H9A	0.222(3)	0.624(3)	0.429(2)	0.018(9)
H9B	0.157(4)	0.731(3)	0.425(2)	0.03(1)
H10A	0.435(3)	0.869(3)	0.227(1)	0.011(8)
H10B	0.567(4)	0.911(3)	0.206(2)	0.04(1)
H10C	0.525(3)	0.967(3)	0.271(2)	0.03(1)
H11A	0.636(4)	0.673(3)	0.189(2)	0.04(1)
H11B	0.649(3)	0.608(3)	0.254(2)	0.03(1)
H11C	0.515(4)	0.631(3)	0.222(2)	0.03(1)
H12A	0.956(4)	0.663(3)	0.325(2)	0.04(1)
H12B	0.827(4)	0.594(3)	0.329(2)	0.03(1)
H12C	0.927(3)	0.600(3)	0.389(2)	0.03(1)
H13A	1.019(3)	0.900(3)	0.405(2)	0.014(8)
H13B	0.923(3)	0.944(3)	0.447(2)	0.018(9)
H13C	0.997(3)	0.839(3)	0.475(2)	0.03(1)
H14A	0.841(3)	0.539(3)	0.492(1)	0.006(8)
H14B	0.939(3)	0.651(3)	0.499(1)	0.010(8)
H14C	0.924(3)	0.582(3)	0.562(2)	0.023(9)
H15A	0.894(4)	0.818(3)	0.628(2)	0.04(1)
H15B	0.889(3)	0.877(3)	0.565(2)	0.023(9)
H15C	0.785(4)	0.871(4)	0.613(2)	0.04(1)
H16A	0.457(3)	0.823(3)	0.672(2)	0.02(1)
H16B	0.595(4)	0.853(4)	0.656(2)	0.04(1)
H16C	0.562(4)	0.767(3)	0.708(2)	0.04(1)
H17A	0.461(4)	0.516(4)	0.658(2)	0.06(1)
H17B	0.342(4)	0.578(3)	0.637(2)	0.03(1)
H17C	0.406(4)	0.482(4)	0.586(2)	0.05(1)
H18A	0.386(4)	0.955(3)	0.487(2)	0.03(1)
H18B	0.366(3)	0.956(3)	0.561(2)	0.03(1)
H18C	0.250(4)	0.962(3)	0.511(2)	0.03(1)
H19A	0.262(3)	0.763(3)	0.625(2)	0.023(9)
H19B	0.184(3)	0.651(3)	0.570(2)	0.018(9)
H19C	0.142(4)	0.777(3)	0.571(2)	0.03(1)
H20A	0.336(3)	0.668(3)	0.254(2)	0.03(1)
H20B	0.310(3)	0.572(3)	0.302(2)	0.03(1)
H20C	0.204(4)	0.636(3)	0.278(2)	0.04(1)
H21A	0.193(4)	0.885(3)	0.324(2)	0.04(1)
H21B	0.334(4)	0.917(3)	0.310(2)	0.04(1)
H21C	0.292(4)	0.940(4)	0.372(2)	0.05(1)
H28A	0.786(3)	0.430(3)	0.215(2)	0.03(1)
H28B	0.713(3)	0.336(3)	0.254(2)	0.02(1)
H29A	0.788(3)	0.119(3)	-0.127(2)	0.017(9)

Table 4-2 (continued). Atomic Parameters for Hydrogen Atoms of **21a**

Atom	X/a	Y/b	Z/c	U(iso)
H29B	0.744(3)	0.233(3)	-0.159(2)	0.021(9)
H30A	1.305(3)	0.123(3)	0.065(2)	0.018(9)
H30B	1.177(3)	0.049(3)	0.052(2)	0.019(9)
H31A	1.111(3)	0.334(3)	0.277(1)	0.014(8)
H31B	1.049(4)	0.440(4)	0.253(2)	0.04(1)
H31C	1.014(3)	0.393(3)	0.316(2)	0.03(1)
H32A	0.862(3)	0.154(3)	0.301(2)	0.03(1)
H32B	0.951(3)	0.101(3)	0.258(1)	0.011(8)
H32C	0.810(4)	0.093(3)	0.232(2)	0.03(1)
H33A	0.535(3)	0.118(3)	0.098(2)	0.021(9)
H33B	0.521(4)	0.176(4)	0.170(2)	0.05(1)
H33C	0.631(3)	0.113(3)	0.159(2)	0.019(9)
H34A	0.528(3)	0.367(3)	0.061(2)	0.020(9)
H34B	0.624(3)	0.466(3)	0.094(1)	0.009(8)
H34C	0.530(3)	0.426(3)	0.135(2)	0.023(9)
H35A	0.608(3)	0.065(3)	-0.028(2)	0.02(1)
H35B	0.529(3)	0.165(3)	-0.008(2)	0.03(1)
H35C	0.526(3)	0.126(3)	-0.082(2)	0.03(1)
H36A	0.633(4)	0.420(3)	-0.024(2)	0.04(1)
H36B	0.589(4)	0.368(4)	-0.096(2)	0.07(2)
H36C	0.713(4)	0.440(4)	-0.072(2)	0.06(1)
H37A	0.929(3)	0.458(3)	-0.057(2)	0.017(9)
H37B	1.042(4)	0.462(3)	-0.095(2)	0.03(1)
H37C	0.919(3)	0.456(3)	-0.133(2)	0.03(1)
H38A	1.108(4)	0.267(3)	-0.174(2)	0.03(1)
H38B	1.008(4)	0.138(4)	-0.192(2)	0.04(1)
H38C	0.980(4)	0.264(4)	-0.216(2)	0.05(1)
H39A	1.255(4)	0.032(3)	-0.075(2)	0.04(1)
H39B	1.189(4)	0.092(3)	-0.137(2)	0.05(1)
H39C	1.114(4)	-0.008(4)	-0.086(2)	0.05(1)
H40A	1.255(4)	0.328(3)	-0.075(2)	0.04(1)
H40B	1.353(4)	0.285(4)	-0.040(2)	0.05(1)
H40C	1.281(3)	0.364(3)	0.000(2)	0.03(1)
H41A	1.338(4)	0.322(3)	0.172(2)	0.03(1)
H41B	1.234(3)	0.379(3)	0.191(2)	0.03(1)
H41C	1.266(3)	0.388(3)	0.120(2)	0.02(1)
H42A	1.139(3)	0.151(3)	0.236(2)	0.023(9)
H42B	1.243(3)	0.090(3)	0.199(2)	0.03(1)
H42C	1.104(3)	0.042(3)	0.188(2)	0.019(9)

Table 4-3. List of Bond Lengths (Å) for Non-Hydrogen Atoms of **21a**

Atom	Atom	Length(sig)
Si1	C1	1.885(3)
Si1	C7	1.873(4)
Si1	C10	1.864(4)
Si1	C11	1.874(4)
Si2	C2	1.880(3)
Si2	C7	1.867(3)
Si2	C12	1.877(4)
Si2	C13	1.877(3)
Si3	C3	1.865(3)
Si3	C8	1.865(3)
Si3	C14	1.875(3)
Si3	C15	1.872(3)
Si4	C6	1.887(3)
Si4	C8	1.859(3)
Si4	C16	1.877(4)
Si4	C17	1.873(4)
Si5	C6	1.890(3)
Si5	C9	1.862(3)
Si5	C18	1.870(4)
Si5	C19	1.868(4)
Si6	C5	1.872(3)
Si6	C9	1.865(3)
Si6	C20	1.873(3)
Si6	C21	1.868(4)
Si7	C22	1.879(3)
Si7	C28	1.881(4)
Si7	C31	1.870(4)
Si7	C32	1.872(4)
Si8	C23	1.883(3)
Si8	C28	1.874(3)
Si8	C33	1.870(4)
Si8	C34	1.867(4)
Si9	C24	1.873(3)
Si9	C29	1.870(3)
Si9	C35	1.877(4)
Si9	C36	1.872(4)
Si10	C27	1.897(3)
Si10	C29	1.863(3)
Si10	C37	1.863(4)
Si10	C38	1.875(4)
Si11	C27	1.888(3)
Si11	C30	1.862(3)
Si11	C39	1.876(4)
Si11	C40	1.870(4)
Si12	C26	1.866(3)

Table 4-3 (continued). List of Bond Lengths (Å) for Non-Hydrogen Atoms of **21a**

Atom	Atom	Length(sig)
Si12	C30	1.862(3)
Si12	C41	1.862(4)
Si12	C42	1.870(3)
C1	C2	1.511(4)
C1	C5	1.372(4)
C2	C3	1.378(4)
C3	C4	1.500(4)
C4	C5	1.519(4)
C4	C6	1.384(4)
C22	C23	1.508(4)
C22	C26	1.377(4)
C23	C24	1.378(4)
C24	C25	1.510(4)
C25	C26	1.511(4)
C25	C27	1.376(4)

Table 4-4. List of Bond Lengths (Å) for Hydrogen Atoms of **21a**

Atom	Atom	Length(sig)
C7	H7A	1.03(4)
C7	H7B	0.96(4)
C8	H8A	0.96(4)
C8	H8B	1.00(4)
C9	H9A	1.00(4)
C9	H9B	0.90(4)
C10	H10A	1.05(4)
C10	H10B	0.94(4)
C10	H10C	0.98(4)
C11	H11A	1.03(4)
C11	H11B	0.97(4)
C11	H11C	0.97(5)
C12	H12A	0.92(5)
C12	H12B	0.95(4)
C12	H12C	1.08(4)
C13	H13A	1.00(4)
C13	H13B	0.95(4)
C13	H13C	1.12(4)
C14	H14A	0.99(4)
C14	H14B	0.97(4)
C14	H14C	1.02(4)
C15	H15A	0.91(5)
C15	H15B	1.03(4)
C15	H15C	0.95(5)
C16	H16A	1.05(4)
C16	H16B	0.97(5)
C16	H16C	0.92(5)
C17	H17A	0.96(5)
C17	H17B	0.98(4)
C17	H17C	1.09(5)
C18	H18A	0.97(4)
C18	H18B	0.92(4)
C18	H18C	1.05(4)
C19	H19A	1.09(4)
C19	H19B	1.00(4)
C19	H19C	1.02(4)
C20	H20A	1.04(4)
C20	H20B	0.94(4)
C20	H20C	0.99(5)
C21	H21A	1.03(5)
C21	H21B	0.95(5)
C21	H21C	0.84(5)
C28	H28A	0.96(4)
C28	H28B	1.03(4)
C29	H29A	1.04(4)

Table 4-4 (contibued). List of Bond Lengths (Å) for Hydrogen Atoms of **21a**

Atom	Atom	Length(sig)
C29	H29B	0.97(4)
C30	H30A	1.00(4)
C30	H30B	0.95(4)
C31	H31A	1.05(4)
C31	H31B	0.94(5)
C31	H31C	0.97(4)
C32	H32A	0.93(4)
C32	H32B	0.98(4)
C32	H32C	0.98(4)
C33	H33A	1.07(4)
C33	H33B	0.96(5)
C33	H33C	0.89(4)
C34	H34A	1.00(4)
C34	H34B	0.93(4)
C34	H34C	0.96(4)
C35	H35A	1.00(4)
C35	H35B	0.99(4)
C35	H35C	0.99(4)
C36	H36A	0.90(5)
C36	H36B	0.94(5)
C36	H36C	0.96(5)
C37	H37A	0.96(4)
C37	H37B	0.97(5)
C37	H37C	0.97(4)
C38	H38A	1.06(5)
C38	H38B	1.10(5)
C38	H38C	0.96(5)
C39	H39A	0.97(5)
C39	H39B	1.09(5)
C39	H39C	1.07(5)
C40	H40A	0.87(5)
C40	H40B	0.95(5)
C40	H40C	0.98(4)
C41	H41A	0.96(4)
C41	H41B	0.97(4)
C41	H41C	0.98(4)
C42	H42A	1.00(4)
C42	H42B	0.94(4)
C42	H42C	1.01(4)

Table 4-5. List of Bond Angles (Å) for Non-Hydrogen Atoms of **21a**

Atom	Atom	Atom	Angle(sig)
C1	Si1	C7	98.4(2)
C1	Si1	C10	117.1(2)
C1	Si1	C11	111.0(2)
C7	Si1	C10	111.5(2)
C7	Si1	C11	109.8(2)
C10	Si1	C11	108.7(2)
C2	Si2	C7	98.6(2)
C2	Si2	C12	112.5(2)
C2	Si2	C13	113.7(2)
C7	Si2	C12	110.2(2)
C7	Si2	C13	110.4(2)
C12	Si2	C13	110.8(2)
C3	Si3	C8	105.0(2)
C3	Si3	C14	111.3(2)
C3	Si3	C15	111.8(2)
C8	Si3	C14	109.6(2)
C8	Si3	C15	110.4(2)
C14	Si3	C15	108.7(2)
C6	Si4	C8	110.2(2)
C6	Si4	C16	109.5(2)
C6	Si4	C17	110.2(2)
C8	Si4	C16	111.2(2)
C8	Si4	C17	107.1(2)
C16	Si4	C17	108.6(2)
C6	Si5	C9	107.1(2)
C6	Si5	C18	106.6(2)
C6	Si5	C19	114.5(2)
C9	Si5	C18	112.4(2)
C9	Si5	C19	110.0(2)
C18	Si5	C19	106.3(2)
C5	Si6	C9	106.4(2)
C5	Si6	C20	110.1(2)
C5	Si6	C21	112.9(2)
C9	Si6	C20	111.2(2)
C9	Si6	C21	108.1(2)
C20	Si6	C21	108.1(2)
C22	Si7	C28	99.0(2)
C22	Si7	C31	114.3(2)
C22	Si7	C32	110.9(2)
C28	Si7	C31	111.0(2)
C28	Si7	C32	109.9(2)
C31	Si7	C32	111.1(2)
C23	Si8	C28	98.7(2)
C23	Si8	C33	111.1(2)
C23	Si8	C34	116.2(2)

Table 4-5 (continued). List of Bond Angles (Å) for Non-Hydrogen Atoms of **21a**

Atom	Atom	Atom	Angle(sig)
C28	Si8	C33	109.2(2)
C28	Si8	C34	111.8(2)
C33	Si8	C34	109.3(2)
C24	Si9	C29	106.4(2)
C24	Si9	C35	109.8(2)
C24	Si9	C36	113.3(2)
C29	Si9	C35	111.5(2)
C29	Si9	C36	107.4(2)
C35	Si9	C36	108.5(2)
C27	Si10	C29	107.3(2)
C27	Si10	C37	107.0(2)
C27	Si10	C38	114.7(2)
C29	Si10	C37	113.0(2)
C29	Si10	C38	108.9(2)
C37	Si10	C38	106.1(2)
C27	Si11	C30	110.0(2)
C27	Si11	C39	110.8(2)
C27	Si11	C40	108.1(2)
C30	Si11	C39	107.5(2)
C30	Si11	C40	111.7(2)
C39	Si11	C40	108.7(2)
C26	Si12	C30	105.5(2)
C26	Si12	C41	111.8(2)
C26	Si12	C42	112.0(2)
C30	Si12	C41	110.3(2)
C30	Si12	C42	109.1(2)
C41	Si12	C42	108.1(2)
Si1	C1	C2	112.1(2)
Si1	C1	C5	138.2(2)
C2	C1	C5	109.7(2)
Si2	C2	C1	114.1(2)
Si2	C2	C3	136.9(2)
C1	C2	C3	108.9(3)
Si3	C3	C2	126.5(2)
Si3	C3	C4	125.9(2)
C2	C3	C4	107.6(3)
C3	C4	C5	106.7(2)
C3	C4	C6	127.1(3)
C5	C4	C6	126.0(3)
Si6	C5	C1	125.9(2)
Si6	C5	C4	126.6(2)
C1	C5	C4	106.9(3)
Si4	C6	Si5	119.6(2)
Si4	C6	C4	122.5(2)
Si5	C6	C4	117.7(2)

Table 4-5 (continued). List of Bond Angles (Å) for Non-Hydrogen Atoms of **21a**

Atom	Atom	Atom	Angle(sig)
Si1	C7	Si2	106.4(2)
Si3	C8	Si4	113.5(2)
Si5	C9	Si6	109.9(2)
Si7	C22	C23	113.6(2)
Si7	C22	C26	136.9(2)
C23	C22	C26	109.5(2)
Si8	C23	C22	113.2(2)
Si8	C23	C24	137.6(2)
C22	C23	C24	109.3(3)
Si9	C24	C23	125.7(2)
Si9	C24	C25	126.4(2)
C23	C24	C25	107.3(3)
C24	C25	C26	106.7(2)
C24	C25	C27	126.9(3)
C26	C25	C27	126.3(3)
Si12	C26	C22	126.6(2)
Si12	C26	C25	126.2(2)
C22	C26	C25	107.1(3)
Si10	C27	Si11	118.8(2)
Si10	C27	C25	117.1(2)
Si11	C27	C25	123.8(2)
Si7	C28	Si8	106.2(2)
Si9	C29	Si10	109.5(2)
Si11	C30	Si12	114.1(2)

PM3 Calculation of Hexasilylfulvene 21a

The geometry optimization of hexasilylfulvene **21a** was carried out by PM3 calculation.[10] The calculated structure of **21a** is shown in Figure 4-9. The LUMO of **21a** is also shown in Figure 4-10. The geometry of **21a** by the X-ray diffraction is approximately reproduced by PM3 calculation. The selected bond angles and lengths of **21a** calculated by PM3 are shown in Figures 4-11 and 4-12. The charge distribution of **21a** is also shown in Figure 4-13.

Consideration of π-MO of **21a** is very important to understand the nature of π-electron system. The energy diagram of **21a** calculated by PM3 is shown in Figure 4-14. The level of LUMO (-0.19 eV) is remarkably stabilized by silyl groups. The schematic drawing of the LUMO of **21a** is shown in Figure 4-15. In the LUMO, C1-C2, C3-C4, and C4-C5 bonds are bonding, while C1-C5, C2-C3, and C4-C6 bonds are antibonding. The π-MO coefficient at the exo carbon atom (C6) is larger than that of five-membered carbon atoms (C1, C2, C3, C4, and C5). Interestingly, the central five-membered ring has similar π-MO to cyclopentadienide ion with 6π-electron system. In addition, the π-MO of the exo C4-C6 bond is antibonding. Thus, it is reasonable to accept that reduction of **21a** may yield the corresponding dianion species; one negative charge is delocalized on the five-membered ring and forms a 5 center / 6π-electron aromatic cyclopentadienide ion, and the other one is almost localized on the exocyclic carbon atom stabilized by two silicon atoms (Si4 and Si5).

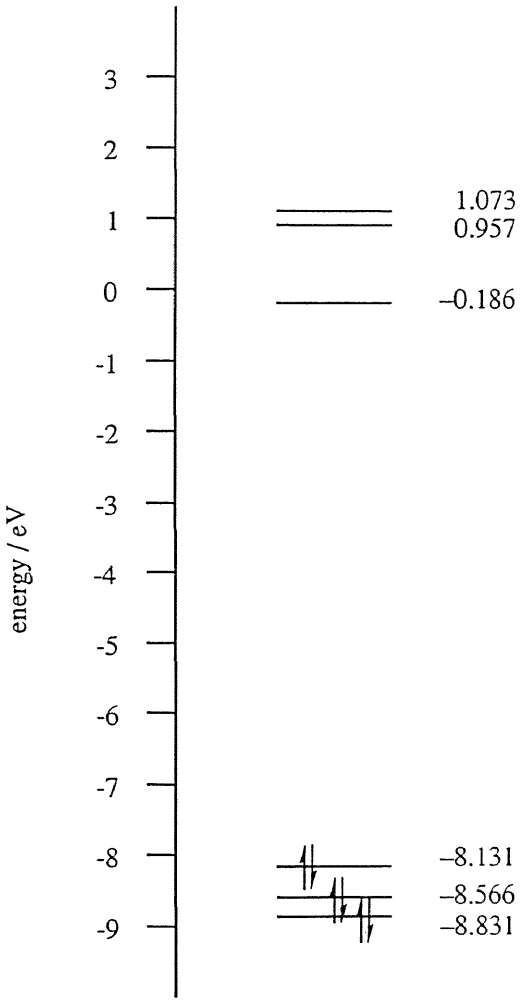

Figure 4-14. Energy diagram of **21a** calculated by PM3.

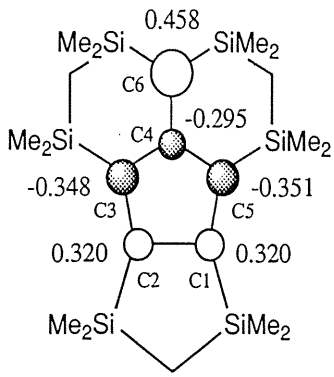

Figure 4-15. Schematic representation of the LUMO of **21a** calculated by PM3.

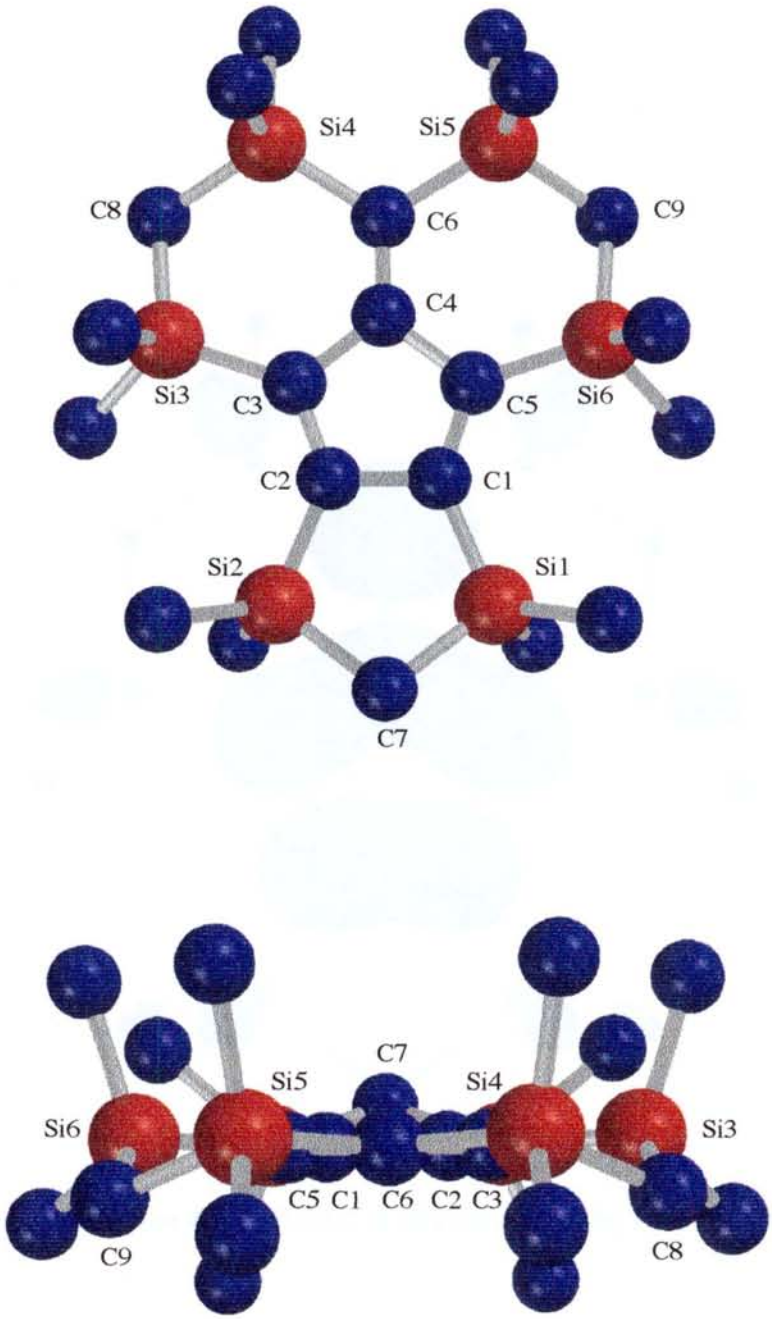

Figure 4-9. Calculated structure of **21a** by PM3 (hydrogen atoms are omitted for the clarity): upper, top view; below, side view.

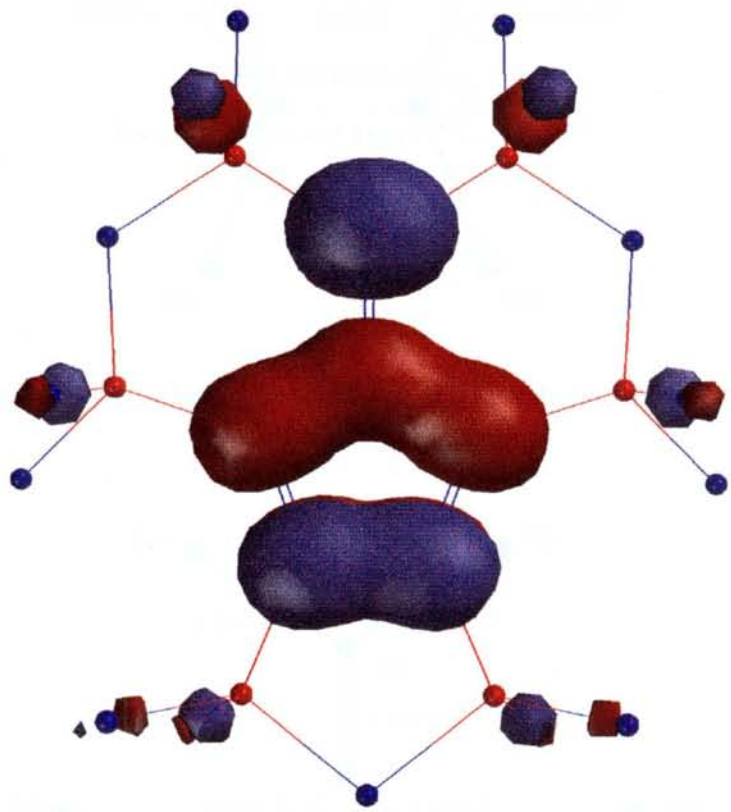

Figure 4-10. LUMO of **21a** calculated by PM3.

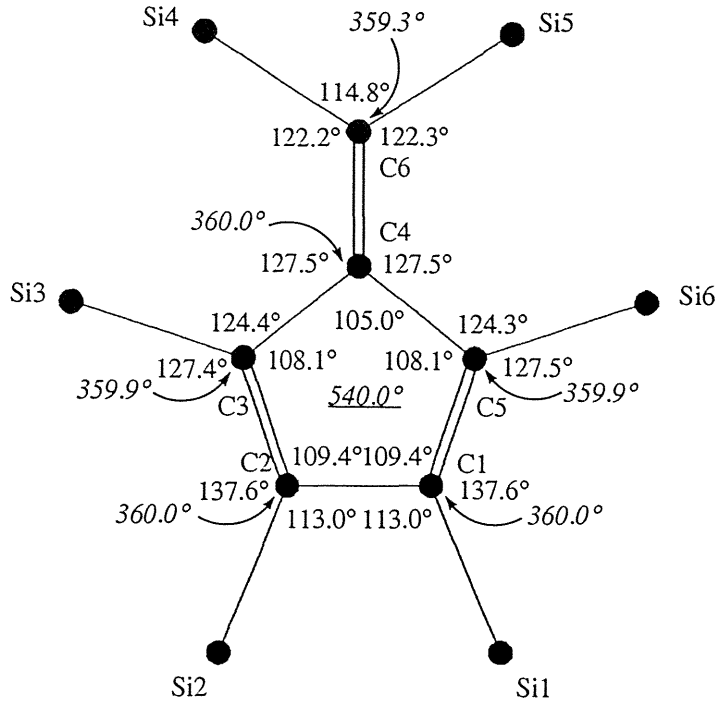

Figure 4-11. Selected bond angles of **21a** calculated by PM3.

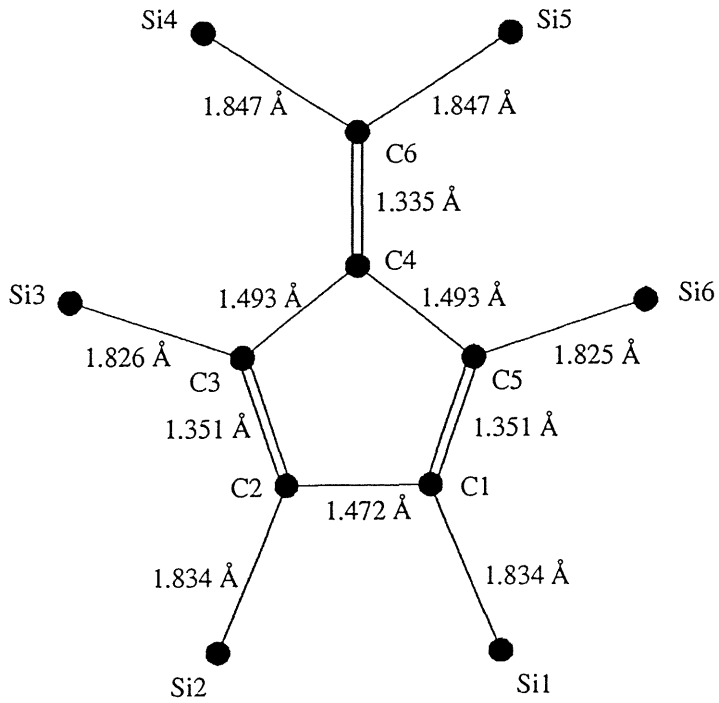

Figure 4-12. Selected bond lengths of **21a** calculated by PM3.

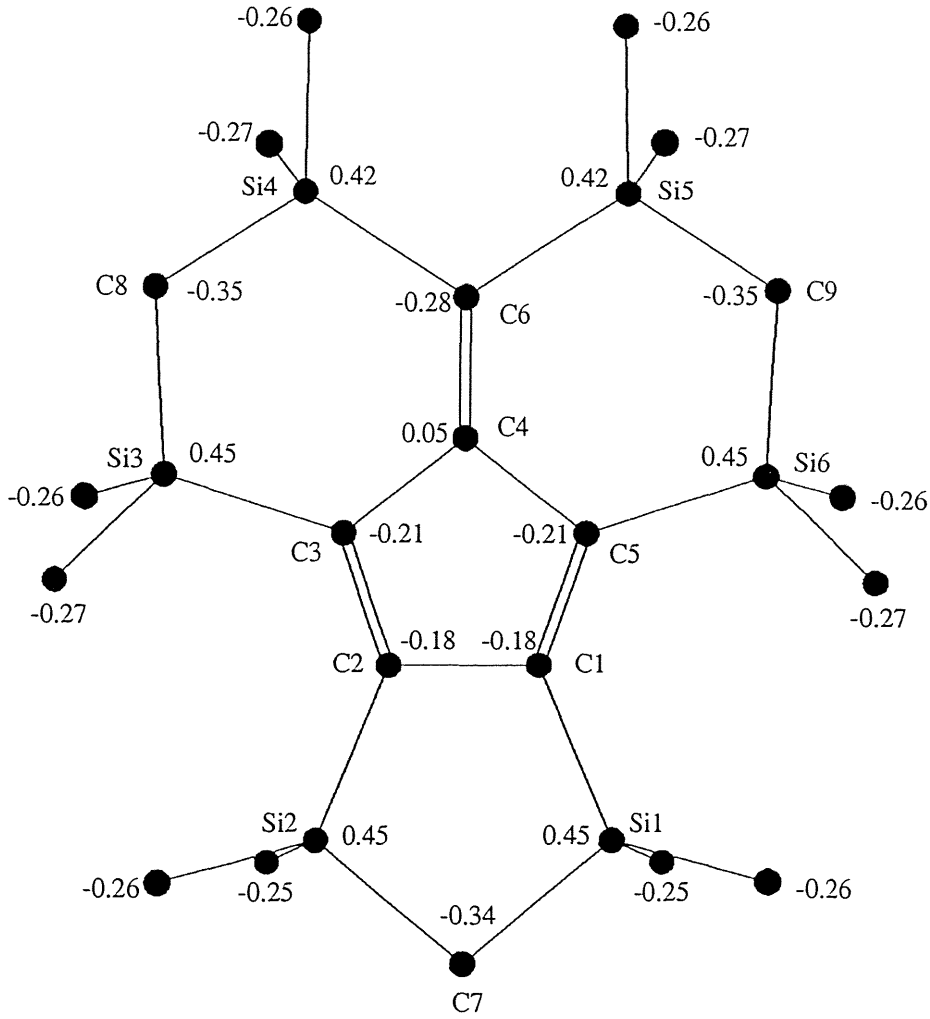

Figure 4-13. Mulliken charge distribution of **21a** calculated by PM3.

Two Electron Reduction of Hexasilylfulvene 21 with Lithium Metal

The reaction of **21a** with excess lithium metal in dry oxygen-free THF at room temperature led to the formation of a yellow solution of the dianion of **21a**. The two electron reduction occurred quantitatively and completed within 1 hour (Scheme 4-7). After the solvent was removed in vacuo, dry degassed heptane was introduced by vacuum transfer. Crystallization from a heptane solution afforded air and moisture sensitive yellow crystals of the dilithium salt of fulvene dianion (**24a**) containing three molecules of THF.

Scheme 4-7

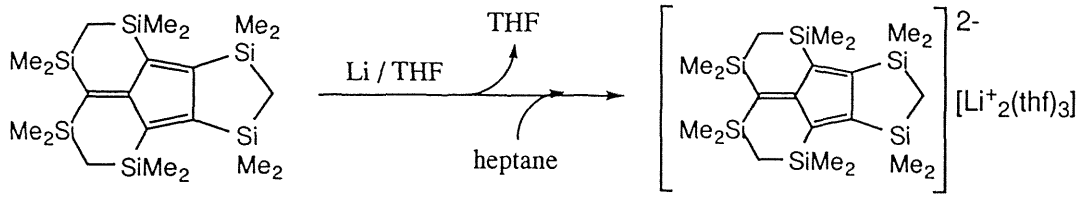

21a **24a**

Fulvene **21b** bridged by siloxane chains also underwent a two electron reduction in THF to yield a yellow solution of the dianion dilithium (**24b**) within 1 hour (Scheme 4-8). The structure of **24a** and **24b** were deduced by NMR spectroscopy, and the structure of **24a** was unequivocally determined by X-ray diffraction.

Scheme 4-8

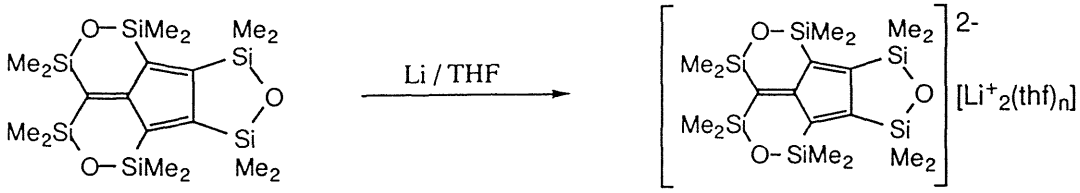

21b **24b**

Molecular Structure of Dilithium Hexasilylfulvene Dianion 24a

The molecular structure of **24a** was unambiguously determined by X-ray crystallography. The dilithium salt **24a** has a monomeric structure and forms contact ion pair (bis-CIP) in the crystals. The ORTEP drawing of **24a** is shown in Figures 4-16 and 4-17. The crystal packing of **24a** is also shown in Figure 4-18. The final atomic parameters of **24a** are listed in Tables 4-6 and 4-7. The atomic distances of **24a** are summarized in Tables 4-8 and 4-9. The bond lengths of **24a** are also summarized in Table 4-10.

Several interesting features of the structure of **24a** can be pointed out. One THF molecule is coordinated with Li1 and two THF molecules are coordinated with Li2. Li1 and Li2 are located above and below of the π-skeleton, respectively. Li1 is situated above the approximate center of the five-membered (Cp) ring. The selected bond lengths of **24a** are shown in Figure 4-19. The lithium-carbon distances for the Cp ring range from 2.164(3) to 2.191(3) Å (av 2.179 Å), so that the Li-to-Cp interaction clearly qualifies as η^5. Li2 is bonded to two carbon atoms (C6 and C9) with distances of 2.136(6) for Li2-C6 and 2.325(6) Å for Li2-C9. The five- and six-membered rings linked by $Me_2SiCH_2SiMe_2$ fragments have the envelope conformation.

The Li distance from the ring centroid (1.795 Å) is comparable to that observed in $[(Ph_2C{=}O)Li{\cdot}\{C_5(SiMe_2H)_5\}]$ (1.818 Å),[11] and somewhat shorter than those observed in $Li(C_5H_4Me)TMEDA$ (1.92 Å),[12] $Li[C_5H_4(SiMe_3)]TMEDA$ (1.93 Å),[13] $[(isodiCp)_2\text{-}Li]^-$,[14] $LiCp_2^-$ (2.008 Å),[15] $[Li_2(TMEDA)_2(C_5H_4Me)]^-$ (2.00 Å).[16] The Li distance from the Cp ring of the tetralithium octasilyltrimethylenecyclopentene tetraanion,[17] bridged by $Me_2SiCH_2SiMe_2$, is also slightly short (1.827 Å), as was the Li distance in **24a**. The relatively short Li distance of **24a** compared with the reported Li distances may be due to the bridged structure consisting of $Me_2SiCH_2SiMe_2$ chains.

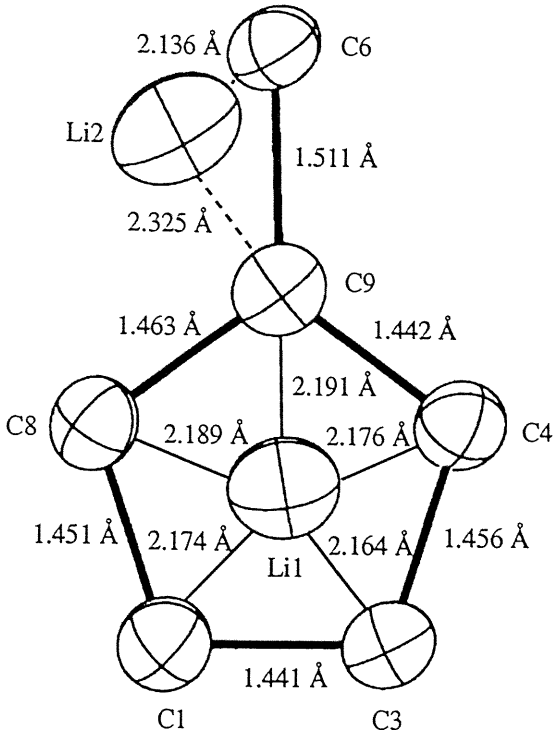

Figure 4-19. Selected bond lengths of **24a**.

Comparison of the structural parameters of **21a** (molecule 2) and **24a** is quite interesting. In **24a**, the central five-membered ring, the exo carbon atom (C6), and Si1, Si2, Si3, Si4, Si6, and C7 atoms become completely coplanar by the two electron reduction. The distance of C6-C9 (1.511(4) Å) is considerably elongated by 0.135(4) Å relative to that of **21a** (1.376(4) Å). The distances of C3-C4 (1.456(4) Å) and C1-C8 (1.451(4) Å) are also stretched by 0.079(4) and 0.073(4) Å compared with **21a** (1.377(4) and 1.378(4) Å, respectively). In contrast, the distances of C1-C3 (1.441(4) Å), C4-C9 (1.442(4) Å), and C8-C9 (1.463(4) Å) of **24a** are shortened by 0.047-0.069 Å (1.508(4), 1.511(4), 1.510(4) Å, respectively, for **21a**). That is, the C-C double bonds of **21a** are elongated, whereas the C-C single bonds are shortened by the reduction. Therefore, the geometry of **24a** reflects the nature of the LUMO of **21a** (Figure 4-15). Thus, the C6-C9, C3-C4, and C1-C8 bonds are antibonding, whereas the C1-C3, C4-C9, and C8-C9 bonds are bonding.

The selected bond angles and lengths of **24a** are shown in Figures 4-20 and 4-21, respectively. The Cp ring is an almost planar equilateral pentagon, as determined by the internal bond angles of 107.7(3)-108.2(3)° (av 108.0°) and the sum of the bond angles (540.0°). The C-C distances of the five-membered ring are 1.441(4)-1.463(4) Å (av 1.451 Å), which are close to those of tetralithium trimethylenecyclopentene tetraanion (av 1.457 Å),[17] but somewhat longer than those of $[(Ph_2C{=}O)Li{\cdot}\{C_5(SiMe_2H)_5\}]$ (av 1.424 Å).[11] One of the negative charge is largely localized at the exocyclic C6 carbon atom and is stabilized by both the Si4 and Si5 atoms, so that this carbon atom is slightly pyramidalyzed (351.4° for the sum of the bond angles). Consequently, the bond lengths of the C6-Si4 bond (1.820(3) Å) and the C6-Si5 bond (1.827(3) Å) in **24a** are shortened markedly compared with those of **21a** (1.888(3) and 1.897(3) Å, respectively) by $p\pi$-σ^* conjugation. The other negative charge is delocalized over the Cp ring to form the cyclopentadienide anion. The X-ray structure of the related dianionic derivative dilithium acepentalenediide has been reported.[18]

The data presented here indicate that the structure of **24a** is a fulvene dianion dilithium, which is stabilized not only by the six silicon atoms but also by the aromatic cyclopentadienide ion.

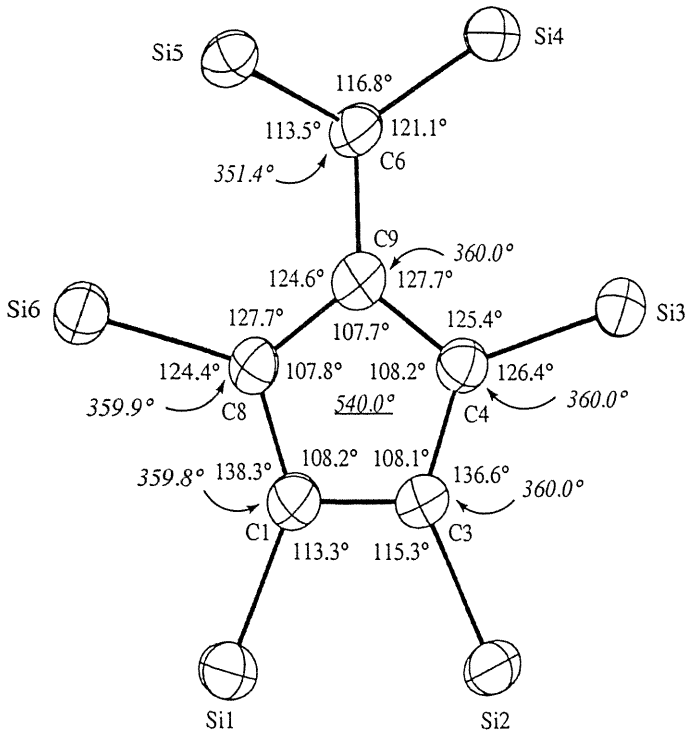

Figure 4-20. Selected bond angles of **24a**.

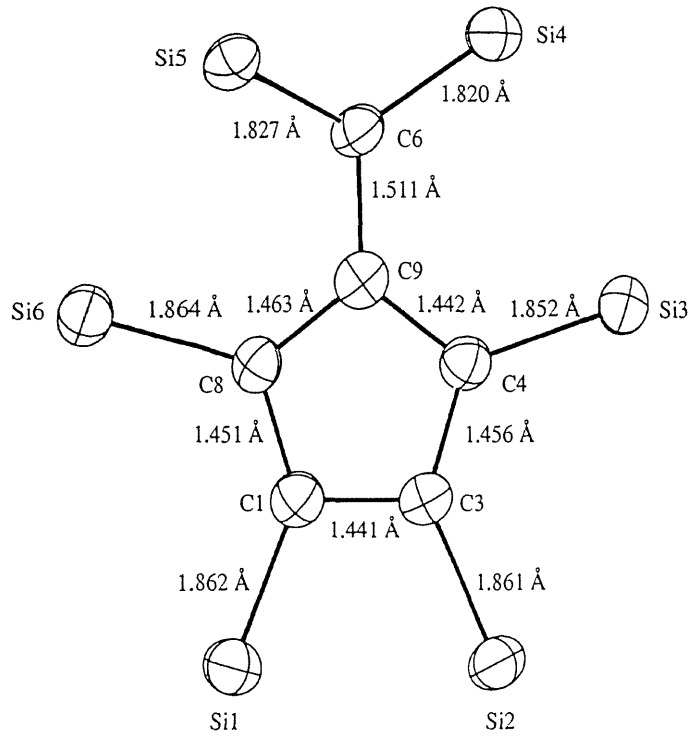

Figure 4-21. Selected bond lengths of **24a**.

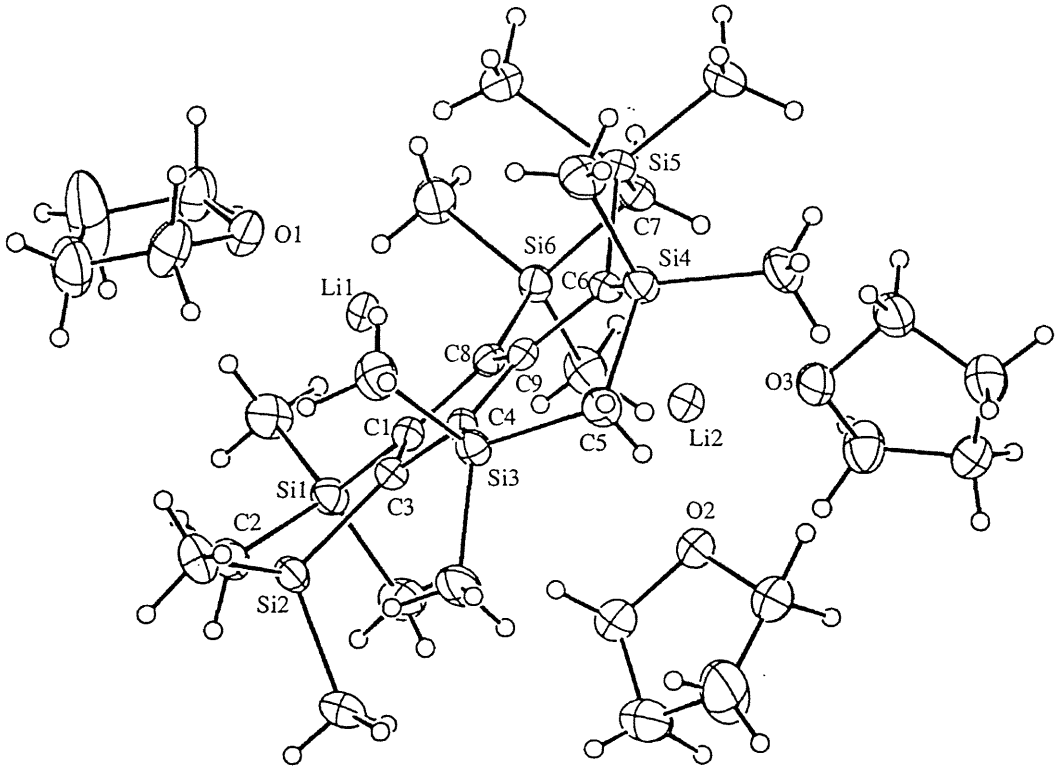

Figure 4-16. ORTEP drawing of **24a**.

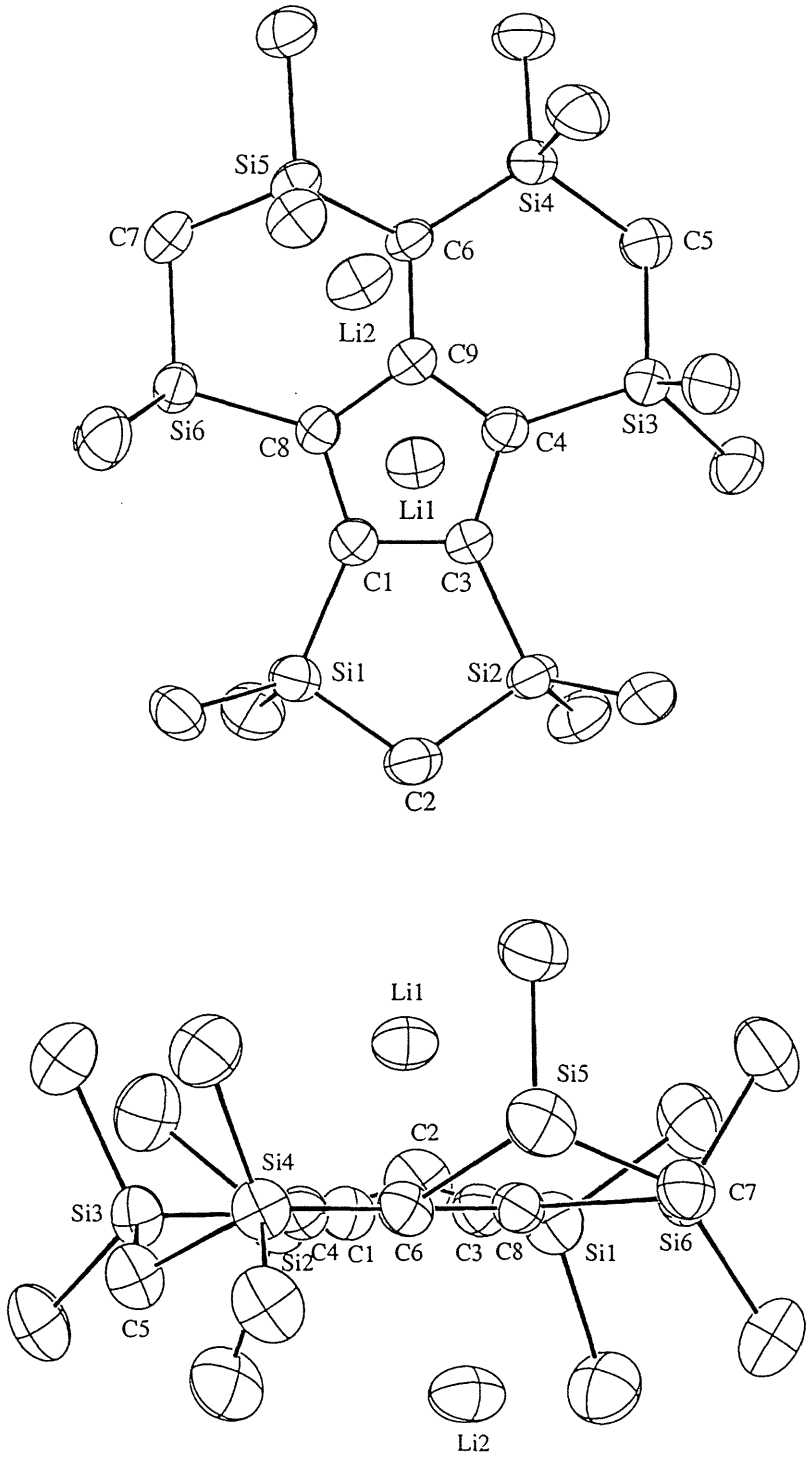

Figure 4-17. ORTEP drawing of **24a** (THF molecules and hydrogen atoms are omitted for the clarity): upper, top view; below, side view.

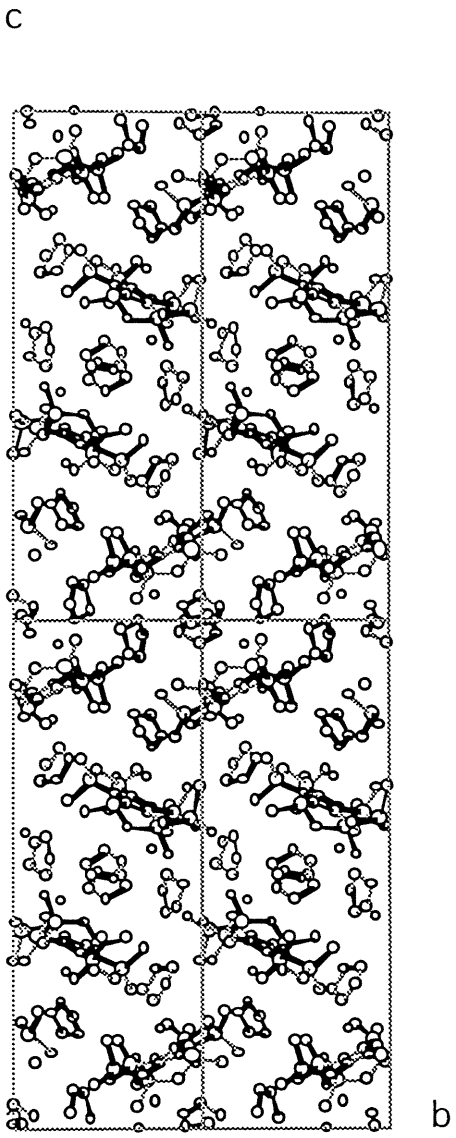

Figure 4-18. Crystal packing of **24a**.

Table 4-6. Atomic Parameters for Non-Hydrogen Atoms of **24a**

Atom	X/a	Y/b	Z/c	U(iso)
Si1	0.50360(6)	0.07700(8)	0.82750(3)	0.0427(4)
Si2	0.30270(6)	-0.08300(7)	0.81550(3)	0.0411(4)
Si3	0.02850(6)	0.04410(7)	0.86180(2)	0.0389(3)
Si4	-0.01250(6)	0.27660(7)	0.90630(2)	0.0399(3)
Si5	0.17540(6)	0.45530(7)	0.88800(2)	0.0385(3)
Si6	0.42150(6)	0.36780(7)	0.87900(2)	0.0386(3)
O1	0.19330(17)	0.24690(20)	0.74810(6)	0.051(1)
O2	0.2838(2)	0.0899(2)	0.9730(1)	0.069(1)
O3	0.31410(18)	0.32770(21)	0.99990(6)	0.059(1)
C1	0.3675(2)	0.1360(2)	0.8458(1)	0.036(1)
C2	0.4441(3)	-0.0468(3)	0.7940(1)	0.050(2)
C3	0.2718(2)	0.0564(2)	0.8410(1)	0.035(1)
C4	0.17400(19)	0.10850(23)	0.85950(8)	0.035(1)
C5	-0.0387(3)	0.1183(3)	0.9059(1)	0.046(1)
C6	0.1380(2)	0.3060(2)	0.8980(1)	0.035(1)
C7	0.3340(2)	0.4785(3)	0.9046(1)	0.043(1)
C8	0.3300(2)	0.2378(2)	0.8672(1)	0.033(1)
C9	0.2092(2)	0.2204(2)	0.8756(1)	0.034(1)
C10	0.5945(3)	0.1713(3)	0.7957(1)	0.058(2)
C11	0.6040(3)	0.0202(4)	0.8735(1)	0.061(2)
C12	0.1914(3)	-0.1335(4)	0.7721(1)	0.058(2)
C13	0.3325(3)	-0.2043(3)	0.8546(1)	0.060(2)
C14	-0.0666(3)	0.0604(4)	0.8102(1)	0.059(2)
C15	0.0337(3)	-0.1133(3)	0.8743(1)	0.058(2)
C16	-0.1243(3)	0.3401(4)	0.8649(1)	0.061(2)
C17	-0.0552(3)	0.3331(4)	0.9589(1)	0.058(2)
C18	0.1490(3)	0.4954(3)	0.8291(1)	0.054(2)
C19	0.0919(3)	0.5663(3)	0.9161(1)	0.053(2)
C20	0.4720(4)	0.4365(4)	0.8296(1)	0.061(2)
C21	0.5541(3)	0.3284(4)	0.9157(1)	0.059(2)
C22	0.1202(3)	0.1801(5)	0.7174(1)	0.071(2)
C23	0.1964(5)	0.1478(5)	0.6836(2)	0.090(3)
C24	0.2884(7)	0.2360(7)	0.6865(2)	0.144(6)
C25	0.2839(4)	0.2987(4)	0.7266(1)	0.068(2)
C26	0.3415(4)	-0.0021(3)	0.9529(1)	0.065(2)
C27	0.3157(6)	-0.1089(5)	0.9766(2)	0.094(3)
C28	0.2180(8)	-0.0778(5)	1.0006(2)	0.133(5)
C29	0.2241(5)	0.0439(4)	1.0078(1)	0.080(3)
C30	0.4109(3)	0.3035(5)	1.0308(1)	0.069(2)
C31	0.3691(4)	0.3204(4)	1.0742(1)	0.068(2)
C32	0.2532(3)	0.3788(4)	1.0657(1)	0.069(2)
C33	0.2479(4)	0.4145(4)	1.0195(1)	0.065(2)
Li1	0.2222(4)	0.2124(5)	0.8064(1)	0.044(2)
Li2	0.2563(5)	0.2413(5)	0.9491(2)	0.053(3)

Table 4-7. Atomic Parameters for Hydrogen Atoms of **24a**

Atom	X/a	Y/b	Z/c	U(iso)
H2A	0.494(3)	-0.117(3)	0.798(1)	0.07(1)
H2B	0.426(3)	-0.028(3)	0.768(1)	0.07(1)
H5A	-0.002(3)	0.091(3)	0.929(1)	0.06(1)
H5B	-0.125(3)	0.097(3)	0.904(1)	0.07(1)
H7A	0.358(2)	0.551(3)	0.897(1)	0.047(8)
H7B	0.347(2)	0.472(2)	0.934(1)	0.035(7)
H10A	0.552(3)	0.203(3)	0.771(1)	0.06(1)
H10B	0.638(3)	0.237(3)	0.813(1)	0.08(1)
H10C	0.652(3)	0.124(3)	0.784(1)	0.07(1)
H11A	0.627(3)	0.079(4)	0.893(1)	0.09(1)
H11B	0.567(3)	-0.037(4)	0.888(1)	0.10(1)
H11C	0.670(3)	-0.021(4)	0.864(1)	0.09(1)
H12A	0.124(4)	-0.140(4)	0.779(1)	0.09(1)
H12B	0.186(4)	-0.084(4)	0.750(2)	0.10(2)
H12C	0.219(4)	-0.206(5)	0.760(2)	0.12(2)
H13A	0.351(3)	-0.268(3)	0.841(1)	0.07(1)
H13B	0.398(3)	-0.185(3)	0.877(1)	0.09(1)
H13C	0.265(4)	-0.235(4)	0.870(1)	0.11(2)
H14A	-0.040(3)	0.007(3)	0.787(1)	0.06(1)
H14B	-0.064(3)	0.128(3)	0.803(1)	0.05(1)
H14C	-0.146(3)	0.034(4)	0.812(1)	0.09(1)
H15A	0.057(3)	-0.156(3)	0.851(1)	0.07(1)
H15B	0.081(3)	-0.129(4)	0.900(1)	0.09(1)
H15C	-0.047(3)	-0.144(4)	0.879(1)	0.09(1)
H16A	-0.108(3)	0.325(4)	0.837(1)	0.10(2)
H16B	-0.196(4)	0.333(4)	0.869(1)	0.10(1)
H16C	-0.118(4)	0.417(4)	0.868(1)	0.10(2)
H17A	-0.015(3)	0.288(3)	0.983(1)	0.07(1)
H17B	-0.140(3)	0.322(3)	0.961(1)	0.08(1)
H17C	-0.041(3)	0.408(3)	0.964(1)	0.06(1)
H18A	0.170(3)	0.578(4)	0.827(1)	0.10(1)
H18B	0.072(4)	0.494(3)	0.819(1)	0.09(1)
H18C	0.190(3)	0.454(4)	0.811(1)	0.08(1)
H19A	0.002(3)	0.563(3)	0.908(1)	0.09(1)
H19B	0.106(2)	0.561(3)	0.948(1)	0.047(8)
H19C	0.116(3)	0.643(4)	0.908(1)	0.07(1)
H20A	0.521(3)	0.490(3)	0.839(1)	0.06(1)
H20B	0.512(4)	0.380(4)	0.815(1)	0.11(2)
H20C	0.410(3)	0.473(3)	0.814(1)	0.07(1)
H21A	0.534(3)	0.299(4)	0.943(1)	0.09(1)
H21B	0.595(3)	0.404(4)	0.923(1)	0.09(1)
H21C	0.596(3)	0.287(4)	0.903(1)	0.07(1)
H22A	0.093(3)	0.110(4)	0.733(1)	0.10(1)
H22B	0.056(4)	0.244(5)	0.709(2)	0.15(2)
H23A	0.228(6)	0.073(6)	0.689(2)	0.17(3)

Table 4-7 (continued). Atomic Parameters for Hydrogen Atoms of **24a**

Atom	X/a	Y/b	Z/c	U(iso)
H23B	0.150(5)	0.139(5)	0.656(2)	0.16(2)
H24A	0.349(5)	0.241(5)	0.670(2)	0.14(2)
H24B	0.336(9)	0.177(9)	0.706(3)	0.19(6)
H25A	0.353(5)	0.311(6)	0.748(2)	0.18(3)
H25B	0.243(6)	0.372(7)	0.715(2)	0.15(3)
H26A	0.305(4)	-0.001(4)	0.924(2)	0.13(2)
H26B	0.431(4)	0.024(4)	0.954(1)	0.10(1)
H27A	0.299(4)	-0.164(4)	0.959(2)	0.10(2)
H27B	0.381(7)	-0.106(7)	1.006(3)	0.16(4)
H28A	0.202(5)	-0.126(6)	1.021(2)	0.16(2)
H28B	0.158(12)	-0.102(13)	0.977(5)	0.16(9)
H29A	0.176(5)	0.115(6)	1.011(2)	0.19(3)
H29B	0.283(4)	0.063(4)	1.036(2)	0.12(2)
H30A	0.481(4)	0.343(4)	1.023(1)	0.11(2)
H30B	0.435(3)	0.226(4)	1.023(1)	0.10(1)
H31A	0.432(4)	0.361(5)	1.093(2)	0.13(2)
H31B	0.359(3)	0.248(4)	1.086(1)	0.09(1)
H32A	0.187(3)	0.326(4)	1.068(1)	0.09(1)
H32B	0.243(3)	0.448(4)	1.082(1)	0.08(1)
H33A	0.171(3)	0.405(4)	1.004(1)	0.09(1)
H33B	0.290(3)	0.491(4)	1.016(1)	0.10(1)

Table 4-8. List of Atomic Distances (Å) for Non-Hydrogen Atoms of **24a**

Atom	Atom	Length(sig)
Si1	C1	1.862(3)
Si1	C2	1.874(4)
Si1	C10	1.876(4)
Si1	C11	1.878(5)
Si2	C2	1.880(4)
Si2	C3	1.861(3)
Si2	C12	1.871(5)
Si2	C13	1.879(4)
Si3	C4	1.852(3)
Si3	C5	1.865(4)
Si3	C14	1.871(4)
Si3	C15	1.875(4)
Si4	C5	1.869(4)
Si4	C6	1.820(3)
Si4	C16	1.888(5)
Si4	C17	1.886(4)
Si5	C6	1.827(3)
Si5	C7	1.877(3)
Si5	C18	1.898(4)
Si5	C19	1.885(4)
Si6	C7	1.870(4)
Si6	C8	1.864(3)
Si6	C20	1.887(5)
Si6	C21	1.880(4)
O1	C22	1.443(5)
O1	C25	1.436(5)
O1	Li1	1.867(5)
O2	C26	1.441(5)
O2	C29	1.451(6)
O2	Li2	1.930(7)
O3	C30	1.433(5)
O3	C33	1.443(5)
O3	Li2	1.944(6)
C1	C3	1.441(4)
C1	C8	1.451(4)
C1	Li1	2.174(6)
C3	C4	1.456(4)
C3	Li1	2.164(6)
C4	C9	1.442(4)
C4	Li1	2.176(6)
C6	C9	1.511(4)
C6	Li2	2.136(6)
C8	C9	1.463(4)
C8	Li1	2.189(5)
C9	Li1	2.191(5)

Table 4-8 (continued). List of Atomic Distances (Å) for Non-Hydrogen Atoms of **24a**

Atom	Atom	Length(sig)
C9	Li2	2.325(6)
C22	C23	1.494(7)
C23	C24	1.476(11)
C24	C25	1.459(9)
C26	C27	1.495(8)
C27	C28	1.466(11)
C28	C29	1.436(9)
C30	C31	1.502(6)
C31	C32	1.504(7)
C32	C33	1.501(6)

Table 4-9. List of Bond Lengths (Å) for Hydrogen Atoms of **24a**

Atom	Atom	Length(sig)
C2	H2A	1.01(4)
C2	H2B	0.86(4)
C5	H5A	0.87(4)
C5	H5B	1.02(4)
C7	H7A	0.92(4)
C7	H7B	0.94(3)
C10	H10A	0.94(4)
C10	H10B	1.04(4)
C10	H10C	0.97(4)
C11	H11A	0.94(5)
C11	H11B	0.94(5)
C11	H11C	0.98(4)
C12	H12A	0.83(5)
C12	H12B	0.89(5)
C12	H12C	0.99(6)
C13	H13A	0.90(4)
C13	H13B	1.00(4)
C13	H13C	1.03(5)
C14	H14A	1.02(4)
C14	H14B	0.83(4)
C14	H14C	0.98(5)
C15	H15A	0.94(4)
C15	H15B	0.95(5)
C15	H15C	1.02(4)
C16	H16A	0.92(5)
C16	H16B	0.86(5)
C16	H16C	0.91(6)
C17	H17A	1.00(4)
C17	H17B	1.00(4)
C17	H17C	0.89(4)
C18	H18A	1.00(6)
C18	H18B	0.91(5)
C18	H18C	0.90(4)
C19	H19A	1.05(5)
C19	H19B	0.99(4)
C19	H19C	0.98(5)
C20	H20A	0.87(4)
C20	H20B	0.94(5)
C20	H20C	0.93(4)
C21	H21A	0.98(5)
C21	H21B	1.02(5)
C21	H21C	0.82(4)
C22	H22A	1.02(5)
C22	H22B	1.07(6)
C23	H23A	0.95(7)

Table 4-9 (contibued). List of Bond Lengths (Å) for Hydrogen Atoms of **24a**

Atom	Atom	Length(sig)
C23	H23B	0.97(6)
C24	H24A	0.91(6)
C24	H24B	1.03(11)
C25	H25A	1.01(7)
C25	H25B	1.03(8)
C26	H26A	0.97(6)
C26	H26B	1.08(5)
C27	H27A	0.85(6)
C27	H27B	1.13(9)
C28	H28A	0.88(7)
C28	H28B	1.01(15)
C29	H29A	1.01(7)
C29	H29B	1.07(6)
C30	H30A	0.99(5)
C30	H30B	0.99(5)
C31	H31A	1.00(5)
C31	H31B	0.94(5)
C32	H32A	0.99(5)
C32	H32B	0.97(5)
C33	H33A	0.98(4)
C33	H33B	1.03(5)

Table 4-10. List of Bond Angles (Å) for Non-Hydrogen Atoms of **24a**

Atom	Atom	Atom	Angle(sig)
C1	Si1	C2	100.5(2)
C1	Si1	C10	119.0(2)
C1	Si1	C11	111.8(2)
C2	Si1	C10	110.3(2)
C2	Si1	C11	108.8(2)
C10	Si1	C11	106.1(2)
C2	Si2	C3	99.8(2)
C2	Si2	C12	111.8(2)
C2	Si2	C13	107.0(2)
C3	Si2	C12	116.0(2)
C3	Si2	C13	114.0(2)
C12	Si2	C13	107.7(2)
C4	Si3	C5	106.9(2)
C4	Si3	C14	112.5(2)
C4	Si3	C15	113.2(2)
C5	Si3	C14	109.9(2)
C5	Si3	C15	107.8(2)
C14	Si3	C15	106.5(2)
C5	Si4	C6	110.0(2)
C5	Si4	C16	106.4(2)
C5	Si4	C17	107.1(2)
C6	Si4	C16	115.3(2)
C6	Si4	C17	113.5(2)
C16	Si4	C17	104.0(2)
C6	Si5	C7	109.4(2)
C6	Si5	C18	112.5(2)
C6	Si5	C19	115.6(2)
C7	Si5	C18	106.9(2)
C7	Si5	C19	107.8(2)
C18	Si5	C19	104.2(2)
C7	Si6	C8	108.9(2)
C7	Si6	C20	106.6(2)
C7	Si6	C21	110.5(2)
C8	Si6	C20	113.5(2)
C8	Si6	C21	109.6(2)
C20	Si6	C21	107.7(2)
C22	O1	C25	108.7(3)
C22	O1	Li1	124.8(3)
C25	O1	Li1	118.8(3)
C26	O2	C29	109.3(4)
C26	O2	Li2	125.2(3)
C29	O2	Li2	123.8(3)
C30	O3	C33	105.3(3)
C30	O3	Li2	129.2(3)
C33	O3	Li2	123.9(3)

Table 4-10 (continued). List of Bond Angles (Å) for Non-Hydrogen Atoms of **24a**

Atom	Atom	Atom	Angle(sig)
Si1	C1	C3	113.3(2)
Si1	C1	C8	138.3(2)
Si1	C1	Li1	127.4(2)
C3	C1	C8	108.2(3)
C3	C1	Li1	70.2(2)
C8	C1	Li1	71.2(2)
Si1	C2	Si2	104.8(2)
Si2	C3	C1	115.3(2)
Si2	C3	C4	136.6(2)
Si2	C3	Li1	124.8(2)
C1	C3	C4	108.1(3)
C1	C3	Li1	71.0(2)
C4	C3	Li1	70.8(2)
Si3	C4	C3	126.4(2)
Si3	C4	C9	125.4(2)
Si3	C4	Li1	124.0(2)
C3	C4	C9	108.2(2)
C3	C4	Li1	70.0(2)
C9	C4	Li1	71.3(2)
Si3	C5	Si4	112.5(2)
Si4	C6	Si5	116.8(2)
Si4	C6	C9	121.1(2)
Si4	C6	Li2	112.1(2)
Si5	C6	C9	113.5(2)
Si5	C6	Li2	108.6(2)
C9	C6	Li2	77.1(2)
Si5	C7	Si6	109.8(2)
Si6	C8	C1	124.4(2)
Si6	C8	C9	127.7(2)
Si6	C8	Li1	123.0(2)
C1	C8	C9	107.8(3)
C1	C8	Li1	70.0(2)
C9	C8	Li1	70.5(2)
C4	C9	C6	127.7(3)
C4	C9	C8	107.7(3)
C4	C9	Li1	70.2(2)
C4	C9	Li2	118.1(3)
C6	C9	C8	124.6(3)
C6	C9	Li1	125.7(3)
C6	C9	Li2	63.6(2)
C8	C9	Li1	70.4(2)
C8	C9	Li2	91.8(2)
Li1	C9	Li2	162.2(3)
O1	C22	C23	105.1(4)
C22	C23	C24	104.8(5)

Table 4-10 (continued). List of Bond Angles (Å) for Non-Hydrogen Atoms of **24a**

Atom	Atom	Atom	Angle(sig)
C23	C24	C25	108.3(6)
O1	C25	C24	106.6(5)
O2	C26	C27	106.1(4)
C26	C27	C28	104.6(5)
C27	C28	C29	107.2(6)
O2	C29	C28	105.4(5)
O3	C30	C31	106.5(3)
C30	C31	C32	105.2(4)
C31	C32	C33	104.2(4)
O3	C33	C32	104.1(4)
O1	Li1	C1	134.1(3)
O1	Li1	C3	133.1(3)
O1	Li1	C4	146.5(3)
O1	Li1	C8	148.4(3)
O1	Li1	C9	159.3(3)
C1	Li1	C3	38.8(2)
C1	Li1	C4	65.3(2)
C1	Li1	C8	38.8(2)
C1	Li1	C9	65.3(2)
C3	Li1	C4	39.2(2)
C3	Li1	C8	65.1(2)
C3	Li1	C9	65.2(2)
C4	Li1	C8	65.0(2)
C4	Li1	C9	38.6(2)
C8	Li1	C9	39.0(2)
O2	Li2	O3	97.2(3)
O2	Li2	C6	132.9(3)
O2	Li2	C9	107.5(3)
O3	Li2	C6	124.9(4)
O3	Li2	C9	153.1(4)
C6	Li2	C9	39.3(2)

PM3 Calculation of Hexasilylfulvene Dianion $21a^{2-}$

The geometry optimization of hexasilylfulvene dianion $\mathbf{21a}^{2-}$ (counter ion free) was also carried out by PM3 calculation.[10] The calculated structure of $\mathbf{21a}^{2-}$ is shown in Figure 4-22. The geometry of $\mathbf{21a}^{2-}$ calculated by PM3 is close to that of dilithium hexasilylfulvene dianion **21a** by the X-ray diffraction. Some differences between crystal structure and calculated structure may be due to the existence of lithium counter cation and THF ligands. The selected bond angles and lengths of $\mathbf{21a}^{2-}$ calculated by PM3 are shown in Figures 4-23 and 4-24. The charge distribution of $\mathbf{21a}^{2-}$ is also shown in Figure 4-25.

Comparison of the calculated parameters of **21a** and $\mathbf{21a}^{2-}$ is also interesting. The change of bond lengths by two electron reduction is wellreproduced by PM3 calculation. The C-C single and double bond lengths of **21a** calculated by PM3 are 1.472-1.493 Å (av 1.486 Å) and 1.335-1.351 Å (av 1.346 Å), respectively. Those of $\mathbf{21a}^{2-}$ are 1.406-1.433 Å (av 1.424 Å) and 1.412-1.417 Å (av 1.413 Å), respectively. The Si-C(sp^2) single bond lengths of $\mathbf{21a}^{2-}$ calculated by PM3 are 1.763-1.799 Å (av 1.782 Å), which are shorter than those of **21a** (1.825-1.847 Å (av 1.836 Å)) due to the $p\pi$-σ^* conjugation.

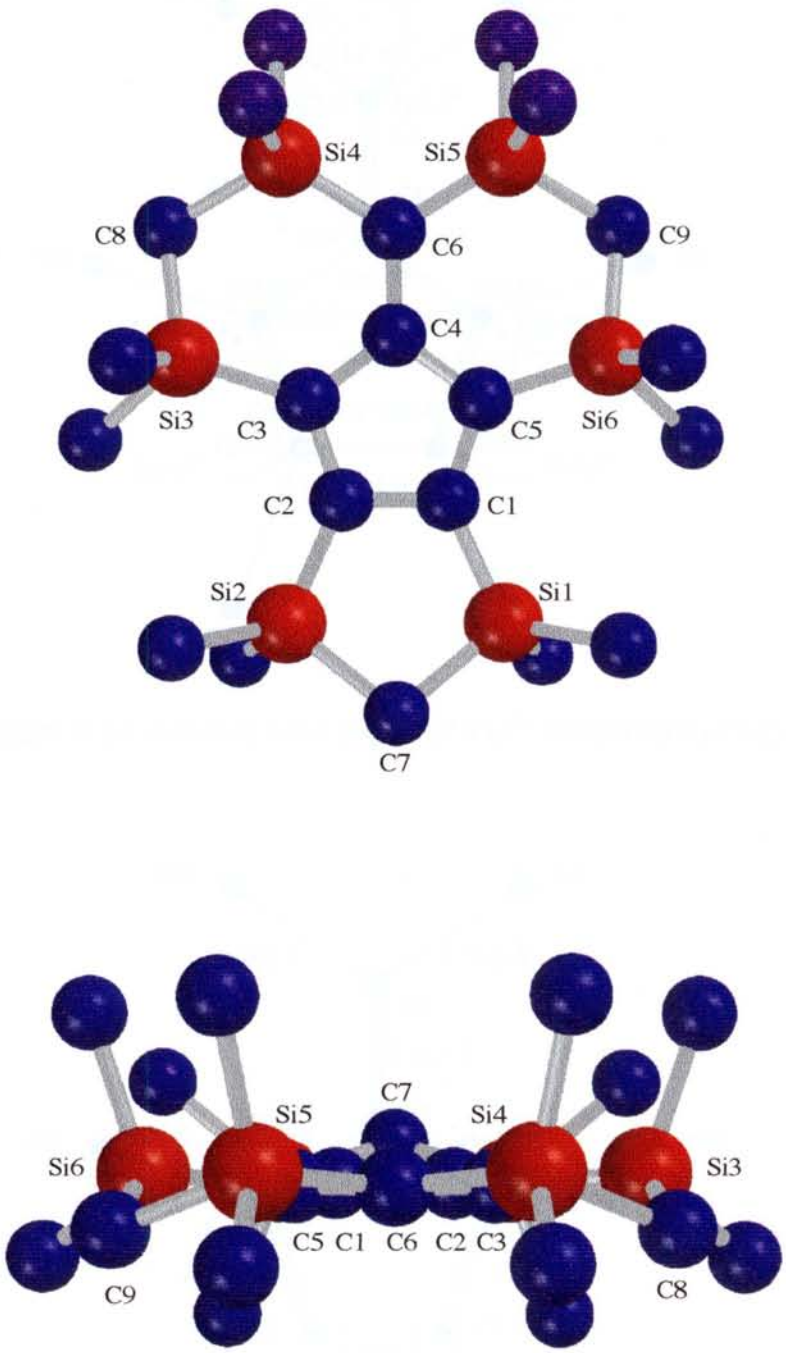

Figure 4-22. Calculated structure of **21a**$^{2-}$ by PM3 (hydrogen atoms are omitted for the clarity): upper, top view; below, side view.

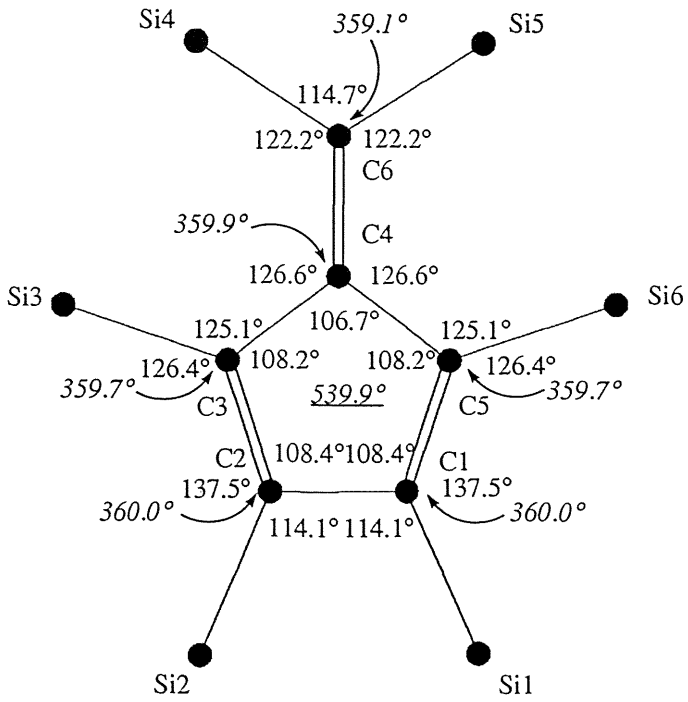

Figure 4-23. Selected bond angles of $\mathbf{21a}^{2-}$ calculated by PM3.

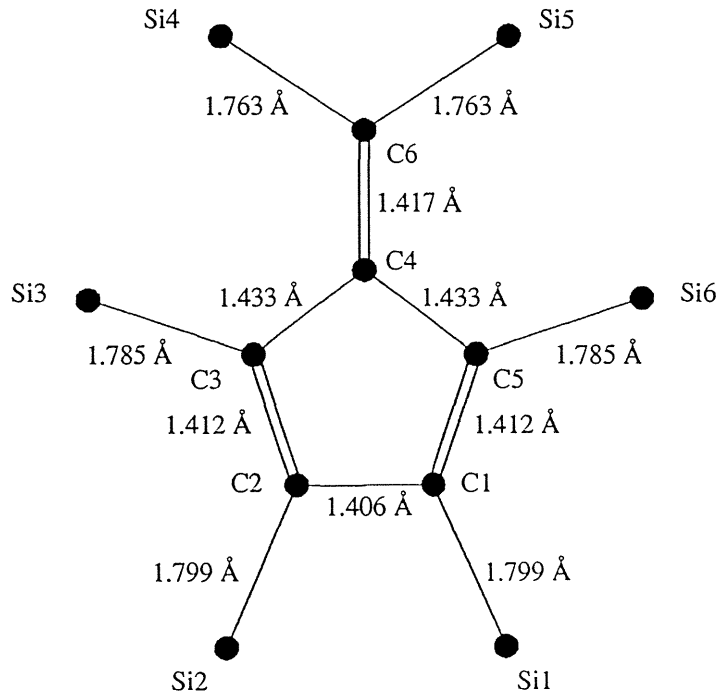

Figure 4-24. Selected bond lengths of $\mathbf{21a}^{2-}$ calculated by PM3.

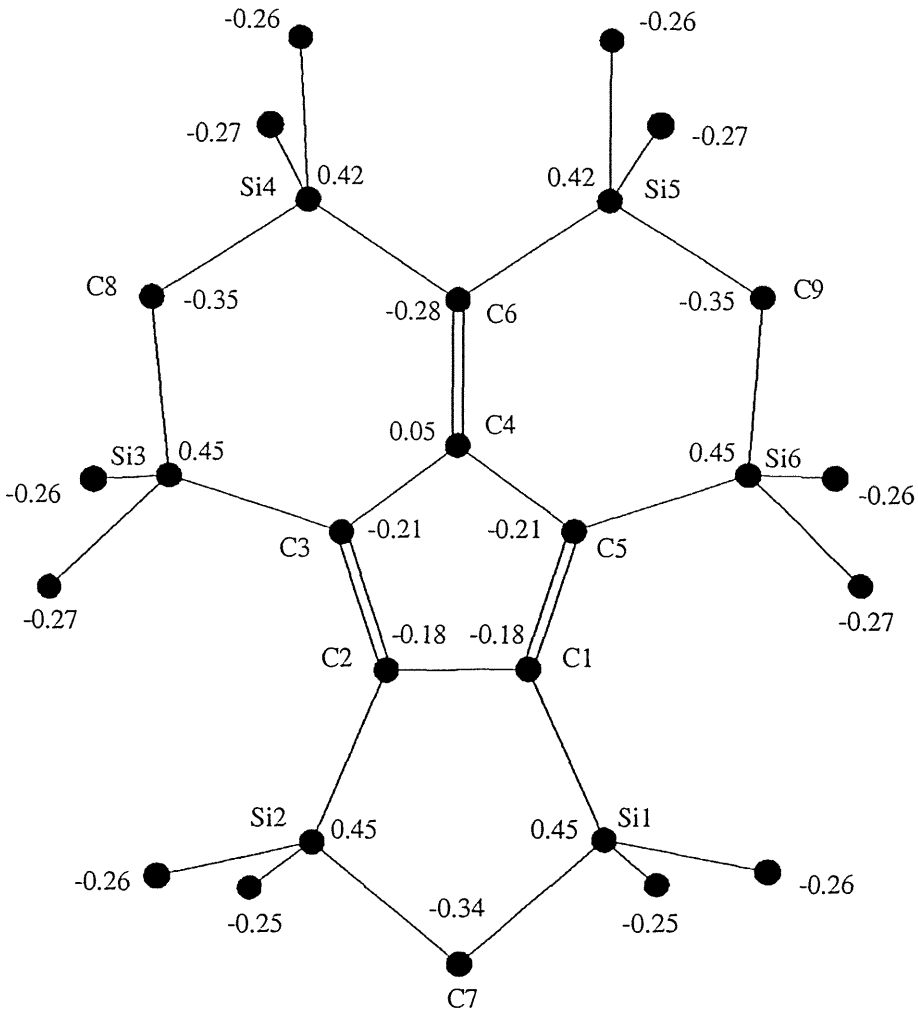

Figure 4-25. Mulliken charge distribution of **21a**$^{2-}$ calculated by PM3.

Structure of Dilithium Hexasilylfulvene Dianion 24 in Toluene-d_8

The structure of **24a** in solution was characterized by ^{1}H, ^{13}C, ^{29}Si, and ^{6}Li NMR spectroscopies. The NMR data of **24a** in toluene-d_8 indicates the highly symmetric bis-CIP structure, as found by the X-ray crystallography. However, the two Li^+ ions of **24a** are not fixed to the π-skeleton and undergo rapid exchange with each other on the NMR time scale, as depicted in Figure 4-26. Thus, the ^{6}Li NMR spectrum of **24a** in toluene-d_8 yielded only one signal, appearing at -3.18 ppm (Figure 4-27). The exchange of the Li^+ ions was not suppressed in the temperature range of 193-298 K. The ^{6}Li NMR chemical shift of **24a** (δ = -3.18) is intermediate between those of $(Me_3Si)_2CHLi$ (δ = 2.46) and $[(Ph_2C{=}O)Li{\cdot}\{C_5(SiMe_2H)_5\}]$ (δ = -7.51).[11]

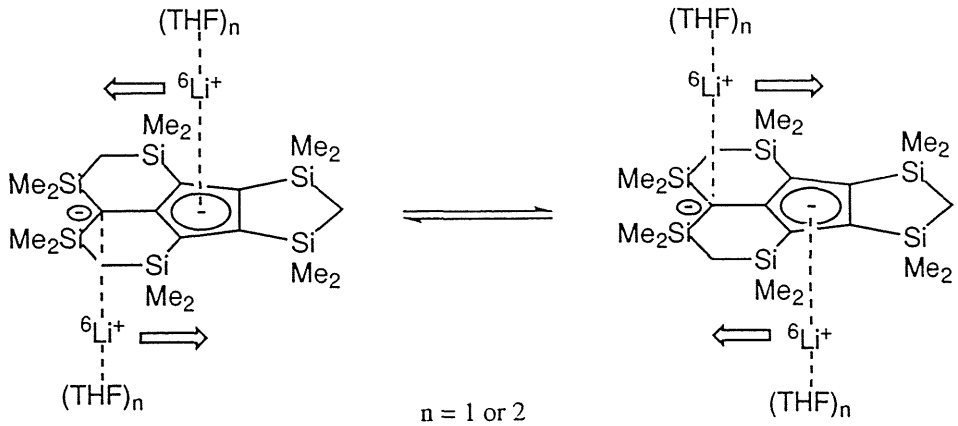

Figure 4-26. Lithium interconversion of **24a**.

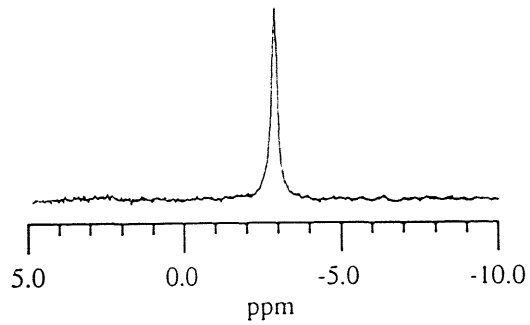

Figure 4-27. ^{6}Li NMR spectrum of **24a** in toluene-d_8 at 298 K.

In the ^{13}C NMR spectrum of **24a**, three sets of methyl carbons (4.4, 5.34, and 6.0 ppm) and two sets of methylene carbons (3.4 and 5.27 ppm) were observed, as well as four sets of quaternary carbons at 30.2 (C6), 112.1 (C4 and C8), 138.6 (C1 and C3), and 164.9 (C9) ppm. The ^{13}C signal of the C6 atom was observed at 30.2 ppm, which is markedly shifted to upper field by 152.7 ppm relative to that of **21a** (182.9 ppm). This shift is due to the negative charge at the exocyclic C6 carbon atom of **24a**. The ^{29}Si NMR spectrum showed three sets of signals at -14.4, -12.5, and -5.4 ppm shifting to upper field, relative to those of **21a**. This suggests that the negative charge is stabilized by the six silyl groups in **24a**.

The same high symmetric bis-CIP formation in toluene-d_8 was also deduced on the basis of the ^{1}H, ^{13}C, ^{29}Si, and ^{6}Li NMR spectra of the dilithium hexasilylfulvene dianion **24b**. The interconversion of the two CIP-Li^+ ions of **24** in solution readily occurs due to the planar structure of the π-system.

Structure of Dilithium Hexasilylfulvene Dianion 24 in THF-d_8

The structure of **24a** in a solvating media such as THF-d_8 was also deduced on the basis of the NMR spectra. The spectral data indicates that bis-CIP formation of **24a** is maintained in THF-d_8 at 298 K. The ^{6}Li NMR spectrum shows one signal at -3.05 ppm (Figure 4-28). Interestingly, upon lowering the temperature, this ^{6}Li signal was decreasing, whereas two new peaks were growing with the same intensity. The ^{6}Li NMR spectrum at 163 K yielded two new peaks appearing at 0.79 and -0.29 ppm. The signal at 0.79 ppm is assigned to the Li^+ ion, which bonded to the π-skeleton (CIP-Li^+). The signal at -0.29 ppm is assignable to the THF solvated species, $[Li^+(THF)_n]$.[19] Thus, at low temperature, CIP-SSIP species (**24a'**) is formed in THF-d_8. There is an unique equilibrium between the two dianion species, **24a** (bis-CIP structure) and **24a'** (CIP-SSIP structure) in THF-d_8 (Scheme 4-9).

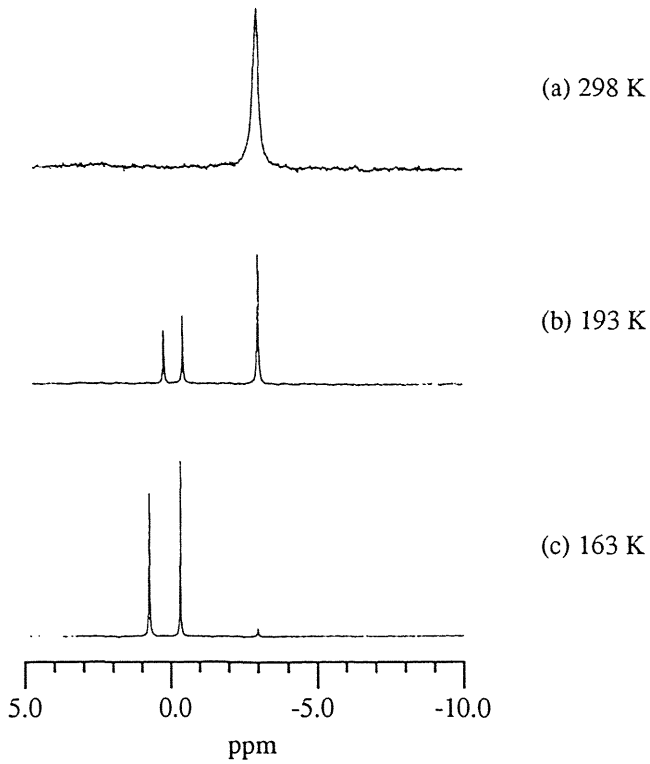

Figure 4-28. ^{6}Li NMR specra of **24a** in THF-d_8: (a) 298 K, (b) 193 K, and (c) 163 K.

Scheme 4-9

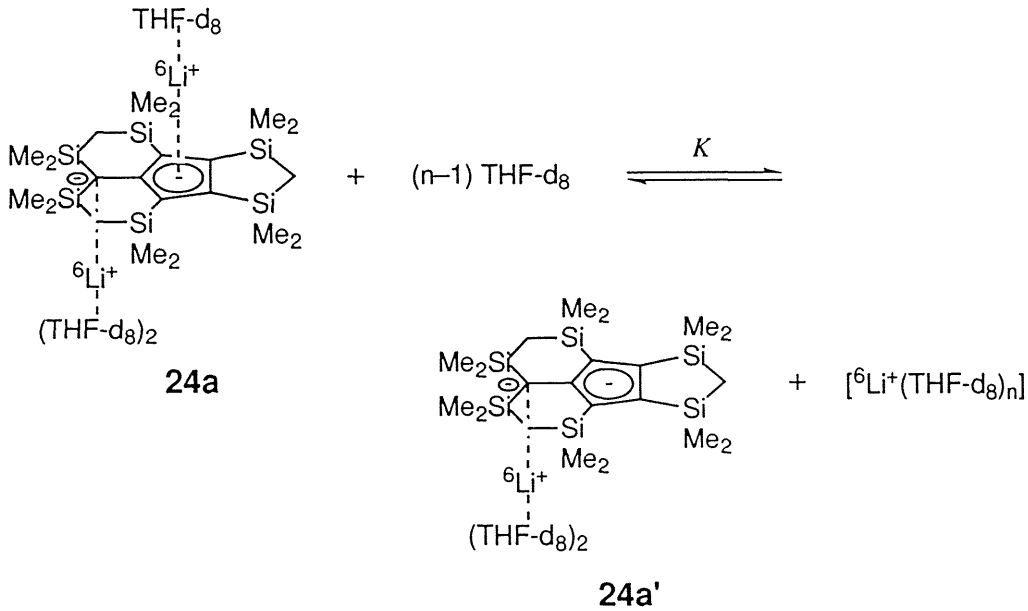

On the other hand, there is no observation of the similar equilibrium of the dilithium salt **24b**. Only one ^{6}Li signal of **24b** was yielded in THF-d_8 at temperature range 298-173 K.

The η^5-coordinated lithium of bis-CIP species (**24a**) is solvated by THF-d_8 to form CIP-SSIP species (**24a'**) at low temperature. Therefore, the π-skeleton of **24a'** has different environments above and below the plane. The six resonances of $SiMe_2$ were found in both ^{1}H and ^{13}C NMR spectrum of **24a'**. In the ^{13}C NMR spectrum of **24a'**, the signal appearing at 23.4 ppm splits into a triplet ($J^{13}C\text{-}^{6}Li$ = 3.5 Hz) due to the coupling with one ^{6}Li (I = 1). The triplet signal is assigned to the exocyclic carbon atom. Thus, the CIP-Li^+ ion of **24a'** is apparently bonded to the exocyclic carbon.

It is quite reasonable that the ^{6}Li chemical shift of -3.05 ppm is the average of the two CIP-Li^+ ions. One is strongly bonded to the exocyclic carbon atom (δ = 0.79) and the other is suited almost above the center of the cyclopentadienide ring. The ^{6}Li chemical shift of the η^5-coordinated lithium is estimated for -6.89 ppm. The appreciable upfield shift (δ = -6.89) is evidently caused by the strong shielding effect by the diamagnetic ring current resulting from 6π-electron aromatic ring system. Thus, the NMR data presented here indicates that the structure of **24a** is a fulvene dianion dilithium, which is stabilized not only by the six silicon atoms but also by the aromatic cyclopentadienide ion.

From the van't Hoff plot, the values of ΔH = -38.3 kJ·mol^{-1} for the equilibrium of the two dianion species (**24a** and **24a'**) can be estimated. The large negative enthalpy suggests that the bis-CIP structure **24a** is the entropy-controlled species, whereas the CIP-SSIP structure **24a'** is the enthalpy-controlled species. The van't Hoff plot is shown in Figure 4-29. The data for the equilibrium is summarized in Table 4-11.

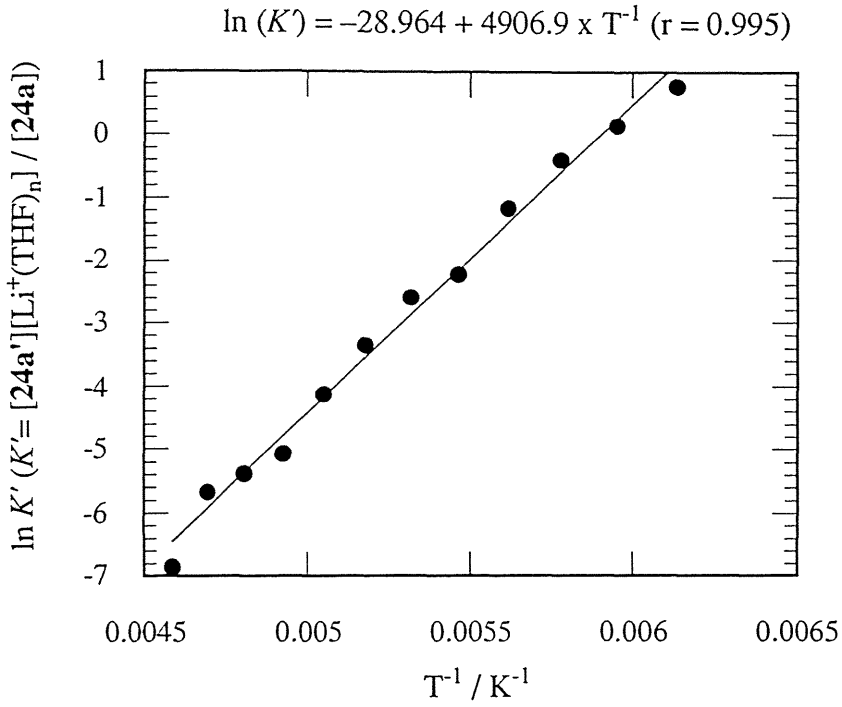

$K = [\mathbf{24a'}][Li^+(THF)_n] / [\mathbf{24a}][THF\text{-}d_8]^{n-1}$

$K' = [\mathbf{24a'}][Li^+(THF)_n] / [\mathbf{24a}] = [\mathbf{24a'}]^2 / [\mathbf{24a}]$

$\ln K' = \Delta S / R - \Delta H / RT$

$\Delta H = -38.3\ kJmol^{-1}$

Figure 4-29. van't Hoff plot ($\ln K'$ vs. T^{-1}) for the equilibrium between **24a** and **24a'** in THF-d_8.

Table 4-11. Data for the equilibrium of the two dianion species **24a** and **24a'** based on ^{6}Li NMR (44 MHz)

T / K	T^{-1} / K^{-1}	[**24a**] (M)	[**24a'**] (M)	[**24a'**]^2 / [**24**] (M)	ln K' [a)]
218	4.59×10^{-3}	8.01×10^{-2}	0.92×10^{-2}	0.00106	-6.853
213	4.69×10^{-3}	7.34×10^{-2}	1.59×10^{-2}	0.00344	-5.671
208	4.81×10^{-3}	7.12×10^{-2}	1.81×10^{-2}	0.00460	-5.381
203	4.93×10^{-3}	6.86×10^{-2}	2.07×10^{-2}	0.00625	-5.076
198	5.05×10^{-3}	5.86×10^{-2}	3.07×10^{-2}	0.01608	-4.130
193	5.18×10^{-3}	4.82×10^{-2}	4.11×10^{-2}	0.03505	-3.351
188	5.32×10^{-3}	3.67×10^{-2}	5.26×10^{-2}	0.07539	-2.585
183	5.46×10^{-3}	3.11×10^{-2}	5.82×10^{-2}	0.10891	-2.217
178	5.62×10^{-3}	1.68×10^{-2}	7.25×10^{-2}	0.31287	-1.162
173	5.78×10^{-3}	0.95×10^{-2}	7.98×10^{-2}	0.67032	-0.400
168	5.95×10^{-3}	0.60×10^{-2}	8.33×10^{-2}	1.15648	0.145
163	6.13×10^{-3}	0.34×10^{-2}	8.59×10^{-2}	2.17024	0.775

a) $K = [\mathbf{24a'}][Li^{+}(THF)_n] / [\mathbf{24a}][THF\text{-}d_8]^{n-1}$, $K' = [\mathbf{24a'}][Li^{+}(THF)_n] / [\mathbf{24a}] = [\mathbf{24a'}]^2 / [\mathbf{24a}]$

Experimental Section

General Methods

^{1}H NMR spectra were recorded on a Bruker AC-300 FT spectrometer. ^{13}C, ^{29}Si, and ^{6}Li NMR spectra were collected on a Bruker AC-300 at 75.5, 59.6, and 44.2 MHz, respectively. ^{6}Li NMR spectra are referenced to 1 M LiCl (1 M = 1 mol dm^{-3}) in methanol / toluene-d_8 or 1 M LiCl in THF-d_8. Mass spectra were obtained on a Shimadzu QP-1000. Electronic spectra were recorded on a Shimadzu UV-2100 spectrometer. The sampling of **24a** for X-ray crystallography was carried out by using a Giken Engineering Service GBX-1200 gas-replacement type glove box.

Materials

Tetrahydrofuran and heptane were dried and distilled from sodium benzophenone ketyl. These solvents were further dried and degassed over a potassium mirror in vacuo prior to use. Toluene-d_8 and THF-d_8 were dried over molecular sieves, and then transferred into a tube covered with potassium mirror prior to use. Lithium-6 (95 atom%) metal was commercially available (Aldrich Chemical Company). 3,3,5,5,8,8,10,10,13,13,15,15-dodecamethyl-3,5,8,10,13,15-hexasilacyclopentadeca-1,6,11-triyne (**11**) was prepared as described in Chapter 2. 3,3,5,5,8,8,10,10,13,13,15,15-dodecamethyl-3,5,8,10,13,15-hexasila-4,9,14-trioxacyclopentadeca-1,6,11-triyne (**20**) and hexasilylfulvene (**21b**) were prepared according to the methods of literature.[7]

Preparation of Hexasilylfulvene (21a)

A mixture of the 3,3,5,5,8,8,10,10,13,13,15,15-dodecamethyl-3,5,8,10,13,15-hexasilacyclopentadeca-1,6,11-triyne (**11**) (227 mg, 0.49 mmol) and [$Mn(CO)_3$(Me-Cp)] (160 mg, 0.73 mmol) in THF (30 ml) was irradiated with a 500 W high-pressure

mercury lamp for 8 h through the cutoff filter ($\lambda > 300$ nm) at room temperature. After removal of the manganese complex, the reaction mixture was chromatographed on silica gel to produce red crystals of **21a** in 26% yield. mp 170 °C; ^{1}H NMR ($CDCl_3$) δ = -0.12 (s, 4 H, CH_2), 0.29 (s, 2 H, CH_2), 0.30 (s, 12 H, CH_3), 0.34 (s, 12 H, CH_3), 0.41 (s, 12 H, CH_3); ^{13}C NMR ($CDCl_3$) δ = 1.8 (CH_2), 1.9 (CH_3), 3.2 (CH_3), 3.4 (CH_2), 3.5 (CH_3), 143.8 (C), 167.1 (C), 168.4 (C), 182.9 (C); ^{29}Si NMR ($CDCl_3$) δ = -13.4, -6.7, -2.4; UV (hexane) λ_{max}/nm (ε) 215 (21000), 298 (19500); HRMS Found: m/z 462.1894. Calcd for $C_{21}H_{42}Si_6$: M, 462.1902.

X-ray Crystallography of Hexasilylfulvene (21a)

Single crystal of **21a** for X-ray diffractions was grown from an ethanol solution. The X-ray crystallographic experiment of **21a** was performed on a DIP2020 image plate diffractometer equipped with graphite-monochromatized Mo-*K*α radiation (λ = 0.71073 Å). Crystal data for **21a** at 130 K: MF = $C_{21}H_{42}Si_6$, MW = 463.09, triclinic, a = 11.333(1) Å, b = 11.877(1) Å, c = 20.749(1) Å, α = 894.883(3)°, β = 97.185(3)°, γ = 95.948(4)°, V = 2773.4(5) Å^3, space group = P1-, Z = 4, D_{caled} = 1.109 g/cm^3. The final R factor was 0.034 (R_w = 0.040) for 8231 reflections with $I_o > 3\sigma(I_o)$. The details of the X-ray experiment are given in Table 4-12.

Table 4-12. Detail of the X-ray Experiment for **21a**

molecular formula	$C_{21}H_{42}Si_6$
molecular weight	463.09
crystal system	triclinic
space group	$P\bar{1}$
cell constants	a = 11.333(1) Å, b = 11.877(1) Å, c = 20.749(1) Å, α = 894.883(3)°, β = 97.185(3)°, γ = 95.948(4)°, V = 2773.4(5) Å^3
Z value	4
D_{calcd}	D_x = 1.109 g cm^{-3}, D_m = 1.100 g cm^{-3}
μ (Mo $K\alpha$)	0.210 mm^{-1}
crystal size	0.35 x 0.30 x 0.30 mm
crystal shape	prism
crystal color	orange
diffractometer	DIP2020 Image plate
radiation	Mo$K\alpha$ (λ = 0.71073 Å) graphite monochromatized rotating anode
temperature	130 K
2θ range	4.08 - 55.94°
number of unique reflections	8231
number of used reflections	8231 ($I > 3\sigma(I)$)
number of parameters	824
data correction	DIP2030K
structure analysis	maXus
refinement	maXus
temperature factors	anisotropic (C and Si) isotropic (H)
$R = \sum \|\|F_o\| - \|F_c\|\| / \sum \|F_o\|$	0.034
$R_w = [\sum w(\|F_o\| - \|F_c\|)^2 / \sum \|F_o\|^2]^{1/2}$	0.040
goodness of fit	S = 1.241

NMR Spectral Data of Hexasilylfulvene (21b) in $CDCl_3$

^1H NMR ($CDCl_3$) δ = 0.29 (s, 24 H, CH_3), 0.34 (s, 12 H, CH_3); ^{13}C NMR ($CDCl_3$) δ = 1.9 (CH_3), 2.5 (CH_3), 3.5 (CH_3), 141.0 (C), 164.7 (C), 168.0 (C), 180.7 (C); ^{29}Si NMR ($CDCl_3$) δ = -0.4, 1.6, 9.2.

Preparation of Dilithium Hexasilylfulvene Dianion (24a).

The crystals of **21a** (22 mg, 0.05 mmol) and lithium metal (30 mg, 4.3 mmol) were placed in a reaction tube with a magnetic stirrer. After degassing, dry oxygen-free THF (1.5 mL) was introduced by vacuum transfer and the mixture was stirred at room temperature to give a yellow solution of the dianion of **21a** within 1 h. After the solvent was removed in vacuo, degassed heptane was introduced by vacuum transfer. Then, after the lithium metal was removed, the solution was cooled to afford yellow crystals of **24a** quantitatively. ^1H NMR (C_7D_8) δ = 0.04 (s, 4 H, CH_2), 0.18 (s, 2 H, CH_2), 0.49 (s, 12 H, CH_3), 0.55 (s, 24 H, CH_3), 1.39 (br.s, 12 H, THF), 3.42 (br.s, 12 H, THF); ^{13}C NMR (C_7D_8) δ = 3.4 (CH_2), 4.4 (CH_3), 5.27 (CH_2), 5.34 (CH_3), 6.0 (CH_3), 25.3 (THF), 30.2 (C), 66.4 (THF), 112.1 (C), 138.6 (C), 164.9 (C); ^{29}Si NMR (C_7D_8) δ = –14.4, -12.5, -5.4; ^6Li NMR (C_7D_8) δ = -3.18.

NMR Spectral Data of 24a in THF-d_8 at 298 K.

^1H NMR (THF-d_8) δ = -0.34 (s, 4 H, CH_2), -0.15 (s, 2 H, CH_2), 0.02 (s, 12 H, CH_3), 0.17 (s, 12 H, CH_3), 0.21 (s, 12 H, CH_3); ^{13}C NMR (THF-d_8) δ = 4.4 (CH_3), 4.6 (CH_2), 5.2 (CH_2), 5.4 (CH_3), 5.9 (CH_3), 30.5 (C), 112.0 (C), 138.7 (C), 164.7 (C); ^{29}Si NMR (THF-d_8) δ = -15.0, -13.2, -6.3; ^6Li NMR (THF-d_8) δ = -3.05.

NMR Spectral Data of 24a' in THF-d_8 at 163 K.

^{1}H NMR (THF-d_8) δ = -0.61 (d, J = 11.9 Hz, 2 H, CH_2), -0.47 (d, J = 11.9 Hz, 2 H, CH_2), -0.36 (br.s, 2 H, CH_2), -0.12 (s, 6 H, CH_3), -0.07 (s, 6 H, CH_3), -0.04 (s, 6 H, CH_3), -0.03 (s, 6 H, CH_3), 0.15 (s, 6 H, CH_3), 0.19 (s, 6 H, CH_3); ^{13}C NMR (THF-d_8) δ = 5.2 (CH_2), 5.6 (CH_3), 5.7 (CH_3), 5.9 (CH_3), 6.4 (CH_2), 6.6 (CH_3), 7.1 (CH_3), 8.6 (CH_3), 23.4 (t, $J^{13C\text{-}6Li}$ = 3.5 Hz, C), 109.1 (C), 138.3 (C), 164.5 (C); ^{29}Si NMR (THF-d_8) δ = -16.2, -13.9, -9.8; ^{6}Li NMR (THF-d_8) δ = 0.79, -0.29.

X-ray Crystallography of Dilithium Hexasilylfulvene Dianion (24a)

Single crystal of **24a** for X-ray diffractions was grown from a heptane solution. The X-ray crystallographic experiment of **24a** was performed on a DIP2020 image plate diffractometer equipped with graphite-monochromatized Mo-$K\alpha$ radiation (λ = 0.71073 Å). Crystal data for **24a** at 180 K: MF = $C_{33}H_{66}Li_2O_3Si_6$, MW = 693.29, monoclinic, a = 11.579(1) Å, b = 11.652(1) Å, c = 31.332(2) Å, β = 95.805(4)°, V = 4205.58(3) Å^3, space group = $P2_1/c$, Z = 4, D_{caled} = 1.095 g/cm^3. The final R factor was 0.045 (R_w = 0.054) for 5783 reflections with $I_o > 3\sigma(I_o)$. The details of the X-ray experiment are given in Table 4-13.

Table 4-13. Detail of the X-ray Experiment for **24a**

molecular formula	$C_{33}H_{66}Li_2O_3Si_6$
molecular weight	693.29
crystal system	monoclinic
space group	$P2_1/c$
cell constants	a = 11.579(1) Å, b = 11.652(1) Å,
	c = 31.332(1) Å, β = 95.805(4)°,
	V = 4205.58(3) Å^3
Z value	4
D_{calcd}	D_x = 1.095 g cm^{-3}, D_m = 1.100 g cm^{-3}
μ (Mo $K\alpha$)	0.2204 mm^{-1}
crystal size	0.40 x 0.30 x 0.30 mm
crystal shape	prism
crystal color	yellow
diffractometer	DIP2020 Image plate
radiation	Mo$K\alpha$ (λ = 0.71073 Å)
	graphite monochromatized rotating anode
temperature	180 K
2θ range	4.08 - 56.4°
number of unique reflections	9273
number of used reflections	5783 ($I > 3\sigma(I)$)
number of parameters	824
data correction	DIP2030K
structure analysis	maXus
refinement	maXus
temperature factors	anisotropic (C, Li, O and Si)
	isotropic (H)
$R = \sum \|\|F_o\| - \|F_c\|\| / \sum \|F_o\|$	0.045
$R_w = [\sum w(\|F_o\| - \|F_c\|)^2 / \sum \|F_o\|^2]^{1/2}$	0.054
goodness of fit	S = 1.668

Preparation of NMR Sample of Dilithium Hexasilylfulvene Dianion (24b).

The crystals of **21b** (51 mg, 0.109 mmol) and lithium metal (30 mg, 4.3 mmol) were placed in a reaction tube with a magnetic stirrer. After degassing, dry oxygen-free THF (1.5 mL) was introduced by vacuum transfer and the mixture was stirred at room temperature to give a yellow solution of the dianion of **21b** within 1 h. After the solvent was removed in vacuo to give **24b** as yellow powder quantitatively, degassed toluene-d_8 was introduced by vacuum transfer. Then, after the lithium metal was removed, the solution of **24b** was used for NMR measurements. ^{1}H NMR (C_7D_8) δ = 0.46 (s, 12 H, CH_3), 0.50 (s, 12 H, CH_3), 0.53 (s, 12 H, CH_3), 1.42 (br.s, 12 H, THF), 3.46 (br.s, 12 H, THF); ^{13}C NMR (C_7D_8) δ = 4.1 (CH_3), 5.2 (CH_3), 5.4 (CH_3), 25.5 (THF), 29.3 (C), 68.5 (THF), 109.4 (C), 135.3 (C), 162.6 (C); ^{29}Si NMR (C_7D_8) δ = -2.0, 1.3, 6.6; ^{6}Li NMR (C_7D_8) δ = -3.10.

NMR Spectral Data of 24b in THF-d_8 at 298 K

^{1}H NMR (THF-d_8) δ = 0.00 (s, 12 H, CH_3), 0.14 (s, 12 H, CH_3), 0.17 (s, 12 H, CH_3); ^{13}C NMR (THF-d_8) δ = 3.9 (CH_3), 4.9 (CH_3), 5.1 (CH_3), 29.3 (C), 109.5 (C), 135.2 (C), 163.2 (C); ^{29}Si NMR (THF-d_8) δ = -2.7, 0.4, 5.8; ^{6}Li NMR (THF-d_8) δ = –2.89.

Molecular Orbital Calculations.

PM3 calculations were performed by Power Macintosh 7600/200 with MACSPARTAN plus program (Ver. 1.1.7).[10] All the calculations were performed with geometry optimization.

References

(1) K.-P. Zeller, "Methoden der Organischen Chemie (Houben-Weyl)" E. Müller, Georg Thieme, Stuttgart, Germany (1985).

(2) (a) K. Ziegler and W. Schäfer, *Ann*, **511,** 101 (1934). (b) G. R. Knox and P. L. Pauson, *J. Chem. Soc.*, **1961,** 4610.

(3) E. D. Bergmann, *Chem. Rev.*, **68,** 41 (1968).

(4) (a) P. Jutzi, *Adv. Organomet. Chem.*, **26,** 217 (1986). (b) C. Schade and P. v. R. Schleyer, *Adv. Organomet. Chem.*, **27,** 169 (1987). (c) A. B. Sannigrahi, T. Kar, B. G. Niyogi, P. Hobza, and P. v. R. Schleyer, *Chem. Rev.*, **90** 1061 (1990). A.-M. Sapse and P. v. R. Schleyer, "Lithium Chemistry: A Theoretical and Experimental Overview", Wiley, New York (1995).

(5) A. Oku, M. Yoshida, and K. Matsumoto, *Bull. Chem. Soc. Jpn.*, **52,** 524 (1979).

(6) T. Kawase, S. Fujino, and M. Oda, *Chem. Lett.*, **1990,** 1683.

(7) (a) H. Sakurai, Y. Nakadaira, A. Hosomi, Y. Eriyama, K. Hirama, and C. Kabuto, *J. Am. Chem. Soc.*, **106,** 8316 (1984). (b) H. Sakurai, *Nippon Kagaku Kaishi*, **1990,** 439.

(8) H. Sakurai, T. Fujii, and K. Sakamoto, *Chem. Lett.*, **1992,** 339.

(9) A. Sekiguchi, K. Ebata, Y. Terui, and H. Sakurai, *Chem. Lett.*, **1991,** 1417.

(10) J. J. P. Stewart, *J. Comput. Chem.*, **10,** 209 (1989).

(11) A. Sekiguchi, Y. Sugai, K. Ebata, C. Kabuto, and H. Sakurai, *J. Am. Chem. Soc.*, **115,** 1144 (1993).

(12) A. Hammel, W. Schwarz, and J. Weidlein, *Acta Crystallogr.*, **C46,** 2337 (1990).

(13) M. F. Lappert, A. Singh, L. M. Engelhardt, and A. H. White, *J. Organomet. Chem.*, **262,** 271 (1984).

(14) F. Zaegel, J. C. Gallucci, P. Meunier, B. Gautheron, M. R. Sivik, and L. A.

Paquette, *J. Am. Chem. Soc.*, **116,** 6466 (1994).

(15) S. Harder and M. H. Prosenc, *Angew. Chem., Int. Ed. Engl.*, **33,** 1744 (1994).

(16) S. D. Stults, R. A. Andersen, and A. Zalkin, *J. Am. Chem. Soc.*, **111,** 4507 (1989).

(17) (a) A. Sekiguchi, T. Matsuo, and C. Kabuto, *Angew. Chem., Int. Ed. Engl.*, **36,** 2462 (1997). (b) A. Sekiguchi, T. Matsuo, and R. Akaba, *Bull. Chem. Soc. Jpn.*, **71,** 41 (1998).

(18) (a) R. Haag, R. Fleischer, D. Stalke, and A. De Merjere, *Angew. Chem., Int. Ed. Engl.*, **34,** 1493 (1995). (b) R. Haag, B. Ohlhorst, M. Noltemeyer, R. Fleischer, D. Stalke, A. Schuster, D. Kuck, and A. De Merjere, *J. Am. Chem. Soc.*, **117,** 10474 (1995).

(19) A. Sekiguchi, M. Ichinohe, T. Nakanishi, and H. Sakurai, *Chem. Lett.*, **1993,** 267.

Chapter 5

Silyl-Substituted Trimethylenecyclopentene Tetraanion with 8C / 12π-Electron System

Summary

Reaction of octasilyltrimethylenecyclopentene (**25**) with lithium metal in THF yielded orange crystals of the tetralithium salt of trimethylenecyclopentene tetraanion (**26**) with 8 center / 12π-electron system. The molecular structure of **26** has been unequivocally established by X-ray crystallography. The tetralithium **26** has a monomeric structure and forms contact ion pairs (CIP) in the crystals. The two lithium atoms (η^5-coordination) are located above and below the center of the five-membered ring, whereas the other two lithium atoms (μ^2-coordination) are bonded to the two exocyclic carbon atoms. The structural parameters of **26** are discussed in comparison to those of the neutral starting molecule of **25**. The structure of **26** in solution has also been discussed on the basis of NMR spectroscopic data. The molecular structure of **26** found in the crystals is maintained in non-polar solvents. The four Li^+ ions of **26** are fixed to the π-skeleton in non-polar solvents, giving CIP with a highly symmetrical structure. However, in a solvating media such as THF-d_8, one of the Li^+ ions above the cyclopentadienide ring is dissociated to yield a solvent separated ion pair (SSIP) due to the solvation of the Li^+ ion. The X-ray crystallography and the NMR data indicate that the structures of **26** is a stable, closed-shell supercharged tetraanion, which is stabilized not only by the eight silicon atoms but also by the aromatic cyclopentadienyl anion.

Introduction

Supercharged anions with extended π-electron systems have attracted considerable interest owing to their unique structures and electronic properties.[1] The existence of a hexaanionic species in the solid state is inferred from the formation of K_6C_{60}, which was characterized by X-ray powder diffraction and ^{13}C NMR spectroscopy.[2] Scott et al. recently reported on the tetralithium salt of the corannulene tetraanion ($C_{20}H_{10}$) and its derivatives (Scheme 5-1).[3] The most recent, and, to our knowledge, the only report on the molecular structure of a rubrene tetraanion (crystallized as a tetrasodium salt; rubrene = 5,6,11,12-tetraphenyltetracene, $C_{42}H_{28}$) that has been confirmed by X-ray crystallography was carried out by Bock et al. (Scheme 5-2 and Figure 5-1).[4]

Scheme 5-1

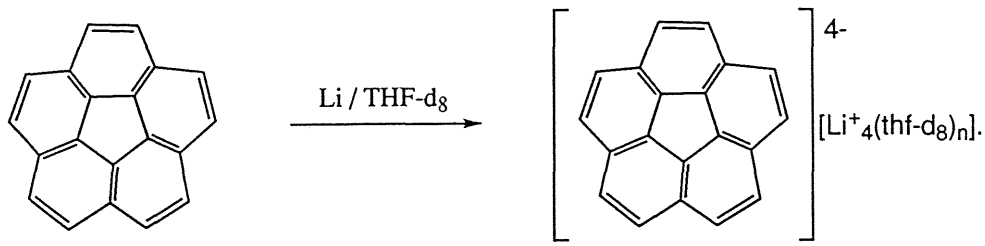

Scheme 5-2

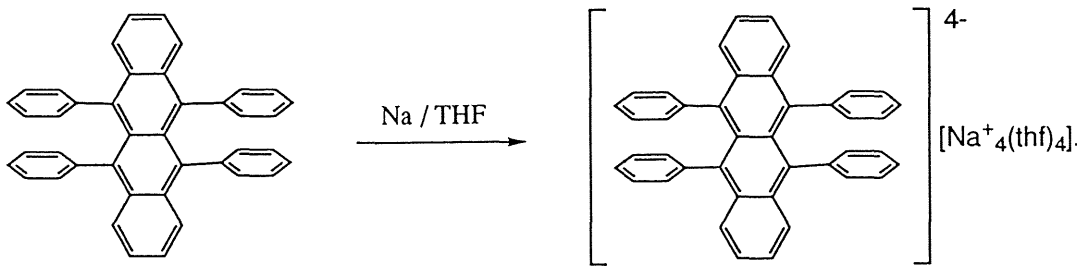

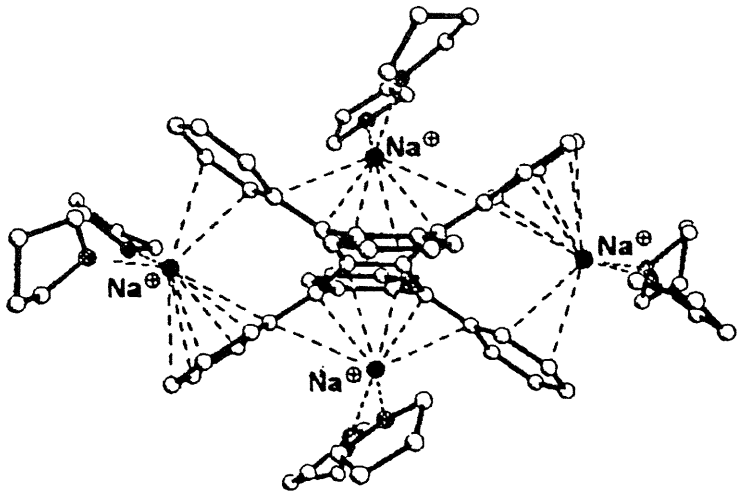

Figure 5-1. Molecular structure of tetrasodium rubrene tetraanion.

Trimethylenecyclopentene (3,4,5-trimethylenecyclopentene) possesses a very unique 8π-electron system based on five-membered ring. One double bond is located in the five-membered ring and three double bonds are situated in the exo position. There has been no studies concerning the anion species of trimethylenecyclopentene derivatives.

In this chapter, synthesis, characterization, and molecular structure of tetralithium octasilyltrimethylenecyclopentene tetraanion as a new silyl-substituted 8C / 12π-electron system are described.

Results and Discussion

Synthesis of Octasilyltrimethylenecyclopentene (25)

Octasilyltrimethylenecyclopentene derivative (**25**) bridged by $Me_2SiCH_2SiMe_2$ chains was prepared by the intramolecular cyclotetramerization of the macrocyclic silyltetrayne (**14**). A mixture of the 3,3,5,5,8,8,10,10,13,13,15,15,18,18,20,20-hexadecamethyl-3,5,8,10,13,15,18,20-octasilacycloicosa-1,6,11,16-tetrayne (**14**) and one molar amount of $[Mn(CO)_3(Me\text{-}Cp)]$ in THF was irradiated with a 500 W high-pressure mercury lamp under the refluxing temperature of THF to produce pale yellow crystals of the persilylated trimethylenecyclopentene derivative (**25**) in 17% yield (Scheme 5-3).

Scheme 5-3

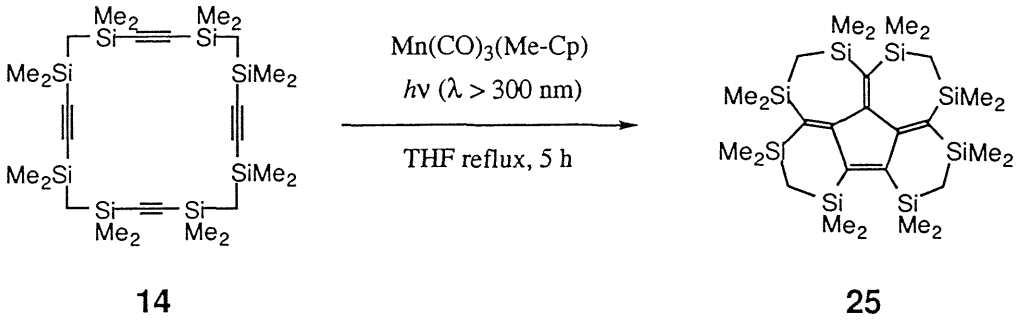

14 **25**

The reaction involves the 1,2-silyl shift in the 1,2-disilyl-substituted acetylene to give 2,2-disilylvinylidene complexes as a reaction intermediate.[5] The 1,2-silyl shift was accelerated by heat, and no trimethylenecyclopentene compounds were furnished at room temperature. The reaction mechanism to produce **25** is not clear at this moment, but a triple 1,2-silyl shift can be involved. The possible mechanism is shown in Scheme 5-4.

Scheme 5-4

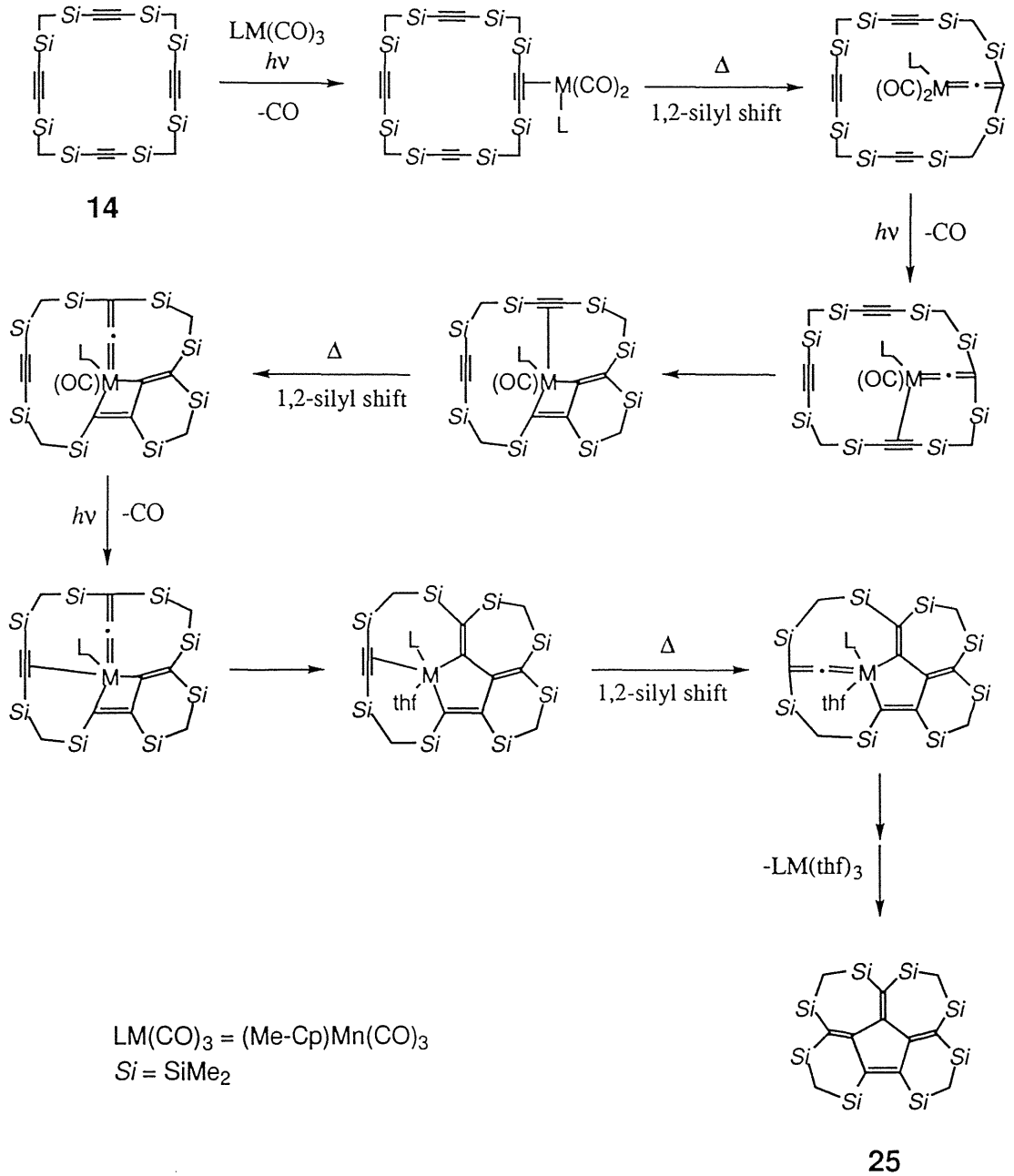

14

25

LM(CO)$_3$ = (Me-Cp)Mn(CO)$_3$

Si = SiMe$_2$

Molecular Structure of Octasilyltrimethylenecyclopentene 25

Octasilyltrimethylenecyclopentene **25** bridged by silmethylene chains could be recrystallized from ethanol. Since there is no crystal structure of the trimethylene-cyclopentene derivative thus far, the molecular structure of **25** has been unequivocally determined by X-ray crystallography. The ORTEP drawing of **25** are shown in Figure 5-2. The crystal packing of **25** is also shown in Figure 5-3. The final atomic parameters of **25** are listed in Tables 5-1 and 5-2. The bond lengths of **25** are summarized in Tables 5-3 and 5-4. The bond angles of **25** are also summarized in Table 5-5.

The selected bond angles and lengths of **25** are shown in Figures 5-4 and 5-5, respectively. The trimethylenecyclopentene derivative **25** is a highly distorted structure and the central five-membered ring is not planar but in an envelope conformation. The angle formed by C1-C2-C3-C5 and C3-C4-C5 plane is 36.2°. The internal bond angles of the five-membered ring are 101.4(4)-109.3(4)° (av 105.2°), and the sum of the bond angles is 526.0°. The appreciable bond alternation between the single and double bonds of π-skeleton of **25** shows the structural feature as a cross-conjugated diene. The C-C single and double bond lengths of **25** are 1.506(7)-1.523(7) Å (av 1.515 Å) and 1.348(7)-1.372(8) Å (av 1.358 Å), respectively.

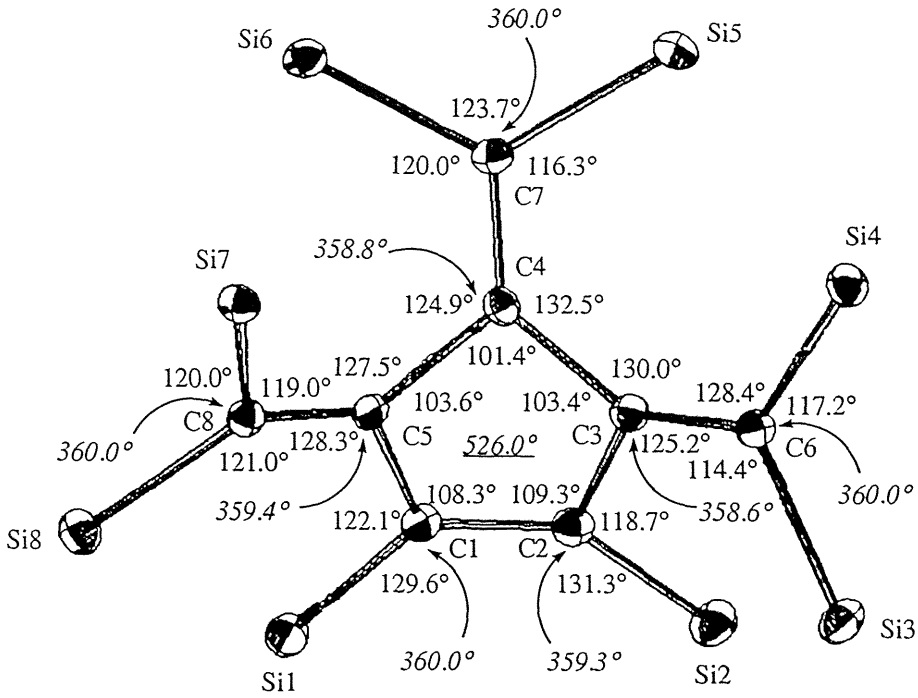

Figure 5-4. Selected bond angles of **25**.

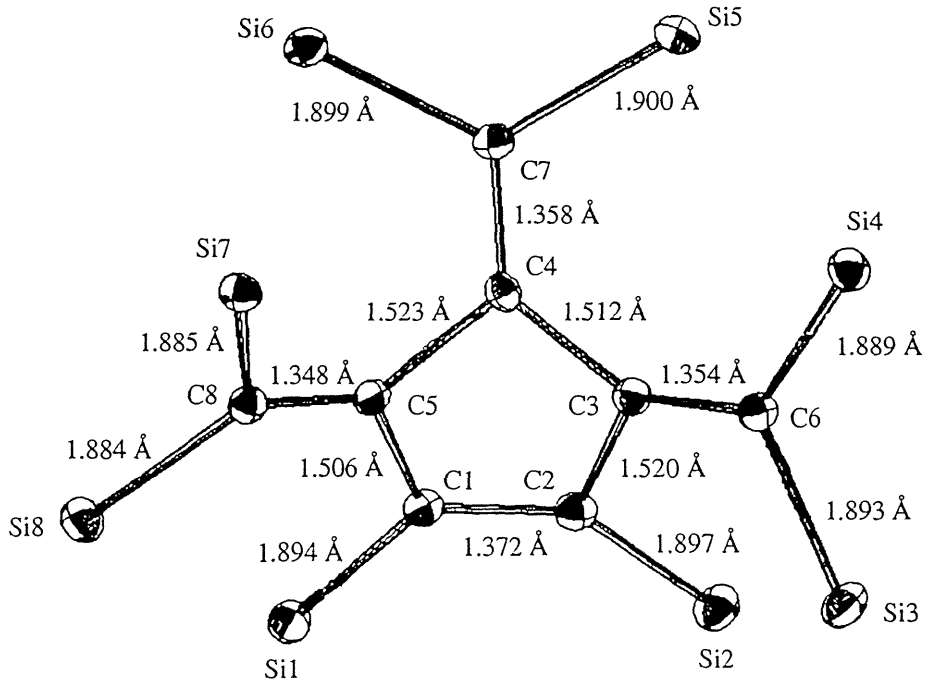

Figure 5-5. Selected bond lengths of **25**.

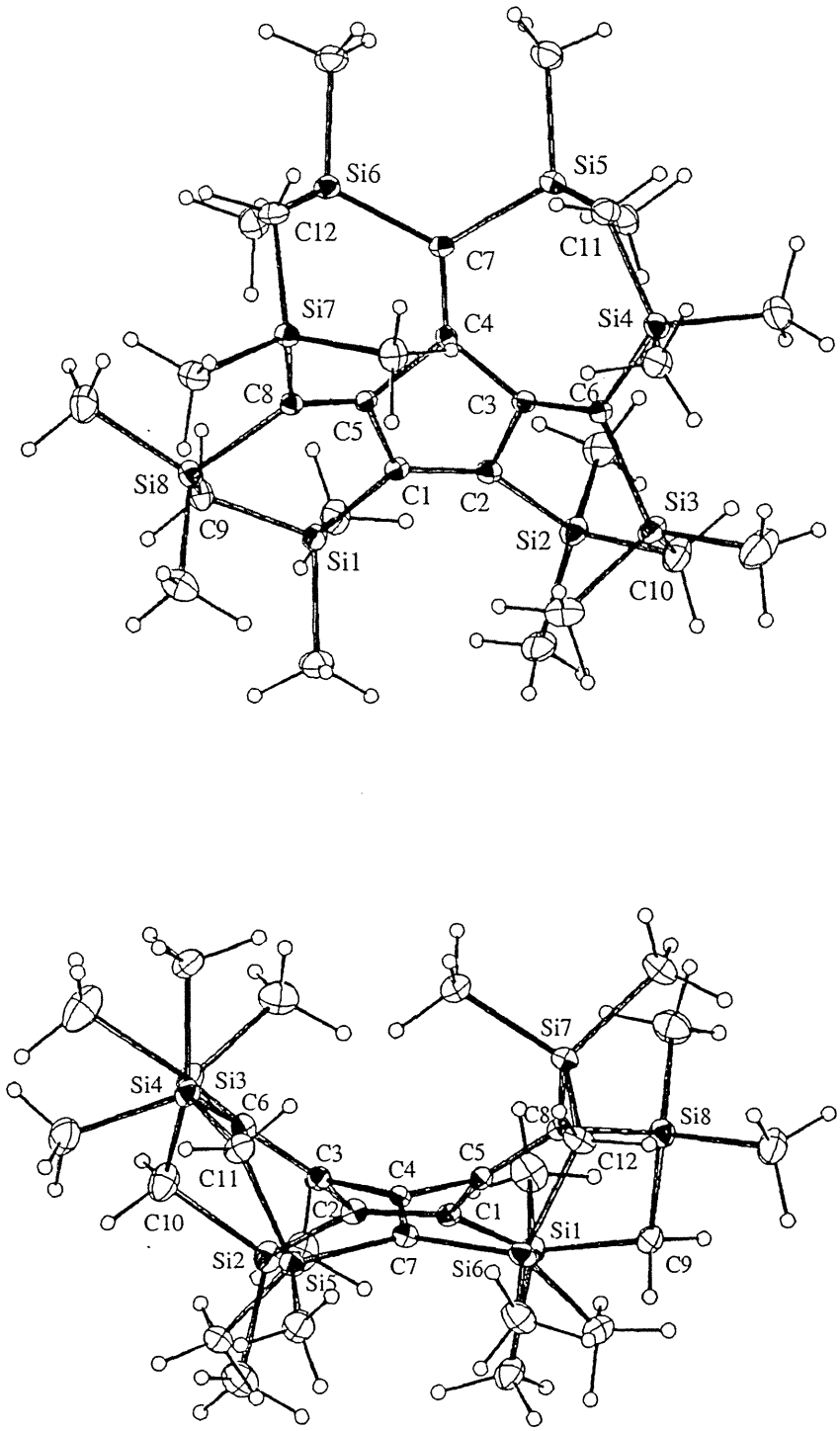

Figure 5-2. ORTEP drawing of **25**: upper, top view; below, side view.

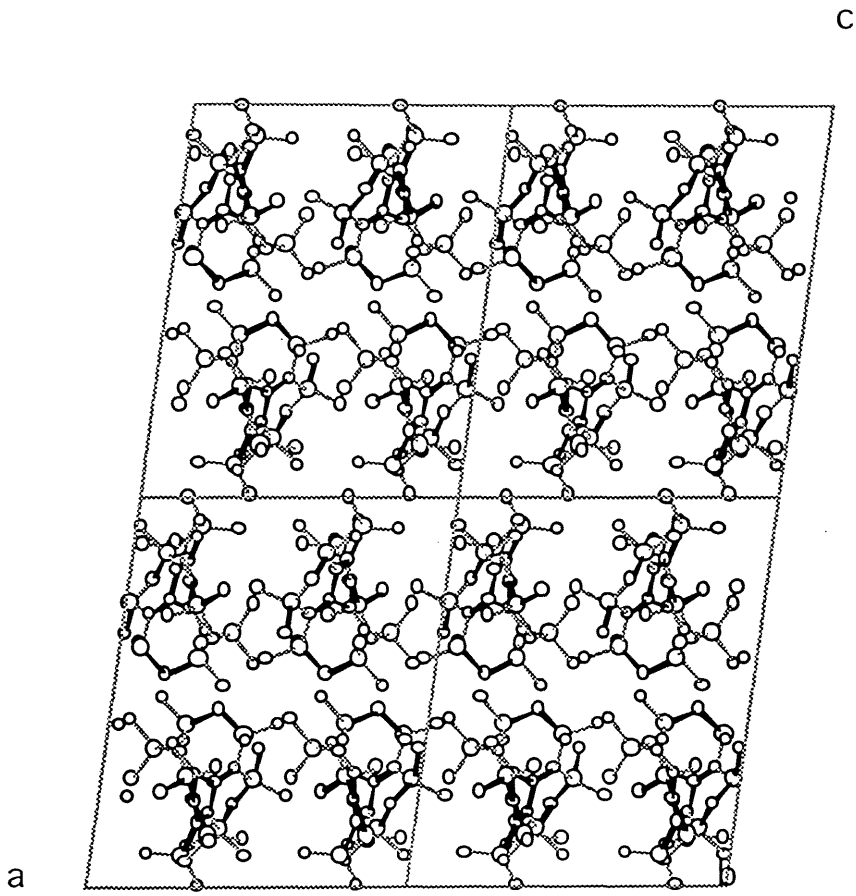

Figure 5-3. Crystal packing of **25**.

Table 5-1. Atomic Parameters[a] for Non-Hydrogen Atoms of **25**

ATOM	X	Y	Z	BEQV
SI1	3894(1)	7261(1)	8542(1)	2.1
SI2	2857(1)	4668(2)	9206(1)	2.4
SI3	3589(1)	2515(1)	8694(1)	2.4
SI4	2688(1)	1896(1)	7166(1)	2.0
SI5	1517(1)	3774(1)	6454(1)	1.9
SI6	2446(1)	6007(1)	5862(1)	2.0
SI7	4323(1)	5400(1)	6134(1)	1.8
SI8	4803(1)	7406(1)	7248(1)	2.1
C1	3526(3)	5921(5)	8082(3)	1.7
C2	3206(3)	4971(5)	8338(3)	1.9
C3	2997(3)	4131(5)	7758(3)	1.7
C4	2930(3)	4845(4)	7115(3)	1.5
C5	3590(3)	5732(4)	7331(3)	1.5
C6	3044(3)	3006(5)	7829(3)	1.9
C7	2356(3)	4895(5)	6541(3)	1.7
C8	4169(3)	6127(4)	6961(3)	1.6
C9	4226(4)	8190(5)	7864(3)	2.4
C10	2999(5)	3131(6)	9356(3)	3.3
C11	2100(4)	2448(5)	6350(3)	2.5
C12	3421(3)	5756(6)	5467(3)	2.3
C21	4835(5)	7048(7)	9210(3)	3.6
C22	3024(5)	7928(5)	8930(3)	2.9
C23	3464(5)	5357(7)	9978(3)	3.6
C24	1731(5)	5071(7)	9136(4)	3.7
C25	3664(6)	969(7)	8840(4)	4.9
C26	4700(4)	3037(7)	8768(4)	3.7
C27	1938(5)	969(6)	7558(4)	3.6
C28	3577(4)	1027(5)	6942(4)	3.0
C29	681(4)	3893(6)	5697(4)	3.2
C30	957(4)	3750(5)	7226(3)	2.6
C31	1568(4)	6029(7)	5133(3)	3.2
C32	2434(4)	7454(6)	6244(4)	3.1
C33	4397(4)	3849(5)	6282(3)	2.8
C34	5347(4)	5787(6)	5847(3)	2.9
C35	5885(4)	7059(7)	7655(4)	3.6
C36	4857(5)	8354(6)	6484(4)	3.3

[a] Positional parameters are multiplied by 10^4. Thermal parameters are given by the equivalent temperature factors (A^2).

Table 5-2. Atomic Parameters[a] for Hydrogen Atoms of **25**

ATOM	X	Y	Z	B
H91	460(4)	886(6)	806(3)	2.6(1.4)
H92	364(4)	842(6)	760(3)	2.9(1.5)
H101	332(4)	299(6)	987(3)	3.3(1.6)
H102	238(4)	275(6)	931(3)	3.2(1.6)
H111	175(4)	179(6)	620(3)	2.9(1.5)
H112	250(4)	260(6)	600(3)	2.8(1.4)
H121	358(4)	641(6)	515(3)	2.6(1.4)
H122	336(4)	521(6)	511(3)	2.8(1.4)
H211	520(4)	649(6)	904(3)	3.1(1.5)
H212	518(4)	782(6)	930(3)	3.3(1.6)
H213	465(4)	676(6)	968(3)	3.2(1.5)
H221	267(4)	738(6)	922(3)	2.8(1.4)
H222	327(4)	856(6)	928(3)	3.3(1.6)
H223	259(4)	829(6)	853(3)	2.9(1.5)
H231	326(4)	521(6)	1041(3)	2.8(1.5)
H232	411(4)	507(6)	1004(3)	3.0(1.5)
H233	346(4)	625(6)	992(3)	2.8(1.5)
H241	140(4)	450(6)	883(3)	2.8(1.4)
H242	153(4)	506(6)	963(3)	3.1(1.5)
H243	165(4)	589(6)	892(3)	3.4(1.6)
H251	370(4)	52(6)	842(3)	3.1(1.5)
H252	419(4)	76(6)	921(4)	3.6(1.6)
H253	310(4)	67(6)	904(3)	3.1(1.5)
H261	493(4)	264(6)	840(3)	3.0(1.5)
H262	472(4)	394(6)	869(3)	3.3(1.6)
H263	504(4)	284(6)	927(3)	3.3(1.6)
H271	214(4)	22(6)	775(3)	2.8(1.5)
H272	171(4)	139(6)	800(3)	3.4(1.6)
H273	141(4)	78(6)	718(3)	3.4(1.6)
H281	383(4)	63(6)	738(3)	2.7(1.4)
H282	335(4)	44(6)	654(3)	3.4(1.6)
H283	403(4)	156(6)	674(3)	3.3(1.6)
H291	81(4)	386(6)	518(3)	2.9(1.5)
H292	29(4)	448(6)	564(3)	2.9(1.5)
H293	26(4)	337(6)	572(3)	2.9(1.5)
H301	133(4)	350(6)	758(3)	2.6(1.4)
H302	75(4)	457(6)	733(3)	3.1(1.5)
H303	43(4)	320(6)	714(3)	2.9(1.5)

[a] Positional parameters are multiplied by 10^4. Thermal parameters are given by the equivalent temperature factors (A^2).

Table 5-2 (continued). Atomic Parameters[a] for Hydrogen Atoms of **25**

H311	106(4)	599(6)	529(3)	2.7(1.4)
H312	158(4)	679(6)	484(3)	3.3(1.5)
H313	161(4)	532(6)	479(3)	3.2(1.5)
H321	194(4)	787(6)	641(3)	3.0(1.5)
H322	288(4)	752(6)	670(4)	3.6(1.6)
H323	259(4)	807(6)	588(4)	3.6(1.6)
H331	434(4)	341(6)	582(3)	2.8(1.5)
H332	500(4)	364(6)	657(3)	3.2(1.5)
H333	392(4)	357(6)	657(3)	2.9(1.5)
H341	555(4)	519(6)	557(3)	2.9(1.5)
H342	527(4)	654(6)	552(3)	3.4(1.6)
H343	581(4)	595(6)	629(3)	2.9(1.5)
H351	618(4)	770(6)	786(3)	3.1(1.5)
H352	587(4)	644(6)	806(3)	3.1(1.5)
H353	625(4)	673(6)	728(3)	3.1(1.5)
H361	480(4)	778(6)	607(3)	3.2(1.5)
H362	434(4)	896(6)	644(4)	3.5(1.6)
H363	543(4)	880(6)	655(4)	3.7(1.6)

[a] Positional parameters are multiplied by 10^4. Thermal parameters are given by the equivalent temperature factors (A^2).

Table 5-3. List of Bond Lengths (Å) for Non-Hydrogen Atoms of **25**

ATOM	-	ATOM		LENGTH(SIG)
SI1	-	C1	=	1.894(6)
SI1	-	C9	=	1.867(7)
SI1	-	C21	=	1.883(9)
SI1	-	C22	=	1.868(7)
SI2	-	C2	=	1.897(6)
SI2	-	C10	=	1.870(8)
SI2	-	C23	=	1.877(8)
SI2	-	C24	=	1.873(9)
SI3	-	C6	=	1.893(6)
SI3	-	C10	=	1.864(8)
SI3	-	C25	=	1.873(11)
SI3	-	C26	=	1.891(9)
SI4	-	C6	=	1.889(6)
SI4	-	C11	=	1.864(7)
SI4	-	C27	=	1.884(8)
SI4	-	C28	=	1.877(7)
SI5	-	C7	=	1.900(6)
SI5	-	C11	=	1.871(7)
SI5	-	C29	=	1.870(8)
SI5	-	C30	=	1.868(7)
SI6	-	C7	=	1.899(6)
SI6	-	C12	=	1.876(7)
SI6	-	C31	=	1.871(8)
SI6	-	C32	=	1.887(7)
SI7	-	C8	=	1.885(6)
SI7	-	C12	=	1.868(7)
SI7	-	C33	=	1.880(7)
SI7	-	C34	=	1.881(8)
SI8	-	C8	=	1.884(6)
SI8	-	C9	=	1.875(6)
SI8	-	C35	=	1.869(8)
SI8	-	C36	=	1.889(8)
C1	-	C2	=	1.372(8)
C1	-	C5	=	1.506(7)
C2	-	C3	=	1.520(8)
C3	-	C4	=	1.512(8)
C3	-	C6	=	1.354(8)
C4	-	C5	=	1.523(7)
C4	-	C7	=	1.358(8)
C5	-	C8	=	1.348(7)

Table 5-4. List of Bond Lengths (Å) for Hydrogen Atoms of **25**

ATOM	-	ATOM		LENGTH(SIG)
C9	-	H91	=	1.04(7)
C9	-	H92	=	1.05(7)
C10	-	H101	=	1.08(7)
C10	-	H102	=	1.10(7)
C11	-	H111	=	0.99(7)
C11	-	H112	=	1.02(7)
C12	-	H121	=	1.05(7)
C12	-	H122	=	0.96(7)
C21	-	H211	=	0.98(7)
C21	-	H212	=	1.08(7)
C21	-	H213	=	1.07(7)
C22	-	H221	=	1.09(7)
C22	-	H222	=	1.07(7)
C22	-	H223	=	1.07(7)
C23	-	H231	=	0.96(7)
C23	-	H232	=	1.09(7)
C23	-	H233	=	1.08(7)
C24	-	H241	=	1.01(7)
C24	-	H242	=	1.06(7)
C24	-	H243	=	1.07(7)
C25	-	H251	=	0.99(7)
C25	-	H252	=	1.07(7)
C25	-	H253	=	1.10(7)
C26	-	H261	=	0.98(7)
C26	-	H262	=	1.09(7)
C26	-	H263	=	1.09(7)
C27	-	H271	=	1.00(7)
C27	-	H272	=	1.10(7)
C27	-	H273	=	1.08(7)
C28	-	H281	=	1.02(7)
C28	-	H282	=	1.08(7)
C28	-	H283	=	1.08(7)
C29	-	H291	=	1.07(7)
C29	-	H292	=	0.93(7)
C29	-	H293	=	0.93(7)
C30	-	H301	=	0.90(7)
C30	-	H302	=	1.07(7)
C30	-	H303	=	1.08(7)
C31	-	H311	=	0.92(7)
C31	-	H312	=	1.08(7)
C31	-	H313	=	1.09(7)
C32	-	H321	=	1.04(7)
C32	-	H322	=	1.07(7)
C32	-	H323	=	1.08(7)
C33	-	H331	=	1.04(7)
C33	-	H332	=	1.09(7)
C33	-	H333	=	1.07(7)
C34	-	H341	=	0.98(7)
C34	-	H342	=	1.10(7)
C34	-	H343	=	1.08(7)
C35	-	H351	=	0.95(7)
C35	-	H352	=	1.09(7)
C35	-	H353	=	1.07(7)
C36	-	H361	=	1.05(7)
C36	-	H362	=	1.10(7)
C36	-	H363	=	1.07(7)

Table 5-5. List of Bond Angles (Å) for Non-Hydrogen Atoms of **25**

ATOM -	ATOM	ATOM	ANGLE(SIG)
C1 -	SI1 -	C9 =	105.6(2)
C1 -	SI1 -	C21 =	112.7(3)
C1 -	SI1 -	C22 =	110.4(2)
C9 -	SI1 -	C21 =	106.8(3)
C9 -	SI1 -	C22 =	110.0(3)
C21 -	SI1 -	C22 =	111.0(3)
C2 -	SI2 -	C10 =	106.5(3)
C2 -	SI2 -	C23 =	116.7(3)
C2 -	SI2 -	C24 =	107.1(3)
C10 -	SI2 -	C23 =	105.4(3)
C10 -	SI2 -	C24 =	111.2(3)
C23 -	SI2 -	C24 =	110.0(3)
C6 -	SI3 -	C10 =	106.3(3)
C6 -	SI3 -	C25 =	117.0(3)
C6 -	SI3 -	C26 =	106.7(3)
C10 -	SI3 -	C25 =	108.3(4)
C10 -	SI3 -	C26 =	112.9(3)
C25 -	SI3 -	C26 =	105.8(4)
C6 -	SI4 -	C11 =	114.3(2)
C6 -	SI4 -	C27 =	106.7(3)
C6 -	SI4 -	C28 =	112.2(2)
C11 -	SI4 -	C27 =	106.0(3)
C11 -	SI4 -	C28 =	108.2(2)
C27 -	SI4 -	C28 =	109.1(3)
C7 -	SI5 -	C11 =	104.0(2)
C7 -	SI5 -	C29 =	116.6(2)
C7 -	SI5 -	C30 =	111.1(2)
C11 -	SI5 -	C29 =	107.4(3)
C11 -	SI5 -	C30 =	112.5(2)
C29 -	SI5 -	C30 =	105.2(3)
C7 -	SI6 -	C12 =	109.1(2)
C7 -	SI6 -	C31 =	114.9(3)
C7 -	SI6 -	C32 =	111.0(2)
C12 -	SI6 -	C31 =	106.4(3)
C12 -	SI6 -	C32 =	111.4(3)
C31 -	SI6 -	C32 =	103.9(3)
C8 -	SI7 -	C12 =	108.2(2)
C8 -	SI7 -	C33 =	109.6(2)
C8 -	SI7 -	C34 =	111.6(2)
C12 -	SI7 -	C33 =	111.1(2)
C12 -	SI7 -	C34 =	111.8(3)
C33 -	SI7 -	C34 =	104.4(3)
C8 -	SI8 -	C9 =	107.4(2)
C8 -	SI8 -	C35 =	112.7(3)
C8 -	SI8 -	C36 =	109.5(2)
C9 -	SI8 -	C35 =	111.0(3)
C9 -	SI8 -	C36 =	106.9(3)
C35 -	SI8 -	C36 =	109.1(3)
SI1 -	C1 -	C2 =	129.6(4)
SI1 -	C1 -	C5 =	122.1(3)
C2 -	C1 -	C5 =	108.3(4)
SI2 -	C2 -	C1 =	131.3(4)

Table 5-5 (continued). List of Bond Angles (Å) for Non-Hydrogen Atoms of **25**

SI2	-	C2	-	C3	=	118.7(3)
C1	-	C2	-	C3	=	109.3(4)
C2	-	C3	-	C4	=	103.4(4)
C2	-	C3	-	C6	=	125.2(5)
C4	-	C3	-	C6	=	130.0(5)
C3	-	C4	-	C5	=	101.4(4)
C3	-	C4	-	C7	=	132.5(5)
C5	-	C4	-	C7	=	124.9(4)
C1	-	C5	-	C4	=	103.6(4)
C1	-	C5	-	C8	=	128.3(4)
C4	-	C5	-	C8	=	127.5(4)
SI3	-	C6	-	SI4	=	117.2(2)
SI3	-	C6	-	C3	=	114.4(4)
SI4	-	C6	-	C3	=	128.4(4)
SI5	-	C7	-	SI6	=	123.7(3)
SI5	-	C7	-	C4	=	116.3(4)
SI6	-	C7	-	C4	=	120.0(4)
SI7	-	C8	-	SI8	=	120.0(2)
SI7	-	C8	-	C5	=	119.0(3)
SI8	-	C8	-	C5	=	121.0(4)
SI1	-	C9	-	SI8	=	112.2(3)
SI2	-	C10	-	SI3	=	110.0(4)
SI4	-	C11	-	SI5	=	114.4(3)
SI6	-	C12	-	SI7	=	111.7(3)

PM3 Calculation of Octasilyltrimethylenecyclopentene 25

The geometry optimization of octasilyltrimethylenecyclopentene **25** was carried out by PM3 calculation.[6] The calculated structure of **25** is shown in Figure 5-6. The LUMO and next LUMO of **25** are also shown in Figures 5-7 and 5-8. The geometry of **25** by the X-ray diffraction is wellreproduced by PM3 calculation. The selected bond angles and lengths of **25** calculated by PM3 are shown in Figures 5-9 and 5-10. The charge distribution of **25** is also shown in Figure 5-11.

The energy diagram of **25** calculated by PM3 is shown in Figure 5-12. The schematic drawings of the LUMO (0.20 eV) and next LUMO (0.43 eV) of **25** are also shown in Figures 5-13 and 5-14, respectively. In the LUMO, C1-C2, C3-C6, and C5-C8 bonds are antibonding, whereas C1-C5 and C2-C3 bonds are bonding. The π-MO coefficients at the central C1 and C2 carbon atoms are larger than that of other carbon atoms as shown in Figure 5-13. Thus, two electron reduction of **25** may produce dianion dimetal complex so that the counter cations may strongly interact with the C1 and C2 carbon atoms. The resulting dianion may be stabilized by Si1 and Si2 silicon atoms. The schematic drawing of the LUMO of **25** is very close to that of hexasilyldimethylene-cyclobutene as described in Chapter 2. Hexasilyldimethylenecyclobutene dianion has the bis(allyl anion) character. Thus, octasilyltrimethylenecyclopentene dianion may also have the bis(allyl anion) character.

Of particular interest of the π-MO of **25** is the next LUMO. The central five-membered ring has similar π-MO to cyclopentadienide ion with 6π-electron system. In addition, the π-MO of the exo carbon-carbon bonds (C3-C6, C4-C7, and C5-C8) are all antibonding. Therefore, it is quite reasonable to assume that reduction of **25** may produce the tetraanion by four electron reduction, which will be stabilized by not only cyclopentadienide ion with 6π-electron system but also by six silicon atoms (Si3, Si4, Si5, Si6, Si7, and Si8).

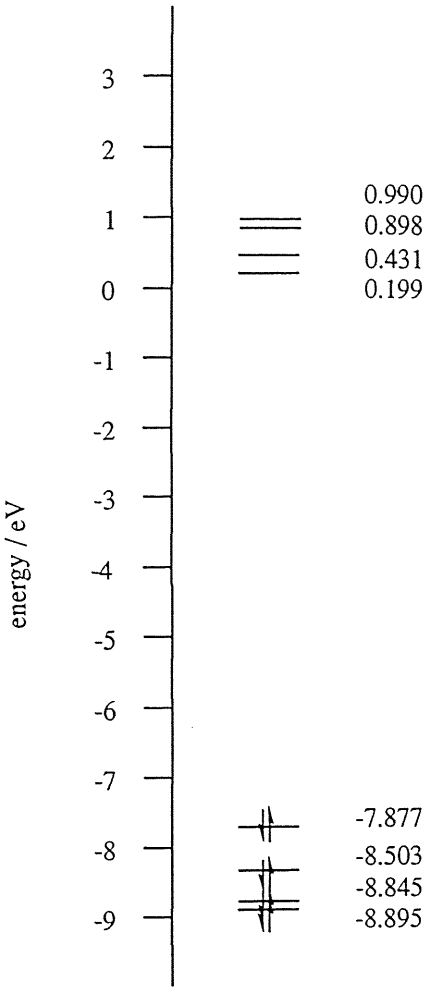

Figure 5-12. Energy diagram of **25** calculated by PM3.

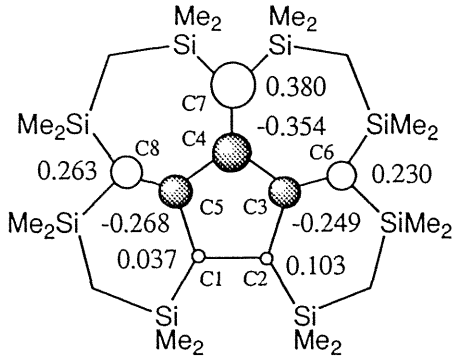

Figure 5-14. Schematic representation of the next LUMO of **25** calculated by PM3.

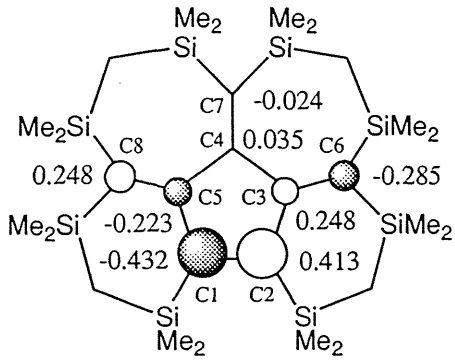

Figure 5-13. Schematic representation of the LUMO of **25** calculated by PM3.

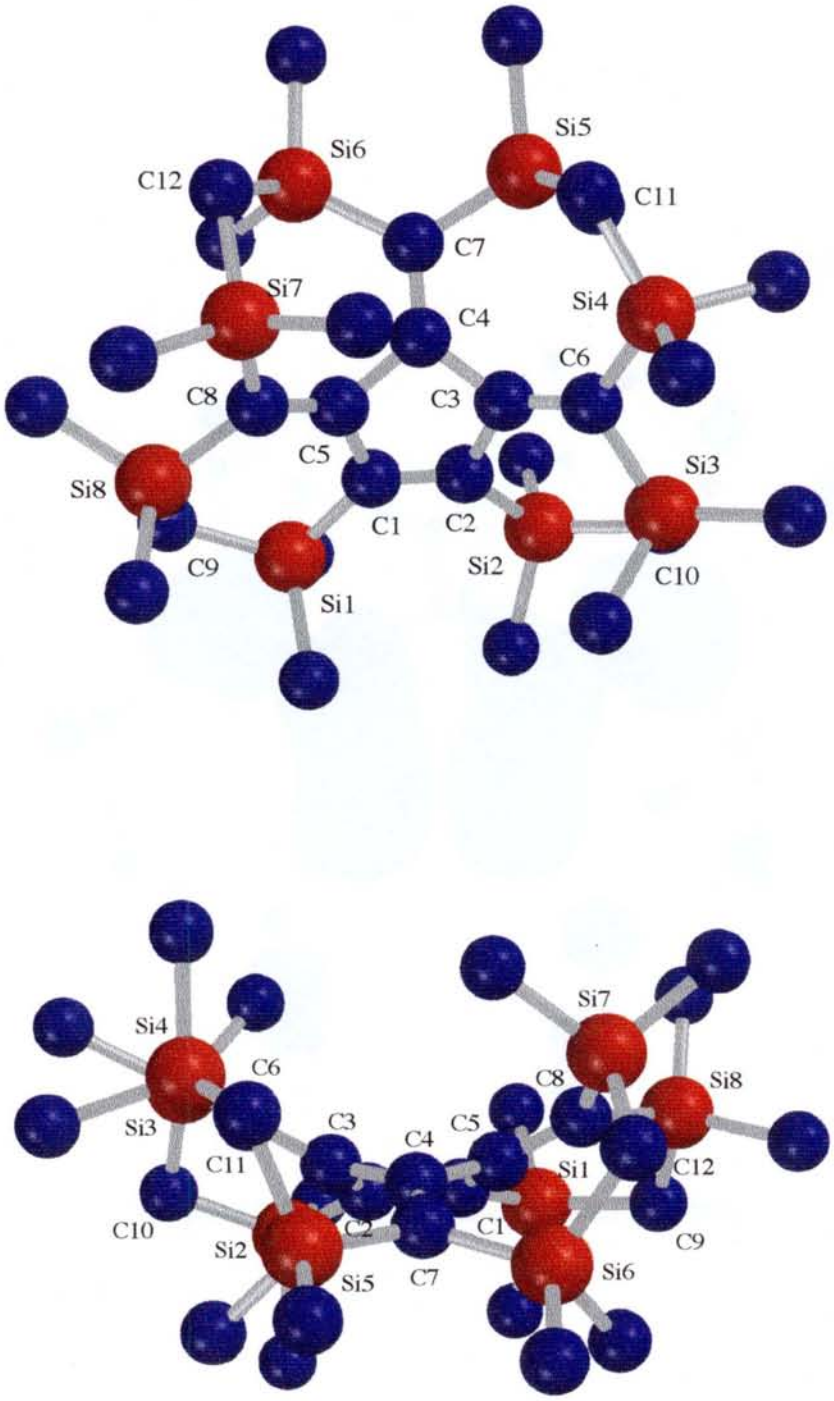

Figure 5-6. Calculated structure of **25** by PM3 (hydrogen atoms are omitted for the clarity): upper, top view; below, side view.

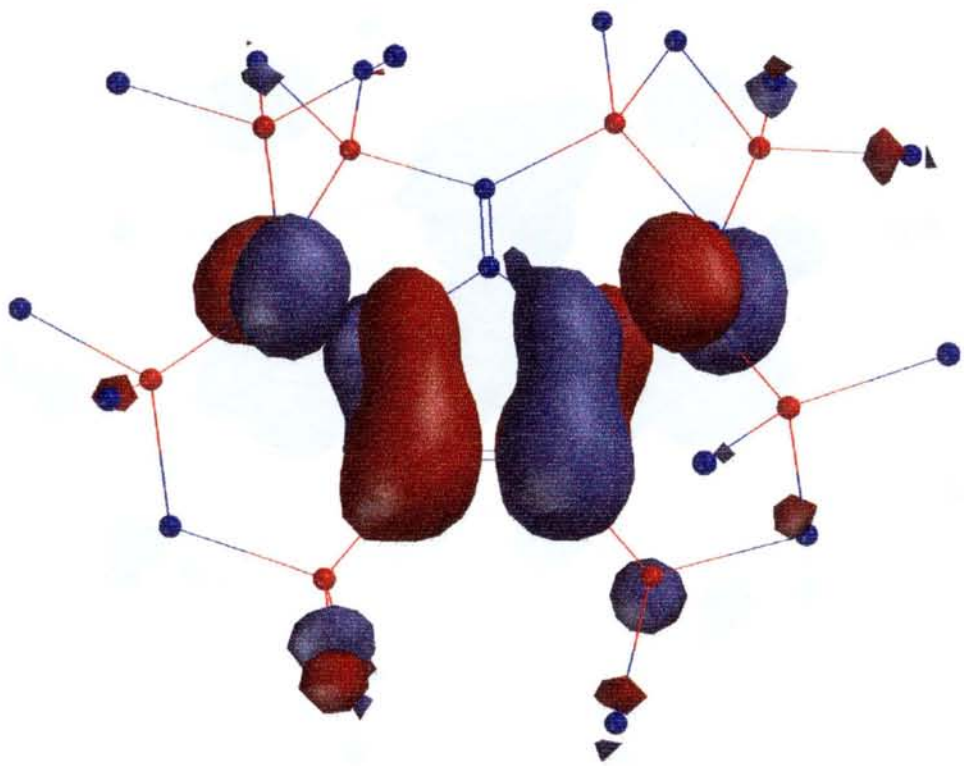

Figure 5-7. LUMO of **25** calculated by PM3.

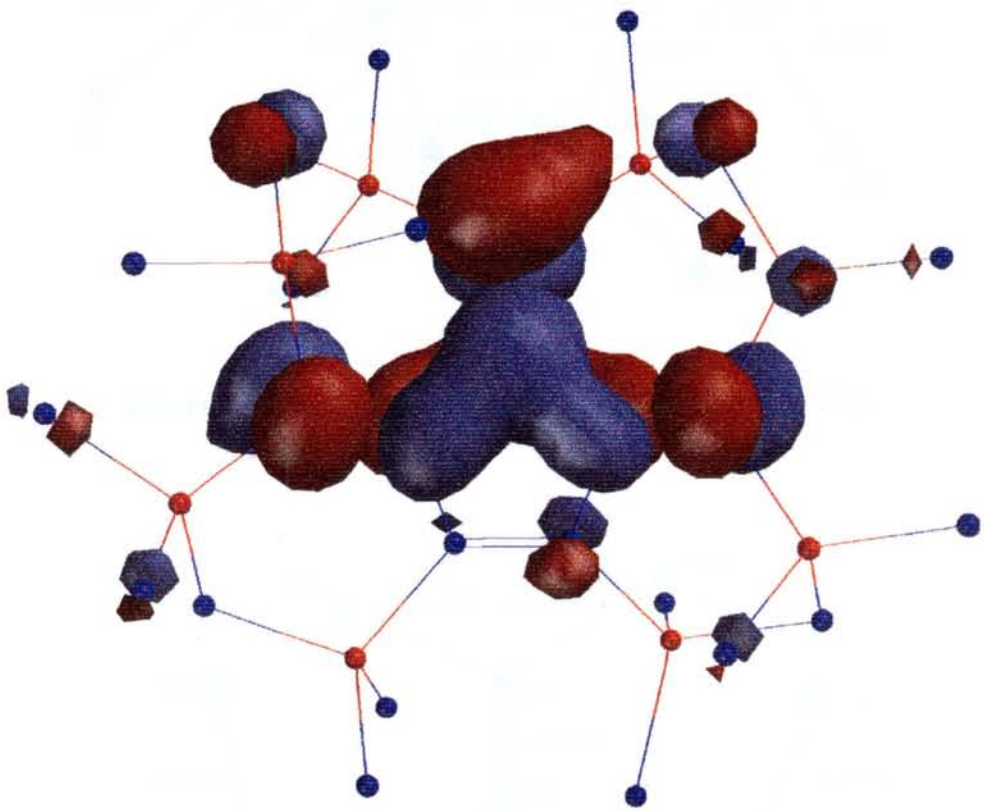

Figure 5-8. next LUMO of **25** calculated by PM3.

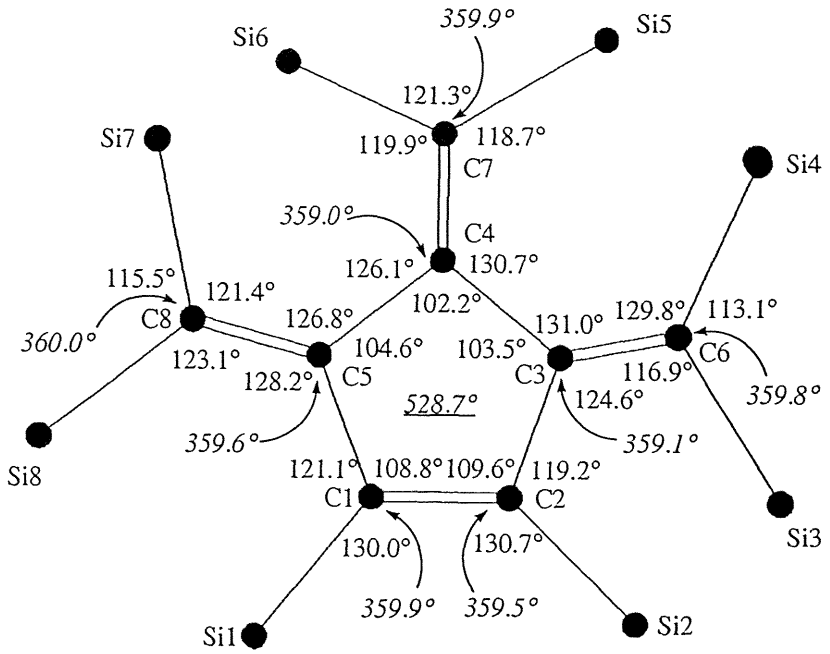

Figure 5-9. Selected bond angles of **25** calculated by PM3.

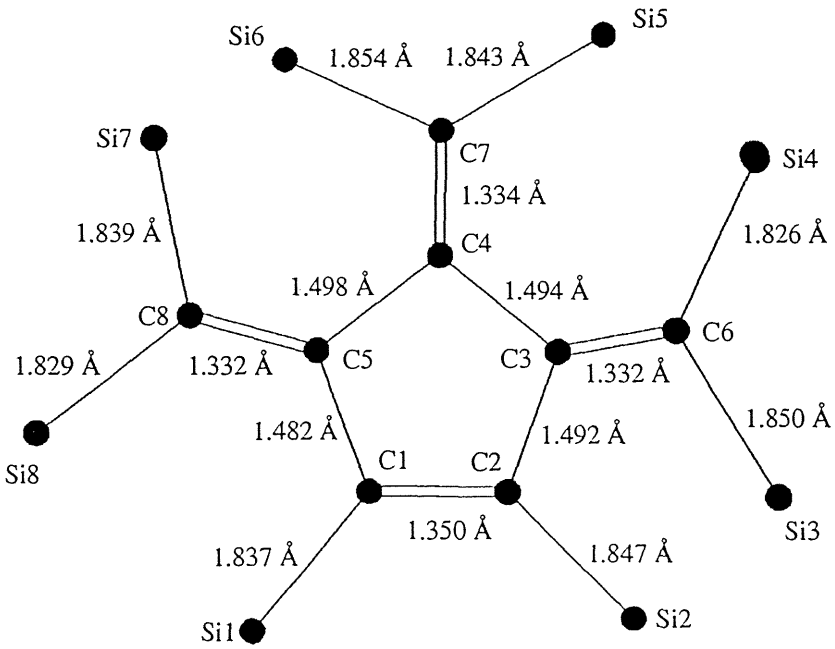

Figure 5-10. Selected bond lengths of **25** calculated by PM3.

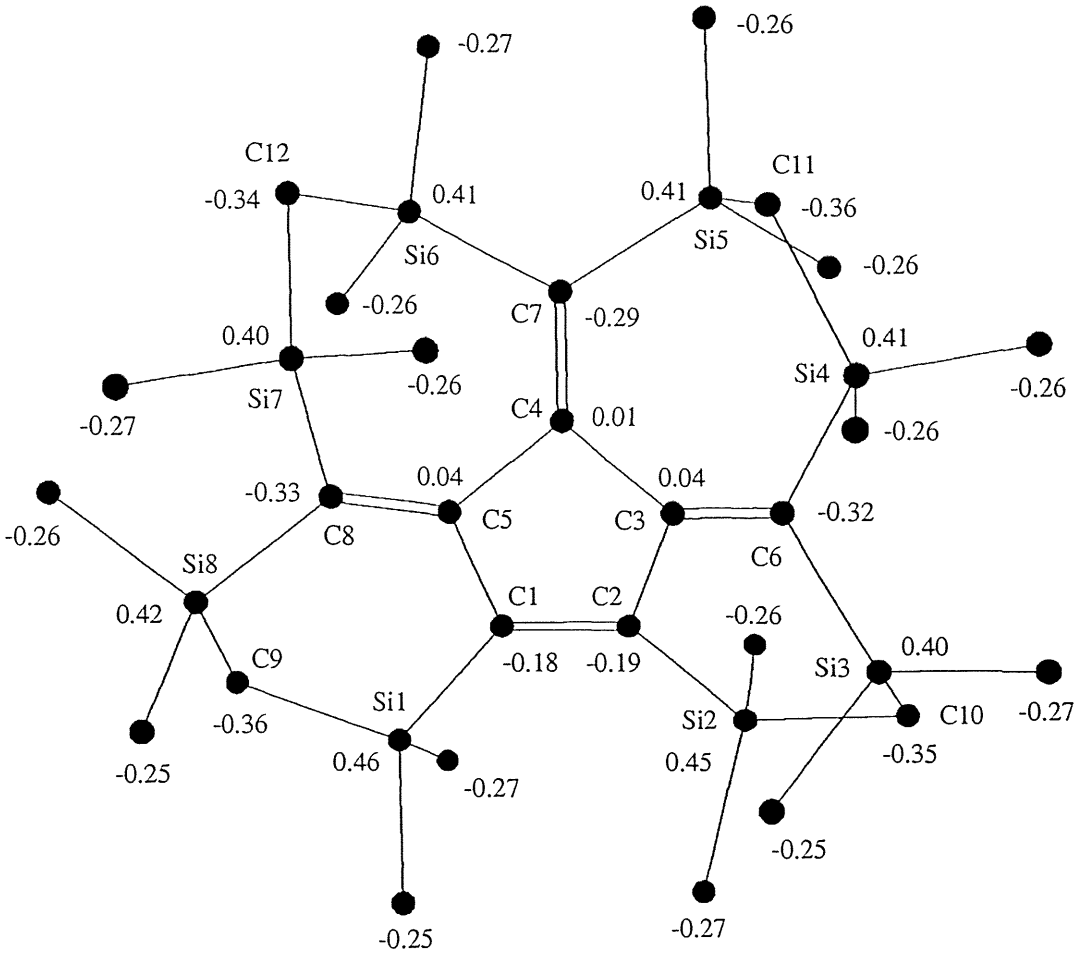

Figure 5-11. Mulliken charge distribution of **25** calculated by PM3.

Cyclic Voltammetry of Octasilyltrimethylenecyclopentene 25

The cyclic voltammetry of **25** in acetonitrile is shown in Figure 5-15. The irreversible reduction peak was observed at -1.38 V (vs. SCE) as a very broad peak. The reduction potential of **25** is close to that of silyl-substituted ethylene derivatives (e.g. –1.20 V for tetrakis(trimethylsilyl)ethylene and -1.22 V for 2,2,2',2',5,5,5',5'-octamethyl-2,2',5,5'-tetrasilabicyclopentylidene). The broad peak potential of **25** suggests the possibility of the multiple reduction. Thus, the four electron reduction is reasonably anticipated by means of the MO calculation and the electrochemistry of **25**.

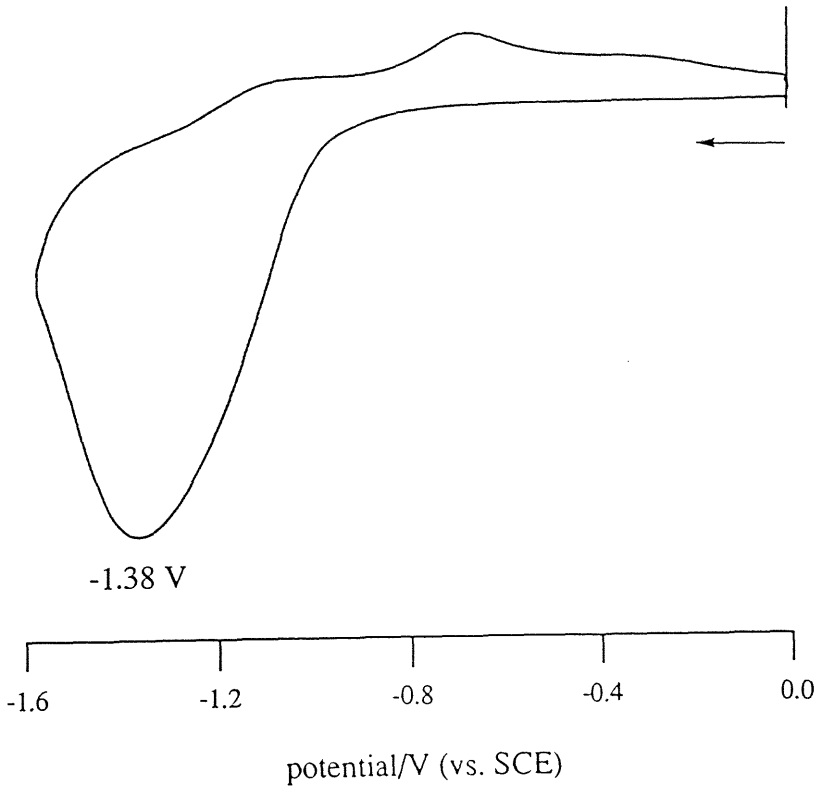

Figure 5-15. Cyclic voltammetry of 25 in acetonitrile (scan rate: 200 mVs^{-1}; conditions: room temperature, under argon).

Four Electron Reduction of Octasilyltrimethylenecyclopentene 25 with Lithium Metal

Reduction of **25** with excess lithium metal in dry oxygen-free THF at room temperature led to the formation of an orange solution of the tetraanion of **25** (Scheme 5-5). The reaction completed within 1 hour. The solvent was removed in vacuo, and then dry degassed hexane was introduced by vacuum transfer. Crystallization from hexane afforded air and moisture sensitive pale orange crystals of the tetralithium salt of octasilyltrimethylenecyclopentene tetraanion (**26**) containing four molecules of THF. The structure of **26** was unequivocally confirmed by NMR spectroscopy and X-ray crystallography. Several attempts to obtain dianion dilithium of **25** by two electron reduction failed due to the facile four electron reduction.

Scheme 5-5

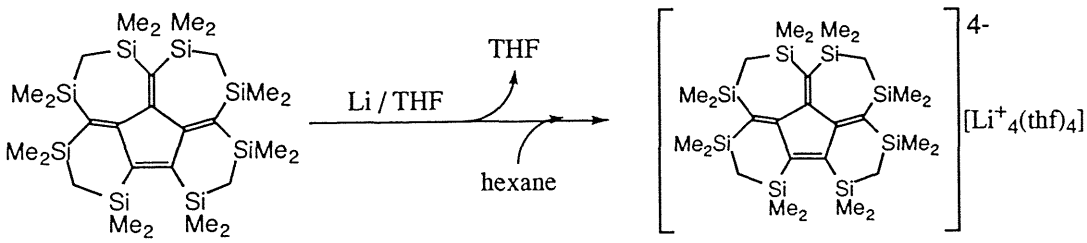

25 **26**

Molecular Structure of Tetralithium Octasilyltrimethylenecyclopentene Tetraanion 26

Figure 5-16 shows the molecular structure of **25**, which was confirmed by X-ray diffraction. The tetralithium **26** has a monomeric structure and forms contact ion pair (CIP) in the crystals. The ORTEP drawing of **26** is also shown in Figure 5-17. The structure shows that the molecule has C_2 symmetry and C1-C2 bond is a crystallographic 2-fold axis. The crystal packing of **26** is shown in Figure 5-18. The final atomic parameters of **3** are listed in Tables 5-6 and 5-7. The atomic distances of **26** are summarized in Tables 5-8 and 5-9. The bond angles of **26** are also summarized in Table 5-10.

Several interesting features of the structures of **26** can be pointed out. One THF molecule is coordinated to each lithium atom. Li1 and Li1* are located above and below the center of the five-membered ring (η^5-coordination). The selected bond lengths of **26** are shown in Figure 5-19. The distances between Li1 and the five-membered carbon atoms (C2, C3, C4, C4*, and C3*) range from 2.132(7) to 2.335(7) Å (av 2.234 Å), which are somewhat longer than those of lithium pentakis(dimethylsilyl)cyclopentadienide [$(Ph_2C{=}O)Li{\cdot}\{C_5(SiMe_2H)_5\}$] (av 2.186 Å).[7] Li2 and Li2* are bonded to the two exocyclic carbon atoms (C1, C6 and C1, C6*) (μ^2-coordination).

A comparison of the structural parameters of **25** and **26** is quite interesting. Eight carbon atoms of the π-skeleton of **26** become completely coplanar by the four electron reduction. The C3-C6, C3*-C6*, and C1-C2 distances in **26** are between 0.179 and 0.186 Å (av 0.182 Å) which are longer than the corresponding distances in **25**. In addition, the C4-C4* distance in **26** is elongated by 0.098 Å. By contrast, the C3-C4, C3*-C4*, C2-C3, and C2*-C3* distances in **26** are between 0.042 and 0.080 Å (av 0.062 Å) which are shorter than those in **25**. That is, the C-C double bonds in **25** are elongated, whereas the C-C single bonds are shortened by the reduction. Therefore, the

geometry of **26** reflects the nature of the LUMO and next LUMO of **26** (Figures 5-13 and 5-14).

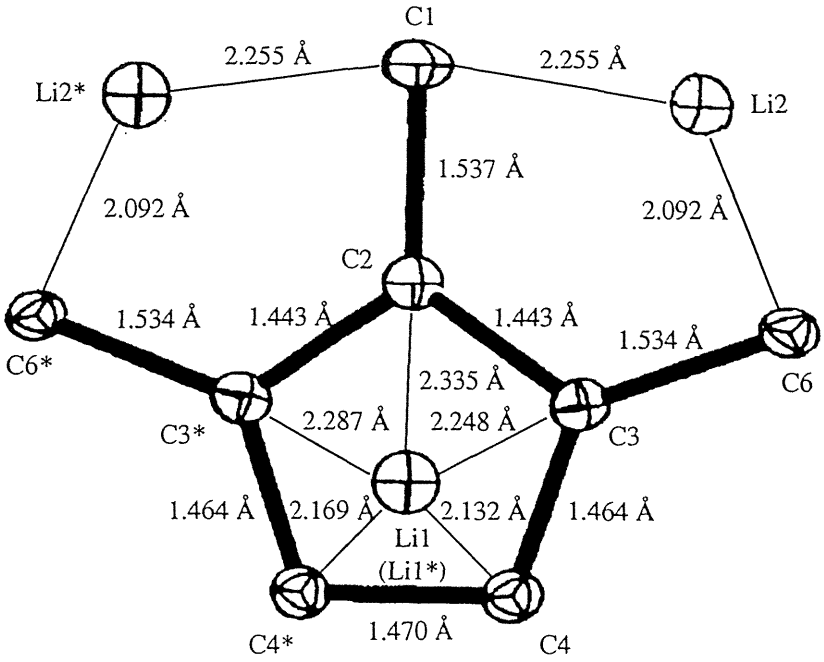

Figure 5-19. Selected bond lengths of **26**.

The selected bond angles and lengths of **26** are shown in Figures 5-20 and 5-21. The five-membered ring is planar and forms an almost equilateral pentagon, as determined by the internal bond angles of 107.4(2)-108.8(4)° (av 108.0°) and the sum of the bond angles (540.0°). The C-C distances of the five-membered ring are 1.443(5)-1.470(7) Å (av 1.457 Å). The bond lengths of the Si-C bonds (C1-Si1, 1.832(3); C6-Si2, 1.809(4); C6-Si3, 1.832(4) Å) of **26** are remarkably shortened compared to those of **25** (1.900(6), 1.893(6), and 1.889(6), respectively), due to the delocalization of the negative charge onto the silicon centers by $p\pi$-σ^* conjugation. The bond lengths of the Si-C (Si-Me and Si-CH_2) bonds of **26** are slightly elongated (about 0.01 Å) relative to those of **2**. The X-ray diffraction data indicate that the structure of **26** is a stable, closed-shell supercharged tetraanion, which is stabilized not only by the eight silicon atoms but also by the aromatic cyclopentadienyl anion.

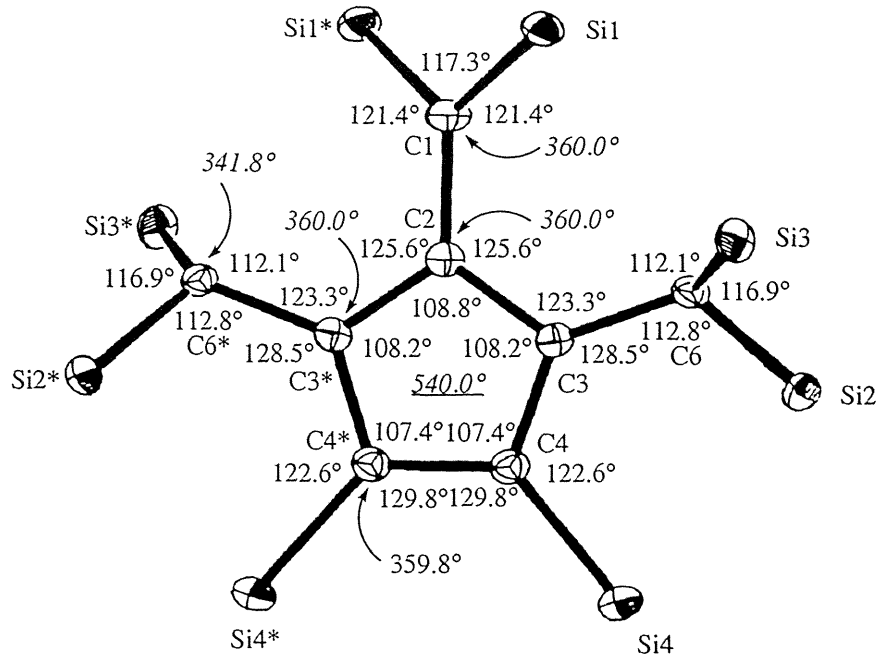

Figure 5-20. Selected bond angles of **26**.

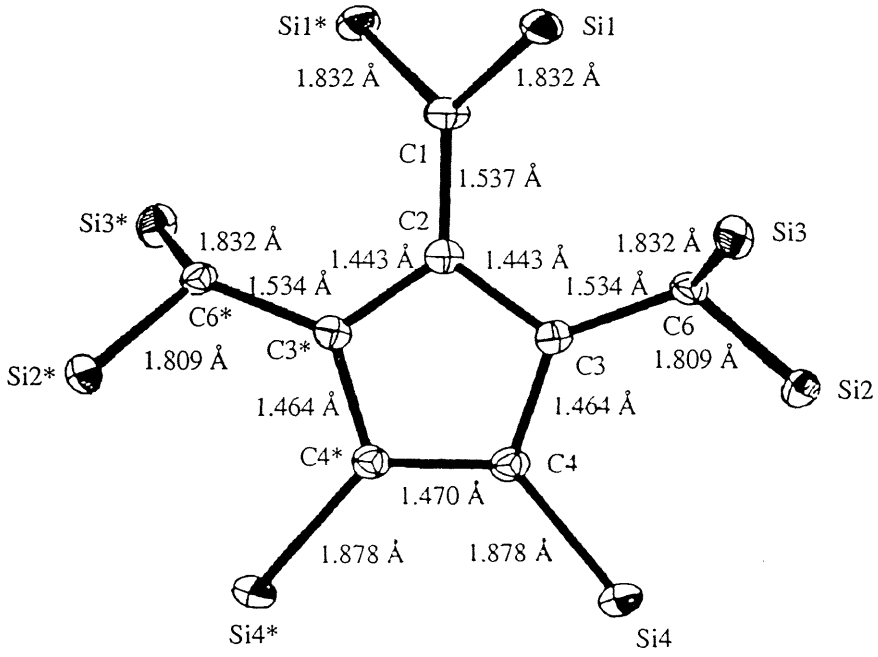

Figure 5-21. Selected bond lengths of **26**.

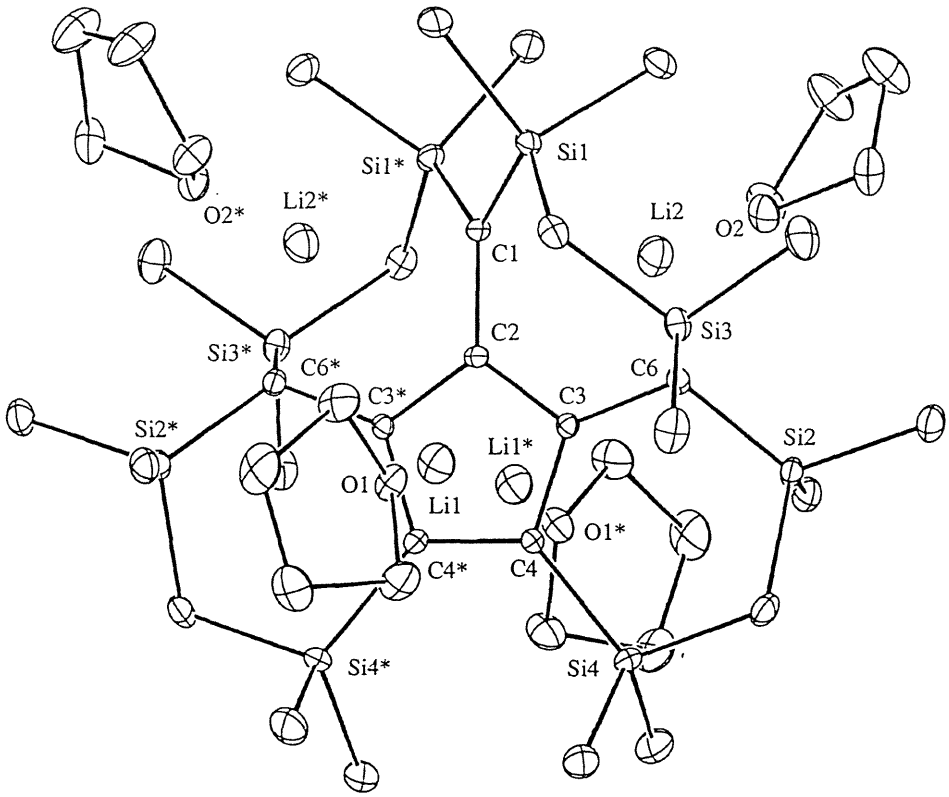

Figure 5-16. ORTEP drawing of **26** (hydrogen atoms are omitted for the clarity).

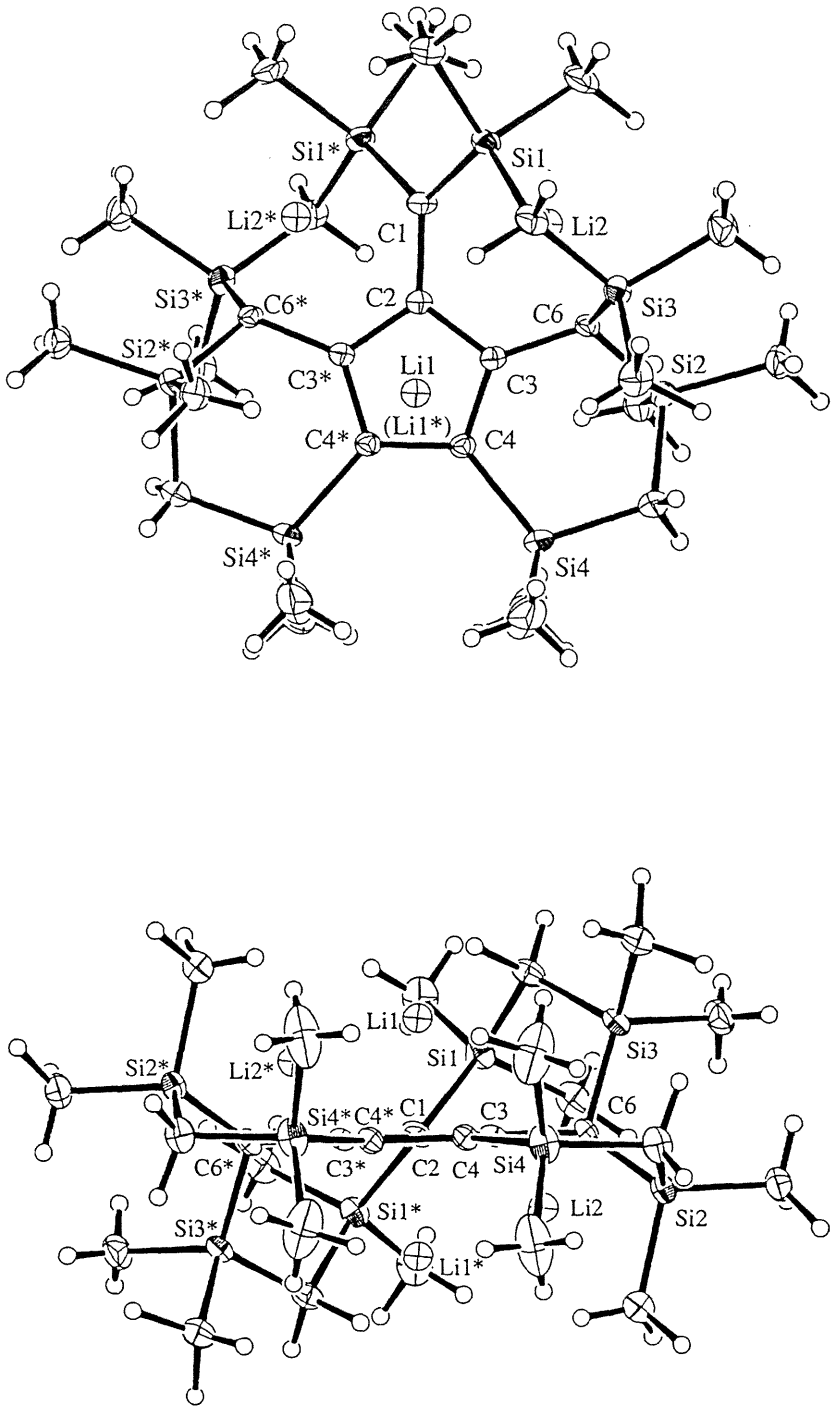

Figure 5-17. ORTEP drawing of **26** (THF molecules are omitted for the clarity): upper, top view; below, side view.

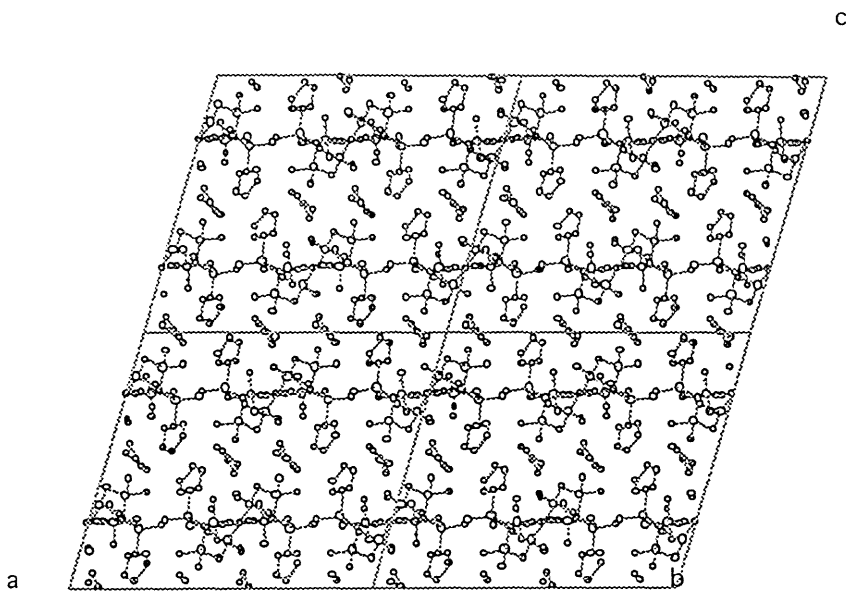

Figure 5-18. Crystal packing of **26**.

Table 5-6. Atomic Parameters for Non-Hydrogen Atoms of **26**

Atom	X/a	Y/b	Z/c	U(iso)
Si1	0.47980(5)	-0.04685(9)	0.81787(6)	0.0333(3)
Si2	0.32678(5)	0.26585(9)	0.72852(6)	0.0317(3)
Si3	0.40089(5)	0.13406(9)	0.85608(5)	0.0330(3)
Si4	0.41750(6)	0.45633(9)	0.75741(7)	0.0422(3)
O1	0.5635(1)	0.3027(2)	0.9419(1)	0.0425(8)
O2	0.3345(1)	0.0000(3)	0.6225(1)	0.0459(9)
C1	0.5000	0.0310(4)	0.7500	0.031(1)
C2	0.5000	0.1564(4)	0.7500	0.024(1)
C3	0.4511(2)	0.2249(3)	0.7574(2)	0.0237(9)
C4	0.4695(2)	0.3389(3)	0.7550(2)	0.0271(10)
C5	0.3434(2)	0.4066(4)	0.7649(3)	0.041(1)
C6	0.3917(2)	0.1800(3)	0.7672(2)	0.0259(9)
C7	0.4711(2)	0.0479(4)	0.8874(2)	0.038(1)
C8	0.5342(3)	-0.1588(4)	0.8575(3)	0.053(2)
C9	0.4069(2)	-0.1284(4)	0.7879(3)	0.047(1)
C10	0.3110(2)	0.2803(4)	0.6317(2)	0.044(1)
C11	0.2531(2)	0.2185(4)	0.7413(3)	0.044(1)
C12	0.4096(2)	0.2453(5)	0.9240(2)	0.051(1)
C13	0.3353(2)	0.0515(5)	0.8673(3)	0.049(1)
C14	0.3971(3)	0.5403(6)	0.6760(5)	0.102(2)
C15	0.4484(3)	0.5531(6)	0.8290(5)	0.102(3)
C16	0.5934(3)	0.2317(5)	0.9967(3)	0.067(2)
C17	0.6422(3)	0.2968(6)	1.0446(3)	0.084(2)
C18	0.6275(3)	0.4127(6)	1.0243(3)	0.089(2)
C19	0.5669(3)	0.4076(5)	0.9751(3)	0.081(2)
C20	0.3276(2)	-0.0157(4)	0.5497(2)	0.054(1)
C21	0.2904(3)	-0.1203(5)	0.5298(3)	0.072(2)
C22	0.2644(3)	-0.1401(5)	0.5891(3)	0.077(2)
C23	0.2792(2)	-0.0420(5)	0.6332(2)	0.057(2)
Li1	0.5319(3)	0.2725(6)	0.8452(3)	0.035(2)
Li2	0.3992(3)	0.0518(6)	0.7016(3)	0.036(2)

Table 5-7. Atomic Parameters for Hydrogen Atoms of **26**

Atom	X/a	Y/b	Z/c	U(iso)
H1	0.476(2)	0.009(4)	0.932(2)	0.06(1)
H2	0.513(2)	0.095(3)	0.904(2)	0.023(10)
H3	0.345(2)	0.399(4)	0.816(2)	0.05(1)
H4	0.317(2)	0.452(4)	0.741(2)	0.05(1)
H5	0.574(2)	-0.137(4)	0.877(2)	0.06(1)
H6	0.534(2)	-0.201(4)	0.833(2)	0.04(1)
H7	0.526(2)	-0.193(4)	0.901(3)	0.08(2)
H8	0.405(2)	-0.164(4)	0.820(2)	0.05(1)
H9	0.407(2)	-0.175(4)	0.755(2)	0.05(1)
H10	0.362(2)	-0.078(4)	0.763(2)	0.05(1)
H11	0.345(2)	0.299(3)	0.619(2)	0.04(1)
H12	0.294(2)	0.227(4)	0.609(2)	0.06(2)
H13	0.273(2)	0.340(4)	0.606(2)	0.07(1)
H14	0.259(2)	0.221(4)	0.791(2)	0.04(1)
H15	0.243(2)	0.154(4)	0.728(2)	0.06(2)
H16	0.215(2)	0.268(4)	0.710(2)	0.07(2)
H17	0.424(2)	0.204(4)	0.975(3)	0.07(2)
H18	0.443(2)	0.284(4)	0.930(2)	0.06(2)
H19	0.360(2)	0.286(4)	0.911(3)	0.08(2)
H20	0.343(2)	0.004(4)	0.895(2)	0.04(1)
H21	0.323(2)	0.005(4)	0.828(2)	0.06(2)
H22	0.304(2)	0.096(4)	0.874(2)	0.07(2)
H23	0.427(3)	0.574(5)	0.669(3)	0.09(2)
H24	0.378(4)	0.500(8)	0.639(5)	0.21(5)
H25	0.373(4)	0.593(8)	0.683(4)	0.18(4)
H26	0.487(3)	0.580(5)	0.839(3)	0.10(2)
H27	0.457(2)	0.516(4)	0.874(2)	0.03(1)
H28	0.416(3)	0.601(5)	0.821(3)	0.08(2)
H29	0.6092	0.1680	0.9794	0.0844
H30	0.5647	0.2038	1.0205	0.0844
H31	0.6819	0.2762	1.0403	0.1033
H32	0.6440	0.2839	1.0928	0.1033
H33	0.6562	0.4450	1.0034	0.1035
H34	0.6275	0.4584	1.0639	0.1035
H35	0.5607	0.4666	0.9414	0.0958
H36	0.5356	0.4162	0.9984	0.0958
H37	0.3667	-0.0218	0.5410	0.0683
H38	0.3070	0.0456	0.5231	0.0683
H39	0.3156	-0.1803	0.5229	0.0903
H40	0.2584	-0.1120	0.4869	0.0903
H41	0.2835	-0.2043	0.6159	0.0942
H42	0.2217	-0.1545	0.5743	0.0942
H43	0.2841	-0.0561	0.6803	0.0691
H44	0.2472	0.0119	0.6175	0.0691

Table 5-8. List of Atomic Distances (Å) for Non-Hydrogen Atoms of **26**

Atom	Atom	Length(sig)
Si(1)	C(1)	1.832(3)
Si(1)	C(7)	1.874(4)
Si(1)	C(8)	1.873(5)
Si(1)	C(9)	1.894(5)
Si(2)	C(5)	1.871(4)
Si(2)	C(6)	1.809(4)
Si(2)	C(10)	1.890(5)
Si(2)	C(11)	1.872(5)
Si(3)	C(6)	1.832(4)
Si(3)	C(7)	1.878(4)
Si(3)	C(12)	1.902(5)
Si(3)	C(13)	1.880(5)
Si(4)	C(4)	1.878(4)
Si(4)	C(5)	1.852(5)
Si(4)	C(14)	1.880(7)
Si(4)	C(15)	1.847(7)
O(1)	C(16)	1.420(6)
O(1)	C(19)	1.441(6)
O(1)	Li(1)	1.913(7)
O(2)	C(20)	1.445(5)
O(2)	C(23)	1.440(6)
O(2)	Li(2)	1.951(7)
C(1)	C(2)	1.537(7)
C(1)	Li(2)	2.255(7)
C(1)	Li(2)	2.255(7)
C(2)	C(3)	1.443(5)
C(2)	C(3)	1.443(5)
C(2)	Li(1)	2.335(7)
C(2)	Li(1)	2.334(7)
C(3)	C(4)	1.464(5)
C(3)	C(6)	1.533(5)
C(3)	Li(1)	2.247(7)
C(3)	Li(1)	2.287(8)
C(4)	C(4)	1.469(7)
C(4)	Li(1)	2.132(7)
C(4)	Li(1)	2.169(8)
C(6)	Li(2)	2.092(8)
C(16)	C(17)	1.486(8)
C(17)	C(18)	1.490(10)
C(18)	C(19)	1.462(9)
C(20)	C(21)	1.529(7)
C(21)	C(22)	1.502(7)
C(22)	C(23)	1.476(7)

Table 5-9. List of Bond Lengths (Å) for Hydrogen Atoms of **26**

Atom	Atom	Length(sig)
C(5)	H(3)	1.03(4)
C(5)	H(4)	0.86(4)
C(7)	H(1)	0.99(5)
C(7)	H(2)	1.09(4)
C(8)	H(5)	0.92(5)
C(8)	H(6)	0.72(4)
C(8)	H(7)	1.04(5)
C(9)	H(8)	0.79(5)
C(9)	H(9)	0.87(5)
C(9)	H(10)	1.19(4)
C(10)	H(11)	0.92(4)
C(10)	H(12)	0.83(5)
C(10)	H(13)	1.15(5)
C(11)	H(14)	0.97(4)
C(11)	H(15)	0.84(5)
C(11)	H(16)	1.11(5)
C(12)	H(17)	1.11(5)
C(12)	H(18)	0.87(5)
C(12)	H(19)	1.19(5)
C(13)	H(20)	0.78(4)
C(13)	H(21)	0.94(5)
C(13)	H(22)	0.94(5)
C(14)	H(23)	0.86(6)
C(14)	H(24)	0.89(10)
C(14)	H(25)	0.90(9)
C(15)	H(26)	0.92(6)
C(15)	H(27)	0.98(4)
C(15)	H(28)	0.92(6)
C(16)	H(29)	0.967
C(16)	H(30)	0.982
C(17)	H(31)	0.973
C(17)	H(32)	0.972
C(18)	H(33)	0.964
C(18)	H(34)	0.975
C(19)	H(35)	0.973
C(19)	H(36)	0.970
C(20)	H(37)	0.963
C(20)	H(38)	0.965
C(21)	H(39)	0.969
C(21)	H(40)	0.968
C(22)	H(41)	0.984
C(22)	H(42)	0.955
C(23)	H(43)	0.941
C(23)	H(44)	0.972

Table 5-10. List of Bond Angles (Å) for Non-Hydrogen Atoms of **26**

Atom	Atom	Atom	Angle(sig)
C(1)	Si(1)	C(7)	109.8(2)
C(1)	Si(1)	C(8)	114.9(2)
C(1)	Si(1)	C(9)	115.1(2)
C(7)	Si(1)	C(8)	109.5(2)
C(7)	Si(1)	C(9)	107.1(2)
C(8)	Si(1)	C(9)	99.8(2)
C(5)	Si(2)	C(6)	108.4(2)
C(5)	Si(2)	C(10)	106.0(2)
C(5)	Si(2)	C(11)	108.9(2)
C(6)	Si(2)	C(10)	113.1(2)
C(6)	Si(2)	C(11)	115.1(2)
C(10)	Si(2)	C(11)	104.9(2)
C(6)	Si(3)	C(7)	110.6(2)
C(6)	Si(3)	C(12)	116.3(2)
C(6)	Si(3)	C(13)	114.2(2)
C(7)	Si(3)	C(12)	104.8(2)
C(7)	Si(3)	C(13)	107.2(2)
C(12)	Si(3)	C(13)	102.9(2)
C(4)	Si(4)	C(5)	110.7(2)
C(4)	Si(4)	C(14)	113.5(3)
C(4)	Si(4)	C(15)	114.1(3)
C(5)	Si(4)	C(14)	104.1(3)
C(5)	Si(4)	C(15)	107.8(3)
C(14)	Si(4)	C(15)	106.0(4)
C(16)	O(1)	C(19)	103.6(4)
C(16)	O(1)	Li(1)	129.3(4)
C(19)	O(1)	Li(1)	126.9(4)
C(20)	O(2)	C(23)	104.9(3)
C(20)	O(2)	Li(2)	135.5(3)
C(23)	O(2)	Li(2)	119.4(3)
Si(1)	C(1)	Si(1)	117.3(3)
Si(1)	C(1)	C(2)	121.4(1)
Si(1)	C(1)	Li(2)	86.3(2)
Si(1)	C(1)	Li(2)	100.5(2)
Si(1)	C(1)	C(2)	121.4(1)
Si(1)	C(1)	Li(2)	100.5(2)
Si(1)	C(1)	Li(2)	86.3(2)
C(2)	C(1)	Li(2)	83.5(2)
C(2)	C(1)	Li(2)	83.5(2)
Li(2)	C(1)	Li(2)	167.0(4)
C(1)	C(2)	C(3)	125.6(2)
C(1)	C(2)	C(3)	125.6(2)
C(1)	C(2)	Li(1)	127.6(2)
C(1)	C(2)	Li(1)	127.5(2)
C(3)	C(2)	C(3)	108.8(4)

Table 5-10 (continued). List of Bond Angles (Å) for Non-Hydrogen Atoms of **26**

Atom	Atom	Atom	Angle(sig)
C(3)	C(2)	Li(1)	68.4(3)
C(3)	C(2)	Li(1)	70.0(3)
C(3)	C(2)	Li(1)	70.0(3)
C(3)	C(2)	Li(1)	68.4(3)
Li(1)	C(2)	Li(1)	104.9(4)
C(2)	C(3)	C(4)	108.2(3)
C(2)	C(3)	C(6)	123.3(3)
C(2)	C(3)	Li(1)	75.0(2)
C(2)	C(3)	Li(1)	73.6(2)
C(4)	C(3)	C(6)	128.5(3)
C(4)	C(3)	Li(1)	66.3(3)
C(4)	C(3)	Li(1)	66.5(3)
C(6)	C(3)	Li(1)	123.8(3)
C(6)	C(3)	Li(1)	126.5(3)
Li(1)	C(3)	Li(1)	109.4(3)
Si(4)	C(4)	C(3)	122.6(3)
Si(4)	C(4)	C(4)	129.8(1)
Si(4)	C(4)	Li(1)	123.2(3)
Si(4)	C(4)	Li(1)	118.1(3)
C(3)	C(4)	C(4)	107.4(2)
C(3)	C(4)	Li(1)	74.8(3)
C(3)	C(4)	Li(1)	75.2(3)
C(4)	C(4)	Li(1)	71.4(3)
C(4)	C(4)	Li(1)	68.7(3)
Li(1)	C(4)	Li(1)	118.7(3)
Si(2)	C(5)	Si(4)	111.2(2)
Si(2)	C(6)	Si(3)	116.9(2)
Si(2)	C(6)	C(3)	112.8(2)
Si(2)	C(6)	Li(2)	111.6(3)
Si(3)	C(6)	C(3)	112.1(2)
Si(3)	C(6)	Li(2)	112.3(3)
C(3)	C(6)	Li(2)	87.3(3)
Si(1)	C(7)	Si(3)	111.1(2)
O(1)	C(16)	C(17)	106.6(5)
C(16)	C(17)	C(18)	105.3(5)
C(17)	C(18)	C(19)	104.1(5)
O(1)	C(19)	C(18)	105.6(5)
O(2)	C(20)	C(21)	105.7(4)
C(20)	C(21)	C(22)	104.2(4)
C(21)	C(22)	C(23)	105.8(4)
O(2)	C(23)	C(22)	105.3(4)
O(1)	Li(1)	C(2)	153.6(4)
O(1)	Li(1)	C(3)	147.3(4)
O(1)	Li(1)	C(3)	149.2(4)
O(1)	Li(1)	C(4)	139.8(4)

Table 5-10 (continued). List of Bond Angles (Å) for Non-Hydrogen Atoms of **26**

Atom	Atom	Atom	Angle(sig)
O(1)	Li(1)	C(4)	141.0(4)
C(2)	Li(1)	C(3)	36.6(1)
C(2)	Li(1)	C(3)	36.4(1)
C(2)	Li(1)	C(4)	63.4(2)
C(2)	Li(1)	C(4)	62.9(2)
C(3)	Li(1)	C(3)	62.3(2)
C(3)	Li(1)	C(4)	39.0(2)
C(3)	Li(1)	C(4)	64.7(2)
C(3)	Li(1)	C(4)	64.6(2)
C(3)	Li(1)	C(4)	38.2(2)
C(4)	Li(1)	C(4)	39.9(2)
O(2)	Li(2)	C(1)	139.9(4)
O(2)	Li(2)	C(6)	125.6(4)
C(1)	Li(2)	C(6)	94.0(3)

PM3 Calculation of Octasilyltrimethylenecyclopentene Tetraanion 25^{4-}

The geometry optimization of octasilyltrimethylenecyclopentene tetraanion $\mathbf{25}^{4-}$ (counter ion free) was also carried out by PM3 calculation.[6] The calculated structure of $\mathbf{25}^{4-}$ is shown in Figure 5-22. The geometry of $\mathbf{25}^{4-}$ calculated by PM3 is close to that of tetralithium octasilyltrimethylenecyclopentene tetraanion **26** by the X-ray diffraction. Some differences between crystal structure and calculated structure may be due to the existence of counter lithium cation and THF ligands. The selected bond angles and lengths of $\mathbf{25}^{4-}$ calculated by PM3 are shown in Figures 5-23 and 5-24. The charge distribution of $\mathbf{25}^{4-}$ is also shown in Figure 5-25.

Comparison of the calculated parameters of **25** and $\mathbf{25}^{4-}$ is also interesting. The change of bond lengths by four electron reduction is wellreproduced by PM3 calculation. The C-C single and double bond lengths of **25** calculated by PM3 are 1.482-1.498 Å (av 1.492 Å) and 1.332-1.350 Å (av 1.337 Å), respectively. Those of $\mathbf{25}^{4-}$ are 1.426-1.444 Å (av 1.435 Å) and 1.416-1.432 Å (av 1.424 Å), respectively. The Si-C(sp^2) single bond lengths of $\mathbf{25}^{4-}$ calculated by PM3 are 1.739-1.798 Å (av 1.768 Å), which are shorter than those of **25** (1.826-1.854 Å (av 1.841 Å)) due to the $p\pi$-σ^* conjugation.

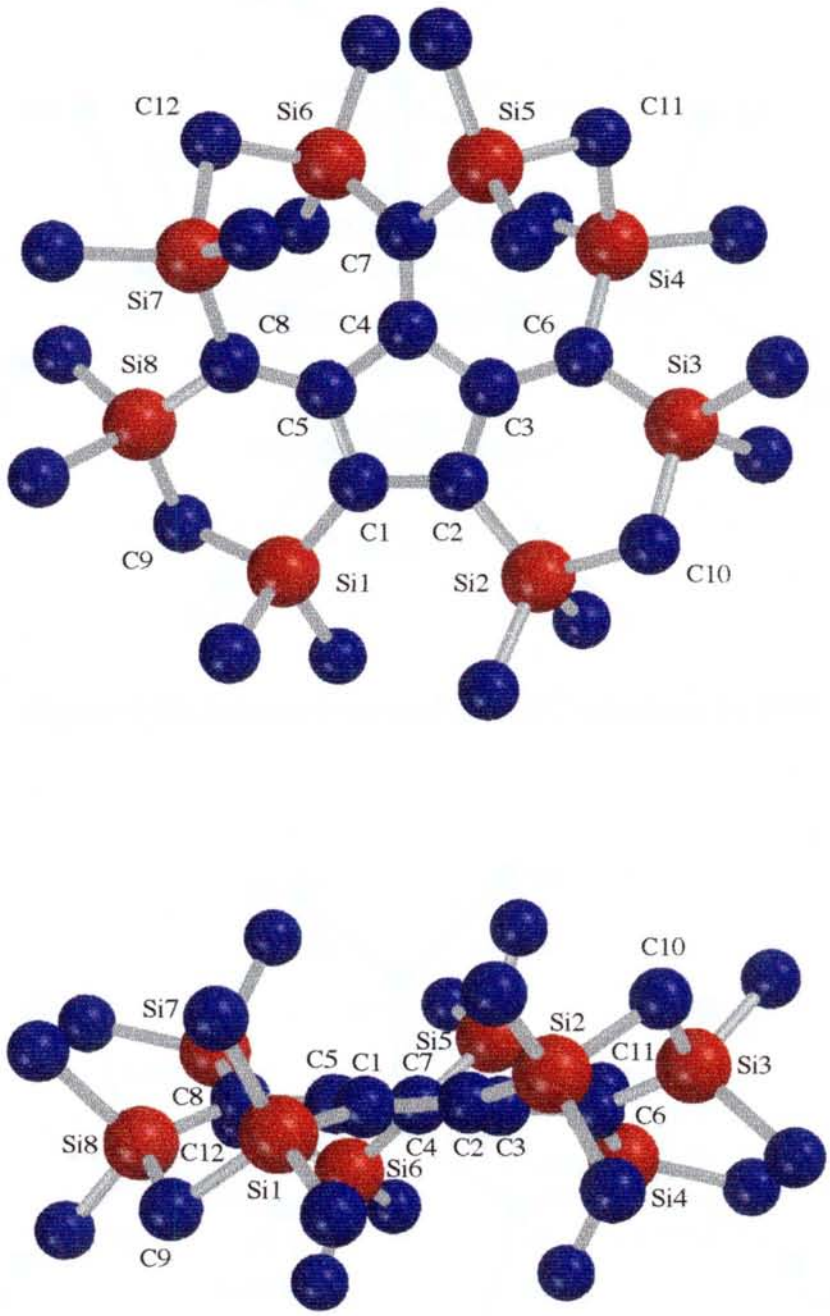

Figure 5-22. Calculated structure of $\mathbf{25}^{4-}$ by PM3 (hydrogen atoms are omitted for the clarity): upper, top view; below, side view.

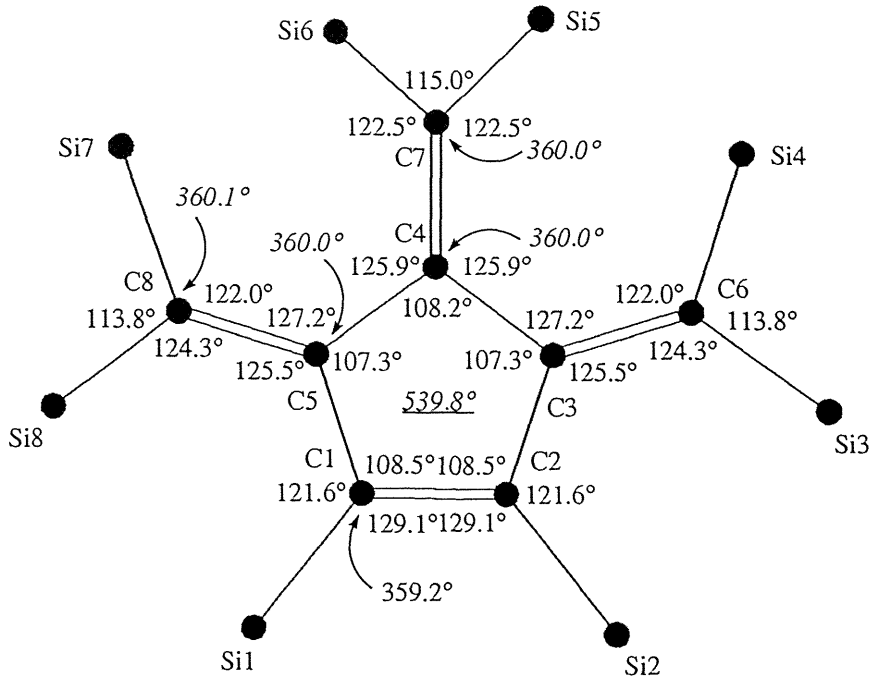

Figure 5-23. Selected bond angles of 25^{4-} calculated by PM3.

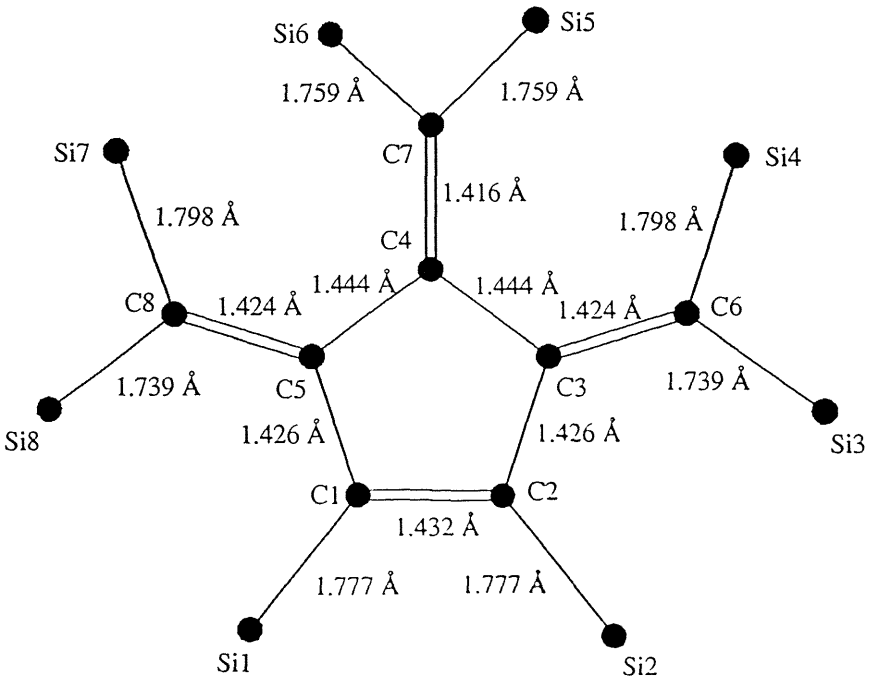

Figure 5-24. Selected bond lengths of 25^{4-} calculated by PM3.

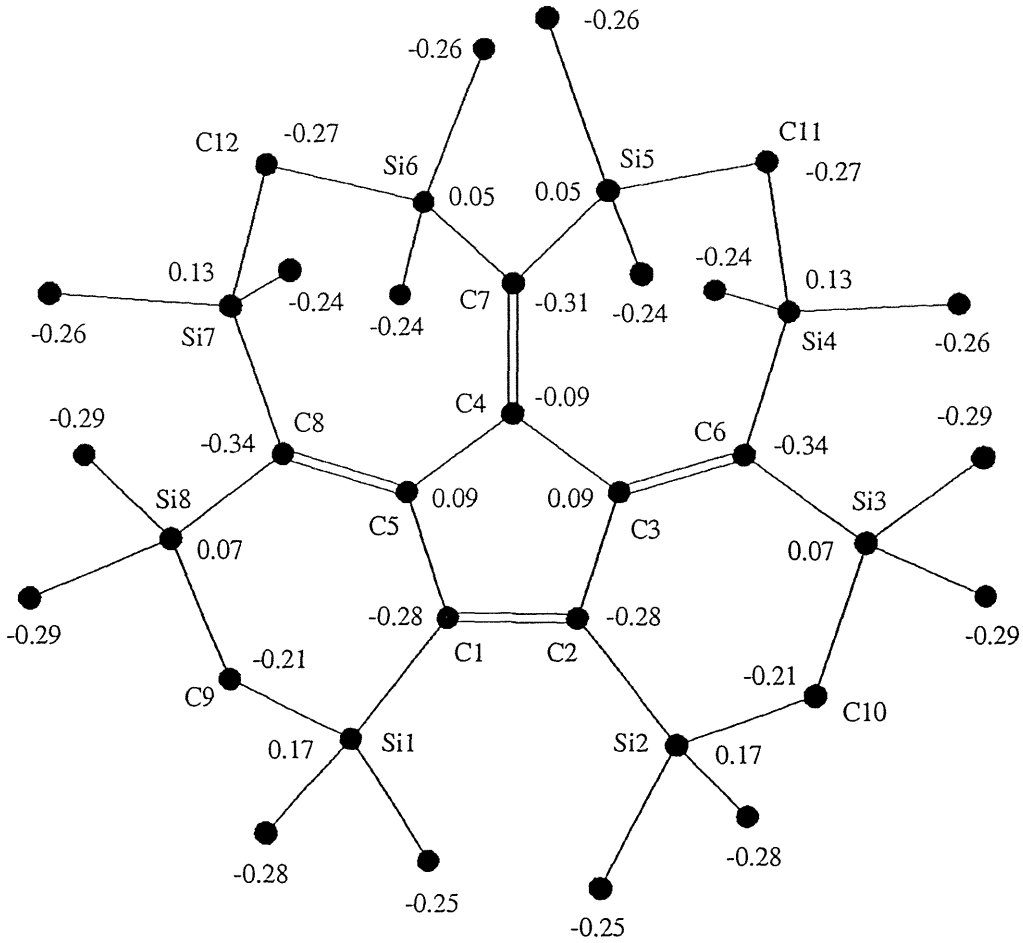

Figure 5-25. Mulliken charge distribution of 25^{4-} calculated by PM3

Structure of Tetralithium Octasilyltrimethylenecyclopentene Tetraanion 26 in Benzene-d_6

The structure of **26** in benzene-d_6 was deduced by ^1H, ^{13}C, ^{29}Si, and ^6Li NMR spectroscopies. The two methyl groups of $SiMe_2$ and two hydrogen atoms of CH_2 were magnetically nonequivalent due to the fixed six- or seven-membered ring, as well as due to the coordination of lithiums. Thus, in the ^1H NMR spectrum of **26** in benzene-d_6, eight sets of methyl groups and four sets of doublet signals of methylene groups with the geminal couplings (13.2 and 13.7 Hz) were found. In the ^{29}Si NMR spectrum, four sets of signals were observed at -16.1, -15.1, -14.5, and -13.2 ppm, shifted to upper field relative to those of **25**. In the ^{13}C NMR spectrum, five sets of quaternary carbon atoms were found at 9.62, 19.7, 107.0, 132.1, and 148.2 ppm. The signal appearing at 19.7 ppm splits into a triplet ($J^{13}C\text{-}^6Li$ = 6.2 Hz) due to the coupling with one ^6Li (I = 1) (Figure 5-26), whereas the signal at 9.62 ppm splits into a quintet ($J^{13}C\text{-}^6Li$ = 2.3 Hz) due to the coupling with two equivalents ^6Li (Figure 5-27). Thus, the triplet signal is assigned to C6 and C6* carbons, and the quintet signal is assigned to C1 carbon. It is apparent that the negative charge is largely delocalized of the three exocyclic carbon atoms (C1, C6, and C6*) in the π-skeleton of **26**, as evidenced by the ^{13}C NMR spectral data. These carbons are remarkably shifted to upper field by 169.3 ppm for C1 and 152.9 ppm for C6 and C6* relative to those of **25**.

Interestingly, the ^6Li NMR spectrum of **26** yielded two signals appearing at -6.27 and 2.47 ppm with the same intensity as shown in Figure 5-28. The appreciable upfield shift at -6.27 ppm is evidently caused by the strong shielding effect by the diamagnetic ring current resulting from the 6π aromatic system. The ^6Li NMR chemical shift (δ = –6.27) is close to that of lithium pentakis(dimethylsilyl)cyclopentadienide [$(Ph_2C{=}O)Li{\cdot}\{C_5(SiMe_2H)_5\}$] (δ = –7.51).[7] Thus, this ^6Li signal is reasonably assigned to Li1 and Li1*, locating at the center of the five-membered ring. On the other hand, the satellite

signal due to the coupling with ^{13}C was observed for the signal of 2.47 ppm ($J^{13}C$–^{6}Li = 6.2 Hz) as shown in Figure 5-29. This ^{6}Li signal is reasonably assigned to Li2 and Li2*, which bonded to the two exocyclic carbon atoms. Thus, the molecular structure of **26** found in the crystals is maintained in non-polar solvents such as benzene-d_6 and toluene-d_8 to give a contact ion pair (CIP).

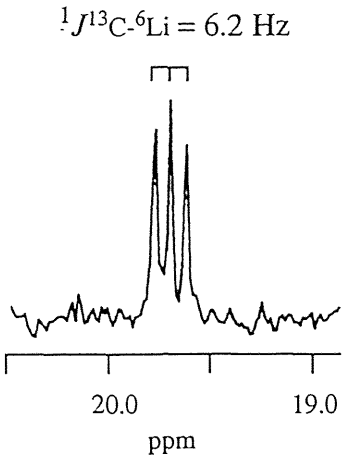

Figure 5-26. 19.6 ppm signal of ^{13}C NMR of **26** in benzene-d_6 at 298 K.

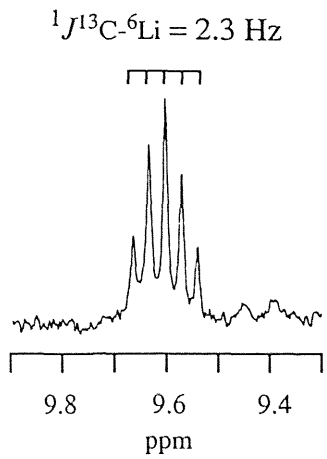

Figure 5-27. 9.62 ppm signal of ^{13}C NMR of **26** in benzene-d_6 at 298 K.

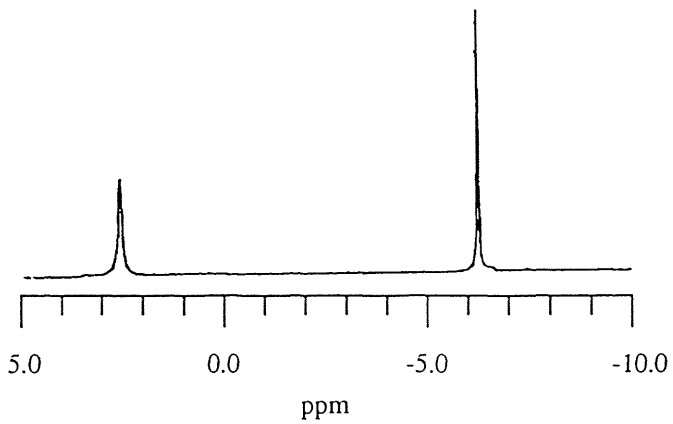

Figure 5-28. ^{6}Li NMR of **26** in benzene-d_6 at 298 K.

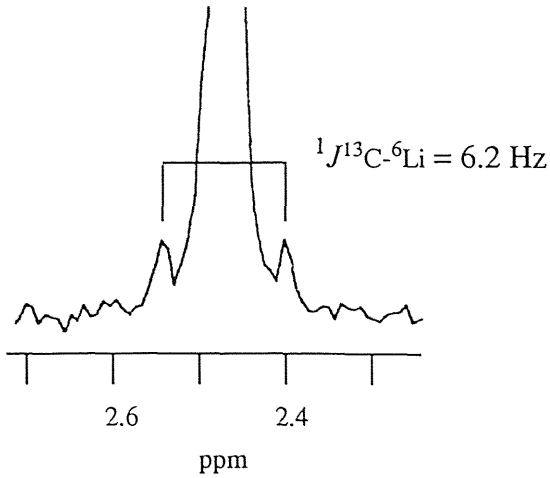

Figure 5-29. 2.47 ppm signal of ^6Li NMR of **26** in benzene-d_6 at 298 K

Structure of Tetralithium Octasilyltrimethylenecyclopentene Tetraanion 26 in THF-d_8

The structure in a solvating media such as THF-d_8, is quite different from that found in non-polar solvents. In ^6Li NMR of **26** in THF-d_8, four signals were observed at -6.56, -0.37, 0.17 and 1.72 ppm with the same intensity as shown in Figure 5-30. The exchange between the four ^6Li signals did not occur even at 60 °C. The satellite signals due to the coupling with ^{13}C were observed for the signals of 0.17 ($J^{13}C$–^6Li = 4.7 Hz) and 1.72 ppm ($J^{13}C$–^6Li = 5.7 Hz), assignable to the Li^+ ion bonded to the π-skeleton (Figures 5-31 and 5-32). It should be noted that none of the satellite signals for -6.56 and -0.37 ppm were found. The ^6Li signal at -6.56 ppm is reasonably assigned to the Li^+ ion located above the cyclopentadienide ring. The chemical shift and the lack of the satellite signals due to ^{13}C suggest that the ^6Li NMR at -0.37 ppm is assignable to the THF solvated species, $[Li^+(thf)_n]$. The signal at δ = -0.37, which is assigned to the solvated Li^+ ion, becomes more intense on addition of ^6LiBr due to the rapid exchange. However, the intensity of the other three signals at δ = -6.56, 0.17, and 1.72 for the Li^+ ions of the

CIP remain unchanged because these ions are bounded to the π-electron system. Thus, one of the two Li^+ ions (either Li1 or Li1*) above the cyclopentadienide ring is dissociated to yield a solvent separated ion pair (SSIP) in a solvating media such as THF-d_8.

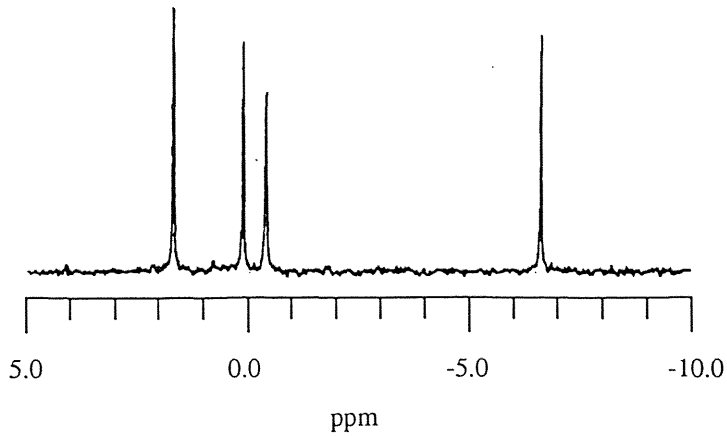

Figure 5-30. ^{6}Li NMR of **26** in THF-d_8 at 298 K.

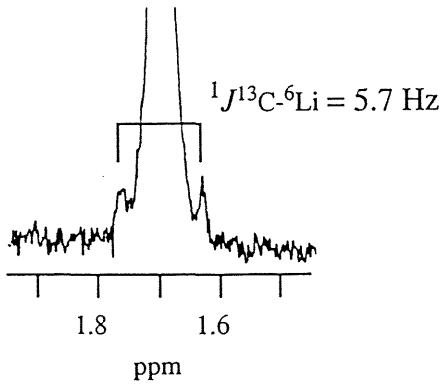

Figure 5-31. 1.72 ppm signal of ^{6}Li NMR of **26** in THF-d_8 at 298 K.

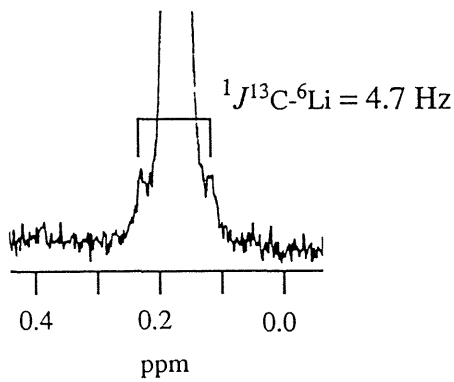

Figure 5-32. 0.17 ppm signal of ^{6}Li NMR of **26** in THF-d_8 at 298 K.

In ^{1}H and ^{13}C NMR spectra of the tetraanion **26** in THF-d_8, sixteen different protons and carbons due to $SiMe_2$ can be observed because of the lack of the symmetry. Four different methylene carbons can also be found. In the ^{13}C NMR spectrum, eight sets of quaternary carbon atoms were found at 8.54, 17.2, 19.1, 108.5, 109.8, 127.9, 139.2, and 143.0 ppm. The signals appearing at 17.2 and 19.1 ppm split into a triplet ($J^{13}C\text{-}^{6}Li$ = 5.7 and 4.7 Hz) due to the coupling with one ^{6}Li (I = 1), respectively (Figures 5-33 and 5-34). The signal at 8.54 ppm splits into a multiplet due to the coupling with two nonequivalent ^{6}Li. Thus, the triplet signals are assigned to C6 and C6* carbons, and the multiplet signal is assigned to C1 carbon. In the ^{29}Si NMR spectrum, eight different signals can be seen at -19.2, -17.1, -15.9, -15.7, -15.2, -14.5, -11.8, and -11.1 ppm.

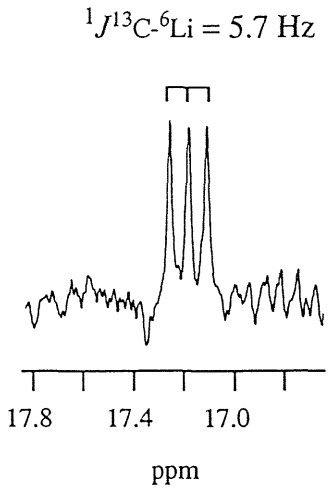

Figure 5-33. 17.2 ppm signal of ^{13}C NMR of **26** in THF-d_8 at 298 K.

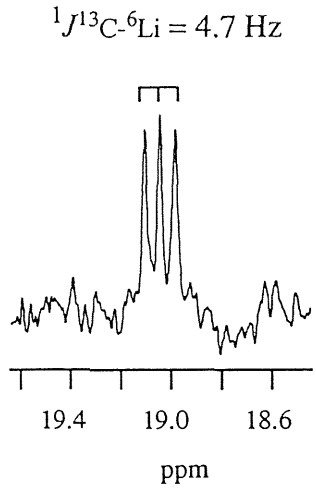

Figure 5-34. 19.1 ppm signal of ^{13}C NMR of **26** in THF-d_8 at 298 K.

Experimental Section

General Methods

^{1}H NMR spectra were recorded on a Bruker AC-300 FT spectrometer. ^{13}C, ^{29}Si, and ^{6}Li NMR spectra were collected on a Bruker AC-300 at 75.5, 59.6, and 44.2 MHz, respectively. ^{6}Li NMR spectra are referenced to 1 M LiCl (1 M = 1 mol dm^{-3}) in methanol / benzene-d_6 or 1 M LiCl in THF-d_8. Mass spectra were obtained on a Shimadzu QP-1000. Electronic spectra were recorded on a Shimadzu UV-2100 spectrometer. Cyclic voltammetry was carried out with a conventional CV cell with a platinum disk as a working electrode, a platinum wire as a counter electrode, and a saturated calomel electrode as a reference electrode in acetonitrile. A Hokuto HA501 Potentiostat/Galvanostat, a Hokuto HB 104 Function Generator, and a YEW Model XY recorder were used for the measurement. Commercially available anhydrous lithium perchlorate (Kishida Kagaku Chameleon Reagent) as a supporting electrolyte was used as received. The sampling of **26** for X-ray crystallography was carried out by using a Giken Engineering Service GBX-1200 gas-replacement type glove box.

Materials

Tetrahydrofuran and hexane were dried and distilled from sodium benzophenone ketyl. These solvents were further dried and degassed over a potassium mirror in vacuo prior to use. Benzene-d_6 and THF-d_8 were dried over molecular sieves, and then transferred into a tube covered with potassium mirror prior to use. Lithium-6 (95 atom%) metal was commercially available (Aldrich Chemical Company). 3,3,5,5,8,8,10,10,13,13,15,15,18,18,20,20-hexadecamethyl-3,5,8,10,13,15,18,20-octasilacycloicosa-1,6,11,16-tetrayne (**14**) was prepared as described in Chapter 3.

Preparation of Octasilyltrimethylenecyclopentene (25)

A mixture of 3,3,5,5,8,8,10,10,13,13,15,15,18,18,20,20-hexadecamethyl-3,5,8,10,13,15,18,20-octasilacycloicosa-1,6,11,16-tetrayne (**14**) (201 mg, 0.33 mmol) and $[Mn(CO)_3(Me\text{-}Cp)]$ (93 mg, 0.43 mmol) in THF (30 ml) was irradiated with a 500 W high-pressure mercury lamp for 5 h through the cutoff filter ($\lambda > 300$ nm) under the refluxing temperature of THF. After removal of the manganese complex, the reaction mixture was chromatographed on silica gel to produce pale yellow crystals of **2** in 17% yield. mp 229–230 °C. ^1H NMR (C_7D_8) δ = -0.28 (d, J = 13.4 Hz, 2 H, CH_2), -0.16 (d, J = 13.4 Hz, 2 H, CH_2), 0.05 (s, 6 H, CH_3), 0.05 (d, J = 13.6 Hz, 2 H, CH_2), 0.18 (s, 6 H, CH_3), 0.21 (s, 6 H, CH_3), 0.23 (s, 6 H, CH_3), 0.26 (s, 6 H, CH_3), 0.29 (s, 6 H, CH_3), 0.30 (s, 6 H, CH_3), 0.31 (s, 6 H, CH_3), 0.43 (d, J = 13.6 Hz, 2 H, CH_2); ^{13}C NMR ($CDCl_3$) δ = 1.00 (CH_3), 1.13 (CH_3), 1.76 (CH_2), 2.54 (CH_3), 3.52 (CH_3), 3.69 (CH_3), 3.99 (CH_3), 4.77 (CH_3), 6.45 (CH_3), 12.0 (CH_2), 134.1 (C), 135.7 (C), 158.6 (C), 172.6 (C), 178.9 (C); ^{29}Si NMR ($CDCl_3$) δ = -13.3, -10.2, –10.0, -9.14; UV (hexane) λ_{max} /nm (ε) 229 (19500), 268 (15500), 309 (11000), 351 (5600). Found: C, 54.37; H 9.35%. Calcd for $C_{28}H_{56}Si_8$: C, 54.47; H 9.14 %.

X-ray Crystallography of Octasilyltrimethylenecyclopentene (25)

Single crystal of **25** for X-ray diffractions was grown from an ethanol solution. The X-ray crystallographic experiment of **25** was performed on a Rigaku-Denki AFC 5R diffractometer equipped with graphite-monochromatized Mo-$K\alpha$ radiation (λ = 0.71069 Å). Crystal data for **25** at 150 K: MF = $C_{28}H_{56}Si_8$, MW = 617.43, monoclinic, a = 16.194(7) Å, b = 11.963(3) Å, c = 19.581(2) Å, β = 97.94(2)°, V = 3757(2) Å^3, space group = $P2_1/a$, Z = 4, D_{calcd} = 1.091 g/cm^3. The final R factor was 0.0799 (R_w = 0.0914) for 6229 reflections with $F_o > 3\sigma(F_o)$. The details of the X-ray experiment are given in Table 5-11.

Table 5-11. Detail of the X-ray Experiment for **25**

molecular formula	$C_{28}H_{56}Si_8$
molecular weight	617.43
crystal system	monoclinic
space group	$P2_1/a$
cell constants	a = 16.194(7) Å, b = 11.963(3) Å, c = 19.581(2) Å, β = 97.94(2)°,
Z value	V = 3757(2) Å^3
D_{calcd}	4
μ (Mo $K\alpha$)	1.109 g cm^{-3}
crystal size	0.295 mm^{-1}
crystal shape	0.40 x 0.30 x 0.30 mm
crystal color	prism
diffractometer	pale yellow
radiation	Rigaku AFC-5R
	Mo$K\alpha$ (λ = 0.710690 Å)
temperature	graphite monochromatized rotating anode
2θ range	150 K
number of unique reflections	3 - 58°
number of used reflections	10452
number of parameters	6229 ($F > 3\sigma(F)$)
data correction	550
	Lorenz and polarization effects
structure analysis	no absorption, no extinction
refinement	direct method
temperature factors	block diagonal least squares methods
	anisotropic (C and Si)
$R = \sum \|\|F_o\| - \|F_c\|\| / \sum \|F_o\|$	isotropic (H, generated by calculation)
$R_w = [\sum w(\|F_o\| - \|F_c\|)^2 / \sum \|F_o\|^2]^{1/2}$	0.0799
	0.0914

Preparation of Tetralithium Octasilyltrimethylenecyclopentene Tetraanion (26).

The crystals of **25** (51 mg, 0.083 mmol) and lithium metal (30 mg, 4.3 mmol) were placed in a reaction tube with a magnetic stirrer. After degassing, dry oxygen-free THF (1.5 mL) was introduced by vacuum transfer and the mixture was stirred at room temperature to give an orange solution of the tetraanion of **25** within 1 h. After the solvent was removed in vacuo, degassed hexane was introduced by vacuum transfer. Then, after the lithium metal was removed, the solution was cooled to afford orange crystals of **26** quantitatively. ^{1}H NMR (C_6D_6) δ = -0.72 (d, J = 13.7 Hz, 2 H, CH_2), –0.20 (d, J = 13.7 Hz, 2 H, CH_2), 0.05 (s, 6 H, CH_3), 0.08 (s, 6 H, CH_3), 0.12 (d, J = 13.2 Hz, 2 H, CH_2), 0.29 (s, 6 H, CH_3), 0.34 (d, J = 13.2 Hz, 2 H, CH_2), 0.54 (s, 6 H, CH_3), 0.56 (s, 6 H, CH_3), 0.61 (s, 6 H, CH_3), 0.62 (s, 6 H, CH_3), 0.63 (s, 6 H, CH_3), 1.32 (br.s, 16 H, THF), 3.56 (br.s, 16 H, THF); ^{13}C NMR (C_6D_6) δ = 5.37 (CH_3), 5.67 (CH_3 X 2), 6.65 (CH_3), 6.90 (CH_3), 6.96 (CH_3), 7.37 (CH_3), 7.53 (CH_3), 9.20 (CH_2), 9.62 (quint, J^{13}C–^{6}Li = 2.3 Hz, C), 11.6 (CH_2), 19.7 (t, J^{13}C–^{6}Li = 6.2 Hz, C), 25.4 (THF), 68.9 (THF), 107.0 (C), 132.1 (C), 148.2 (C); ^{29}Si NMR (C_6D_6) δ = –16.1, -15.1, -14.5, -13.2; ^{6}Li NMR (C_6D_6) δ = -6.27, 2.47.

NMR Spectral Data of 26 in THF-d_8 at 298 K.

^{1}H NMR (THF-d_8) δ = -0.90 (d, J = 12.6 Hz, 1 H, CH_2), -0.74 (d, J = 12.6 Hz, 1 H, CH_2), -0.62 (d, J = 12.6 Hz, 1 H, CH_2), -0.46 (d, J = 12.6 Hz, 1 H, CH_2), -0.40 (d, J = 12.6 Hz, 1 H, CH_2), -0.36 (d, J = 12.3 Hz, 1 H, CH_2), -0.35 (d, J = 12.6 Hz, 1 H, CH_2), -0.26 (s, 3 H, CH_3), -0.24 (s, 3 H, CH_3), -0.23 (s, 3 H, CH_3), -0.22 (s, 3 H, CH_3), –0.11 (s, 3 H, CH_3), -0.08 (s, 3 H, CH_3), -0.01 (s, 3 H, CH_3), 0.01 (s, 3 H, CH_3), 0.04 (s, 3 H, CH_3), 0.05 (s, 3 H, CH_3), 0.12 (s, 3 H, CH_3), 0.16 (s, 3 H, CH_3), 0.20 (s, 6 H, CH_3 X 2), 0.22 (s, 3 H, CH_3), 0.27 (s, 3 H, CH_3); ^{13}C NMR

(THF-d_8) δ = 2.92 (CH_3), 6.02 (CH_3), 6.56 (CH_3), 6.92 (CH_3 X 2), 6.98 (CH_3), 7.56 (CH_3), 7.57 (CH_3), 7.58 (CH_3), 7.64 (CH_3), 8.18 (CH_3), 8.54 (m, CLi_2), 8.79 (CH_3), 8.92 (CH_3), 9.25 (CH_3), 9.59 (CH_3), 10.2 (CH_2), 10.8 (CH_3), 11.2 (CH_2), 11.5 (CH_2), 11.7 (CH_2), 17.2 (t, $J^{13}C-^{6}Li$ = 5.7 Hz, C), 19.1 (t, $J^{13}C-^{6}Li$ = 4.7 Hz, C), 108.5 (C), 109.8 (C), 127.9 (C), 139.2 (C), 143.0 (C); ^{29}Si NMR (THF-d_8) δ = -19.2, -17.1, -15.9, -15.7, -15.2, -14.5, -11.8, –11.1; ^{6}Li NMR (THF-d_8) δ = -6.56, -0.37, 0.17, 1.72. The assignment of ^{1}H and ^{13}C signals were performed by DEPT and C-H COSY experiments, indicating that one doublet signal of CH_2 (ca. -0.22 ppm) was obscured by overlapping signals of methyl groups.

X-ray Crystallography of Tetralithium Octasilyltrimethylenecyclopentene Tetraanion (26)

Single crystal of **26** for X-ray diffractions was grown from a hexane solution. The X-ray crystallographic experiment of **26** was performed on a Rigaku-Denki AFC 5R diffractometer equipped with graphite-monochromatized Cu-*K*α radiation (λ = 1.54718 Å). Crystal data for **26** at 286 K: MF = $C_{44}H_{88}Li_4O_4Si_8$, MW = 933.62, monoclinic, a = 22.94(1) Å, b = 12.257(4) Å, c = 20.164(7) Å, β = 106.49(3)°, V = 5435(3) $Å^3$, space group = *C*2/c, Z = 4, D_{calcd} = 1.141 g/cm^3. The final R factor was 0.0574 (R_w = 0.0650) for 3546 reflections with $I_o > 3\sigma(I_o)$. The details of the X-ray experiment are given in Table 5-12.

Molecular Orbital Calculations

PM3 calculations were performed by Power Macintosh 7600/200 with MACSPARTAN plus program (Ver. 1.1.7).[6] All the calculations were performed with geometry optimization.

Table 5-12. Detail of the X-ray Experiment for **26**

molecular formula	$C_{44}H_{88}Li_4O_4Si_8$
molecular weight	933.62
crystal system	monoclinic
space group	*C2/c*
cell constants	a = 22.94(1) Å, b = 12.257(4) Å,
	c = 20.164(7) Å, β = 106.49(3)°,
Z value	V = 5435(3) Å^3
D_{calcd}	4
μ (Cu $K\alpha$)	1.141 g cm^{-3}
crystal size	mm^{-1}
crystal shape	0.20 x 0.20 x 0.20 mm
crystal color	prism
diffractometer	orange
	Rigaku AFC-5R
temperature	Cu$K\alpha$ (λ = 1.54718 Å)
2θ range	graphite monochromatized rotating anode
number of unique reflections	283 K
number of used reflections	8 - 120°
number of parameters	4301
data correction	3546 ($I > 3\sigma(I)$)
	374
structure analysis	Lorenz and polarization effects
refinement	no absorption, no extinction
temperature factors	direct method
	block diagonal least squares methods
$R = \sum \|\|F_o\| - \|F_c\|\| / \sum \|F_o\|$	anisotropic (C, Li, O and Si)
$R_w = [\sum w(\|F_o\| - \|F_c\|)^2 / \sum \|F_o\|^2]^{1/2}$	isotropic (H generated by calculation)
	0.0574
	0.0650

References

(1) For reviews, see: (a) K. Müllen, *Chem. Rev.*, **84,** 603 (1984). (b) M. Rabinovitz, *Top. Curr. Chem.*, **14,** 99 (1988). (c) A. M. Sapse, P. v. R. Schleyer, "Lithium Chemistry: A Theoretical and Experimental Overview", Wiley, New York (1995).

(2) (a) O. Zhou, J. E. Fischer, N. Coustel, S. Kycia, Q. Zhu, A. R. McGhie, W. J. Romanow, J. P. McGauley Jr, A. B. Smith III, and D. E. Cox, *Nature,* **351,** 462 (1991). (b) R. Tycko, G. Dabbagh, M. J. Rosseinsky, D. W. Murphy, R. M. Fleming, A. P. Ramirez, and J. C. Tully, *Science,* **253,** 884 (1991).

(3) (a) A. Ayalon, M. Rabinovitz, P.-C. Cheng, and L. T. Scott, *Angew. Chem., Int. Ed. Engl.,* **31,** 1636 (1992). (b) A. Ayalon, A. Sygula, P.-C. Cheng, M. Rabinovitz, P. W. Radideau, and L. T. Scott., *Science,* **265,** 1065 (1994). (c) M. Baumgarten, L. Gherghel, M. Wagner, A. Weitz, M. Rabinovitz, P. W. Radideau, and L. T. Scott., *J. Am. Chem. Soc.*, **117,** 6254 (1995).

(4) H. Bock, K. Gharagozloo-Hubmann, C. Näther, N. Nagel, and Z. Havlas, *Angew. Chem., Int. Ed. Engl.*, **35,** 631 (1996).

(5) (a) H. Sakurai, *Nippon Kagaku Kaishi,* **1990,** 439. (b) H. Sakurai, *Pure Appl. Chem.*, **68,** 327 (1996). (c) H. Sakurai, T. Fujii, and K. Sakamoto, *Chem. Lett.*, **1992,** 339.

(6) J. J. P. Stewart, *J. Comput. Chem.*, **10,** 209 (1989).

(7) A. Sekiguchi, Y. Sugai, K. Ebata, C. Kabuto, and H. Sakurai, *J. Am. Chem. Soc.*, **115,** 1144 (1993).

Chapter 6

Silyl-Substituted [5]Radialene with 10C / 10π-Electron System

Summary

The intramolecular reaction of 3,3,6,6,8,8,11,11,14,14,16,16,19,19,21,21-hexadecamethyl-3,6,8,11,14,16,19,21-octasilacyclohenicosa-1,4,9,12,17-pentayne (**27**) with excess molar amount of $[Mn(CO)_3(Me\text{-}Cp)]$ in THF under photochemical and refluxing conditions produced persilylated [5]radialene derivative (**28**).

Introduction

Polyanion species have attracted considerable interest due to their structure and electronic properties, which were described in chapter 5. Polyanion species of π-electron systems have many interesting and important problems, delocalization of π-electrons, distribution of negative charge, formation of ion pairs, solvation of counter cation, and so on. The dynamic behavior of counter cation is also a notable subject on the polyanion species.

The author has revealed the structure and properties of fulvene dianion (chapter 4) and trimethylenecyclopentene tetraanion (chapter 5) in this dissertation. These anion species, which are based on five-membered ring, are nonbenzenoid aromatic compounds. The five-membered ring of these molecules become cyclopentadienide ion with 5C / 6π-electron system by the reduction, respectively. Especially, the aromatic stabilization of cyclopentadienide ion contributes to the formation of tetralithium salt of octasilyltrimethylenecyclopentene tetraanion despite the electrostatic repulsion of four negative charges.

On the other hand, dimethylenecyclobutene dianion (chapter 2) and [4]radialene dianion (chapter 3), which are based on four-membered ring, are nonaromatic compounds. The author has also revealed that the aromaticity of cyclobutadiene dianion is somewhat weaker than those of cyclopentadienide ion (chapter 1).

[5]Radialene (pentamethylenecyclopentane) possesses a very unique 10π-electron system based on five-membered ring. [5]Radialene has a particular arrangement with a high symmetric framework. [5]Radialene is also a moiety of corannulene ($C_{20}H_{10}$) and fullerene (C_{60}). Although there has been some papers on the anion species of both corannulene[1] and fullerene,[2] the anion species of [5]radialene is hitherto unknown.

Stable ten-component sandwich compounds have been characterized in which four lithium ions reside between two tetraanions derived from corannulene or its alkyl-substituted derivatives and four lithium ions decorate the exterior (Figure 6-1).[1b] In THF solution, the four lithium ions inside the sandwich can exchange environments with the four external lithium atoms, but the two tetraanion decks of sandwich never separate from each other on the NMR time scale. Theoretical calculations point to a "stacked bowl" conformation and a low energy barrier for synchronous double inversion of the tetraanion bowls in the solvated sandwich compounds (Figure 6-2).

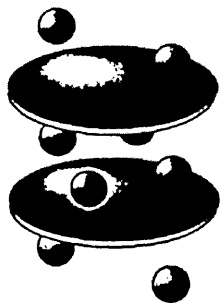

Figure 6-1. Formal representation of the side view of dimers from two corannulene tetraanion (disks) and eight lithium cations (balls).

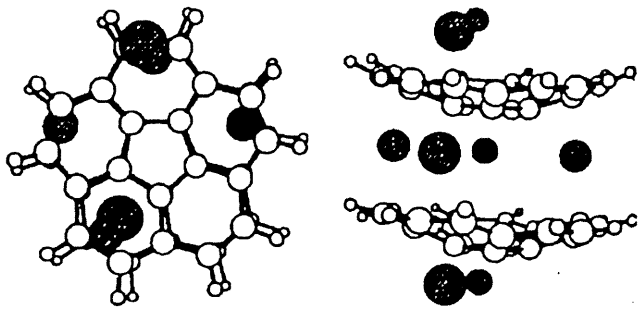

Figure 6-2. Minimum-energy geometry calculated (MNDO) for the corannulene^{4-} / 4 Li^{+} dimer.

In this chapter, synthesis and characterization of persilylated [5]radialene as a new silyl-substituted 10C / 10π-electron system as a precursor of the polyanion species are described.

Results and Discussion

Synthesis of Persilylated [5]Radialene 28

[5]Radialene (pentamethylenecyclopentane) has a special arrangement of 10π-electron. The synthetic methods of [5]radialene are very limited, and there are only a few reports on the synthesis of [5]radialene derivatives.[3] The author has demonstrated that the intramolecular cyclotrimerization of the silacyclotriynes with manganese complexes to give a variety of persilyl-substituted π-electron systems, such as dimethylenecyclobutene derivatives.[4] The author has also demonstrated that the silacyclotetrayne undergo the intramolecular cyclization by $[Mn(CO)_3(Me\text{-}Cp)]$ with the formation of persilylated [4]radialene and trimethylenecyclopentene with an eight π-electron system in chapters 3 and 5. All of these reactions involves the 1,2-silyl shift in the 1,2-disilyl-substituted acetylene to give 2,2-disilylvinylidene complexes as a reaction intermediate. The intriguing 1,2-silyl shift is a general reaction in cyclic and acyclic bissilylacetylene promoted by $[Mn(CO)_3(Me\text{-}Cp)]$ or $[Mn(CO)_3Cp]$.[5] The persilylated [5]radialene derivative (**28**) has been synthesized in a similar manner via the intramolecular cyclization of macrocyclic pentayne linked by disilmethylene ($Me_2SiCH_2SiMe_2$) and dimethylsilylene ($SiMe_2$) chains.

The precursor of 3,3,6,6,8,8,11,11,14,14,16,16,19,19,21,21-hexadecamethyl-3,6,8,11,14,16,19,21-octasilacyclohenicosa-1,4,9,12,17-pentayne (**27**) was prepared by the coupling reaction of 2,10-dichloro-2,5,5,7,7,10-hexamethyl-2,5,7,10-tetrasila-undeca-3,8-diyne with Grignard reagent prepared from 3,3,5,5,8,8,10,10-octamethyl-3,5,8,10-tetrasiladodeca-1,6,11-triyne and ethylmagnesium bromide in a satisfactory yield (Scheme 6-1).

Scheme 6-1

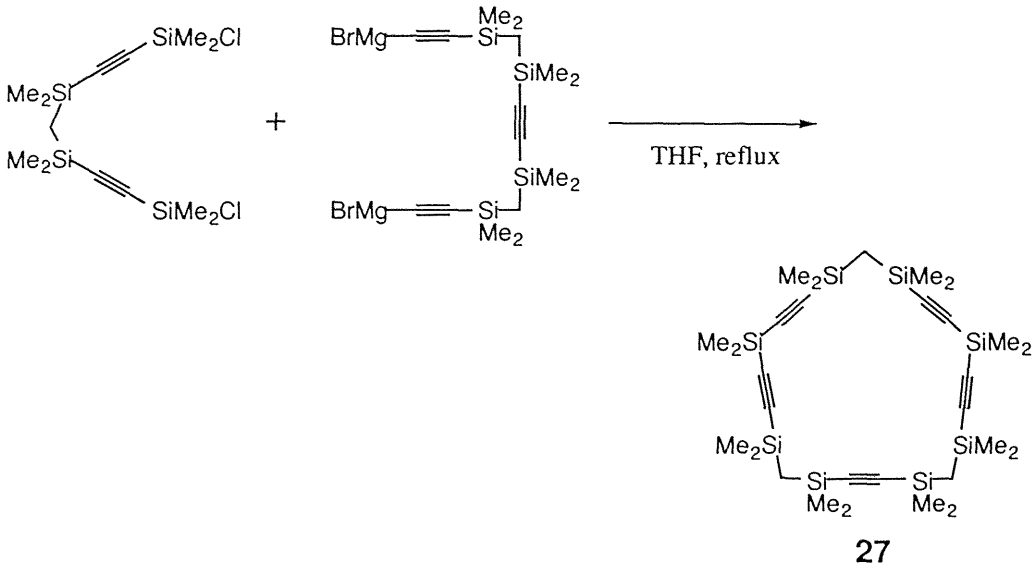

27

A mixture of macrocyclic pentayne **27** and a large molar excess of $[Mn(CO)_3(Me\text{-}Cp)]$ in THF was irradiated with a 500 W high-pressure mercury lamp under the refluxing temperature of THF to produce orange crystals of the persilylated [5]radialene derivative (**28**) in 2.3% yield (Scheme 6-2).

Scheme 6-2

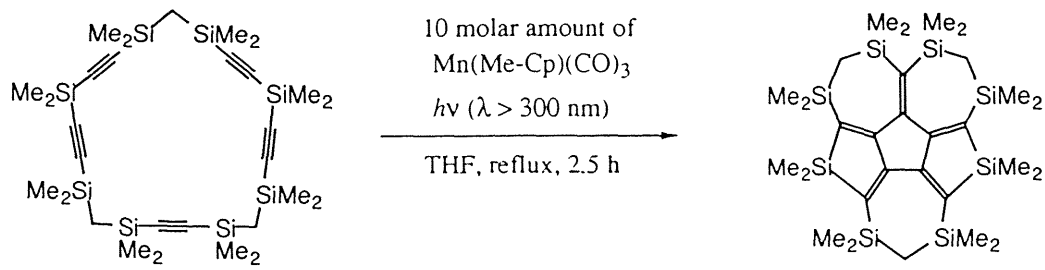

27 28

The reaction mechanism remains unclear at this moment; nevertheless, a quintuple 1,2-silyl shift must be involved in the formation of **28**. The 1,2-silyl shift was accelerated by heat, and no radialene compounds were furnished at room temperature. The possible mechanism is shown in Scheme 6-3. However, the use of one molar amount of the manganese complexes resulted in a formation of the dimethylenecyclobutene derivative (**29**) as pale yellow crystals in 15% yield (Scheme 6-4). The products are reflected by the equivalent of manganese complexes for **27**. The same results were given by using $[Mn(CO)_3(Cp)]$.

Scheme 6-4

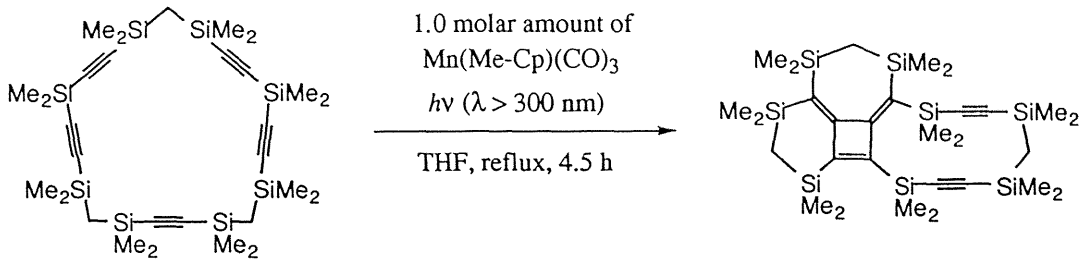

27 **29**

Oligomerization of acetylene, catalyzed by transition metal complexes, is a very important class of reactions to lead to benzene as a trimer and cyclooctatetraene as a tetramer.[6] Although the isolated yield is low, persilylated [5]radialene **28** is a first manner of the cyclopentamerization of acetylene units. Compounds **28** and **29** were fully characterized by NMR spectroscopy.

Scheme 6-3

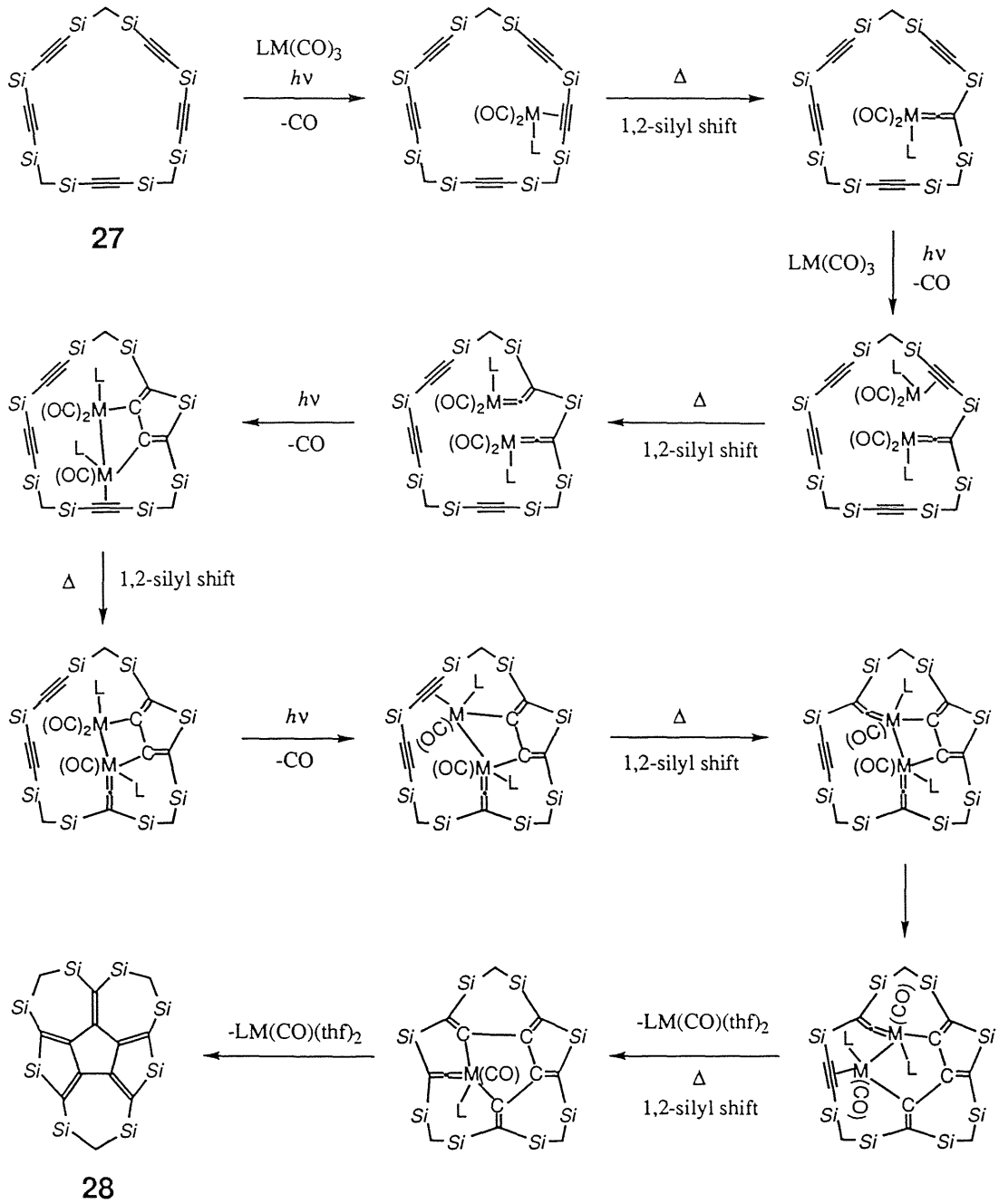
LM(CO)3
hν
-CO
Δ
1,2-silyl shift
27
28
-LM(CO)(thf)2
LM(CO)3 = (Me-Cp)Mn(CO)3
Si = SiMe2

Experimental Section

General Methods

^{1}H NMR spectra were recorded on a Bruker AC-300 FT spectrometer. ^{13}C and ^{29}Si NMR spectra were collected on a Bruker AC-300 at 75.5 and 59.6 MHz, respectively. Mass spectra were obtained on a Shimadzu QP-1000. Electronic spectra were recorded on a Shimadzu UV-2100 spectrometer.

Materials

Tetrahydrofuran and hexane were dried and distilled from sodium benzophenone ketyl.

Preparation of 3,3,6,6,8,8,11,11,14,14,16,16,19,19,21,21-hexadecamethyl-3,6,8,11,14,16,19,21-octasilacyclohenicosa-1,4,9,12,17-pentayne (27)

3,3,5,5,8,8,10,10-octamethyl-3,5,8,10-tetrasiladodeca-1,6,11-triyne (10.04 g, 0.030 mol) in THF (20 ml) was added to a THF solution of ethylmagnesium bromide (180 ml, 0.067 mol) to produce the Grignard reagent. The THF solution of the resulting Grignard reagent and 2,10-dichloro-2,5,5,7,7,10-hexamethyl-2,5,7,10-tetrasilaundeca-3,8-diyne (10.97 g, 0.030 mol) in THF (180 ml) were added dropwise slowly to refluxing THF (500 ml). After the addition, the reaction mixture was heated overnight. The mixture was poured in hexane and hydrolyzed with dilute hydrochloric acid, followed by extraction with hexane. The organic layer was washed with water and dried over anhydrous sodium sulfate. After evaporation of the solvent, the residue was distilled under reduced pressure to give the crude pentayne (27) (120-200 °C / 0.1 mmHg,

Kugelrohr distillation). Recrystallization from ethanol gave pure colorless crystals of **27** in 39% yield. mp 68–69 °C. ^{1}H NMR ($CDCl_3$) δ = 0.00 (s, 4 H, CH_2), 0.03 (s, 2 H, CH_2), 0.22 (s, 12 H, CH_3), 0.25 (s, 24 H, CH_3), 0.28 (s, 12 H, CH_3); ^{13}C NMR ($CDCl_3$) δ = 0.1 (CH_3), 0.9 (CH_3 x 2), 1.0 (CH_3), 3.2 (CH_2 x 2), 110.1 (C), 110.2 (C), 114.8 (C), 115.7 (C x 2); ^{29}Si NMR ($CDCl_3$) δ = -42.7, -19.6, -18.9, -18.8; UV (hexane) λ_{max} /nm (ε) 209 (5800), 218 (3900). Found: C, 55.03; H 8.79%. Calcd for $C_{29}H_{54}Si_8$: C, 55.52; H 8.67 %.

Preparation of Persilylated [5]radialene (28)

A mixture of 3,3,6,6,8,8,11,11,14,14,16,16,19,19,21,21-hexadecamethyl-3,6,8,11,14,16,19,21-octasilacyclohenicosa-1,4,9,12,17-pentayne (**27**) (400 mg, 0.64 mmol) and [$Mn(CO)_3$(Me-Cp)] (1396 mg, 6.40 mmol) in THF (35 ml) was irradiated with a 500 W high-pressure mercury lamp for 2.5 h through the cutoff filter (λ > 300 nm) under the refluxing temperature of THF. After removal of the manganese complex, the reaction mixture was chromatographed on silica gel to produce orange crystals of **28** in 2.3% yield. mp 140–142 °C. ^{1}H NMR ($CDCl_3$) δ = 0.10 (s, 2 H, CH_2), 0.13 (s, 12 H, CH_3), 0.14 (s, 12 H, CH_3), 0.15 (s, 12 H, CH_3), 0.29 (s, 12 H, CH_3), 0.29 (s, 4 H, CH_2); ^{13}C NMR ($CDCl_3$) δ = -2.3 (CH_3), 1.1 (CH_3), 1.5 (CH_3), 3.0 (CH_3), 4.9 (CH_2), 11.7 (CH_2), 143.3 (C), 144.9 (C), 157.0 (C), 163.2 (C), 164.7 (C), 172.0 (C); ^{29}Si NMR ($CDCl_3$) δ = -12.0, -10.0, -8.4, 30.9; UV (hexane) λ_{max} /nm (ε) 264 (44600), 379 (2800), 428 (2700). Found: C, 55.28; H 8.68%. Calcd for $C_{29}H_{54}Si_8$: C, 55.52; H 8.67 %.

Preparation of Persilylated Dimethylenecyclobutene (29)

A mixture of 3,3,6,6,8,8,11,11,14,14,16,16,19,19,21,21-hexadecamethyl-3,6,8,11,14,16,19,21-octasilacyclohenicosa-1,4,9,12,17-pentayne (**27**) (198 mg, 0.316 mmol) and $[Mn(CO)_3(Me\text{-}Cp)]$ (69 mg, 0.316 mmol) in THF (35 ml) was irradiated with a 500 W high-pressure mercury lamp for 4.5 h through the cutoff filter (λ > 300 nm) under the refluxing temperature of THF. After removal of the manganese complex, the reaction mixture was chromatographed on silica gel to produce pale yellow crystals of **30** in 15% yield. mp 130-131 °C. ^1H NMR ($CDCl_3$) δ = -0.17 (s, 2 H, CH_2), -0.16 (s, 2 H, CH_2), 0.01 (s, 2 H, CH_2), 0.13 (s, 6 H, CH_3), 0.15 (s, 6 H, CH_3), 0.17 (s, 6 H, CH_3), 0.18 (s, 6 H, CH_3), 0.22 (s, 6 H, CH_3), 0.31 (s, 6 H, CH_3), 0.38 (s, 6 H, CH_3), 0.41 (s, 6 H, CH_3); ^{13}C NMR ($CDCl_3$) δ = 0.9 (CH_3), 1.1 (CH_2), 1.2 (CH_3), 1.7 (CH_3), 1.8 (CH_2), 2.7 (CH_3), 2.8 (CH_3), 3.2 (CH_3), 3.6 (CH_3), 3.7 (CH_3), 7.6 (CH_2), 114.5 (C), 116.1 (C x 2), 116.5 (C), 119.6 (C), 121.5 (C), 172.6 (C), 173.0 (C), 176.4 (C), 184.2 (C); ^{29}Si NMR ($CDCl_3$) δ = -33.7, -28.6, -19.3, –19.2, -16.5, –7.6, -6.8, -6.3; UV (hexane) λ_{max} /nm (ε) 250 (26500), 280 (sh. 9600), 324 (sh. 5100). Found: C, 55.44; H 8.92%. Calcd for $C_{29}H_{54}Si_8$: C, 55.52; H 8.67 %.

References

(1) (a) A. Ayalon, M. Rabinovitz, P.-C. Cheng, and L. T. Scott, *Angew. Chem., Int. Ed. Engl.*, **31,** 1636 (1992). (b) A. Ayalon, A. Sygula, P.-C. Cheng, M. Rabinovitz, P. W. Radideau, and L. T. Scott., *Science,* **265,** 1065 (1994). (c) M. Baumgarten, L. Gherghel, M. Wagner, A. Weitz, M. Rabinovitz, P. W. Radideau, and L. T. Scott., *J. Am. Chem. Soc.*, **117,** 6254 (1995).

(2) (a) O. Zhou, J. E. Fischer, N. Coustel, S. Kycia, Q. Zhu, A. R. McGhie, W. J. Romanow, J. P. McGauley Jr, A. B. Smith III, and D. E. Cox, *Nature,* **351,** 462 (1991). (b) R. Tycko, G. Dabbagh, M. J. Rosseinsky, D. W. Murphy, R. M. Fleming, A. P. Ramirez, and J. C. Tully, *Science,* **253,** 884 (1991).

(3) (a) M. Iyoda, H. Otani, M. Oda, Y. Kai, Y. Baba, and N. Kasai, *J. Chem. Soc., Chem. Commun.*, **1986,** 1794. (b) Z. Yoshida and T. Sugimoto, *Angew. Chem. Int. Ed. Engl.*, **27,** 1573 (1988). (c) K. Kano, T. Sugimoto, Y. Misaki, T. Enoki, H. Hatakeyama, H. Oka, Y. Hosotani, and Z. Yoshida, *J. Phys. Chem.*, **98,** 252 (1994).

(4) K. Ebata, T. Matsuo, T. Inoue, Y. Otsuka, C. Kabuto, A. Sekiguchi, and H. Sakurai, *Chem. Lett.*, **1996,** 1053.

(5) H. Sakurai, T. Fujii, and K. Sakamoto, *Chem. Lett.*, **1992,** 339.

(6) (a) W. Reppe, O. Schlichting, K. Klager, and T. Toepel, *Ann. Chem.*, **560,** 1 (1948). (b) W. Reppe and W. J. Schweckendiek, *Ann. Chem.*, **560,** 104 (1948).

List of Publications

(1) Intramolecular Oligomerization of Disilalkylene {-$Me_2Si(CH_2)_nSiMe_2$-} Bridged Cyclic Triacetylenes.

K. Ebata, T. Matsuo, T. Inoue, Y. Otsuka, C. Kabuto, A. Sekiguchi, and H. Sakurai, *Chem. Lett.*, **1996**, 1053.

(2) Persilylated Dimethylenecyclobutene Dianion Dilithium as the First 6C-8π Allyl Anion System.

A. Sekiguchi, T. Matsuo, K. Ebata, and H. Sakurai, *Chem. Lett.*, **1996**, 1133.

(3) A Supercharged Anion with a Silyl-Substituted Eight-Center, Twelve-Electron π System: Synthesis and Characterization of the tetralithium salt of an Octasilyl-Substituted Trimethylenecyclopentene Tetraanion.

A. Sekiguchi, T. Matsuo, and C. Kabuto, *Angew. Chem., Int. Ed. Engl.*, **36**, 2462 (1997).

(4) Tetraanion Tetralithium with 8 Center/12 Electron π-System Stabilized by Silyl Groups. Synthesis and Characterization.

A. Sekiguchi, T. Matsuo, and R. Akaba, *Bull. Chem. Soc. Jpn.*, **71**, 41 (1998).

(5) Octasilyl[4]radialene Dianion Dilithium with an Eight-Center, Ten-Electron π System. Synthesis and Characterization, and Evidence for a Lithium Walk on the π-Skeleton.

A. Sekiguchi, T. Matsuo, and H. Sakurai, *Angew. Chem., Int. Ed. Engl.*, **37**, 1661 (1998).

(6) Synthesis and Reduction of Octasilyl[4]radialene. Structure and Dynamic Study of [4]Radialene Dianion with Eight-Center Ten-Electron π-System.

T. Matsuo, A. Sekiguchi, M. Ichinohe, K. Ebata, and H. Sakurai, *Bull. Chem. Soc. Jpn.*, **71**, 1705 (1998).

(7) The First Isolation and Full Characterization of Fulvene Dianion. Synthesis and X-ray Structure of Silyl-substituted Fulvene Dianion Dilithium.

T. Matsuo, A. Sekiguchi, M. Ichinohe, K. Ebata, and H. Sakurai, *Organometallics*, **17**, 3143 (1998).

(8) Isolation and Molecular Structure of Persilylated [5]Radialene: Intramolecular Cyclization of a Macrocyclic Pentayne with $Mn(CO)_3$(Me-Cp).

T. Matsuo, H. Fure, and A. Sekiguchi, *Chem. Lett.*, **1998**, 1101.

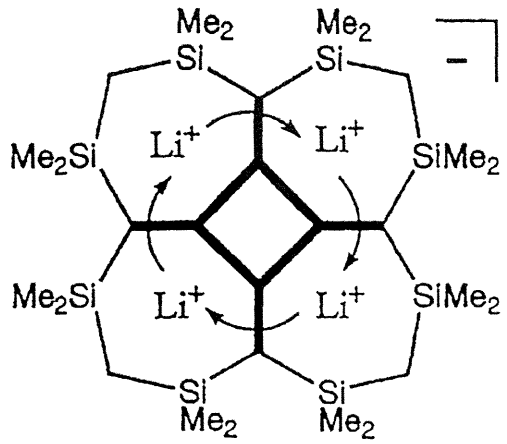

A novel Li^+ walk (top) on the π-electron system of the dilithium salt of the octasilyl[4]radialene dianion (structure depicted in the center) takes place at 298 K in THF.

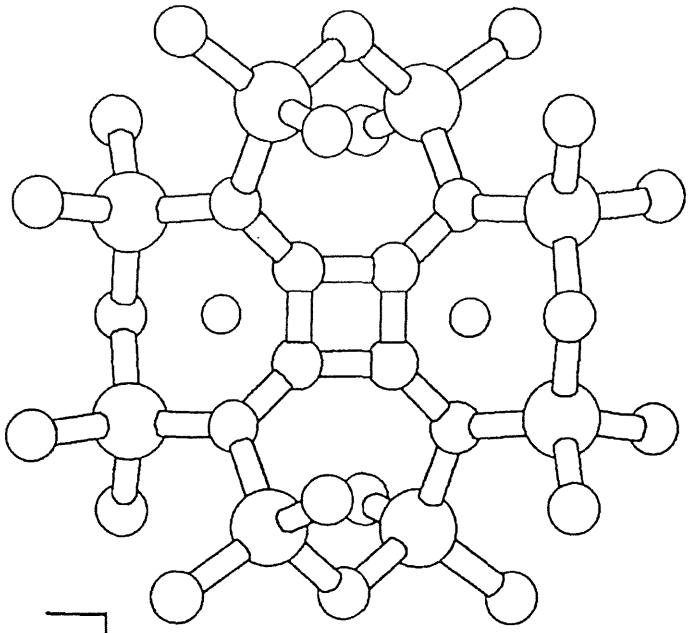

The walking Li^+ ion is bound as a contact ion pair (CIP), the other as a solvent-separated ion pair (SSIP).

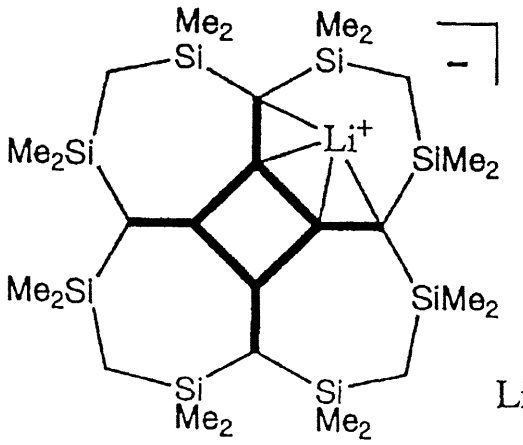

At 173 K the Li^+ walk is suppressed so that Li^+ is fixed at one site on the framework (bottom). Find out more on the following pages.